UNIVERSITY OF CALIFORNIA
Radiation Laboratory

Cover Sheet
Do not remove

INDEX NO. UCRL 483
This document contains 275 pages
This is copy 2 of 3 Series C

OFFICIAL USE ONLY

Issued to Chem. Div.

[redacted]
Classification

Each person who receives this document must sign the cover sheet in the space below

Route to	Noted by	Date	Route to	Noted by	Date
	R.K. Wakerling	11/14/49			
R.L.T.	✓				
	CHEMISTRY DIVISION		✓		
Loan to	K. Gunter	11/25/62			
11 Chem Div. 11		1/10/64			

DISCLAIMER

UCRL 483

UNIVERSITY OF CALIFORNIA

Radiation Laboratory

Contract No. W-7405-eng-48

HIGH ENERGY BOMBARDMENT PRODUCTS OF THORIUM

Thesis by W. Wayne Meinke

November 9, 1949

Berkeley, California

UCRL 483

Oak Ridge Declassification

DISTRIBUTION: Series A. November 9, 1949

	Copy Numbers
Declassification Officer	1-4
Publication Officer	5
Patent Department	6-7
Area Manager	8
Information Division	9

INFORMATION DIVISION
Radiation Laboratory
Univ. of California
Berkeley, California

High Energy Bombardment Products of Thorium

W. Wayne Meinke
Department of Chemistry and Radiation Laboratory
University of California, Berkeley, California

ABSTRACT

Five and possibly six artificial alpha-decay chains collateral to the four radioactive decay families have been prepared by bombardment with the 184-inch cyclotron of the University of California Radiation Laboratory. A number of the members of these chains have been studied to characterize their radioactive properties. A few have also been studied to determine the variation of their yield with particle energy.

The trend in the alpha half-lives of the protactinium isotopes has been determined by milking experiments to determine the orbital electron capture decay/alpha decay ratio. Two neutron deficient isotopes of emanation (element 86) have been discovered in the spallation products of thorium with high energy particles and a new neutron excess isotope of protactinium has been identified in low energy bombardments of thorium.

Table of Contents

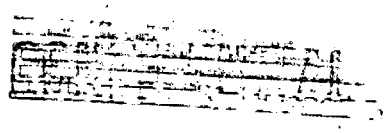

High Energy Bombardment Products of Thorium

W. Wayne Meinke

Foreward

The presence of four charged particle accelerators on the Berkeley campus presents many varied possibilities for nuclear chemical work. Both the 184-inch cyclotron and the 60-inch cyclotron can give large yields of nuclear reaction products. The major problems in characterizing these reaction products are chemical ones involving the application of ordinary analytical procedures to the target separations.

This dissertation discusses the results of these applications to several rather unrelated phases of nuclear work. In Chapter 1 both the production by high energy bombardment and the characterization of five artificial collateral alpha-decay chains are discussed. The variations of yield with particle energy for several of the parents of these chains was studied and presented in Chapter 2. Chapter 3 presents the results of experiments designed to study the trend in alpha half-lives in the protactinium isotopes. Chapter 4 discusses some new neutron deficient isotopes of emanation found in thorium bombardments while Chapter 5 presents evidence for a new neutron-excess isotope of protactinium. The Appendices present for easy reference important information on excitation functions and chemical procedures.

An isotope chart which includes most of the latest values for isotopes in the heavy region is shown on the next page. The values listed are taken primarily from the Table of Isotopes by G. T. Seaborg and I. Perlman, Rev. Mod. Phys. 20, 585 (1948).

ISOTOPE CHART

(HEAVY REGION)

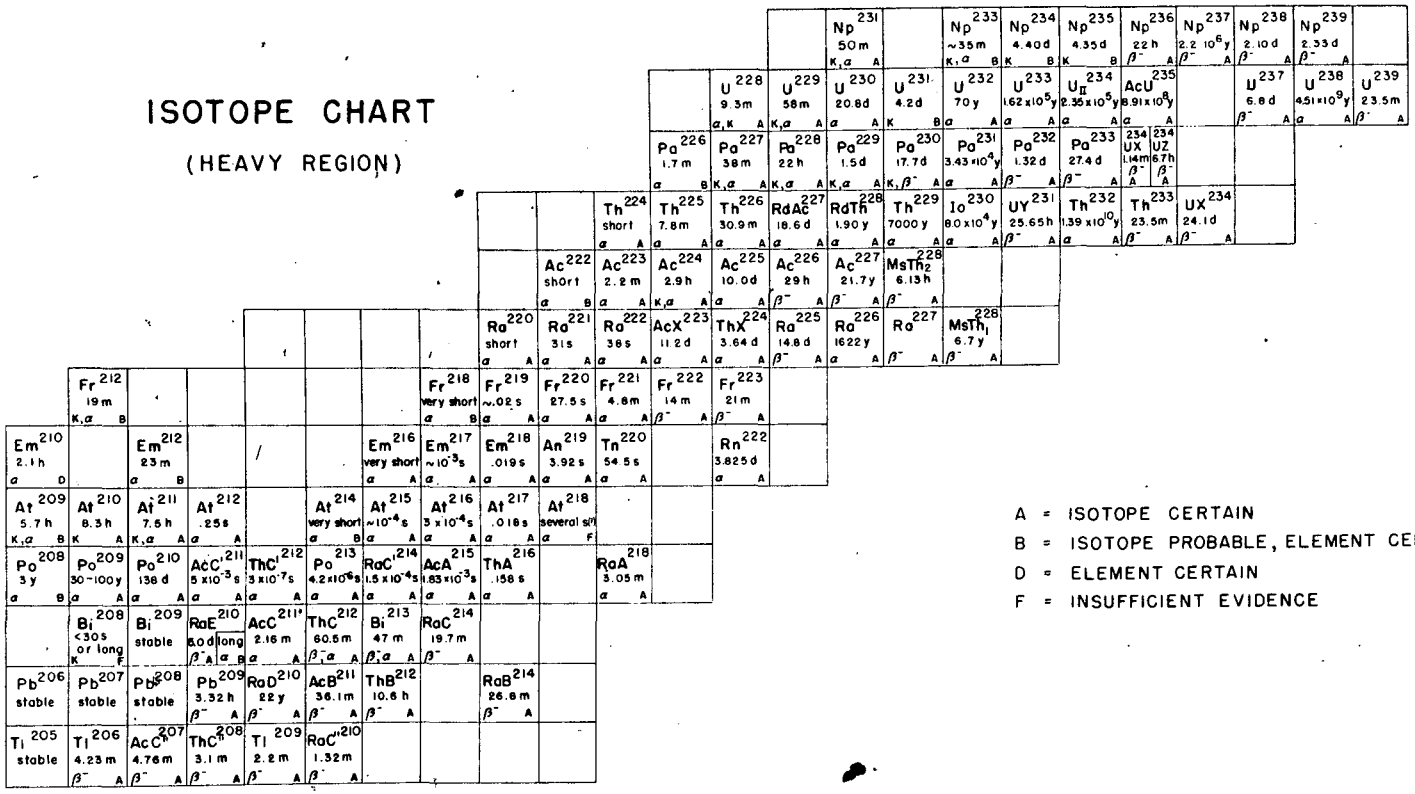

A = ISOTOPE CERTAIN

B = ISOTOPE PROBABLE, ELEMENT CERTAIN

D = ELEMENT CERTAIN

F = INSUFFICIENT EVIDENCE

Chapter I

Artificial Collateral Alpha-Decay Chains

I. Introduction

The Berkeley 184-inch cyclotron has opened up many new fields of research with its full energy beams of 194-Mev deuterons, 388-Mev alpha-particles and, more recently, 348-Mev protons. These new vistas have not been confined to physical problems alone, for the chemist has found that the high energies make possible many reactions previously thought impossible.

Probably the most spectacular of these is the spallation reactions in which the impinging high energy particles split off or "spall" fragments of many units of mass and atomic number from the target nucleus.[1,2] With this type of reaction it is possible to reach many new isotopes previously thought unattainable and in addition to produce rather large amounts of known isotopes that were previously scarce. It has also been possible to induce fission in elements like bismuth[3], lead, and tantalum[4] with these high energy particles.

This cyclotron furnishes more than enough energy to reach and permit exploration of all (d,xn), (α,xn), and (p,xn) reactions producing isotopes with workable half-lives. Hence for the first time it has been possible to completely explore the neutron deficient side of the stable isotopes, an investigation which is limited only by the speed with which chemical procedures can separate the product material, by the contaminating radioactivity of other isotopes of the element separated, and the speed and design of equipment used between the end of bombardment and the counting of the sample.

By bombarding thorium with these high energy deuterons and alpha-particles, we have artificially produced by (d,xn) and (α,xn) reactions, five and possibly

six alpha-decay chains,[5,6] collateral to the four radioactive decay families. These chains being with the protactinium isotopes Pa^{228}, Pa^{227}, and Pa^{226}, and the uranium isotopes U^{229}, U^{228}, and possibly U^{227}, although progenitors have been produced and identified in some cases.[7] A large amount of a seventh chain, the Pa^{230} - U^{230} series which has been reported by Studier and Hyde[8], is also formed in these bombardments. All of these chains decay by alpha emission into the natural radioactive families (or the artificially produced 4n + 1 family[9 - 11]) although in some of the heavier members of the chains orbital electron capture may be favored in the branching decay.

The protactinium or uranium parent controls the decay of the other members of the chain. After chemical separation of these fractions the decay of the alpha-particles was measured by the use of both standard alpha-particle counting devices and an alpha-particle pulse analyzer[12] equipped with a fast sample-changing mechanism. Through the use of the latter we observed a number of alpha-particle groups and determined their energies.

These collateral chains have been identified by physical or chemical separation and identification of radioactive end products of decay which are common both to the chain and to a radioactive family. In some cases where it has not been possible to perform these separations, we have based our assignment on regularities in alpha decay systematics.[13-15]

In many cases where their half-lives and abundances have permitted, individual members of the chains have been studied.

II. Radioactive Collateral Series Found in Bombardments

Soon after 80 Mev deuteron bombardments of thorium, a number of alpha groups are prominent in the pulse analysis of a protactinium fraction. All of these groups appear to decay with the 38.3-minute half-life of the protactinium parent. They are due to the following collateral branch of the 4n + 3 radioactive

family:

$$Pa^{227} \xrightarrow[38.3\ m]{\alpha} Ac^{223} \xrightarrow[2.2\ m]{\alpha} Fr^{219} \xrightarrow[0.02s]{\alpha} At^{215} \xrightarrow[10^{-4}\ s]{\alpha} Bi^{211}(AcC) \xrightarrow[2.16\ m]{\alpha}$$

$$Tl^{207}(AcC'') \xrightarrow[4.76\ m]{\beta^-} Pb^{207}(stable)$$

The branching which arises from orbital electron capture by Pa^{227} is not shown. The mass type was identified by observation of the characteristic energy and half-life of the Bi^{211}(AcC) alpha-particles, the half-life of the beta emitting Tl^{207} (AcC''), and the growth of 18.6-day Th^{227}(RdAc) as an orbital-electron-capture branching decay product of the Pa^{227}.

After the decay of the above series, a second group of alpha-particle emitters can be resolved. This second series, which decays with the 22-hour half-life of its protactinium parent, is a collateral branch of the 4n radioactive family as follows:

$$Pa^{228} \xrightarrow[22h]{\alpha} Ac^{224} \xrightarrow[2.9\ h]{\alpha} Fr^{220} \xrightarrow[27.5\ s]{\alpha} At^{216} \xrightarrow[3x10^{-4}\ s]{\alpha}$$

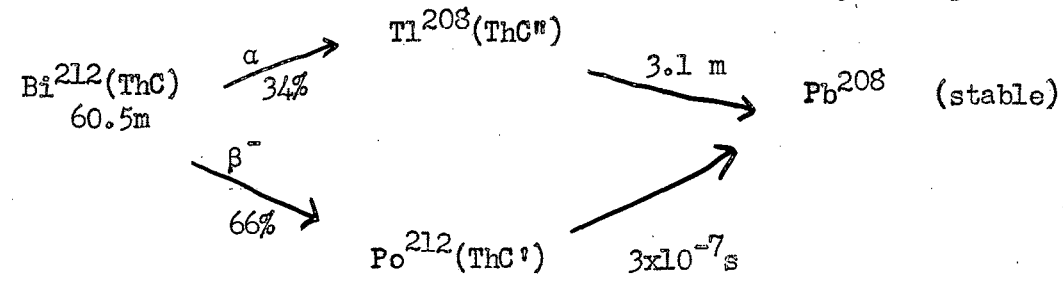

The branch which arises from orbital electron capture by Pa^{228} and Ac^{224} is not shown. The mass type was identified through observation of the characteristic radioactive properties of the Bi^{212}(ThC) and its daughters, chemical identification of Bi^{212}(ThC), the growth of Th^{228}(RdTh) as an orbital-electron-capture branching decay product of the Pa^{228}, and the growth of Ra^{224} (ThX) as a similar product of the Ac^{224}.

The irradiation of thorium with 100 Mev alpha particles resulted in the observation of the following collateral branch of the artificial 4n + 1, neptunium, radioactive family shown with Po^{213} and its decay products:

$$U^{229} \xrightarrow[58\ min]{\alpha} Th^{225} \xrightarrow[8.0\ min.]{\alpha} Ra^{221} \xrightarrow[30\ sec]{\alpha} Em^{217} \xrightarrow[10^{-3}\ sec]{\alpha}$$

$$Po^{213} \xrightarrow[4.2\times10^{-6}\ sec]{\alpha} Pb^{209} \xrightarrow[3.32\ hr.]{\beta^-} Bi^{209}\ (stable)$$

The mass type was identified by observation of the characteristic energy of the Po^{213} alpha-particles as well as the growth of 1.5-day Pa^{229} as the electron-capture branching decay product of U^{229} and the growth of 10.0 day Ac^{225} as the electron-capture decay product of Th^{225}.

Soon after 120-Mev alpha bombardments of thorium the uranium fraction contains another series of five alpha-emitters, which is apparently a collateral branch of the 4n family:

$$U^{228} \xrightarrow[9.3min]{\alpha} Th^{224} \xrightarrow[very\ short]{\alpha} Ra^{220} \xrightarrow[very\ short]{} Em^{216} \xrightarrow[very\ short]{\alpha}$$

$$Po^{212}(ThC') \xrightarrow[3\times10^{-7}\ sec.]{\alpha} Pb^{208}\ (stable)$$

The 9.3 minute half-life of U^{228} controls the decay rate of the series. The mass type was identified by observation of the characteristic energy of the Po^{212}(ThC') alpha-particles and the growth of 22-hour Pa^{228} as an electron-capture branching decay product of U^{228}.

Immediately after a 150-Mev deuteron bombardment of thorium, the protactinium fraction shows a series of alpha-particle emitters whose rate of decay is controlled by the 1.7-minute half-life of the parent with the subsequent members all too short-lived to be isolated and separately studied. Although the mass type has not yet been identified through known daughters as above, general considerations with regard to the method of formation and half-life of the parent substance, and

the energies of all the members of the series suggest a collateral branch of the 4n + 2 family:

$$Pa^{226} \xrightarrow[1.7\ min]{\alpha} Ac^{222} \xrightarrow[short]{\alpha} Fr^{218} \xrightarrow[very\ short]{\alpha} At^{214} \xrightarrow[very\ short]{\alpha}$$

$$Bi^{210}(RaE) \xrightarrow[5\ day]{\beta^-} Po^{210} \xrightarrow[138\ day]{\alpha} Pb^{206}\ (stable)$$

Similarly immediately after bombardment, a uranium fraction seems to show a series of alpha emitters which decay with the one to two minute half-life of the parent. This latter series has not been definitely established but if the existence of U^{227} is proven, it will be a collateral branch of the 4n + 3 family:

$$U^{227}(?) \xrightarrow[1\text{-}2\ min]{\alpha} Th^{223} \xrightarrow{\alpha} Ra^{219} \xrightarrow{\alpha} Em^{215} \xrightarrow{\alpha} Po^{211} \xrightarrow[5x10^{-3}\ sec]{\alpha} Pb^{207}(stable)$$

III. Experimental Methods

A variety of techniques must be employed in working with isotopes whose half-lives range from days to microseconds. These techniques range from laborious chemical separations of one element from all other elements to electronic methods measuring the time between two successive alpha pulses.

For isotopes that have half-lives of a day or so, chemical procedures must be used that insure complete separation from even small quantities of contaminating activities and there is no time limitation on these procedures. If, on the other hand, the desired isotope has a half-life of less than an hour the requisite of purity may still be imposed but the chemistry must now also be rapid -- a factor of two in speed being preferable to a factor of two in purity. In general, physical methods must be relied upon to measure and identify isotopes of half-lives of less than a minute. Counting techniques must also be geared to the half-life of the substance.

A. Types of Bombardments

The first requirement is to obtain a good bombardment, i.e. to obtain as good a product yield as is possible with the beam and target material available. In this work where yield is all important the internal beam of the cyclotron is used, except when other arrangements can meet a special need (with consequent lowering of yield). This internal beam usually gives about one microampere of deuteron and proton current and about one-tenth of this amount for alpha-particles. The electrostatically deflected beam (reducing the current available by a factor of at least 100) and the external beam (reducing the current by a factor of about 50,000)were unsatisfactory for our work.

In general, foils of thorium metal were bombarded in the internal beam either for a half-life of the activity desired or until a considerable amount of that activity had built up. The target foils, measuring about 1.5 inches by 0.5 inches, were clamped into a holder which could be mounted on the probe of the cyclotron and inserted into the tank to intercept the beam. The energy with which the particles hit the target was determined by the radius at which the leading edge of the target foils were set.

In our first bombardments several five-mil foils were stacked on top of each other to increase the reaction yields. Later, however, upon the suggestion of A. Ghiorso, a target holder which would enable a target to be bombarded on edge was designed by L. Magnusson. Sketches of this holder are shown in Figs. 1-6. The holder is put on the end of the 184-inch cyclotron probe in such a way that it requires the beam to traverse the width of the thorium foil instead of its thickness. Hence for the same weight of target material in foil form a factor increase of at least 10 in yield can be obtained by using this target holder. It was only by the application of this concept of bombarding a target "on edge" that we were able to obtain enough yield in many reactions to obtain the data we required.

ITEM	DESCRIPTION	4A9822-1C	4A9822-2C	4A9822-3C
4A9772B	SUPPORT	1	1	1
4A9781-1C	SPACER	1		
4A9781-2C	SPACER		1	
4A9781-3C	SPACER			1
4A9791	SIDE BLOCK	1	1	1
4A9801	JAW BLOCK	1	1	1
4A9811-1A	JAW	1		
4A9811-2A	JAW		1	
4A9811-3A	JAW			1
AB2971	BAYONET	1	1	1
1	MACH. SCR. 4-40 X 3/16 LG. RD. HD.	2	2	2
2	MACH. SCR. 4-40 X 3/16 LG. FIL. HD.	2	2	2
3	MACH. SCR. 4-40 X 3/8 LG. FT. HD.	2	2	2
4	MACH. SCR. 10-24 X 5/16 FIL. HD.	1	1	1
5	MACH. SCR. 4-40 X 3/8 RD. HD.	1	1	1

SHOWN ON					
ISSUED TO	DATE ISSUED	DELIVER TO	JOB NO.	DATE REQ'D	MAKE

CHANGE LETTER	DRAWN BY	CHECK BY	DATE	CHANGE
A	H.T.		8-3-48	4A9772 WAS 4A9771
B	H.T.		10-22-48	ADDED AB2971 ITEM 5
C	JWL	HPR	5-5-49	ADDED 4A9822-2C & 4A9822-3C

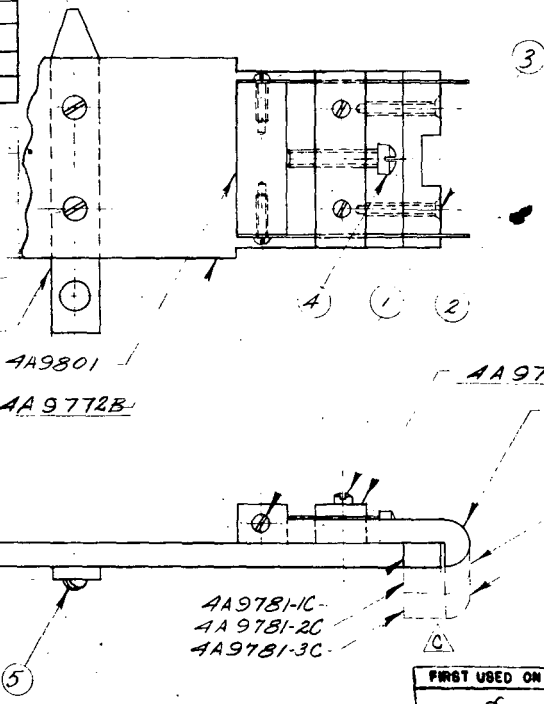

DWG NO	
4A9822-3C	3/4 FOIL TARGET
4A9822-2C	1/2 FOIL TARGET
4A9822-1C	1/4 FOIL TARGET

FIG. 1

FIRST USED ON 140-22

ROUGH FINISH FINISH

GOOD FINISH FINISH

MACHINED DIMENSIONS ±.010 UNLESS OTHERWISE SPECIFIED

MATERIAL

184" CYCLOTRON

PROBE HEAD-FOIL TARGET HOLDER ASSEMBLY

RADIATION LABORATORY
UNIVERSITY OF CALIFORNIA—BERKELEY

DRAWN BY	CHECK BY	DATE
H. THOMAS		7-23-48

APPROVED BY

SCALE FULL SIZE

DRG. NO. 4A9822C

SHOWN ON	4A9822					
ISSUED TO	DATE ISSUED	DELIVER TO	JOB NO.	DATE REQ'D	MAKE	

CHANGE LETTER	DRAWN BY	CHECK BY	DATE	CHANGE
A	MacT		8-3-48	RE-DESIGNED & RE-DRAWN - WAS 4A9771
B	JWL	HPR	5-5-49	5/8 added

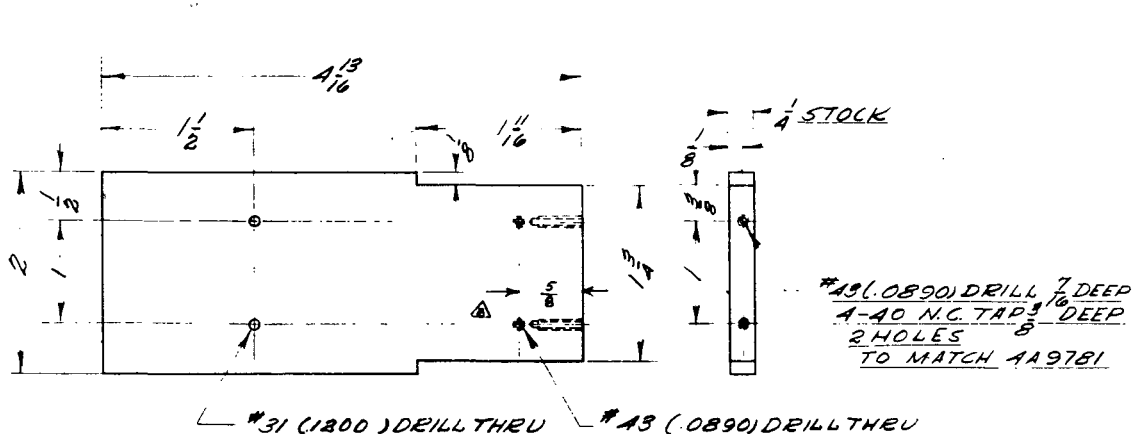

FIG. 2

184" CYCLOTRON
PROBE HEAD-FOIL TARGET HOLDER SUPPORT

FIRST USED ON 140.22

RADIATION LABORATORY
UNIVERSITY OF CALIFORNIA—BERKELEY

DRAWN BY	CHECK BY	DATE
H. THOMAS		8-3-48

APPROVED BY

SCALE FULL-SIZE

DRG. NO. 4A9772B

MATERIAL COPPER

FINISH

MACHINED DIMENSIONS ±.010 UNLESS OTHERWISE SPECIFIED

"ALBANENE" No. 1951, K & E CO., N.Y. REG. U.S. PAT. OFF.

SHOWN ON	4A9822								FIRST USED ON 140.22
ISSUED TO	DATE ISSUED	DELIVER TO	JOB NO.	DATE REQ'D	MAKE				

ROUGH ϕ FINISH — FINE ff FINISH
GOOD f FINISH — GRIND G FINISH

MACHINED DIMENSIONS ± .010 UNLESS OTHERWISE SPECIFIED

RADIATION LABORATORY DRG. NO. 4A9801

UNIVERSITY OF CALIFORNIA–BERKELEY

DRAWN BY	CHECK BY	DATE
M. THOMAS		7-21-48

APPROVED BY | SCALE FULL-SIZE

184" CYCLOTRON

PROBEHEAD-FOIL TARGET HOLDER

JAW BLOCK

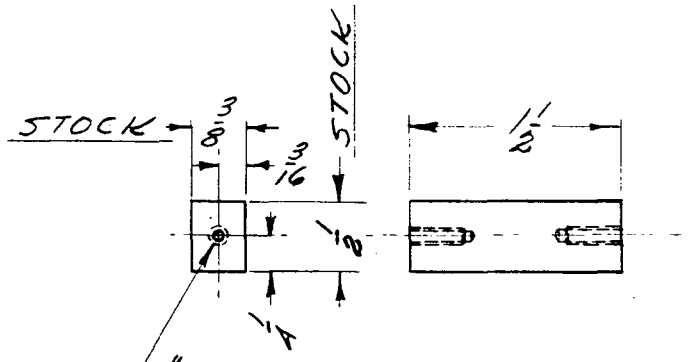

FIG. 3

MATERIAL BAR 3/8 × 1/2 COPPER

CHANGE LETTER	DRAWN BY	CHECK BY	DATE	CHANGE

"ALBANENE" 195L K. & E. CO., N. Y.
REG. U. S. PAT. OFF.

SHOWN ON	4A9822							FIRST USED ON	14-0-22
ISSUED TO		DATE ISSUED		DELIVER TO		JOB NO.		DATE REQ'D	MAKE

ROUGH ⌀ FINISH FINE ff FINISH
GOOD f FINISH GRIND G FINISH
MACHINED DIMENSIONS ± .010 UNLESS OTHERWISE SPECIFIED

RADIATION LABORATORY

DRG. NO. 4A9781C

UNIVERSITY OF CALIFORNIA—BERKELEY

DRAWN BY	CHECK BY	DATE
M. THOMAS		7-21-48

APPROVED BY

SCALE FULL-SIZE

184" CYCLOTRON
PROBE HEAD-FOIL TARGET HOLDER
SPACER

DRG. NO.	"W"	
4A9781-1C	1/4	
4A9781-2C	1/2	
4A9781-3C	3/4	

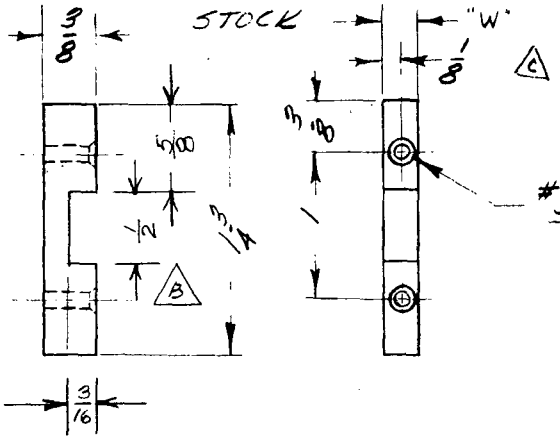

#31 (1200) DRILL THRU
C'SINK FOR
4-40 NC. FLAT
HEAD MACHINE SCREW
2 HOLES TO MATCH 4A9772
A

FIG. 4

CHANGE LETTER	DRAWN BY	CHECK BY	DATE	CHANGE
				4A9781-2C & 3C added
C	JWL	HPR	5-5-49	4A9781-1C was 4A9781B
B	JWL	HPR	12-20-48	1/2" Well O.K.-CA
A	HRT		8-3-48	4A9772 WAS 4A9771

MATERIAL COPPER

"ALBANENE" 195L K. & E. CO., N. Y.
REG. U. S. PAT. OFF.

-p11-

SHOWN ON	4A9822							FIRST USED ON 140-22
ISSUED TO	DATE ISSUED	DELIVER TO	JOB NO.	DATE REQ'D	MAKE			

ROUGH ϕ FINISH — FINE ff FINISH
GOOD f FINISH — GRIND G FINISH
MACHINED DIMENSIONS ± .010 UNLESS OTHERWISE SPECIFIED

RADIATION LABORATORY — DRG. NO. 4A 9811A
UNIVERSITY OF CALIFORNIA—BERKELEY

DRAWN BY	CHECK BY	DATE
APPROVED BY	SCALE FULL-SIZE	

184" CYCLOTRON
PROBE HEAD-FOIL TARGET HOLDER
JAW

DRG. NO.	"L"	
4A9811-1A	½	
4A9811-2A	3/4	
4A9811-3A	1	

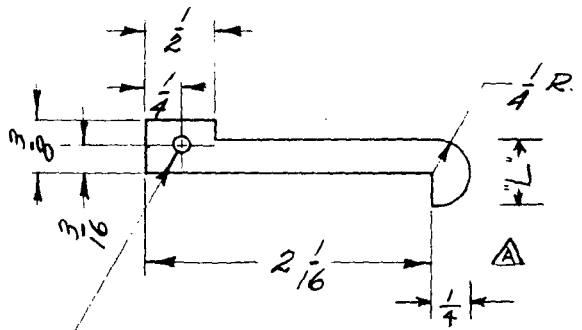

31 (.1200) DRILL THRU
1 HOLE
TO MATCH 4A9801

FIG. 5

CHANGE LETTER	DRAWN BY	CHECK BY	DATE	CHANGE
				4A9811-2A & 3A added
A	JWL		5-5-49	4A9811-1A was 4A9811

MATERIAL SHEET .032 BRASS

"ALBANENE" 195L K. & E. CO., N. Y.
REG. U. S. PAT. OFF.

SHOWN ON								FIRST USED ON 140-22
ISSUED TO	DATE ISSUED	DELIVER TO	JOB NO.	DATE REQ'D	MAKE			

ROUGH ⌀ FINISH FINE ff FINISH
GOOD f FINISH GRIND G FINISH
MACHINED DIMENSIONS ± .010 UNLESS OTHERWISE SPECIFIED

RADIATION LABORATORY
DRG. NO. 4B2971
UNIVERSITY OF CALIFORNIA—BERKELEY

DRAWN BY	CHECK BY	DATE
H. THOMAS		10-22-48

APPROVED BY
SCALE FULL-SIZE

184" CYCLOTRON
PROBE HEAD - FOIL TARGET HOLDER
BAYONET

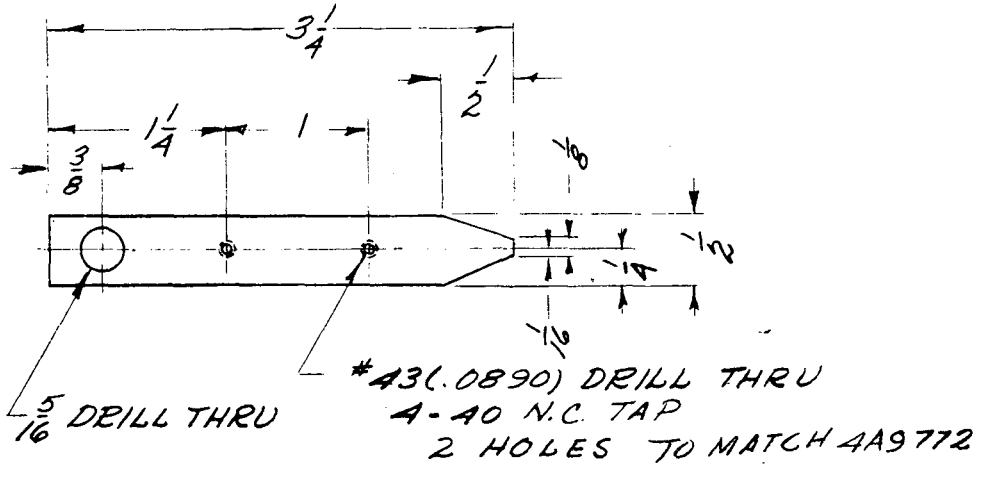

FIG. 6

MATERIAL BAR 1/8 X 1/2 BRASS

CHANGE LETTER	DRAWN BY	CHECK BY	DATE	CHANGE

"ALBANENE" 1951 K. & E. CO., N. Y.
REG. U. S. PAT. OFF.

It should be mentioned that the parts in Figs. 4 and 5 are replaceable and can be discarded when they become too active. Since these are the only holder parts, besides the target itself, that come in contact with the beam, the holder can be used many times even with the hottest of beams. These parts also can be made to give a one-quarter, one-half, or three-quarter-inch clamping base for the targets and have been used to clamp one and one half inch pieces of 25-mil thorium for bombardment.

When isotopes with long half-lives were desired, 25-mil pieces of thorium were used to increase the total yield of the protactinium or uranium. However if the time for chemistry had to be short, pieces of thorium five-mil or less were used to insure rapid solution and a small amount of target bulk to work up.

In some cases, thorium nitrate powder wrapped in aluminum foil was used as a target in order to eliminate the solution time. These bombardments in the vacuum chamber were not successful, however, since the salt outgassed too much and prevented the attainment of a vacuum sufficiently high to proceed with the bombardment.

Saturated thorium nitrate solution was bombarded in the external beam in hopes of reducing the elapsed time between shutdown and counting of the samples. The bombardment was not successful however since too little activity was formed by the external beam.

B. Fast Target Set-up. The Jiffy Probe

When we realized that speed was really at a premium for two of our series --- the 1.7-minute Pa^{226} and the U^{227} series of about the same half-life --- we began using the jiffy probe in our bombardments. This probe, a long hollow tube with a thin concave aluminum end-window, can be inserted into the tank of the cyclotron. The inside of this tube is kept at atmospheric pressure, the window being strong enough to withstand the vacuum of the tank. A "rabbit" holding a target is blown by compressed air to the front of the tube, the target being placed as close to

the window as possible. At the end of bombardment it is possible to remove the target within a few seconds by blowing it out the rear of the probe tube with compressed air. Thorium metal targets were bombarded on edge in this set-up, while thorium nitrate salts were bombarded in a small brass cylinder that fit on the end of the rabbit. In the bombardment, the beam current hitting the target is reduced by a factor of at least 10.

In our early runs, the rabbit was delivered through a flexible tubing which ran from the end of the jiffy probe to outside the shielding. This process, however, required at least one-half minute and we found it faster to catch the rabbit at the end of the probe tube. The rabbit was caught in a lead "suitcase" which made it possible to carry the target around with little exposure to radiation.

In these runs then, after bombardments the order of a minute were made with the jiffy probe set-up, the doors of the cyclotron were opened immediately and the target blown out into the suitcase. This suitcase was then carried to a Health Chemistry truck where we made a combined solution and extraction of the target while we were being driven up to the chemistry building. There the sample was plated out and counted. This method took a minimum of 3.3 minutes from shutdown to pulse analysis for protactinium chemistry and 4.5 minutes for uranium chemistry.

These fast manual runs were wearing on personnel and were so inconsistent that at least ten bombardments had to be made for every good run on the short half-life reactions.

Hence, in conjunction with the Health Chemistry Group, we have planned and built a pneumatic tube carrier system which will bring a target automatically from the head of the jiffy probe to a laboratory in the Chemistry building. Since this system is only now being completed and tested, the increased speed it affords will apply to future work on the short-lived series. The pneumatic tube itself can bring a carrier from the cyclotron to the Chemistry building in eight seconds; the rabbit can be blown out of the jiffy probe in about four seconds, making the total

time elapsed between end of bombardment and the beginning of chemistry about 12 seconds.

New powder target holders designed for use with the pneumatic system are sketched in Figs. 7-9 and pictured in Fig. 10. The thorium nitrate to be bombarded is placed in the front third of the tube, the remaining space being taken up by a copper slug. The entire cartridge is locked in place on the cartridge clip and the loading end is locked shut to prevent opening before the cartridge is removed by special tongs (shown in Figs. 11-13 and pictured in Fig. 14.). Only when the bayonets of the tongs are inserted in the cartridge clip can the cartridge be removed from the clip, or the end of the cartridge opened to allow the radioactive contents to be poured out. These target holders and tongs were designed for this problem by G. T. Saunders of the Health Chemistry group and combine a maximum of safety with maximum speed and ease of handling. It should be mentioned that the end of the pneumatic tube system has an automatic positioning device which will bring the rabbit to rest in exactly the same position each time. Consequently, the tongs can be rapidly inserted at the same angle for every run.

Equipment for carrying the rabbit from the jiffy probe tube into the pneumatic tube carrier and for positioning the cartridge at the end of a run was designed by George Edwards of the cyclotron engineering staff.

N. C. Lee of the Health Chemistry Group has designed a new target holder to permit bombardment of thin strips of metal on edge in the "jiffy probe beam". This holder conveniently uses the same clip as the powder cartridge. The metal strip bombardments will be used if it is found impossible to obtain enough yield of certain reactions with the salt.

The pneumatic tube coupled with the jiffy probe will greatly facilitate bombardments investigating the short-lived series of Pa^{226} and U^{227}.

4H2452

LIST OF MATERIAL		
ITEM OR PART NUMBER	DESCRIPTION	Nº REQ'D
4H2392	CARTRIDGE	1
4H2411	CLOSURE	1
4H2401	SPRING	1
4H2421	PIN	1
1	SCREW, 2-56 X 1/4 LONG, FL. H'D MACH. ST. STEEL	1
2	" " X 1/4 " " " " "	1

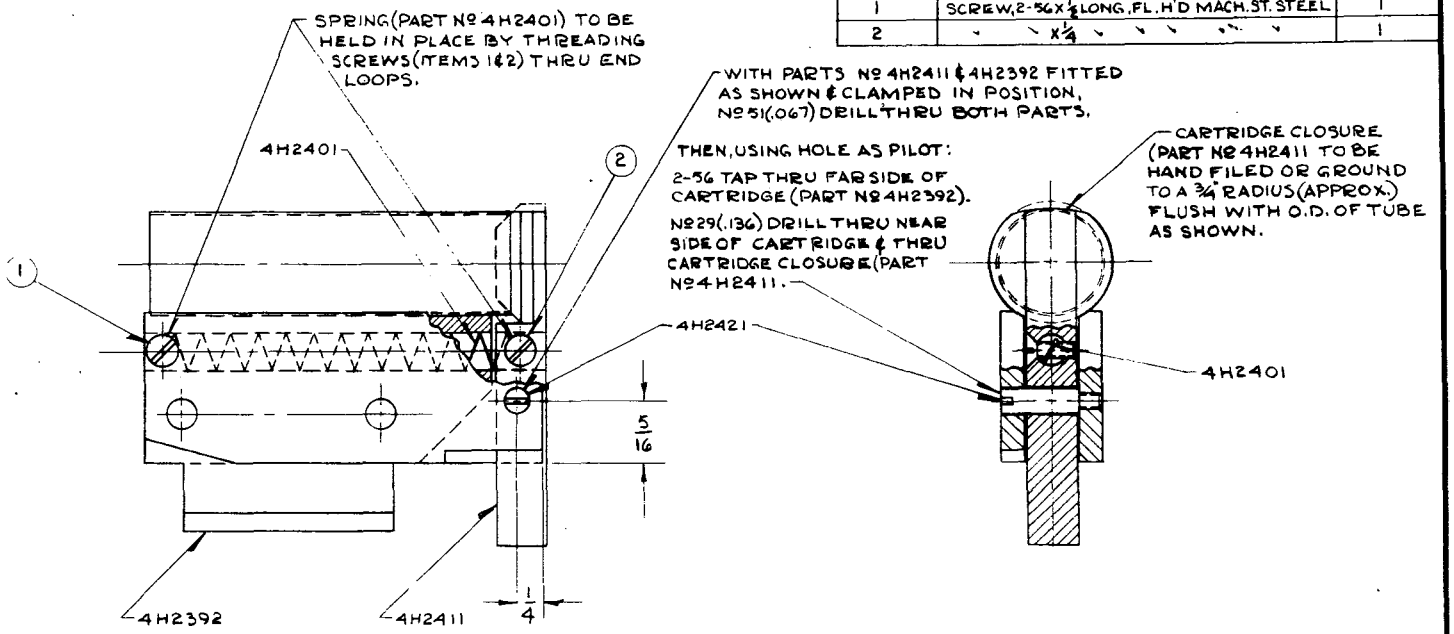

FIG. 7

Change Letter	Drawn By	Check By	Date	CHANGES
✓				

FINISHES: SAW CUT, FLAME CUT, SHEAR; ROUGH MACHINE; AVERAGE MACHINE; SMOOTH MACHINE

SHOP NOTES: UNLESS OTHERWISE SPECIFIED
1. TOLERANCES ± 1/64 ON DIMENSIONS
2. BREAK EDGES 1/64 MAX.
3. 30° CHAMFER ENDS OF ALL SCREW THREADS
4. 1½ PITCH THREAD RELIEF WITH ROUND NOSE TOOL ON MACH. CUT SCREW THREADS

SHOP ORDERS: JOB NO.; SERIAL NO.; DATE ISSUED; DATE REQD.; NO. REQD.; DELIVER TO

DESIGN JOB NO. 140-22

184" CYCLOTRON-BREECH LOADING PROBE
POWDER TARGET HOLDER
SHOWN ON ASSEMBLY
SCALE DOUBLE
DO NOT SCALE THIS DRAWING
DRAWN BY POMEROY
DATE 8-5-49
CHECKED BY
APPR. BY

RADIATION LABORATORY
UNIVERSITY OF CALIFORNIA—BERKELEY

4H2452

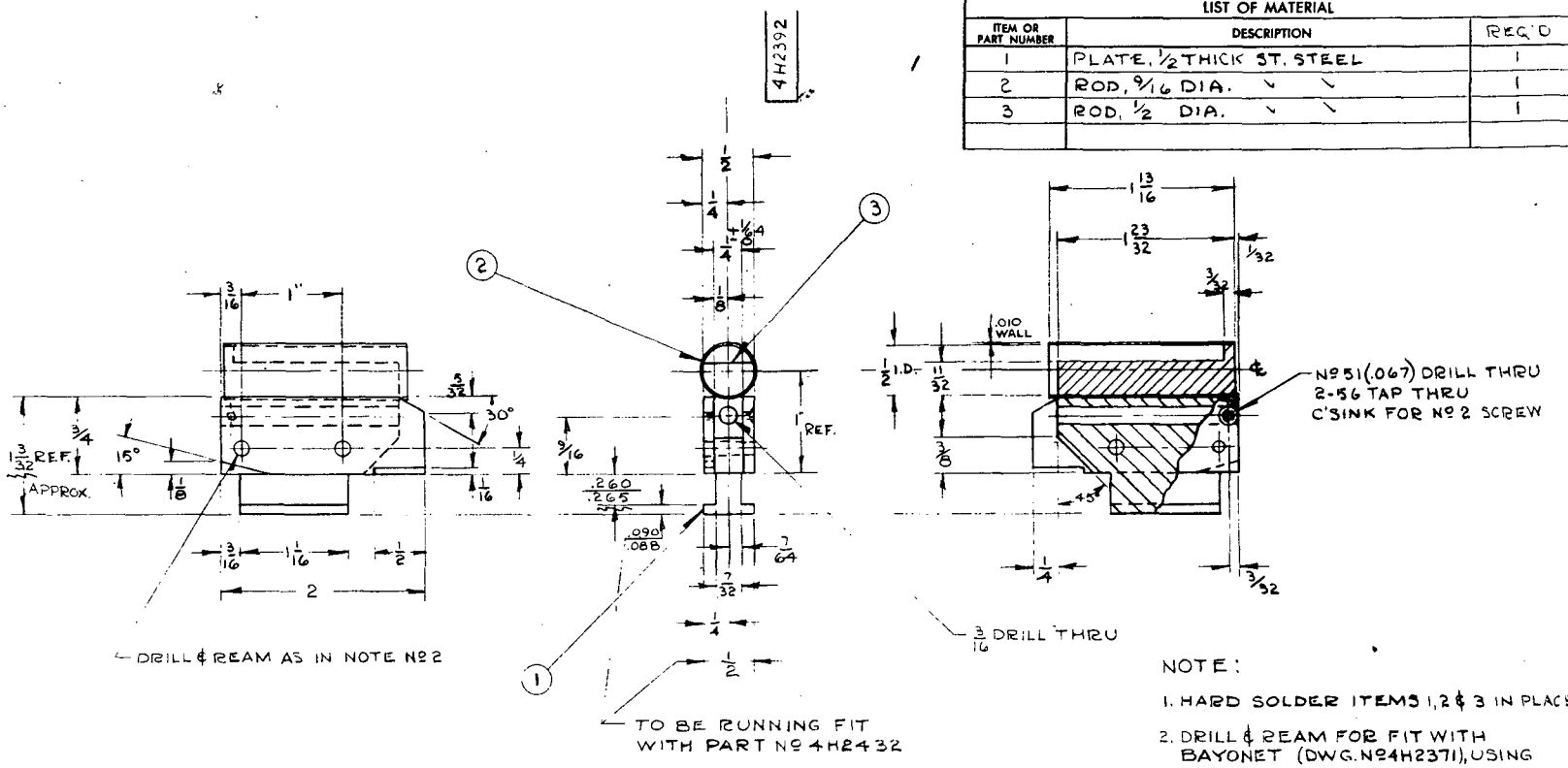

LIST OF MATERIAL		
ITEM OR PART NUMBER	DESCRIPTION	REQ'D
1	PLATE, 1/2 THICK ST. STEEL	1
2	ROD, 9/16 DIA.	1
3	ROD, 1/2 DIA.	1

NOTE:

1. HARD SOLDER ITEMS 1, 2 & 3 IN PLACE.
2. DRILL & REAM FOR FIT WITH BAYONET (DWG. Nº 4H2371), USING JIG TO INSURE INTERCHANGEABILITY OF PARTS. CARTRIDGE & BAYONET TO FIT SNUGLY IN EITHER POSITION WITH .010 TO .030 CLEARANCE BETWEEN MATING FLATS.

√ FINISH ALL OVER

FIG. 8

Change Letter	Drawn By	Check By	Date	CHANGES

FINISHES: SAW CUT, FLAME CUT, SHEAR; ROUGH MACHINE; AVERAGE MACHINE; SMOOTH MACHINE

SHOP NOTES: UNLESS OTHERWISE SPECIFIED
1. TOLERANCES ± .010 ON DIMENSIONS
2. BREAK EDGES 1/64 MAX.
3. 30° CHAMFER ENDS OF ALL SCREW THREADS
4. 11½ PITCH THREAD RELIEF WITH ROUND NOSE TOOL ON MACH. CUT SCREW THREADS

SHOP ORDERS: JOB NO. | SERIAL NO. | DATE ISSUED | DATE REQD. | NO. REQD. | DELIVER TO

DESIGN JOB NO. 140-22
SHOWN ON 4H2452

.84" CYCLOTRON ~ BREECH LOADING PROBE
POWDER TARGET HOLDER
CARTRIDGE
SCALE FULL
DO NOT SCALE THIS DRAWING
DRAWN BY Pomeroy DATE 7-18-49
CHECKED BY
APPR. BY

RADIATION LABORATORY
UNIVERSITY OF CALIFORNIA—BERKELEY

4H2392

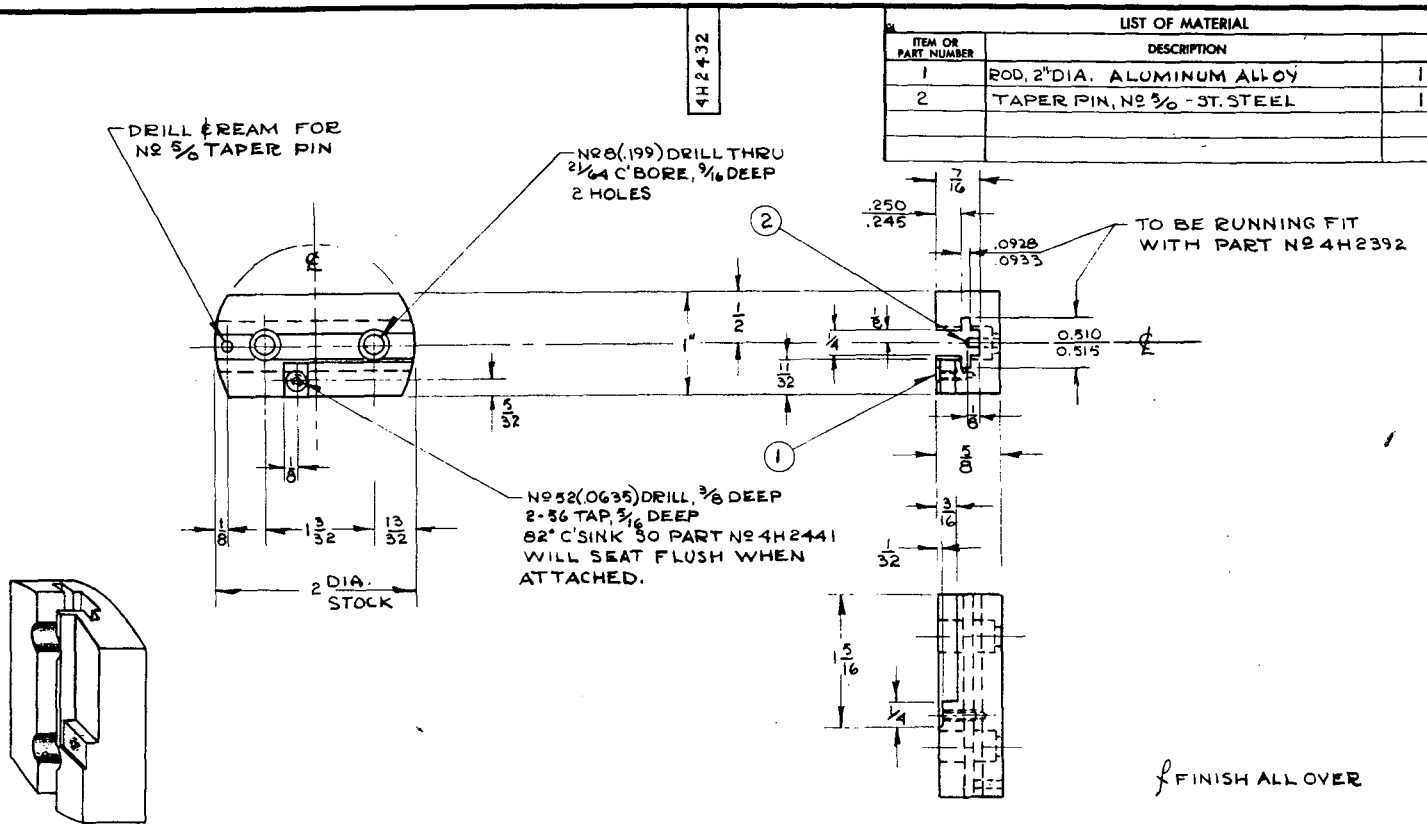

FIG. 9

					FINISHES	SHOP NOTES	SHOP ORDERS	DESIGN JOB NO.	184" CYCLOTRON - BREECH LOADING PROBE		
					SAW CUT, FLAME CUT, SHEAR	UNLESS OTHERWISE SPECIFIED	JOB NO.	140-22	POWDER TARGET HOLDER		
					ROUGH MACHINE	1. TOLERANCES + ON DIMENSIONS =	SERIAL NO.	SHOWN ON	CARTRIDGE CLIP		
					AVERAGE MACHINE	2. BREAK EDGES 1/64 MAX.	DATE ISSUED	4H2453	SCALE FULL	RADIATION LABORATORY	
					SMOOTH MACHINE	3. 30° CHAMFER ENDS OF ALL SCREW THREADS	DATE REQD.		DO NOT SCALE THIS DRAWING	UNIVERSITY OF CALIFORNIA—BERKELEY	
✓						4. 11½ PITCH THREAD RELIEF WITH ROUND NOSE TOOL ON MACH. CUT SCREW THREADS	NO. REQD.		DRAWN BY POMEROY	DATE 7-18-49	4H2432
Change Letter	Drawn By	Check By	Date	CHANGES			DELIVER TO		CHECKED BY A Brown	APPR. BY	

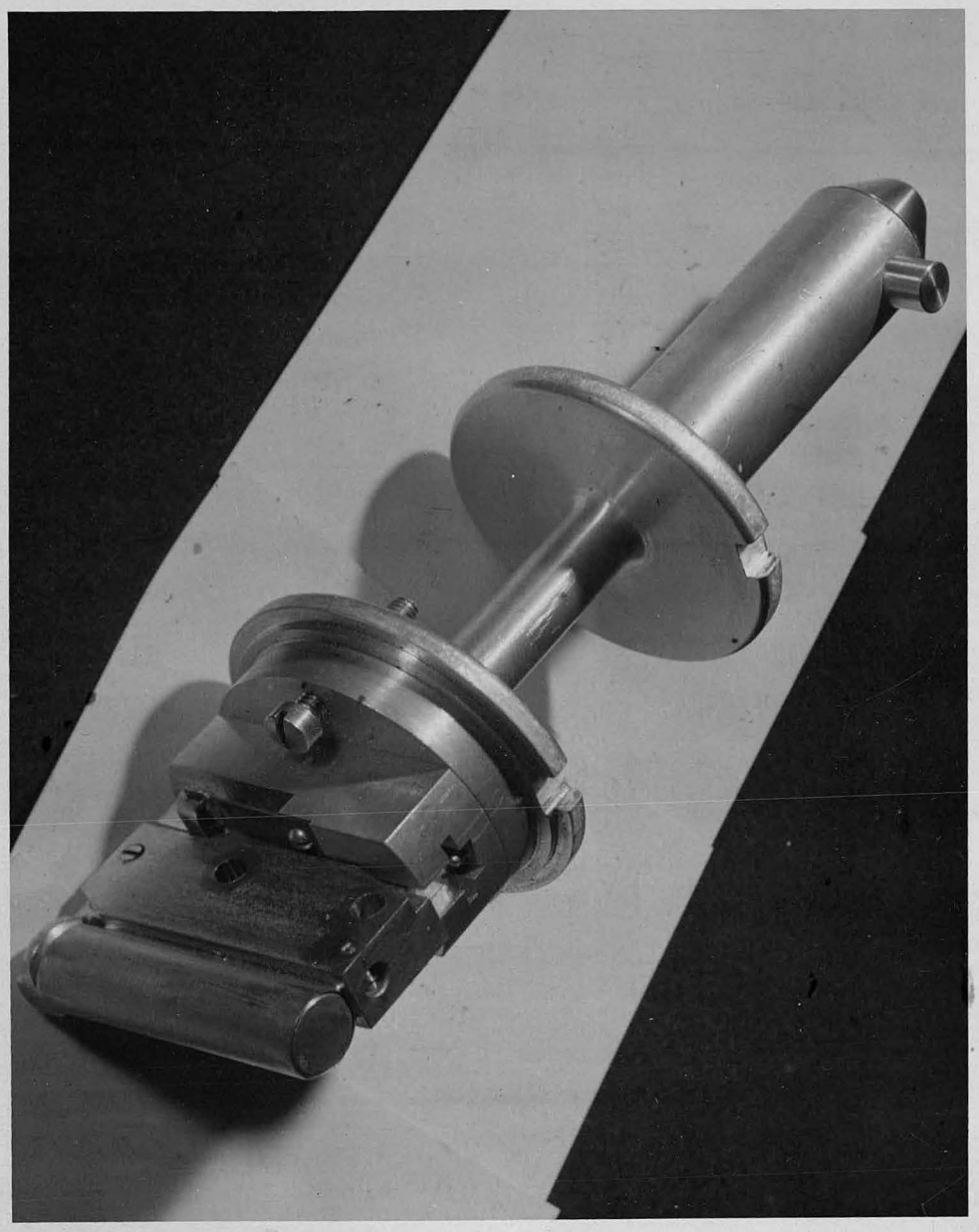

FIG. 10

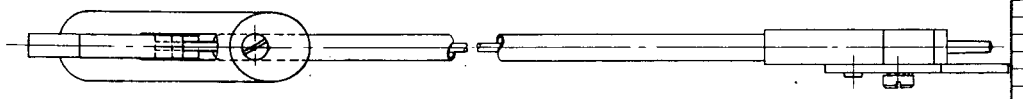

LIST OF MATERIAL		
ITEM OR PART NUMBER	DESCRIPTION	NR REQ'D
3F2072	HANDLE	1
3F5001-1	CONNECTOR TUBE -18	1
3F4991-1	PULL ROD 19 3/8	1
3F4282	TRIGGER	1
3F5021	TRIGGER BUSHING	1
3F5031-1	SLOTTED SCREW	1
4H2323	HEAD	1
4H2331	SPRING	1
4H2341	SLIDE PIN	1
4H2351	JAW	1
4H2361	JAW PIVOT	1
4H2371	BAYONET	1
1	SCREW, 10-24 X 1" LG. FLAT H'D. MACH. ST. STEEL	1
2	SET SCREW 8-32 X 3/16 LG. SKT H'D. CUP PT. ST. STEEL	2
3	SCREW, 5-40 X 1/2 LONG, FLAT H'D. MACH. ST. STEEL	3

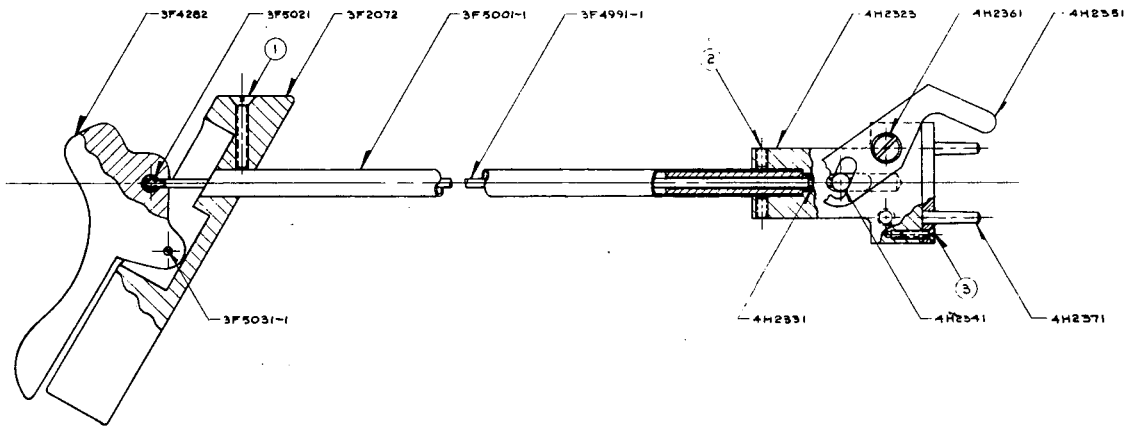

4H2383

FIG. II

CHANGES	FINISHES	SHOP NOTES	SHOP ORDERS	DESIGN JOB NO.	184" CYCLOTRON
	SAW CUT, FLAME CUT, SHEAR	UNLESS OTHERWISE SPECIFIED	JOB NO.	140-22	BREECH LOADING PROBE
	ROUGH MACHINE	1. TOLERANCES ± ON DIMENSIONS —	SERIAL NO.	SHOWN ON	POWDER TARGET HOLDER TONGS ASSEMBLY
	AVERAGE MACHINE	2. BREAK EDGES 1/64 MAX.	DATE ISSUED	SCALE FULL	RADIATION LABORATORY, UNIVERSITY OF CALIFORNIA—BERKELEY
	SMOOTH MACHINE	3. 90° CHAMFER ENDS OF ALL SCREW THREADS	DATE RECD.	DO NOT SCALE THIS DRAWING	
		4. 1½ PITCH THREAD RELIEF WITH ROUND NOSE TOOL ON MACH. CUT SCREW THREADS	NO. RECD.	DRAWN BY POMEROY	DATE 7-22-49
			DELIVER TO	CHECKED BY	APPR. BY

4H2383

LIST OF MATERIAL		
ITEM OR PART NUMBER	DESCRIPTION	
	½ PLATE — ALUMINUM ALLOY	

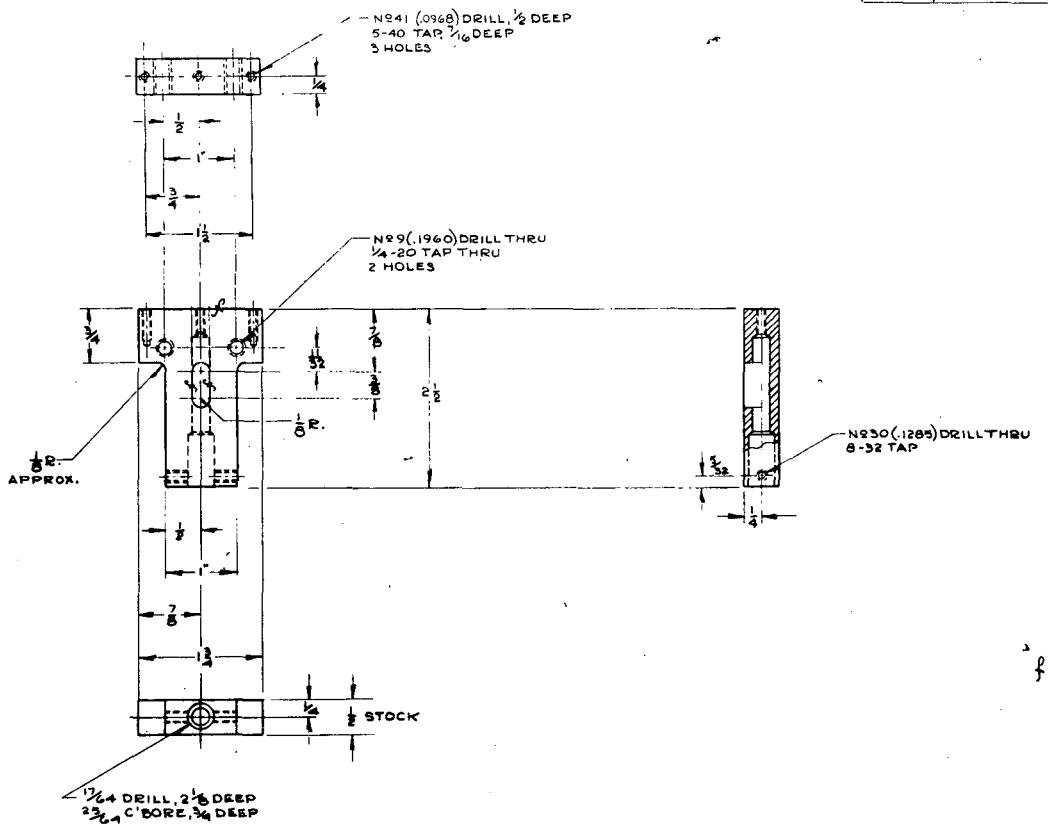

4H2323

f FINISH ALL OVER

FIG. 12

CHANGES	FINISHES	SHOP NOTES	SHOP ORDERS	DESIGN JOB NO.	184" CYCLOTRON-BREACH LOADING PROBE
	SAW CUT, FLAME CUT, SHEAR	UNLESS OTHERWISE SPECIFIED	JOB NO.	140-22	POWDER TARGET HOLDER TONGS
	ROUGH MACHINE	1. TOLERANCES ON DIMENSIONS ± .010	SERIAL NO.	SHOWN ON 4H2383	HEAD
	AVERAGE MACHINE	2. BREAK EDGES 1/64 MAX.	DATE ISSUED	SCALE FULL	RADIATION LABORATORY, UNIVERSITY OF CALIFORNIA—BERKELEY
	SMOOTH MACHINE	3. 30° CHAMFER ENDS OF ALL SCREW THREADS	DATE RECD.	DO NOT SCALE THIS DRAWING	
		4. 1½ PITCH THREAD RELIEF WITH ROUND NOSE TOOL ON MACH. CUT SCREW THREADS	NO. RECD.	DRAWN BY POMEROY DATE 7-18-49	4H2323
			DELIVER TO	CHECKED BY Al Brown APPR. BY	

SHOWN ON				JOB NO.	SER. NO.	DATE ISSUED	DATE REQ'D

NO. REQ'D	DELIVER TO	4H2371
MATERIAL	MATERIAL LIST	

ITEM Nº	DESCRIPTION	REQ'D
1	PLATE, 3/16 ST. STEEL	1
2	Nº2 TAPER PIN X 13/16 LONG-ST. ST.	2

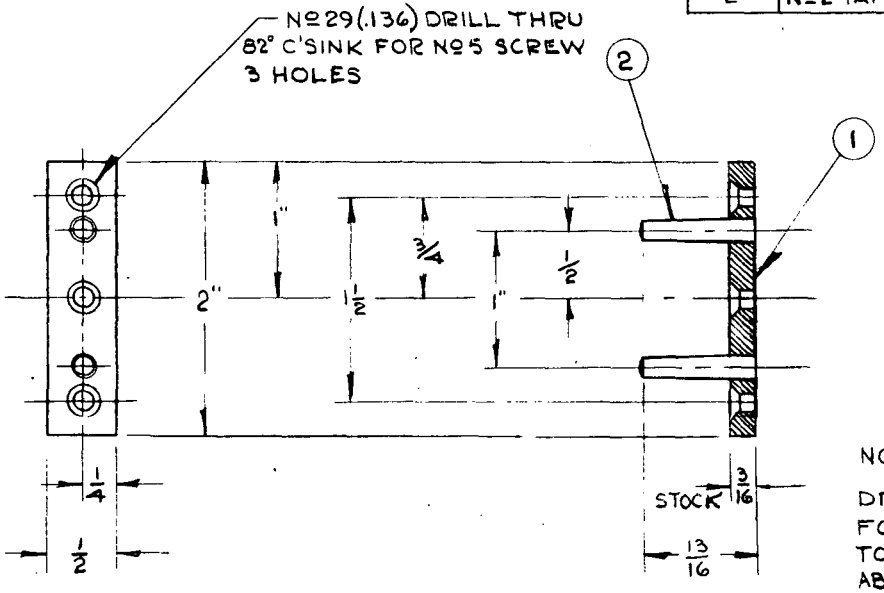

FIG. 13

NOTE:

DRILL & REAM ITEM (1) FOR TAPER PINS USING JIG TO INSURE INTERCHANGE-ABILITY OF CARTRIDGE (DWG. Nº 4H2392) CARTRIDGE & TAPER PIN PLATE TO FIT SNUGLY IN EITHER POSITION, WITH .010 TO .030 CLEARANCE BETWEEN FLAT MATING PORTIONS.

Change Letter	Drawn By	Check By	Date	CHANGES

SAW CUT, FLAME CUT, SHEAR
ROUGH MACHINE
AVERAGE MACHINE
SMOOTH MACHINE

UNLESS OTHERWISE SPECIFIED
1. TOLERANCES ON DIMENSIONS ± .010
2. BREAK EDGES 1/64 MAX.
3. 30° CHAMFER ENDS OF ALL SCREW THREADS
4. 11½ PITCH THREAD RELIEF WITH ROUND NOSE TOOL ON MACH. CUT SCREW THREADS

SCALE FULL		184" CYCLOTRON-BREECH LOADING PROBE
DESIGN JOB NO. 140-22	DATE	POWDER TARGET HOLDER TONGS
DRAWN BY POMEROY	7-18-49	BAYONET
CHECK BY W. Brown	8-2-49	RADIATION LABORATORY, UNIVERSITY OF CALIFORNIA, BERKELEY — 4H2371
APPR. BY		

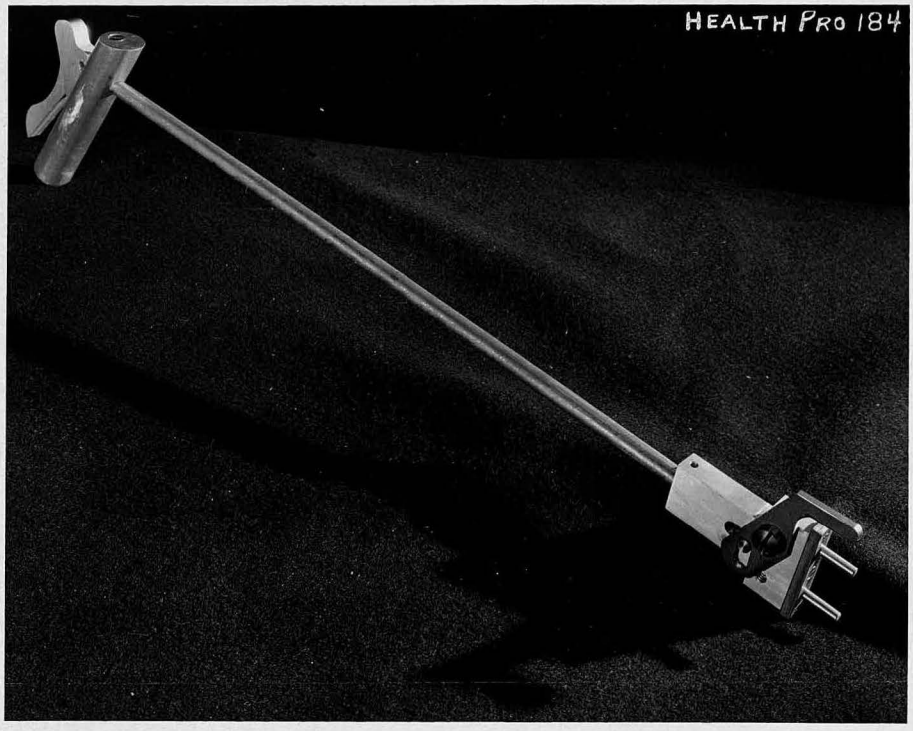

FIG. 14 POWDER TARGET HOLDER TONGS

C. Target Chemistry

Thorium targets are very active when they are removed from the internal beam of the 184-inch cyclotron. Much of this activity comes from fission products of the thorium which are present in good yield, although there is also some activity due to high yield spallation products. Hence the first steps in any chemical separation must be done very carefully to avoid overexposure to the radiation.

Our first targets were worked up in a hood in a "cave" of lead bricks. This shielding was satisfactory for most bombardments, since tongs could be used to handle especially "hot" solutions, but the radioactive spray formed on solution of the target presented a constant problem. The hood of course did a good job in keeping the majority of this spray under control but there was always the possibility of some of the spray getting out into the room.

Consequently the Health Chemistry Group designed and built a lead shielded "Berkeley Box" in which solution, etc., can be done in an enclosed box shielded with one inch of lead. Pictures of the box are shown in Figs. 15 and 16, while a view through the three-inch lead glass window is shown in Fig. 17. It is still necessary that all manipulation be done manually (since the center tong pictured was quite useless) but small tongs and lead bricks can be used inside the box to cut down radiation on the hands. Complete chemical processes from solution through precipitations and solvent extractions can be done in these boxes. These boxes are ideal for the first few steps in the chemical procedure for cyclotron targets where the desired product is separated from the bulk of extraneous activity. In these first processes the time consumed inside a box or outside a box is about the same and of course the added protection weights the scale heavily in favor of box work. Once the contaminating activity is reduced to a reasonable level, however, the chemistry is speeded up if the remainder of the work is done in an open hood. These remarks of course apply to our bombardments of thorium where the gross target activity

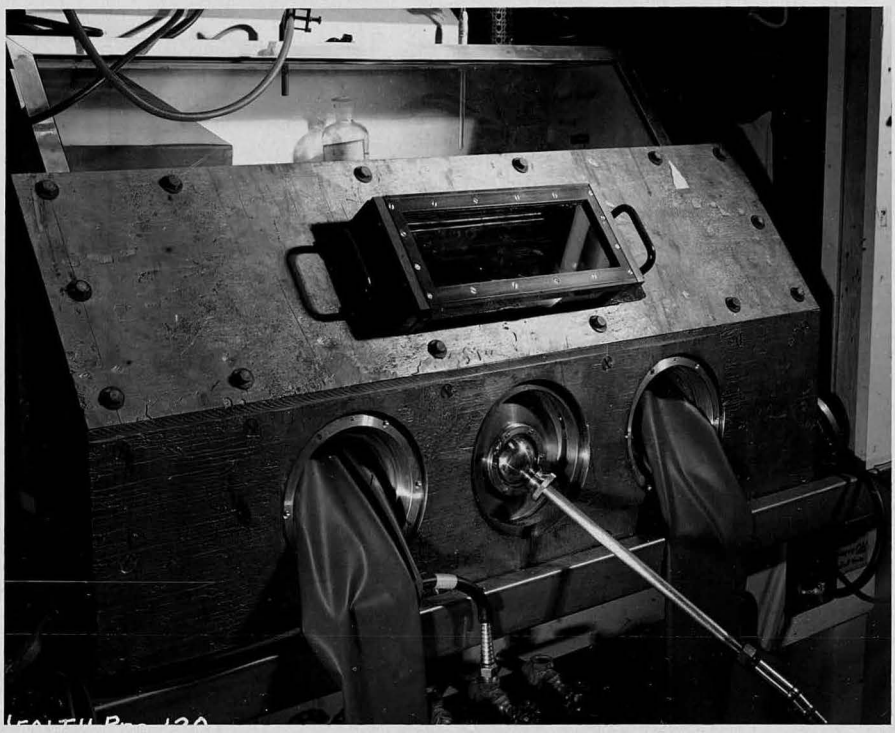

FIG. 15 LEAD SHIELDED BERKELEY BOX

FIG. 16 LEAD SHIELDED BERKELEY BOX

FIG. 17 VIEW THROUGH 3 INCH LEAD GLASS AND LEAD SHIELDED BERKELEY BOX

was many hundred times greater than the activity of any one isotope we were seeking.

Since we were seeking protactinium half-lives varying from a day to minutes, the chemistry required varied from bombardment to bombardment. We found that for bombardments in which we wanted Pa^{227} or Pa^{226} a single extraction with a solution of trifluorothenoylacetone (TTA)[16] in benzene was sufficient to separate these isotopes from all other alpha emitters. Admittedly zirconium and hafnium and probably columbium fission products are also extracted but these are all Geiger activities and do not affect the alpha counting. For protactinium samples that had to be followed for more than six hours however it was necessary for good resolution in pulse analyses, to separate the protactinium from these Geiger activities by di-isopropyl ketone extraction.

In general the chemistry for short half-life targets (see Appendix II, Procedure 91-2) involves solution of the thorium metal in concentrated nitric acid to which a few drops of 0.2 M ammonium fluosilicate has been added to speed up the solution (see Appendix II, Procedure 90-4). This solution is diluted to about 4 N acid and extracted with an equal volume of TTA-benzene solution. The phases are separated and aliquots of the organic layer are plated out on platinum.

For longer half-life targets the more complicated procedure given in Appendix II, Procedure 91-1 was used. This procedure involved precipitation of the protactinium on MnO_2, solution of this precipitate with hydroxylamine and further precipitation on MnO_2 if needed to reduce the volume, di-isopropyl ketone extraction of the protactinium from acid solution, washing to separate small amounts of fission products which might have come through, and finally TTA-benzene extraction of the protactinium and plating of this organic layer to give weightless plates. The MnO_2 precipitations insure that the protactinium is absolutely pure radioactively from all other activities. For the characterization of the Pa^{228} series however it was

only
necessary/to eliminate the zirconium and columbium fission products by di-isopropyl ketone extraction which when combined with the TTA-benzene extraction provided enough purity for alpha counting. For Geiger counting of protactinium isotopes the entire procedure as listed above must be used.

For uranium alpha emitters, the procedure used by Newton[17] involving ether extraction of the uranium from 10 N ammonium nitrate solutions was used. Crane's procedure (see Appendix II, Procedure 92-1) would be necessary for absolute Geiger purity, but it was found satisfactory for our experiments to just ether extract and wash the ether with several portions of saturated ammonium nitrate solutions before finally washing into water and plating.

When the jiffy probe and thorium nitrate targets are used to speed up the chemistry the salt is dissolved directly in a mixture of the extracting medium and the organic extracting agent, allowing the stirring for solution to also serve as the stirring for extraction.

D. Milking of Daughter Activities

Once the parent of the chains has been isolated chemically the daughter members rapidly grow into equilibrium with it and all of the activities decay with the half-life of the parent. These daughter activities can, however, be studied separately by removing them in some manner from the parent activity (i.e. milking).

This separation from the parent can be accomplished chemically or by some physical means which exploits the peculiar properties of different elements or of alpha emission in general.

1. Chemical Milkings A very satisfactory method of separating the daughters -- if the half-life of the daughters is long enough to permit such work-- is by making actual chemical separations. Wherever possible in our work we have chemically separated the daughters to definitely prove their atomic number.

Protactinium daughters of uranium isotopes have been separated by the same TTA-benzene extractions used for separations from target materials.

Tracer thorium was separated by zirconium phosphate precipitations which are quite specific for carrying Th^{+4} from other elements in the heavy region. Since this phosphate precipitate was much too bulky to pulse analyse, it was metathesized first to the fluoride (using lanthanum as carrier for the thorium) and then to the lanthanum hydroxide which was finally dissolved in hydrochloric acid and plated as lanthanum chloride (see Appendix II, Procedure 90-3).

Actinium was separated by lanthanum fluoride-hydroxide precipitation cycles (from a solution containing barium as a holdback for radium), along with zirconium phosphate scavenges to remove the thorium (a modification of Procedure 89-2, Appendix II).

Bismuth can be separated by precipitations of lead sulfide, the precipitate being dissolved in hot concentrated hydrochloric acid and then reprecipitated. The lead is finally separated from the bismuth by sulfate precipitations (see Appendix II, Procedure 83-3).

2. Milkings by Flaming Several elements in the heavy region are volatile when flamed. Hence in our work it was possible to rid the sample of emanation isotopes (and if these isotopes had had a reasonable half-life it would have been possible to collect them as described in Procedure 86-1, Appendix II) by merely heating the platinum plate in a flame. Francium also can be at least partially flamed off a plate since the -1 state appears to disproportionate into the metal and a higher state. The metal sublimes off the plate, the higher state decomposing back into the -1 state and the process repeating itself. Certain states of astatine can also be flamed off plates and when collected may even appear to act like a gas.

In none of our studies did we collect the above elements directly after flaming. We looked instead for the indrect effect of growth of the remaining sample with a given half-life, as the isotope that had been flamed off grew back into equilibrium with the parent.

3. Recoil Milkings A third and very powerful method of separating daughters from the parent activities[18] takes advantage of the recoil imparted to an isotope by the emission of an alpha-particle. If an electric field is imposed between a sample plate and another plate, these recoil daughter atoms will be collected on the negative plate. On this collector plate then there can be none of the first members of the series present on the original plate although there may be varying amounts of subsequent members of the series. Similarly if a double recoil transfer is made, collecting a recoil fraction from the first recoil plate, neither the first nor second members of the series can be present. This procedure can be extended to triple recoils, etc., if enough activity is available initially. One should remember that if the half-life of an intermediate isotope in the series is very short (seconds or less) it will decay immediately into the next series member. The yield of this recoil collection is of course not 100% but more like 10%. If enough activity is available, however, this procedure is very useful in establishing half-lives and mass assignments.

An adaption of this method developed by A. Ghiorso has made possible half-life determinations ranging from 30 seconds to about 20 milliseconds. Basically, the apparatus consists of a 13-inch diameter rotating metal disc which is wired electrically to act as the collector for recoil fragments, a sample holder which positions the sample face down over the outer rim of the disc, and an alpha counting chamber which can be positioned along the outer rim of the disc. The disc is rotated at a known speed, under the parent sample. Recoiling daughter activities are collected along the rim of the disc and are counted by the slit window of the alpha chamber. By positioning the chamber at different degrees of arc from the source, counts of different intensities are registered. By plotting the activity at a certain angle against that angle, we obtain a logarithmic decay curve from which the half-life can be calculated.

A much more flexible modification of this apparatus has been designed and is being built. It will have three counting chambers which can be moved along the periphery of the disc. When these three chambers are correctly positioned, a half-life can be obtained from only one run. This will be an important consideration since short-lived parents like the Pa^{226}, U^{227}, and U^{228} series decay too much during a set of runs to obtain much useful data with the old set-up. Even with the longer-lived series, the background on the turntable builds up very rapidly and at the end of four runs this background makes the values quite uncertain.

A further application of the recoil principle can be made with any alpha counting chamber. A very active sample is inserted into a regular alpha chamber and allowed to remain until its daughters are in equilibrium with the chamber. Some of the recoil fragments collect on the chamber and, if the original source is removed rapidly, the decay of these recoil fragments can be followed. This method can also be applied to the pulse analyzer and will be described later.

E. Alpha Counting

In these collateral chain experiments alpha particles were counted in an ordinary argon ionization chamber. The pulses were fed into an amplifier and registered through a scale of 512 counting circuit. Counting losses through coincidence for this counting set-up appear to be negligible even at fairly high counting rates.

To minimize manual counting over long periods of time, we used a recording "trafficounter". This was so arranged that the alpha or Geiger scaling circuit could actuate the counting mechanism to register the counts from a sample. Furthermore the stamping times were variable and could be set from intervals as short as 0.05 minutes to 64 minutes. This mechanism made possible many of our medium short half-life determinations and also freed us from routine counting of a single sample.

In this work we were primarily interested in alpha emitters. When Geiger counting was required, however, the equipment described in Chapter 2 was used.

F. Alpha-Pulse Analysis

A few scattered pieces of our data were obtained from alpha and Geiger counting but most of our results were made possible by the 48-channel, differential alpha-pulse analyzer.[12] Furthermore, the part of the pulse analyzer which made it possible to obtain so much data in a short amount of time was the fast sample-changing mechanism designed by A. Ghiorso and shown in Fig. 18. With this mechanism, samples were introduced first into a small air lock (shown with a circular cap in the front of the picture)which could be evacuated and filled with the counting gas mixture without disturbing the main counting volume of the gas mixture. This small lock reduced the time required for insertion of a sample into the chamber and counting it. In addition it was possible to leave the top of the lock open when extra speed was required and merely to rely on the flow of counting gas out of the chamber to displace the air from the sample. The resolution of the instrument was understandably poorer in the latter case but was sufficient for some experiments.

Samples were placed on a turn table which could be turned manually from beneath. With the lock open, the table is free to turn to any position. When closed, however, the lock is sealed against the table, keeping the bulk of the chamber at the required gas pressure while the lock can be at air, vacuum, or pressure.

The pulse analyzer itself has 48 electronic channels, each of which counts all alpha pulses within a certain energy range. Since these ranges are continuous, when a plot is made of number of counts per channel against channel number a picture is obtained of the alpha spectrum between two particular predetermined energy values. Such a picture for the U^{230} series is shown in Fig. 19, where the energy scale is indicated and the different isotopes in the series are shown with their alpha energies.

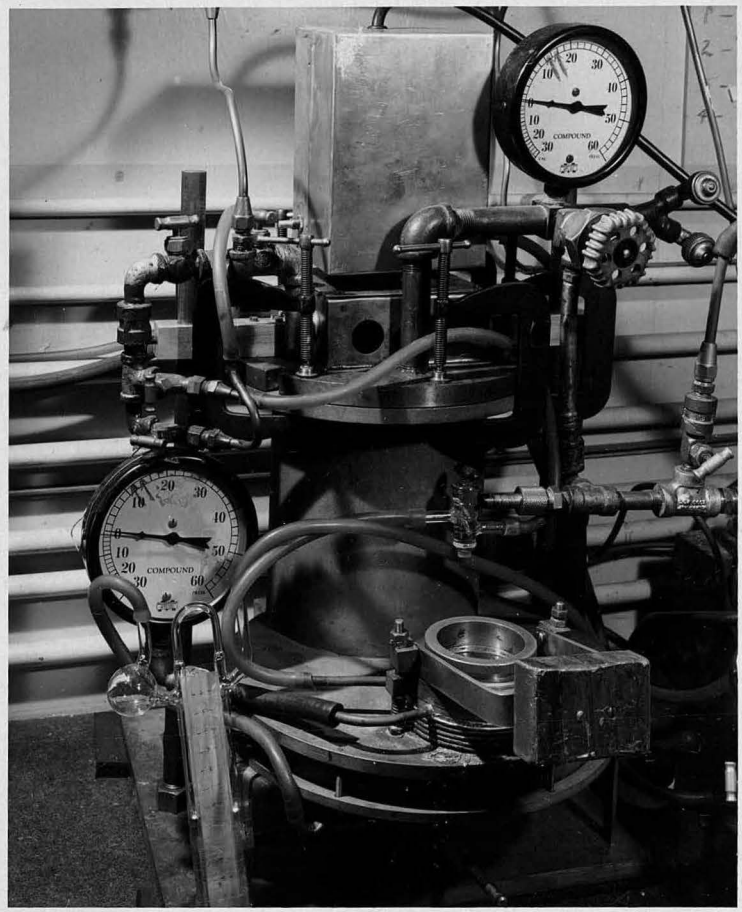

FIG. 18 ALPHA-PARTICLE PULSE ANALYSER CHAMBER WITH FAST SAMPLE-CHANGING MECHANISM.

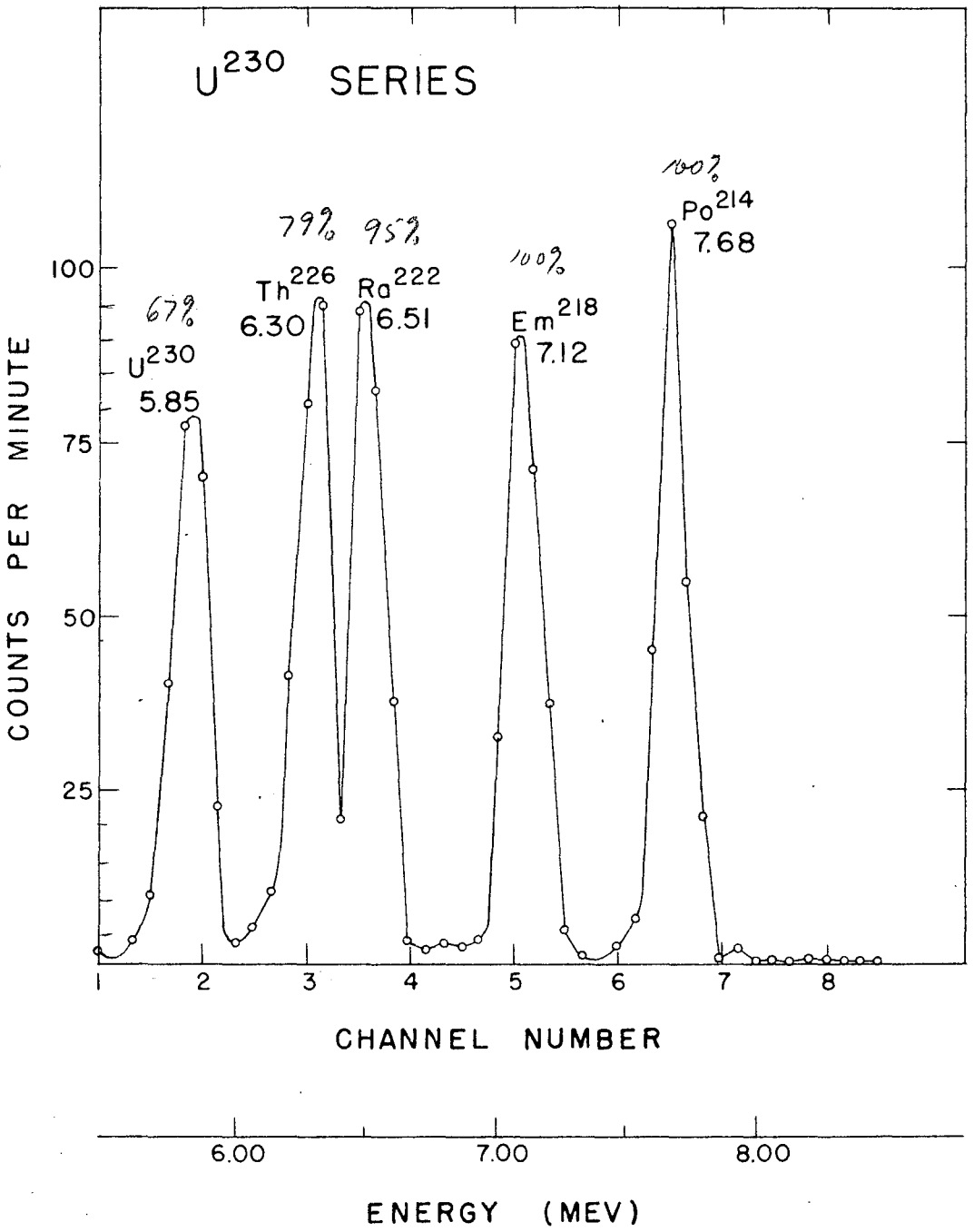

Fig. 19. Alpha-pulse analysis curve of the U^{230} series. A #3 collimator with a thin Zapon coating covered the sample.

The energy limits of the 48 channels can be varied electronically to give either a general picture of a wide energy region or a more detailed picture of some of the fine points of the spectrum.

The pulse analyzer was used to sort out the different series since by checking the decay of certain peaks we were able to determine half-lives of the isotopes. Furthermore, pulse analysis furnished a check on our chemistry since it indicated whether there were any alpha emitting isotopes present besides those of the element separated and its daughters.

All the energies of the alpha emitting isotopes of the collateral chains were determined by alpha pulse analyses, standardization of the instrument being made by calibration against natural radioactive series, the energies of which have been determined very accurately with a magnetic alpha-ray spectrograph. The alpha energies reported for the chains probably have a maximum error of $\pm$ 50 Kev and a minimum error of $\pm$ 10 Kev, depending upon the ease of resolution of the alpha peaks. All energies given in this report are particle energies and not disintegration energies — i.e., the energy carried off by recoil of the atom has not been added.

Collimation was usually required for pulse analysis of samples of these collateral chains to prevent loss of counts from long range alpha particles of very short half-life. The collimators used were sieve-like discs of brass with about one-sixteenth-inch diameter holes and the following thicknesses: #1 = $\sim$ 12 mils, #2 = $\sim$ 22.5 mils, #3 = $\sim$ 33 mils. This collimator is placed over the sample in the chamber, preventing counting of any alpha particles except those coming up through the holes of the collimator. This then insures that parent and daughter alphas will not be counted in coincidence as one very high energy alpha pulse and hence be registered as a coincidence loss. Most of the pulse analysis diagrams included in this chapter were taken with collimation. This collimation reduces the geometry of counting to about 10%.

One unusual effect observed in counting well-collimated samples was that the first peak of a series was definitely lower than the rest. The explanation apparently was that atoms were being recoiled through the collimator into the chamber proper and hence had a higher geometry for subsequent disintegrations of the daughter activities. A thin coating of Zapon over the collimator corrected this.

A few limitations of pulse analysis should be mentioned here. Since thin, almost weightless plates of samples are required it is almost mandatory that carrier-free chemistry be done. Thick samples cause poor resolution of the alpha peaks and often make identification of mixtures of peaks impossible. There is a limit to the amount of Geiger activity that can be tolerated before resolution of the alpha peaks is affected. The resolution becomes poor whenever the Geiger activity reaches the level of from 10^5 - 10^6 counts per minute of soft electrons. The tolerance for hard beta particles is higher. In our bombardments additional chemistry could always separate the protactinium from this excess Geiger contamination.

A modification of recoil techniques mentioned previously is applicable here. The parent plate is suspended face down in the lock over the catcher plate which rests on the turntable. The lock is evacuated, allowing recoil atoms from the upper plate to be collected on the catcher plate. By bringing the lock up to counting gas pressure, opening it, and rotating the turntable, the recoil plate can be pulse analyzed a few seconds after the end of the collection period.

G. Very Short Half-Life Determinations

We have mentioned previously that the rotating disc method could be applied to determinations of half-lives down to about 20 milliseconds. Below this, however, some electronic measuring set-up is required. Studier and Hyde[8] mention a simple electronic device used in their measurement of the 0.019 second Em^{218} half-life. Our requirements were much more stringent than theirs, however, since we expected half-lives from the millisecond range down to half a microsecond. In addition, we

would have to distinguish between members of several series.

An apparatus which we hoped would meet our requirements was designed and built by R. Dorr and A. Ghiorso. The time scale of this apparatus was divided up electronically into three equal segments with a counting dial for each segment. An alpha pulse would trigger the circuit and if another pulse followed within the first segment of time it was recorded on the first dial; the second segment, the second dial, etc. The apparatus was so designed that it could only trigger the circuit for a certain segment of the pulse analyzer spectrum and record only when pulses occurred in another segment of the spectrum. In other words it could be set to trigger on one peak of a series and record on another. The time scale of the apparatus could be varied and when set so that the second interval had half the counts of the first etc., indicated the half-life of the parent. Background correction of course had to be made for random counts which were not related as parent-daughter. A few preliminary values have been obtained with this apparatus but their accuracy can definitely be improved.

IV. Experimental Results

This section lists the results of our experiments with the collateral series and briefly describes the means by which we obtained our values. Half-life and energy values in parentheses in the tables have been estimated from alpha systematics curves of alpha energy versus half-life for the same kind of nuclei (i.e., even-even, even-odd, etc.). (See Figs. 54-57 at end of Chapter.)

A. The Pa^{226} Series

This series, along with the U^{230} series, constitutes a collateral branch of the uranium or 4n + 1 family. Fig. 20 shows a block diagram of this family. Since this series is always found with considerable Pa^{227} series present, it has been hard to obtain good, definitive, pulse analyses. Fig. 21 presents our best pulse analysis to date, the other peaks being isotopes of the Pa^{227} series showing through.

ARTIFICIAL COLLATERAL RADIOACTIVE SERIES

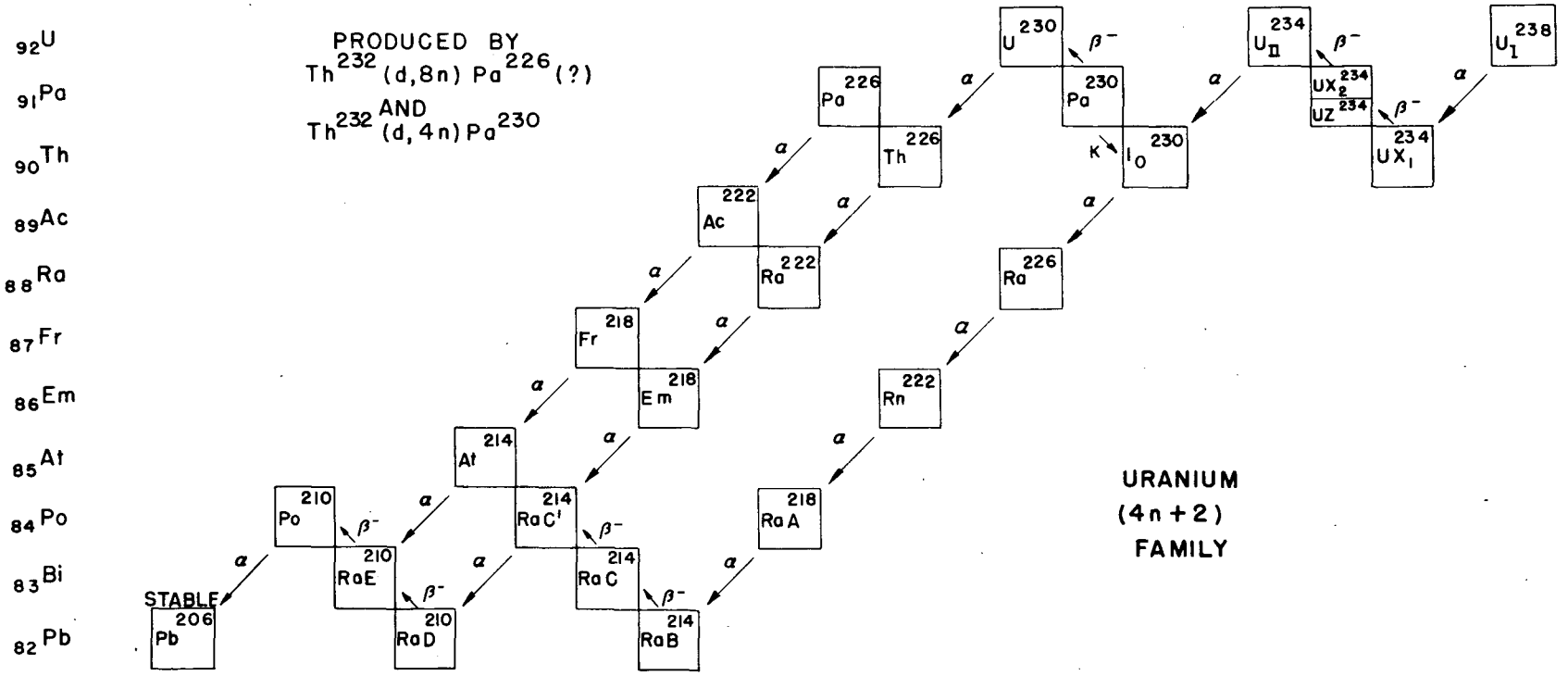

FIG. 20

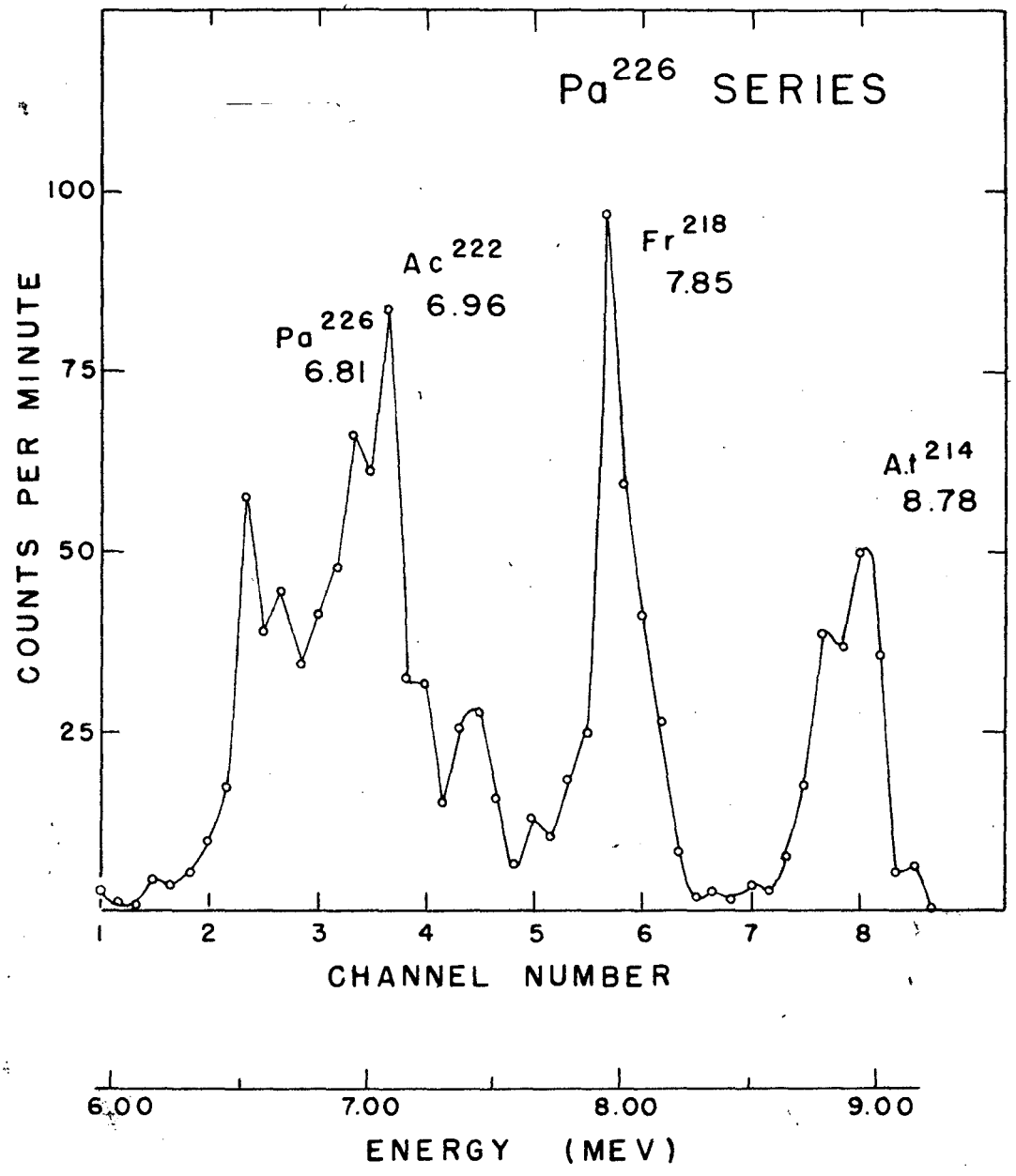

Fig. 21. Alpha-pulse analysis curve of the Pa^{226} series from a 1.5 minute bombardment of thorium nitrate in the jiffy probe with 150-Mev deuterons. This curve represents a 0.5 minute count of the protactinium fraction and was started 3.3 minutes after shutdown. Contamination is from the Pa^{227} series alphas. A #3 collimator was used.

In the matter of about 10 minutes all evidences of Pa^{226} decayed out of the sample leaving a pure sample of Pa^{227} as shown by Fig. 22. If the Pa^{227} series alpha groups are extrapolated back to the time of the first pulse analysis (which incidentally was 3.3 minutes after shutdown), and these values subtracted from the curve in Fig. 21, a new curve showing alphas due only to Pa^{226} series is obtained (Fig. 23).

A summary of data for this series is presented in Table 1. The radioactive properties of RaE and Po^{210} are the accepted values taken from the literature.[7]

Table 1

Pa^{226} Collateral Series Data

Isotope	Type of Radiation	Half-Life	Energy of Radiation (Mev)
Pa^{226}	α	1.78 ± 0.15 min.	6.81
Ac^{222}	α	(pred 30 sec)	6.96
Fr^{218}	α	(pred 5×10^{-3} sec)	7.85
At^{214}	α	(pred 2×10^{-6} sec)	8.78
Bi^{210}(RaE)	β^-	5.0 days	1.17
Po^{210}	α	140 days	5.298
Pb^{206}	Stable		

1. Pa^{226} Our early experiments assigned the 38.3 minute protactinium isotope (now assigned to Pa^{227}) to this isotope, since we thought we found a few counts of Po^{210} in a bismuth fraction chemically milked from the protactinium isotope. The polonium proved to be contamination however, and other milking experiments indicated the correct assignment for the 38.3 minute isotope. Apparently then Pa^{226} had a considerably shorter half-life than 38 minutes.

Our shortest time for chemically separating a protactinium fraction from a thorium metal target bombarded on the regular probe with the internal beam was

Fig. 22. Alpha-pulse analysis curves showing the decay of the Pa^{226} series, leaving the Pa^{227} series. Pulse analysis made on the protactinium fraction of a 1.5 minute bombardment of thorium nitrate in the jiffy probe with 150 Mev deuterons. The counts indicated were for 0.5 minute intervals and were started at the following times after shutdown:

A: 3.3 minutes

B: 6.0 minutes

C: 10.5 minutes

A #3 collimator was used.

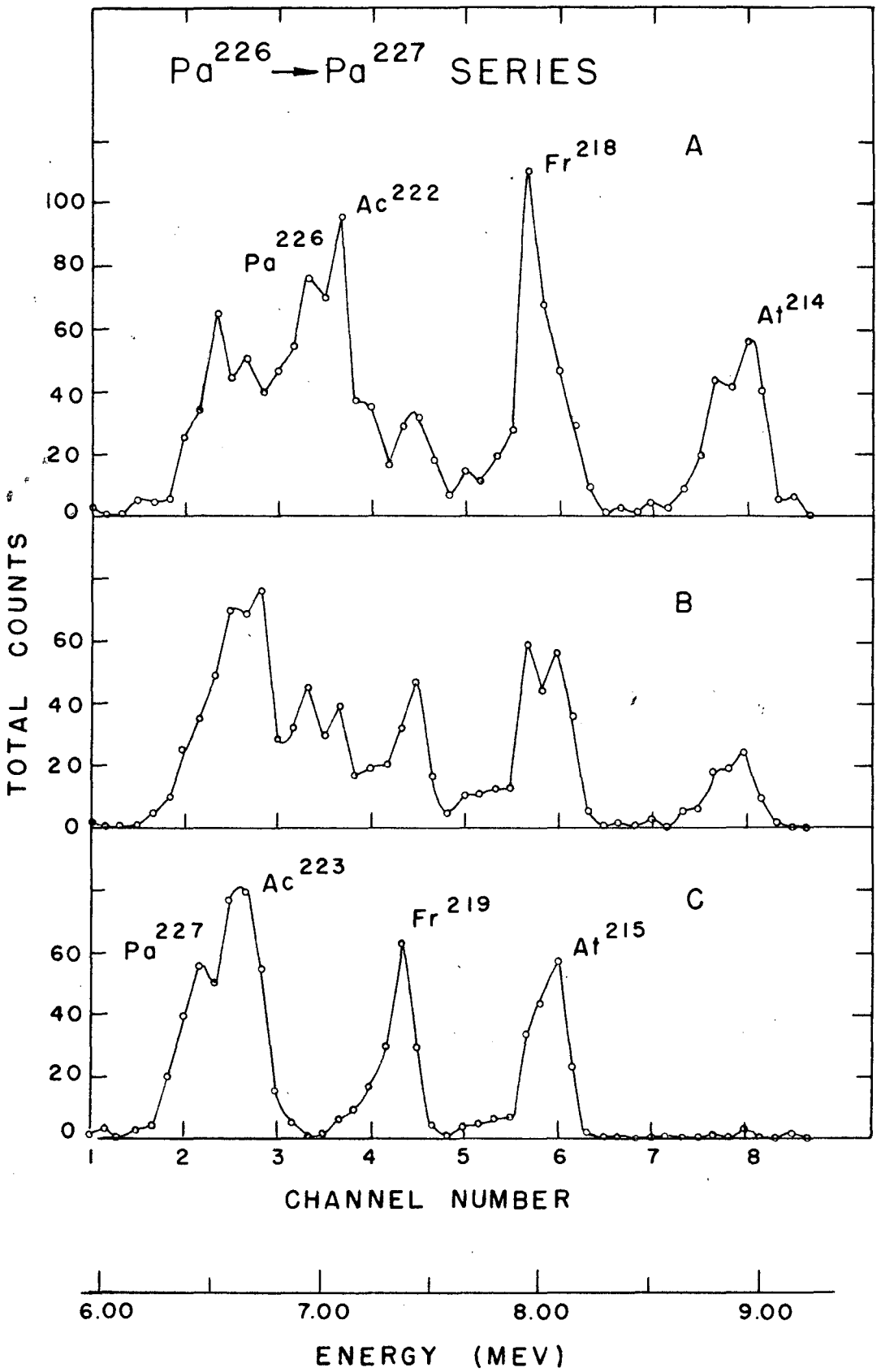
Pa226 → Pa227 SERIES
A
B
C
Pa226
Ac222
Fr218
At214
Pa227
Ac223
Fr219
At215
TOTAL COUNTS
CHANNEL NUMBER
ENERGY (MEV)
6.00
7.00
8.00
9.00

Fig 22

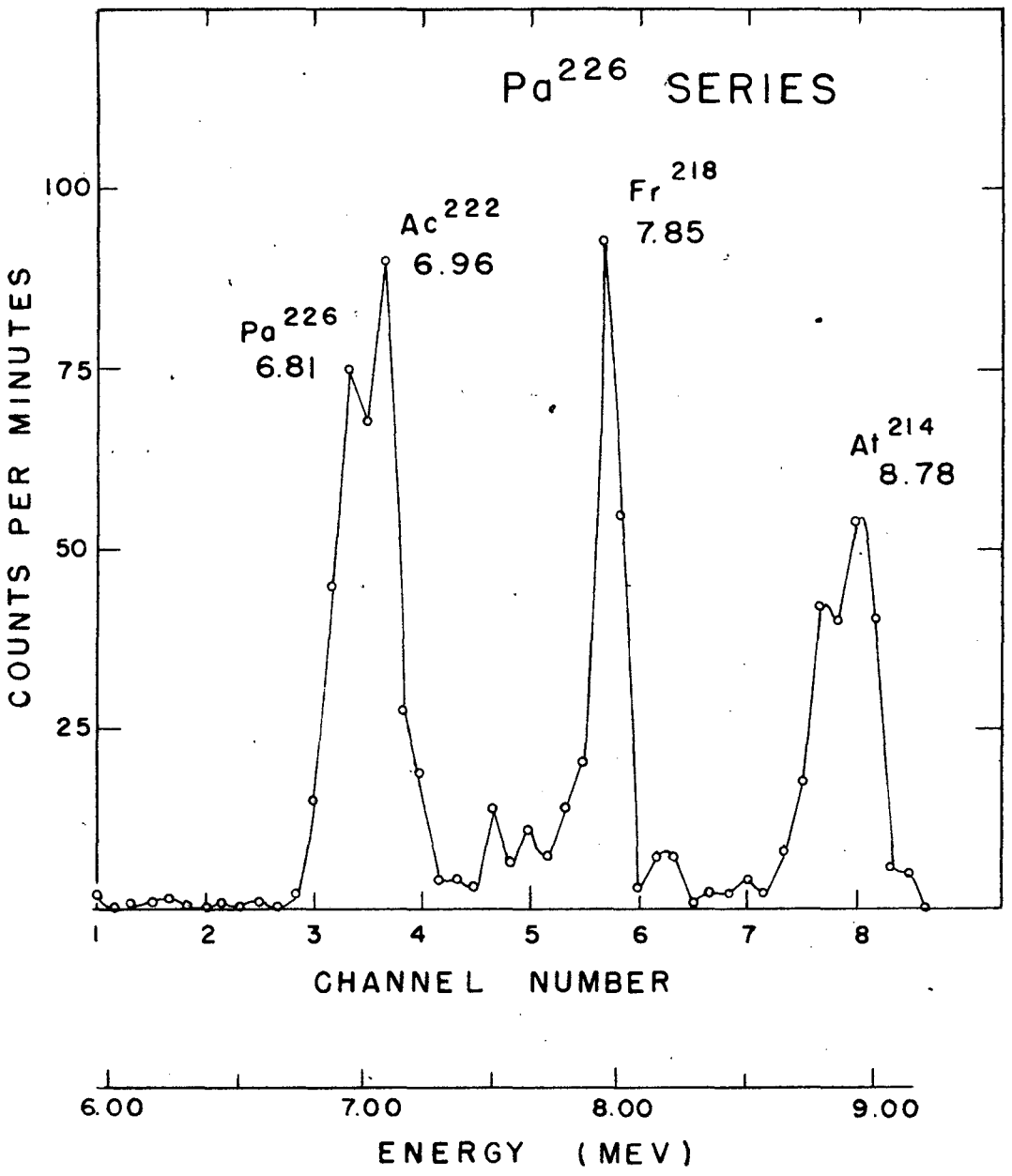

Fig. 23. Resolved alpha-pulse analysis curve of the Pa^{226} series from which the Pa^{227} series peaks shown in Fig. 21 have been subtracted.

16 minutes from shutdown to counter. This however was relatively slow and the only activity found was Pa^{227} and daughters.

We next tried bombarding one mil thorium metal foil in the jiffy probe set-up with full energy deuterons and after many bombardments were able to establish the existence of a short-lived protactinium series that decayed out in a few minutes. However the best chemistry time was six minutes from shutdown to counter and always at the first count the Pa^{227} activity was overwhelming.

We even tried bombarding a saturated solution of thorium nitrate in the external deuteron beam of the cyclotron. This did speed up the separation time by a minute or so but the beam proved too weak to give much Pa^{227} activity, let alone Pa^{226}.

Finally the jiffy probe "rabbit" was modified so that powders could be bombarded in it and we tried bombarding thorium nitrate with deuterons. Several bombardments at full energy indicated that we had shortened our time from shutdown to counting to about 4.5 minutes but the yields were still low and the ratio of Pa^{227}/Pa^{226} was still unfavorable.

Several months elapsed before any more bombardments for this isotope were made and in the meantime we began to understand a little more about the excitation function of the (d,xn) reactions (see Chapter 2) -- although we still did not realize that the peak yield of their excitation function rises a factor of 20 above the yield at full energy.

Thorium nitrate in the jiffy probe was bombarded with 150-Mev deuterons in our subsequent work on this isotope. Two bombardments were sufficient to give us the pulse analyses shown above, with our chemistry time cut down to 3.3 minutes from shutdown to the beginning of pulse analysis. By following the decay of the longest range alpha peak (assumed to be At^{214} from systematics) we obtained a half-life of 1.78 ± 0.15 minutes for the Pa^{226} (Fig. 24). In this 1.5 minute bombardment

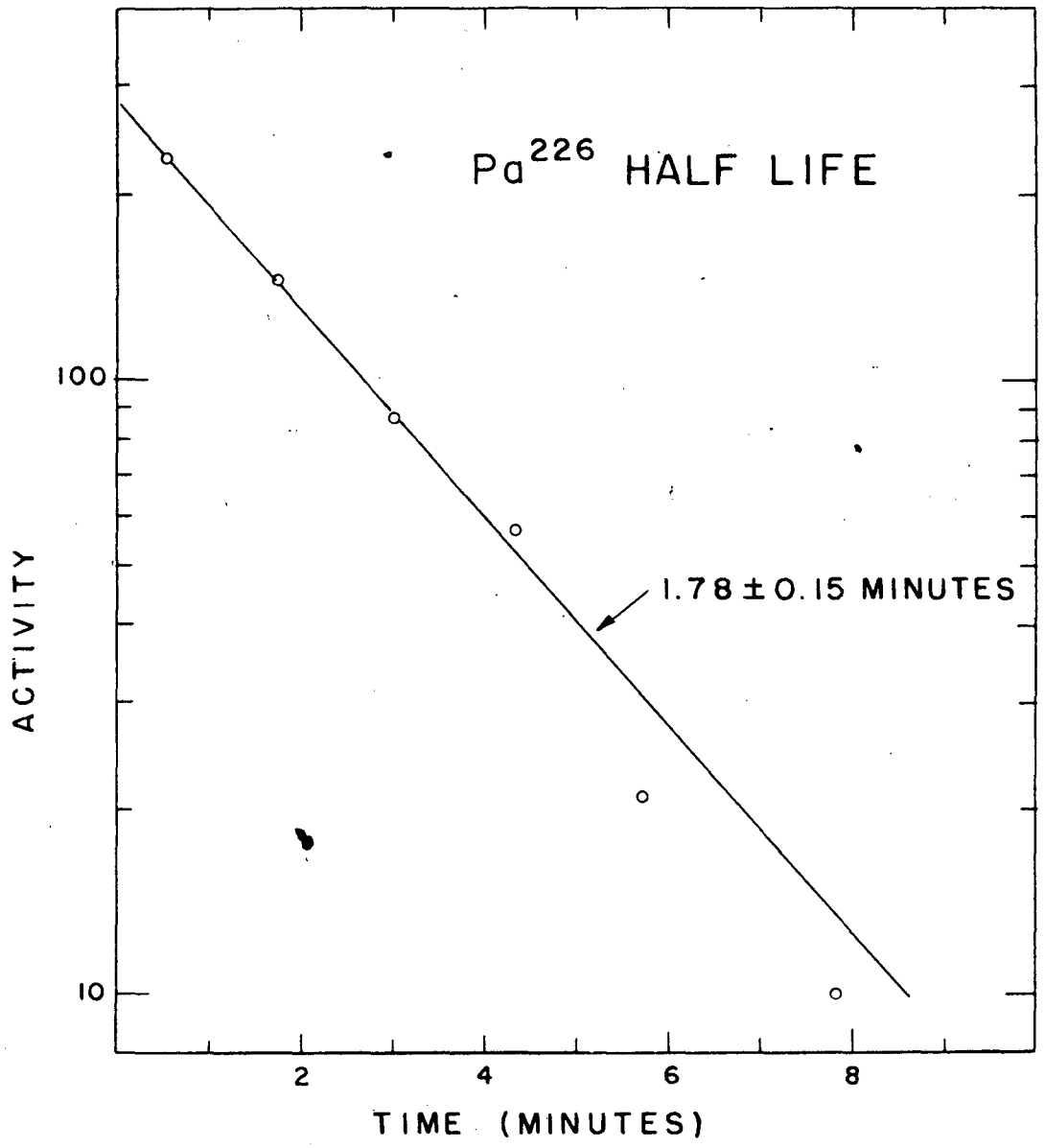

Fig. 24. Determination of the Pa^{226} half-life from the decay of the At^{214} peak in the series of pulse analyses shown in part in Fig. 22.

of thorium nitrate in the jiffy probe we obtained about 10^6 alpha counts per minute of the Pa^{226}, extrapolated to shutdown.

Since in the pulse analysis we were unable to detect any alpha peaks of Th^{226} and daughters along with the Pa^{227}, once the Pa^{226} had decayed out, we can set a limit of ≤ 1 for the K/α branching ratio of Pa^{226}.

2. Other Members of the Pa^{226} Series It was not possible in the two final bombardments mentioned above to obtain any data other than the half-life of the Pa^{226} and the alpha energies of the series members. The assignment of mass numbers to these daughter isotopes was made purely on the basis of alpha energy systematics (see discussion and figures at the end of this chapter). It can be seen that these systematics are a powerful tool in assigning masses now that sufficiently good alpha data has been collected.

When the pneumatic tube-jiffy probe combination is ready for operation and can bring jiffy probe targets into the laboratory within 12 seconds, we hope to shorten our 3.3 minute chemistry by at least a minute and also be able to do many experiments in one day. We should be able to determine the half-lives of the Ac^{222} and Fr^{218} by the rotating disc recoil method and possibly the At^{214} half-life by electronics. We also hope to be able to build up enough activity to be able to milk for the Bi^{210} and Po^{210} daughters to definitely establish the mass assignment of the series.

B. The Pa^{227} Series

This series is collateral to the actinium or 4n + 3 family and is shown in the block diagram of Fig. 25. Its five alpha peaks dominate pulse analyses of protactinium fractions for from five to six hours after thorium bombardments with 80 to 125 Mev deuterons and corresponding energies of protons or alpha-particles. A pulse analysis curve of the five alpha peaks is shown in Fig. 26.

ARTIFICIAL COLLATERAL RADIOACTIVE SERIES

PRODUCED BY

$Th^{232}(d, 7n)\ Pa^{227}$

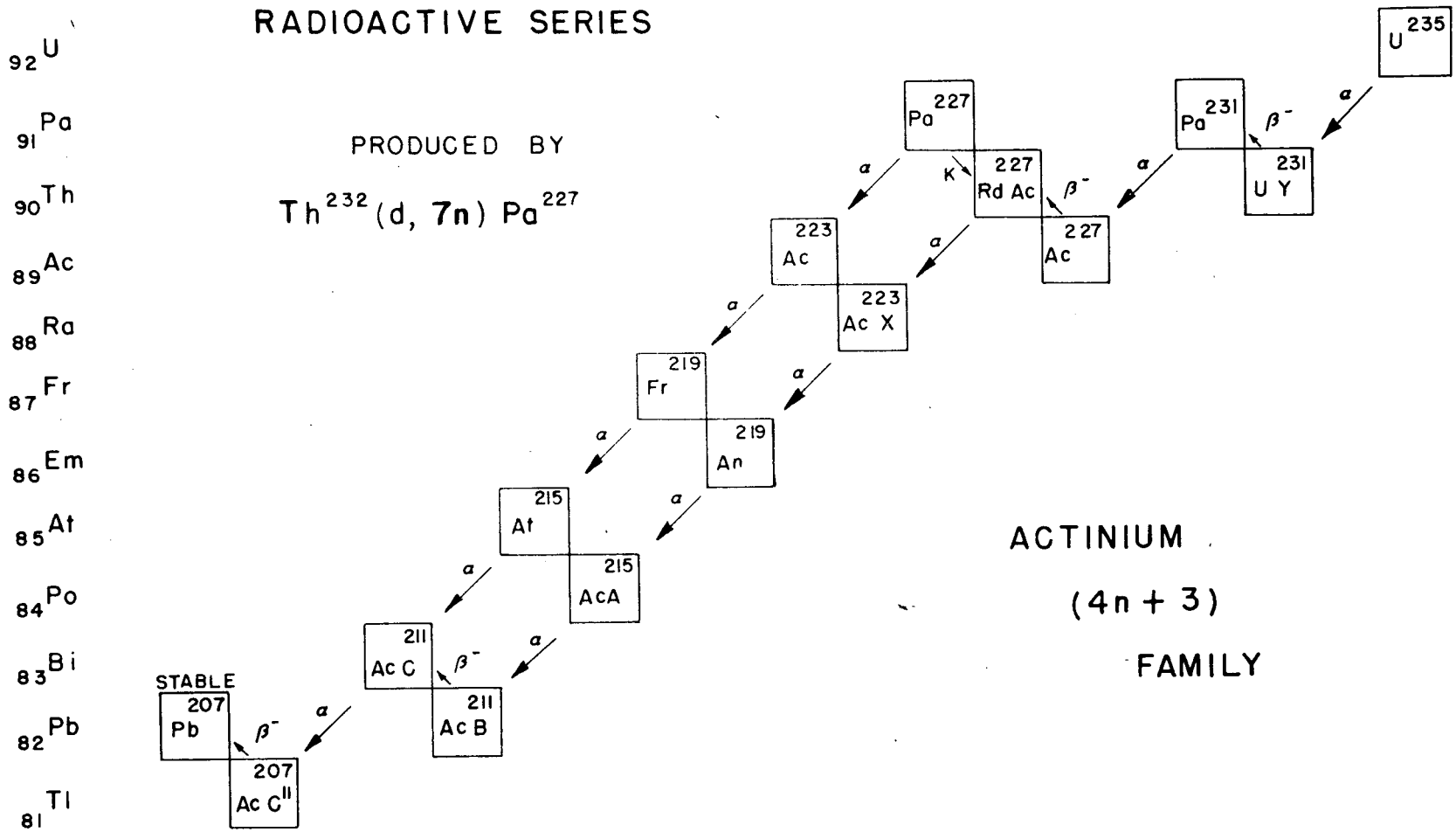

ACTINIUM

(4n + 3)

FAMILY

FIG. 25

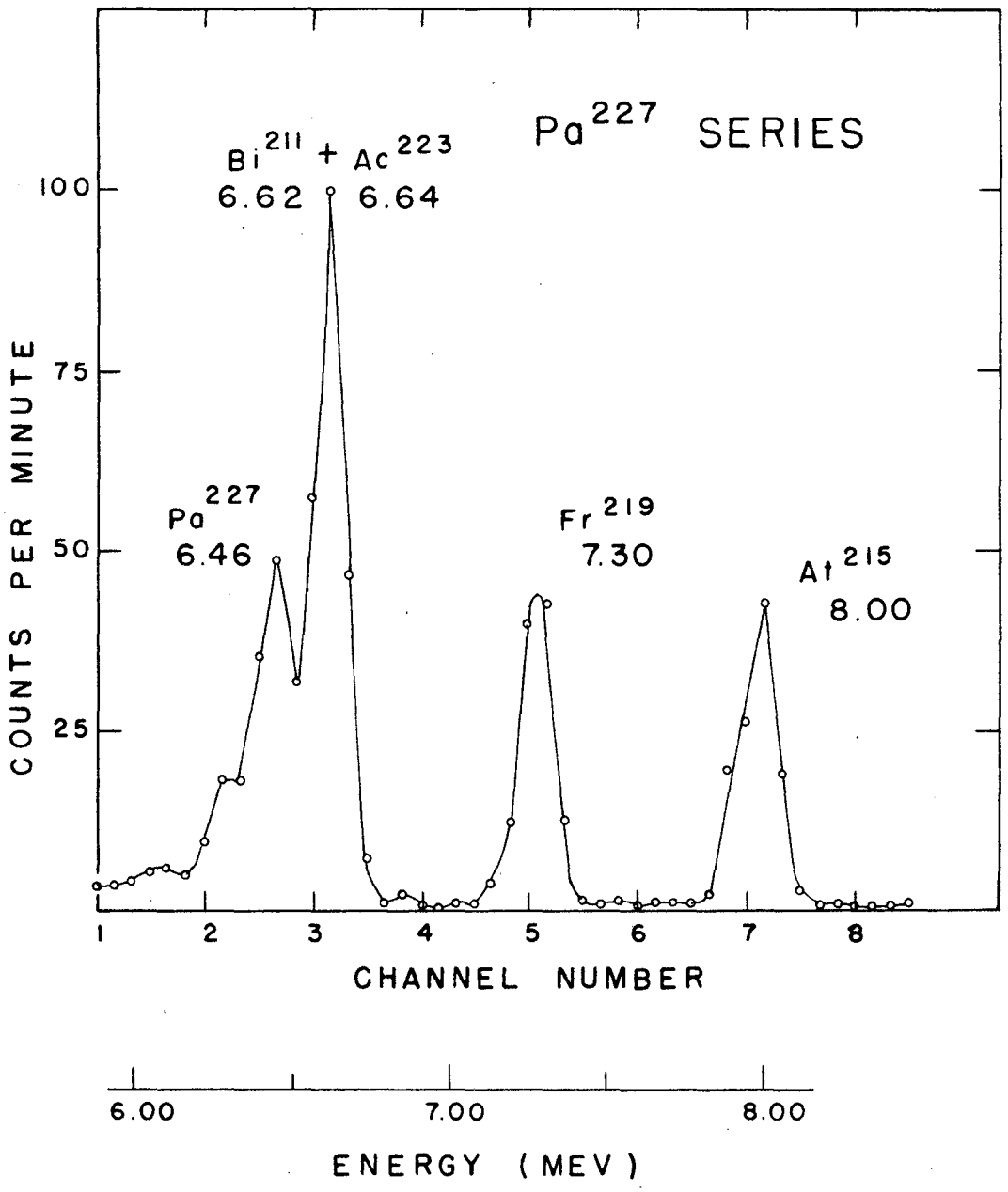

Fig. 26. Alpha-pulse analysis curve of the Pa^{227} series in the protactinium fraction from a thorium metal bombardment. A #2 collimator was used.

When we first encountered this series it looked much like the 30.9 minute Th^{226} and daughters on the pulse analysis, and since it actually decayed with a half-life of about 30 minutes this similarity was even more marked. However the fact that the first peak of this series was much higher than the other two peaks, was unexplainable if the series was considered to be Th^{226} contamination. We proved that this was a new series however by showing that thorium could not come through our chemistry. Furthermore when we pulse analyzed simultaneously a sample of U^{230} series and this other series we found that the curves did not completely superimpose (Fig. 27). These results indicate that the energies of the long range groups of each series are not identical and hence the series are different.

Further work established definitely that the series was the Pa^{227} series. About six hours after shutdown the series gives way to the Pa^{228} and Pa^{229} alpha peaks as shown in Fig. 28. Since the U^{230} series present from Pa^{230} decay is always growing in, the sample shown in part C of the figure was freshly separated from daughters before pulse analysis. Our latest data on the members of this series are presented in Table 2. The radioactive properties of AcC and AcC" are the accepted values taken from the literature.[7]

Table 2
Pa^{227} Collateral Series Data

Isotope	Type of Radiation	Half-Life	Energy of Radiation (Mev)
Pa^{227}	α (~85%) K (~15%)	38.3 ± 0.3 min.	6.46
Ac^{223}	α (99%)	2.2 ± 0.1 min.	6.64
Fr^{219}	α	0.02 sec ± 10%	7.30
At^{215}	α	10^{-4} sec ± 20%	8.00
Bi^{211} (AcC)	α (99.7%)	2.16 min	6.619
Tl^{207} (AcC")	β^-	4.76 min	1.47
Pb^{207}	Stable		

Fig. 27 Alpha-pulse analysis curves showing the results of simultaneously counting samples of pure Pa^{227} series (A) and pure U^{230} series (B) to give C.

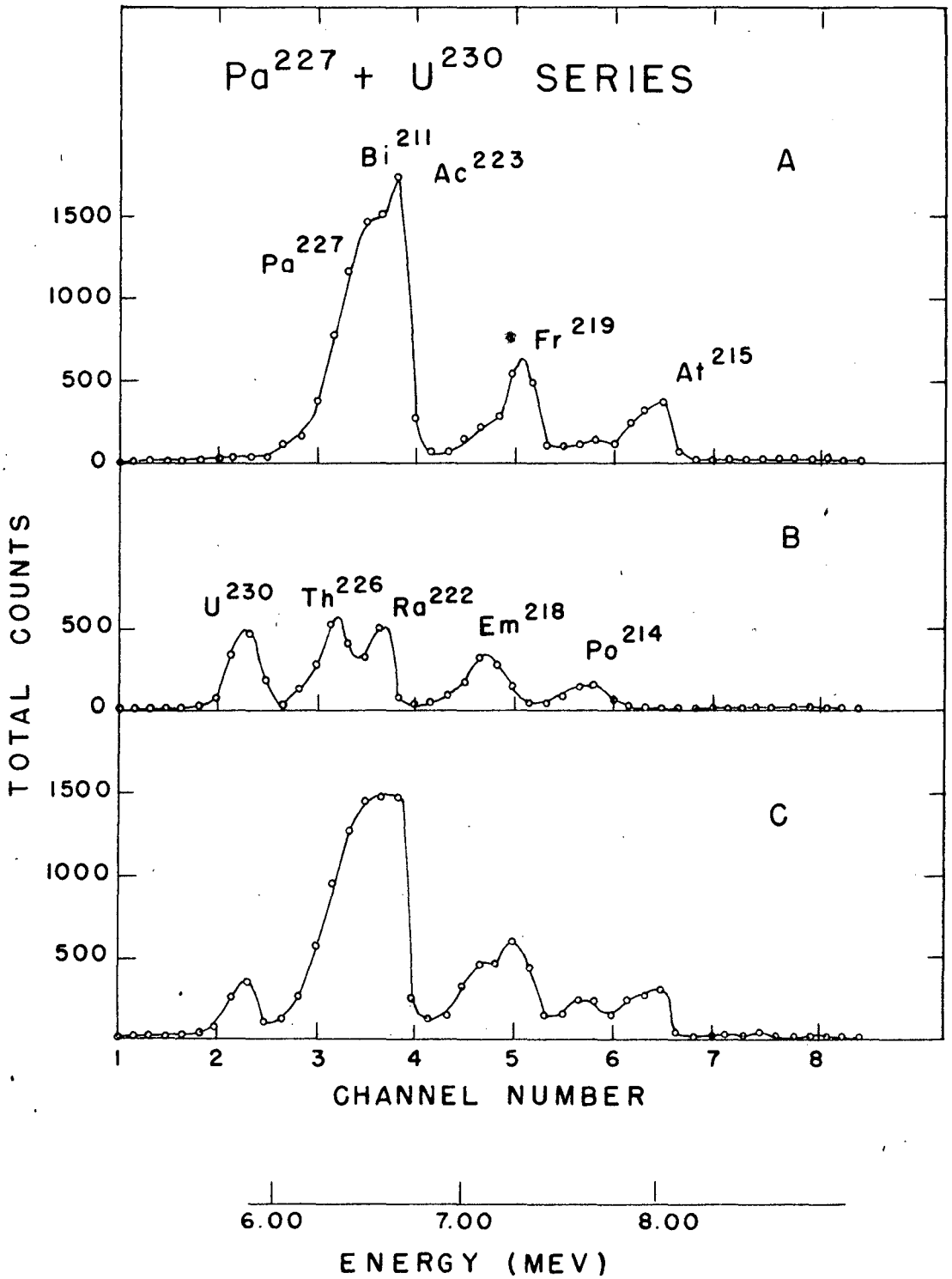
Pa227 + U230 SERIES
A
Bi211
Ac223
Pa227
Fr219
At215
1500
1000
500
0
B
U230
Th226
Ra222
Em218
Po214
500
0
C
1500
1000
500
TOTAL COUNTS
1
2
3
4
5
6
7
8
CHANNEL NUMBER
6.00
7.00
8.00
ENERGY (MEV)

Fig 11

Fig. 28. Alpha-pulse analysis curves showing the decay of the Pa^{227} series, leaving the Pa^{228} and Pa^{229} alpha groups. Pulse analysis made on the protactinium fraction of a 20-minute bombardment of thorium metal with 60-Mev deuterons. The pulse analyses were made on three different samples; A and B without collimation and C with a #3 collimator. The counts lasted about eight minutes and started at the following times after shutdown:

A: 1 hour

B: 7 hours

C: 9 hours

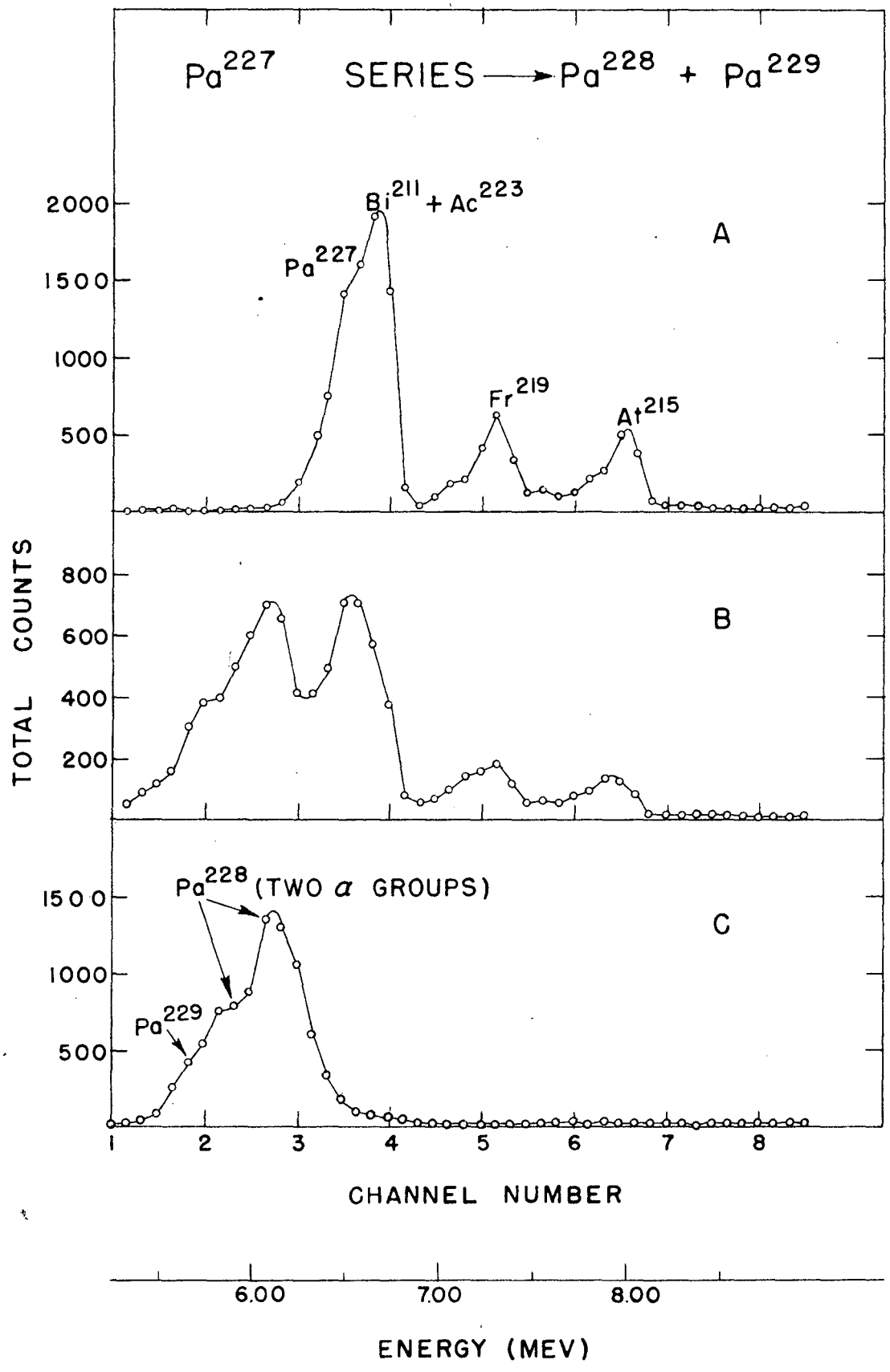
Pa227 SERIES → Pa228 + Pa229
Bi211 + Ac223
Pa227
Fr219
At215
A
B
C
Pa228 (TWO α GROUPS)
Pa229
TOTAL COUNTS
2000
1500
1000
500
800
600
400
200
1500
1000
500
1
2
3
4
5
6
7
8
CHANNEL NUMBER
6.00
7.00
8.00
ENERGY (MEV)

Fig. 5

1. Pa^{227} Since it is possible to obtain this isotope in very high yield and since it is the only protactinium isotope in evidence for a period of five or six hours after bombardment, we have been able to do some rather amazing experiments with it and its daughters. Half life determinations from following the gross alpha counts of the series gave a value of 38.3 ± 0.3 minutes. The counts of successive samples were registered by a "trafficounter" on ticker tape. Later they were normalized to the "hottest" counting sample and plotted as in Fig. 29.

By chemically milking a sample of thorium (including Th^{230} as tracer to determine chemical yield) from a known amount of Pa^{227} we were able to determine the branching ratio of this isotope. The Pa^{227} which had been previously separated from thorium was allowed to decay in TTA-benzene solution for 40 minutes and then the daughters washed from the organic layer with nitric acid. This acid was washed three times with fresh TTA-benzene solution to extract the protactinium which had washed out of the original organic layer, correction being made for the time this protactinium decays while in contact with the milking solution.

The Pa^{227} was allowed to decay only one half-life to reduce the amount of Th^{228} present from the large orbital electron branching decay of Pa^{228}. With this milking time, pulse analysis showed twice as much Th^{227} present as Th^{228} (the original bombardment being made with 60 Mev deuterons). Enough of the 18.6 day Th^{227} was present in the milked sample to indicate a K/α ratio of 0.18 with an error of $\pm$ 0.02.

Further evidence that the Th^{227} came from the 38.3 minute protactinium isotope was given when successive milkings for thorium of the protactinium sample indicated that the parent of the Th^{227} was decaying with about a 35 minute half-life.

By a double recoil experiment collecting and pulse analyzing Bi^{211} alpha particles from the series, it was possible to observe their 6.62 Mev energy and 2.16 minute decay.

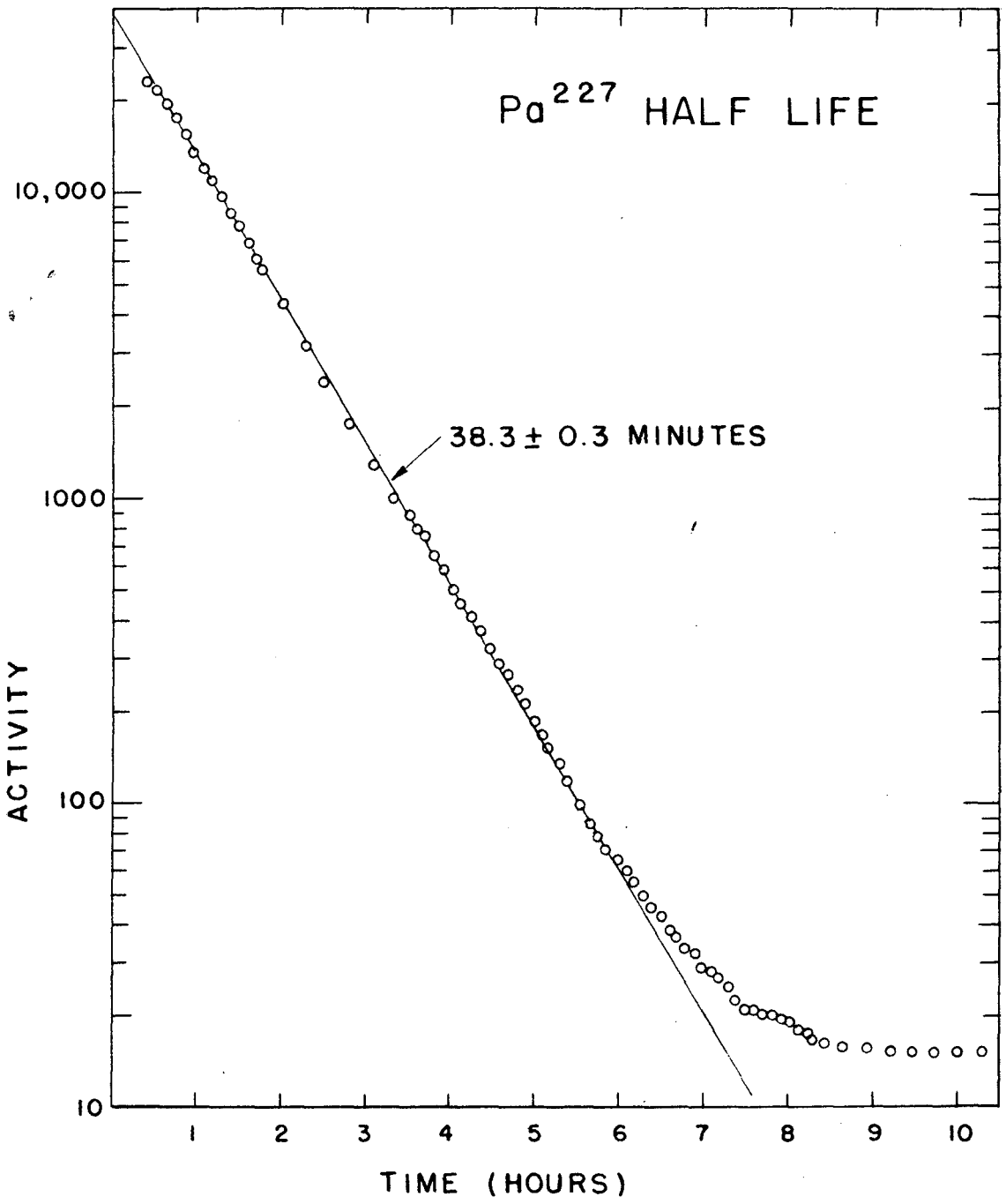

Fig. 29. Determination of the Pa^{227} half-life from the gross alpha decay of the protactinium fraction whose pulse analyses are shown in Fig. 28. Time indicated is time after shutdown.

Furthermore it was possible by a triple recoil experiment to collect enough of the Tl^{207} daughter to follow its 4.76 minute decay (Fig. 30), and even to take a rough absorption curve to check its energy.

The absolute cross sections and relative yields for this isotope are discussed in Chapter 2 of this report.

2. Ac^{223} Recoil atoms collected from Pa^{227} series plates decayed with a half-life of about 2.5 minutes. This value however was a combination of the half-life of the already known 2.16 minute Bi^{211} and Ac^{223}. Since their half-lives are so close together it is impossible to resolve one curve from the other.

Another method of attack was more successful. Recoils were collected from a a large plate of the Pa^{227} series for 10 minutes to insure equilibrium between the sample plate and the collector plate. The collector was then removed and successive one-minute recoil samples taken from it for a period of about 10 minutes. Bi^{211}, the only alpha activity present on the second recoil plates, was followed for about two minutes for each sample, all the counting of successive second recoils being done on one alpha counter and the counts recorded with a trafficounter. The decays of the Bi^{211} were extrapolated back through the best 2.16 minute line to the time of separation of this second recoil from its Ac^{223} parent. These extrapolated values are plotted in Fig. 31 where the time scale denotes minutes after removal of the first recoil plate from its Pa^{227} parent. Statistics on some of the Bi^{211} points is rather bad but it can be seen that the extrapolated values are in reasonable agreement. The half-life of Ac^{223} by this method is 2.2 ± 0.1 minutes. The only assumption made was that the efficiency of recoil for the Bi^{211} atoms was the same during the ten minutes of the experiment. This assumption appears reasonable since field conditions, etc., were invarient.

Data on the branching ratio of this isotope were also obtained from recoil experiments. A very large sample of Pa^{227} and daughters (probably about 10^9 alpha

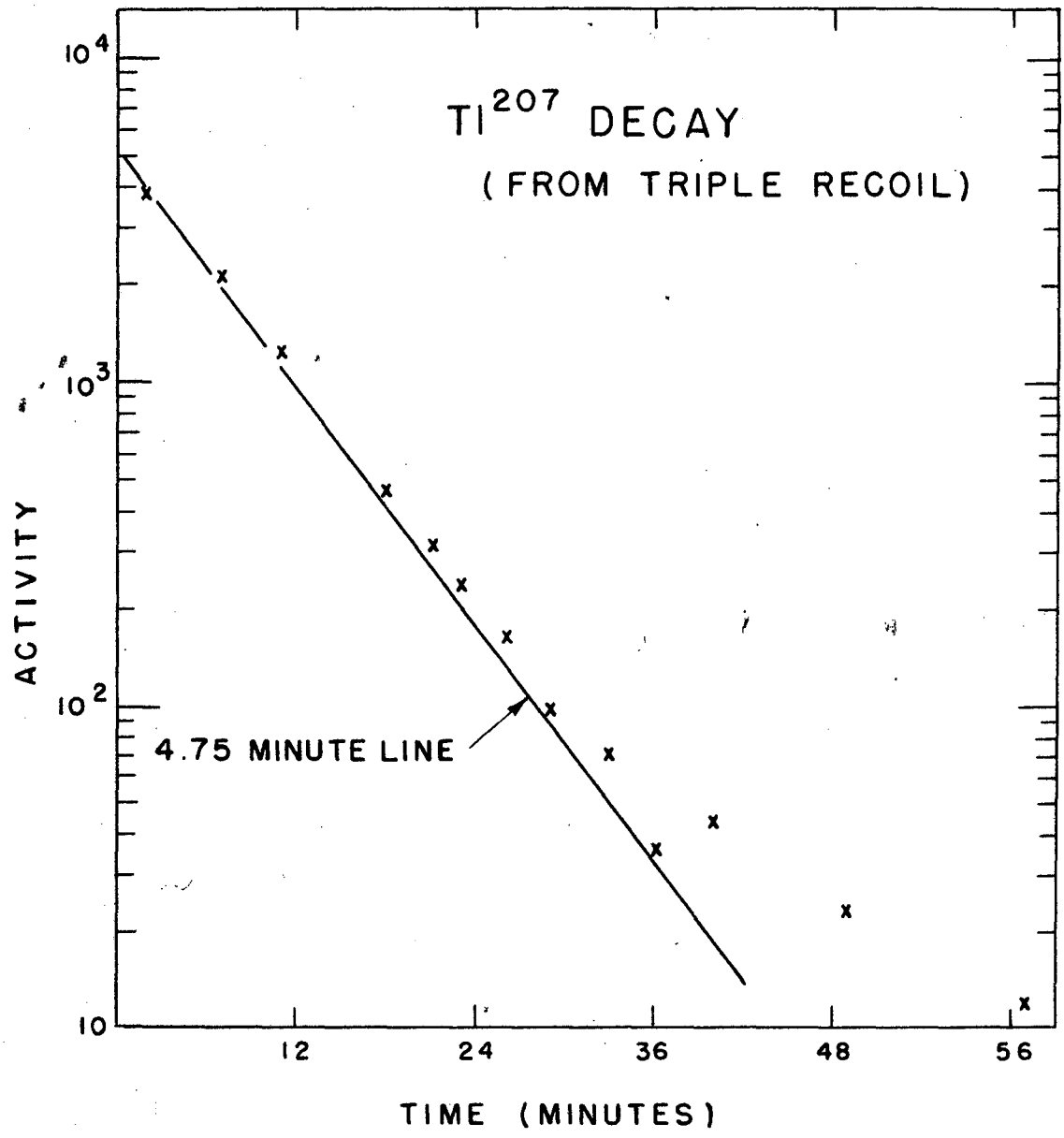

Fig. 30. Decay of a triple recoil sample from a large amount of Pa^{227} series. Accepted half-life for Tl^{207} is 4.76 minutes.

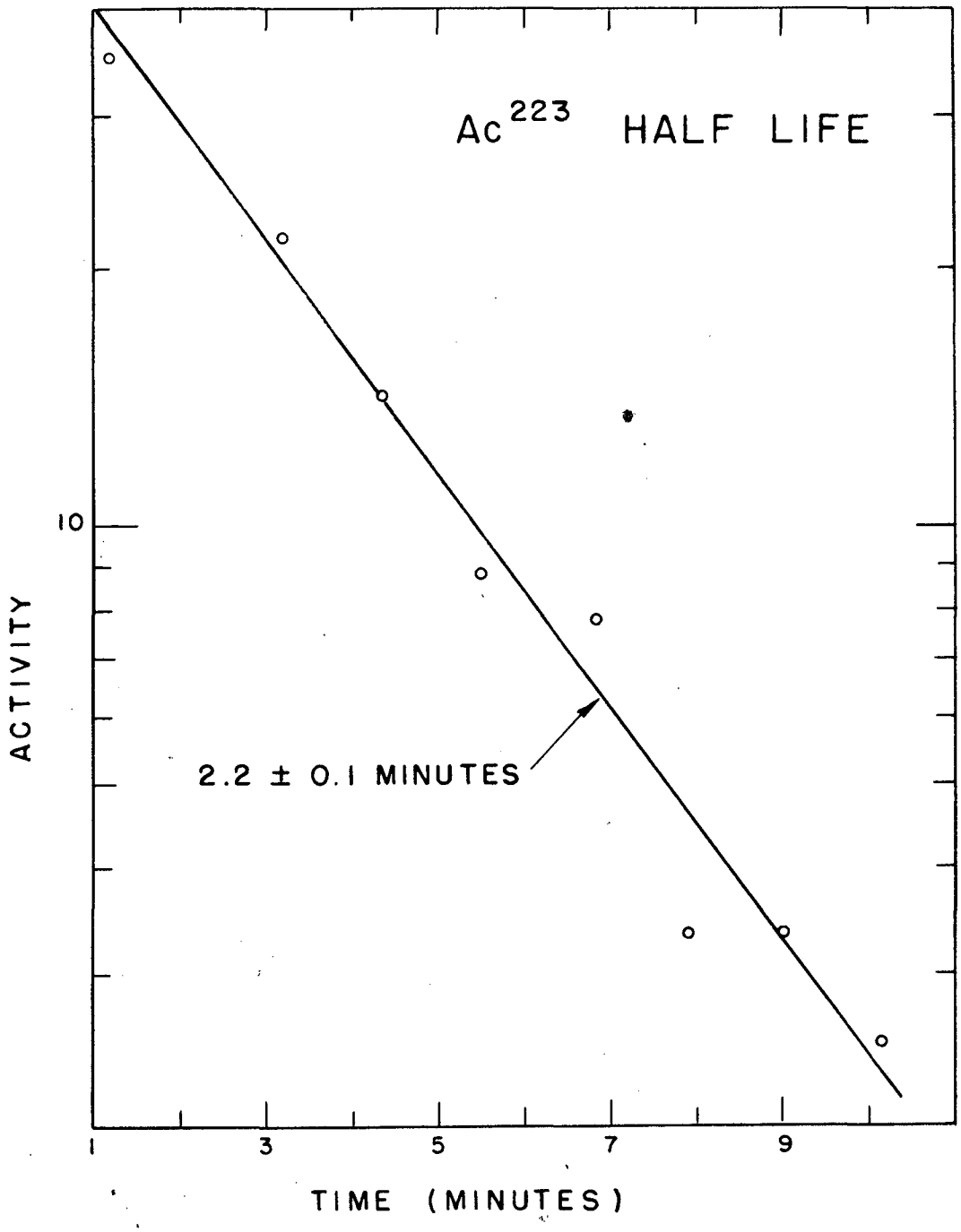

Fig. 31. Determination of the half-life of Ac^{223} by the method of successive second recoils. Time indicated is time after removal of first recoil sample from the Pa^{227} parent.

counts or more per minute) was used as a parent for a ten minute recoil growth. This recoil sample was allowed to decay for about 15 days and finally pulse analyzed to determine the amount of Ra^{223} present. This pulse analysis was not too straightforward since in the Ra^{223} peak there was also some contribution from Ra^{224} and Ac^{225}. A correction can be made for the latter two however by counting the Po^{212} and Po^{213} peaks. Since these alpha peaks do not have a short-lived alpha parent but come instead from Bi^{212} and Bi^{213} respectively, both beta emitters, there is no coincidence loss in their counting and they are a true indication of the amount of Ra^{224} and Ac^{225} present in the sample. (The Po^{212} must be corrected for the branching of the Bi^{212} however.) This then gives the amount of Ac^{223} decaying by orbital electron capture to Ra^{223}.

The amount of Ac^{223} decaying by alpha emission was estimated in the following manner. Recoil samples were grown for a period of several seconds from the parent Pa^{227} sample and then followed down in an alpha counter for decay. The Ac^{223} and Bi^{211} equilibrium decay line was then extrapolated back to the end of the recoil growth time and these values plotted. Three such samples were taken and the best 38.3 minute line drawn through them. A point on the line at the middle of the growth period of the large recoil sample gave an indication of the amount of activity that was recoiling over at that time. It was then assumed that 1/7 of this gross alpha recoil activity was due to Ac^{223} alpha particles; if the Ac^{223} is recoiled over there are four alphas contributing, if the Fr^{219} recoils over there is only the one Bi^{211} alpha and similarly for the At^{215} and the Bi^{211}. The efficiency of recoils was assumed constant over the time of the experiment and independent of the alpha energy of the parent atom.

A comparison of the number of atoms decaying by alpha emission and the number by orbital electron capture shows that the K/α branching ratio for Ac^{223} is 0.01.

3. Fr^{219} From alpha systematics we expected a short half-life for this isotope. The electronic determination gave a value of about 20 milliseconds, within 10% or so.

To check both this value and the principle of the rotating disc recoil method, we mounted a sample of about 4×10^6 alpha counts per minute of the Pa^{227} above the disc and rotated it at a speed of one revolution per second. Apparently about one half to one percent of the recoils were collected on the disc, enough to determine that the half-life of this francium isotope was approximately 20 milliseconds. The three points obtained are shown in Fig. 32.

4. At^{215} The half-life of this isotope has been determined electronically to be about 10^{-4} seconds, within about 20%.

It is interesting to note that the energy we obtain for the At^{215} alpha-particles is several hundred kilovolts less than the 8.4 Mev value reported[19] for At^{215} as formed by the beta-particle branching decay of Po^{215}(AcA).

C. The Pa^{228} Series

This series, collateral to the thorium or 4n family, is the longest-lived (22 hours) of the new chains we have found. It is shown in block diagram in Fig. 33. This series is produced in somewhat lower yield than the Pa^{230} - U^{230} series in thorium bombardments and hence samples will always contain the two series. Since the Pa^{230} is a beta emitter, however, pure samples for alpha-pulse analysis of the Pa^{228} (and the Pa^{229} which is also present) can be obtained immediately after chemical purification. But within an hour or so after purification, the U^{230} series grows in, obscuring the remaining members of the Pa^{228} series in pulse analysis.

Consequently the pulse analysis of Pa^{228} (Fig. 34) also includes Pa^{229} but does not include any of the Pa^{228} daughters. Fig. 35 indicates the decay of a protactinium fraction, with varying amounts of U^{230} series grown in in A, B, and C.

The data for this series are summarized in Table 3. The radioactive properties for ThC, ThC', and ThC'' are the accepted values taken from the literature.[7]

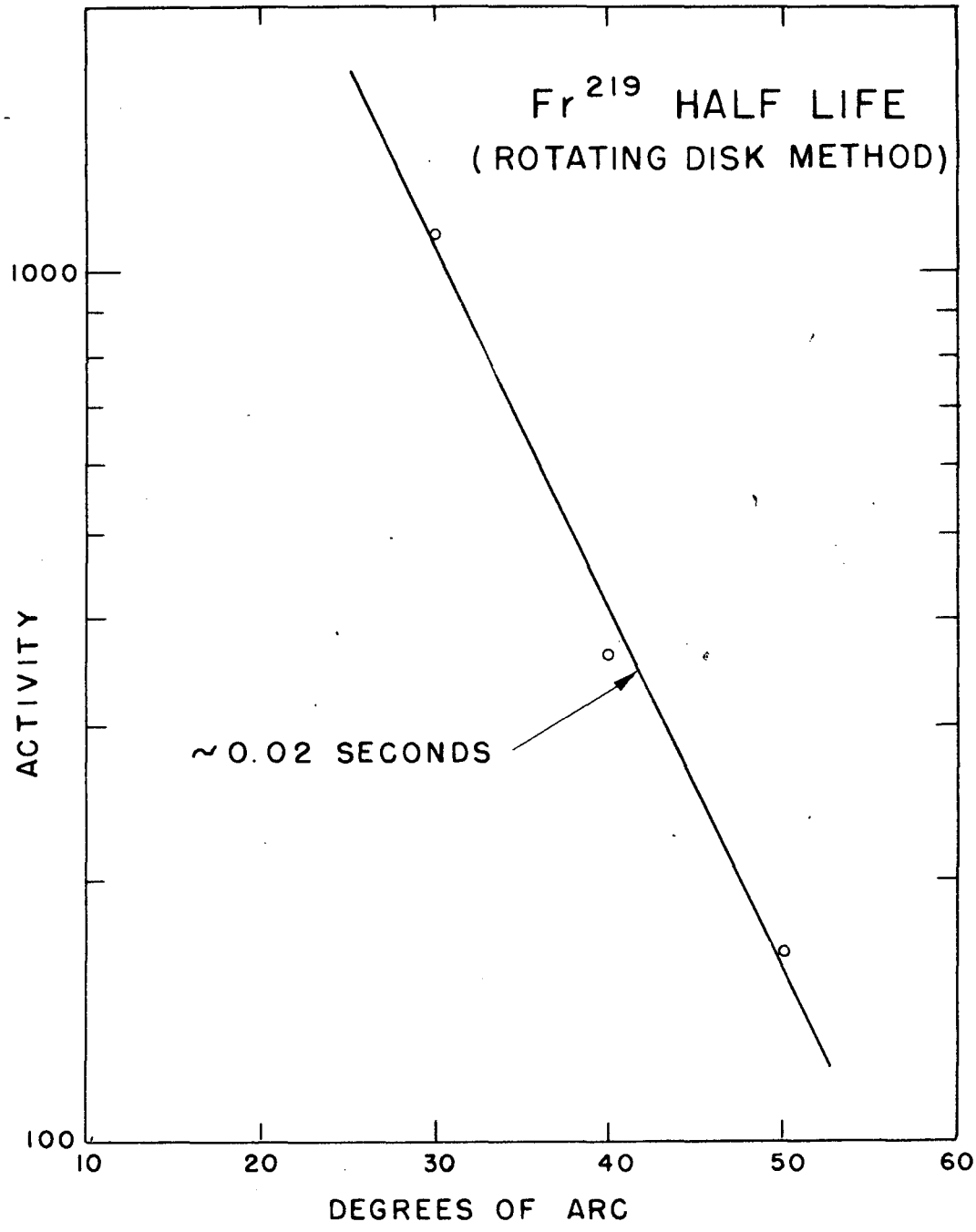

Fig. 32. Determination of the half-life of Fr^{219} by the rotating disc recoil method.

ARTIFICIAL COLLATERAL RADIOACTIVE SERIES

PRODUCED BY

$Th^{232}(d, 6n)Pa^{228}$

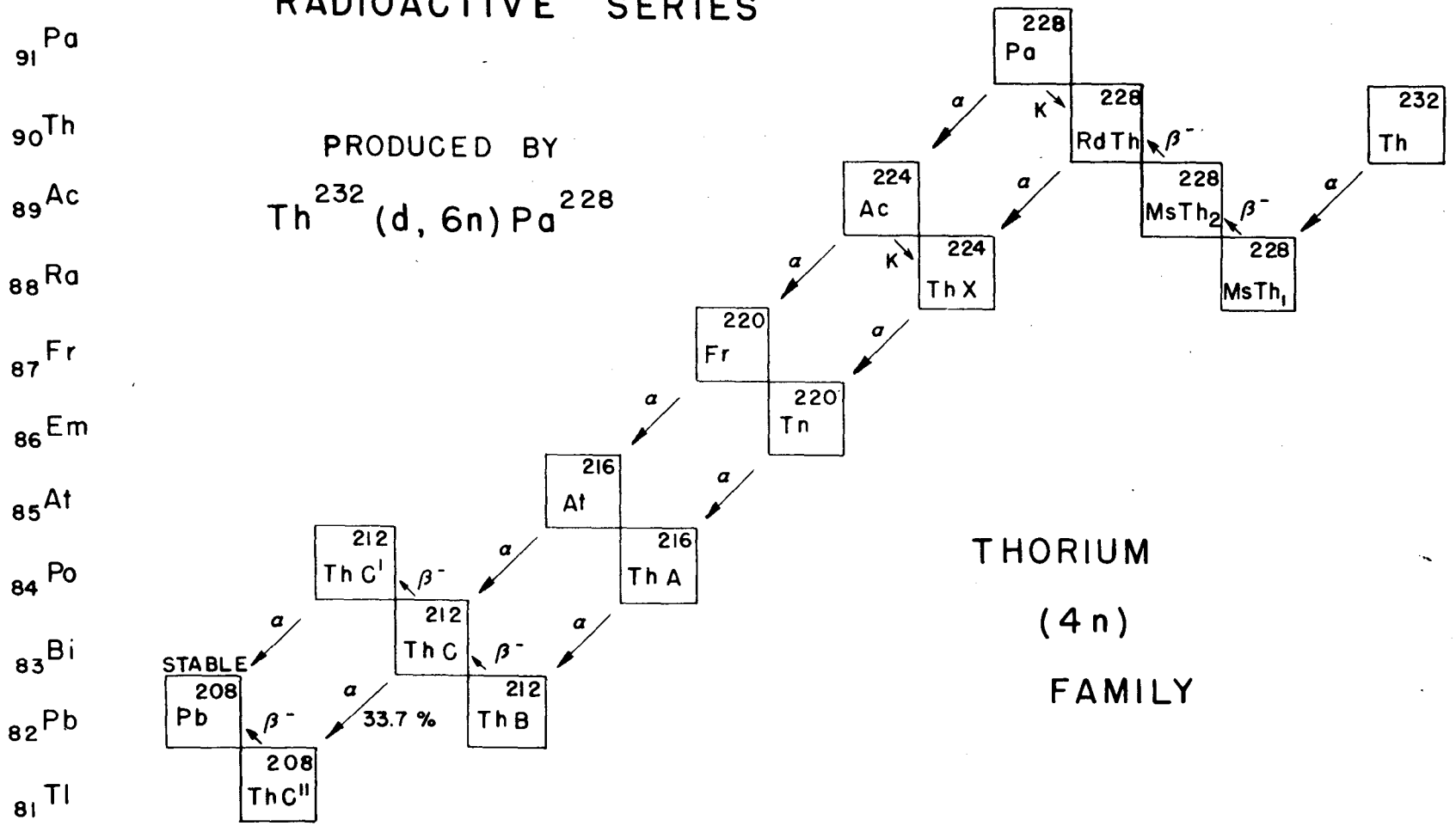

THORIUM

(4n)

FAMILY

FIG. 33

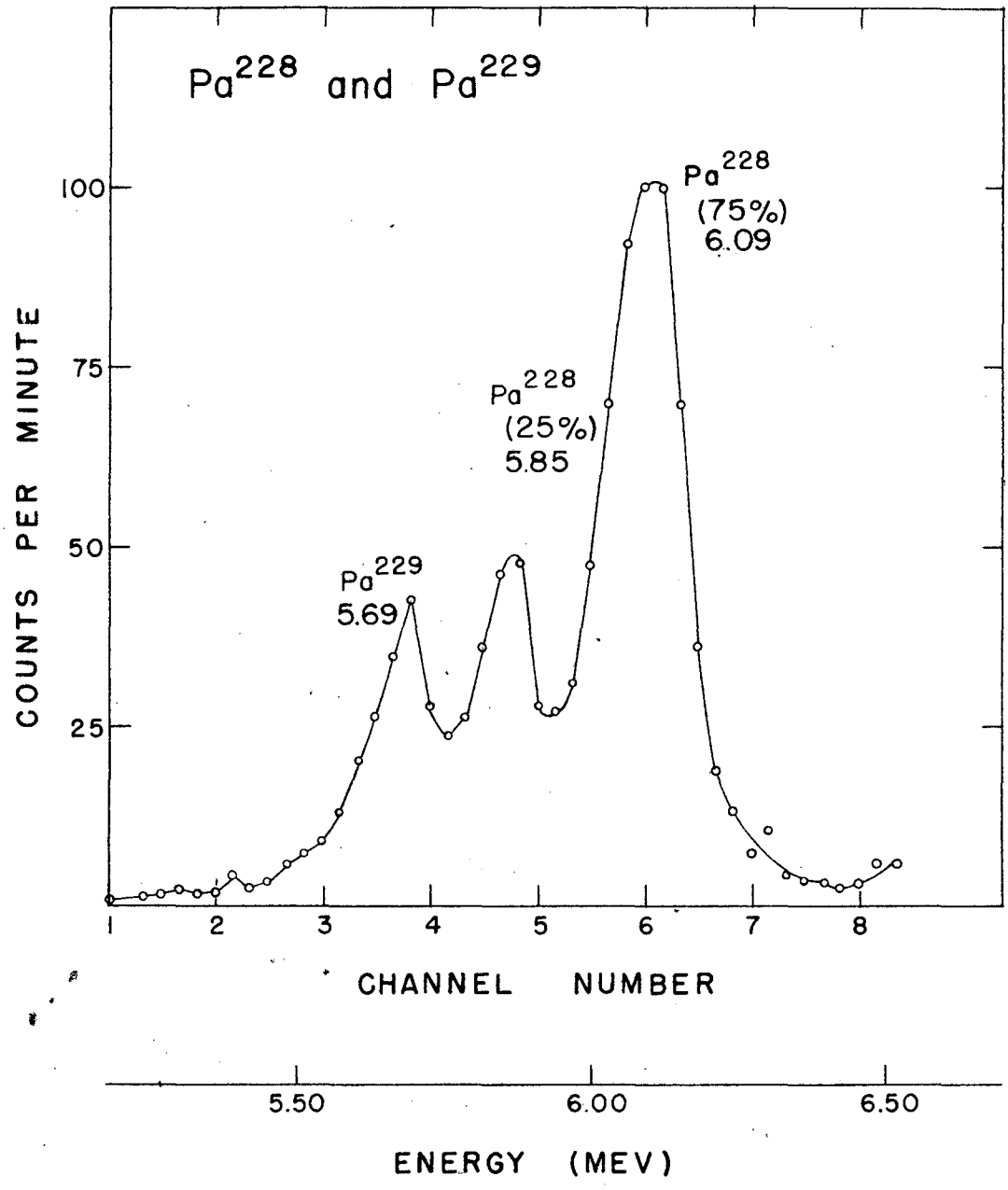

Fig. 34. Alpha-pulse analysis curve of the Pa^{228} and Pa^{229} alpha groups after complete decay of the Pa^{227} series. This sample purified from daughter activities immediately before counting. No collimation used.

Fig. 35. Alpha-pulse analysis curves showing the decay of the protactinium fraction from thorium bombardment with varying amounts of U^{230} series grown into the samples. The fractions are from a six hour bombardment of thorium metal with 60-Mev deuterons.

Sample A was counted for 13 minutes, 3.6 days after shutdown and 90 minutes after chemical separation from daughters.

Sample B was counted for 25 minutes, 7.27 days after shutdown and 28 minutes after chemical separation from daughters.

Sample C was counted for 114 minutes, 10.62 days after shutdown and 2 hours, 20 minutes, after chemical separation from daughters.

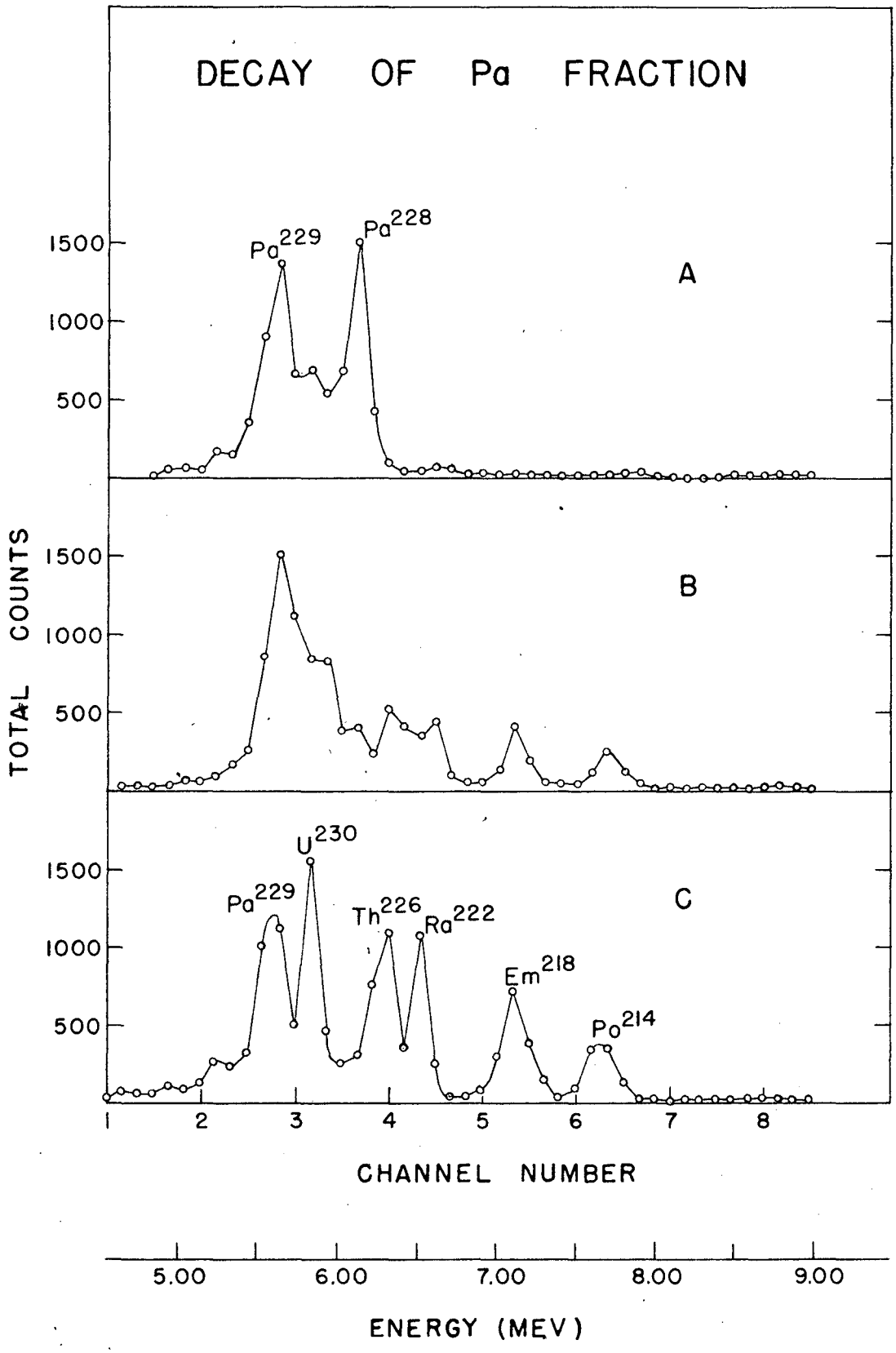
DECAY OF Pa FRACTION
Pa229
Pa228
A
B
C
U230
Pa229
Th226
Ra222
Em218
Po214
1500
1000
500
TOTAL COUNTS
1
2
3
4
5
6
7
8
CHANNEL NUMBER
5.00
6.00
7.00
8.00
9.00
ENERGY (MEV)

Fig. 35

Table 3

Pa^{228} Collateral Series Data

Isotope	Type of Radiation	Half-Life	Energy of Radiation (Mev)
Pa^{228}	α(~2%) K(~98%)	22 ± 1 hr.	6.09(75%) 5.85(25%)
Ac^{224}	α(~10%) K(~90%)	2.9 ± 0.2 hr.	6.17
Fr^{220}	α	27.5 ± 1.5 sec.	6.69
At^{216}	α	3×10^{-4} sec ±10%	7.79
Bi^{212}(ThC)	α(34%) β⁻(66%)	60.5 min	6.081(27%) 6.042(70%) 2.20
Tl^{208}(ThC'')	β⁻	3.1 min	1.72
Po^{212}(ThC')	α	3×10^{-7} sec	8.776
Pb^{208}	Stable		

1. Pa^{228} In the measurement of the half-life of Pa^{228} there arises a problem of resolution of pulse analysis curves since the 1.5 day Pa^{229} is always found with Pa^{228} to a greater or less extent. Even when a bombardment is planned for maximum Pa^{228} yield and minimum Pa^{229} yield there will not be a difference of more than 20 or so between the two isotopes and by the time the Pa^{228} has decayed through one or two half-lives the Pa^{229} will become appreciable and affect the decay curve. Fig. 36A shows such a maximized bombardment.

Since the energies of the Pa^{228} and Pa^{229} are quite close together (6.09 and 5.85 for the two groups of Pa^{228} and 5.69 for Pa^{229}) good resolution of consecutive pulse analyses is difficult and inaccurate. There is always a question as to just how much tail of the Pa^{228} peak to subtract in the resolution. A preliminary value of 22 hours was obtained from rough resolutions of several successive pulse analyses taken over a period of two half-lives of the Pa^{228}. This method however gives no

Fig. 36. Alpha-pulse analysis curves showing the decay of Pa^{228} and Pa^{229} peaks against a fixed amount of long-lived Pa^{231} tracer. All samples were counted immediately after separation from their daughters.

Sample A was counted for 13.1 minutes, 10 hours after shutdown.

Sample B was counted for 8.0 minutes, 3.05 days after shutdown.

Sample C was counted for 17 minutes, 9.05 days after shutdown.

The protactinium fraction was from an 80-Mev deuteron bombardment of thorium metal.

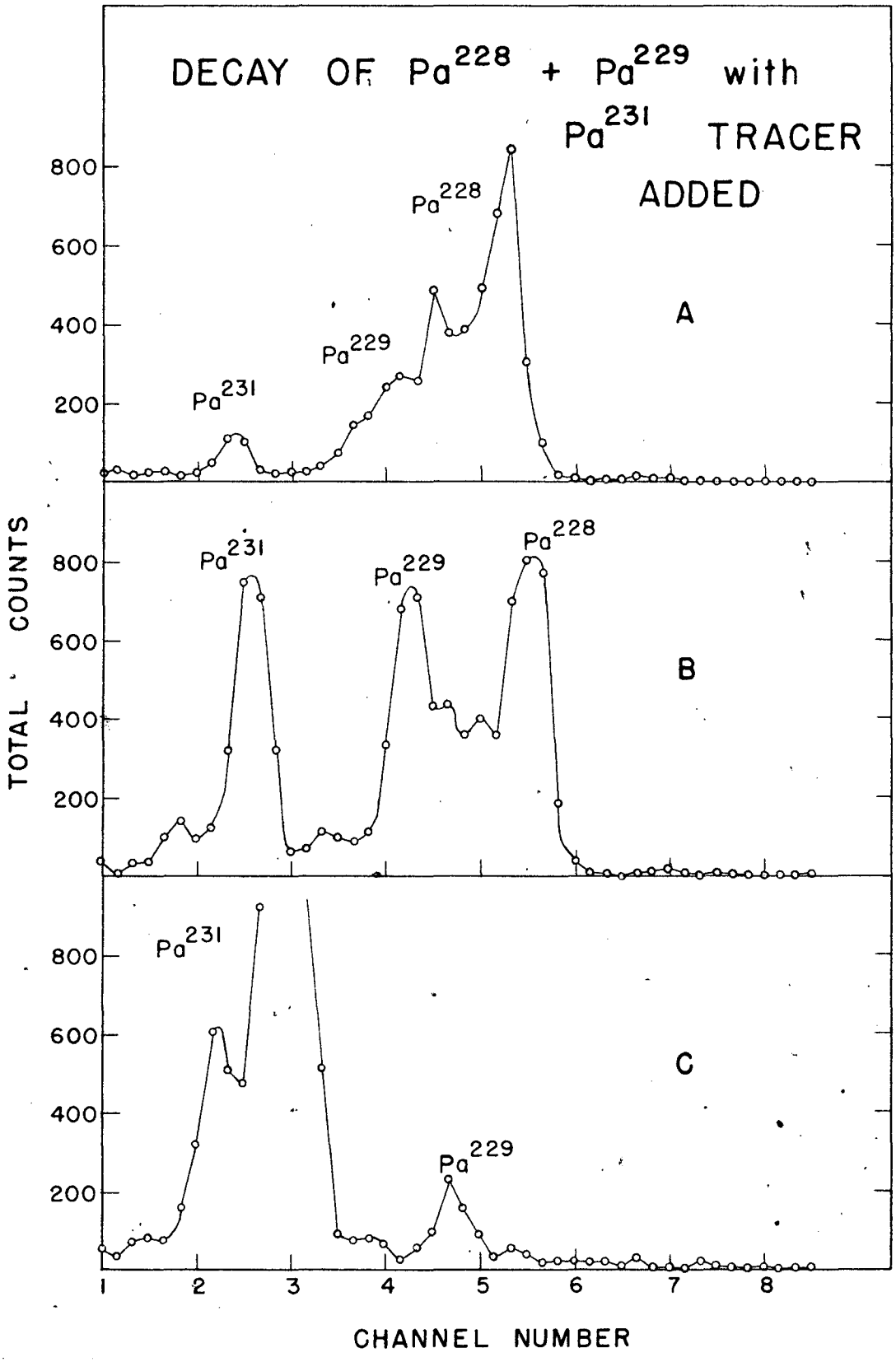

(ENERGY SCALES OF A, B, & C ARE NOT IDENTICAL)

Fig 36

method for estimating the error or observing trends in the half-life measurements and it was consequently discarded in favor of a better method.

This other method consisted of counting the entire group of peaks representing the Pa^{228} and Pa^{229} from pulse analysis and obtaining the ratio of these counts to long-lived Pa^{231} tracer added at the beginning of the experiment. These counts were taken at about 12 hour intervals and the ratios plotted to represent the decay of the peaks. New samples which had been freshly separated from their daughters were used for each point, making the use of tracer Pa^{231} imperative. This chemical separation was necessary to clean out Pa^{230} - U^{230} series alphas which tend to obscure the Pa^{228} and Pa^{229} peaks.

Figure 37 represents the total decay of the group of peaks while Fig. 36 shows a pulse analysis at the beginning, in the middle and at the end of the set of samples. From the group of pulse analyses obtained, several different types of resolutions were made before we finally arrived at the value of 22 ± 1 hours. The dotted line resolution indicated in Fig. 37 resolved the Pa^{229} from Fig. 36C (nine day sample) and through this plotted value drew a 1.5 day line. This Pa^{229} line was then subtracted from the original points and a 21.8 hour line obtained.

Another method resolved the Pa^{228} from the first sample and from the next to the last sample. A line connecting these points gives a 22.7 hour line. It is difficult to obtain more points for this curve since when the alpha peaks of the two isotopes approach the same size, the error in resolution is greatest.

Still another method resolved the Pa^{229} from the 5.5 day sample, drew a 1.5 day line through this point and subtracted this line from the experimental points to obtain a line of half-life 22.0 hours.

Examining the resolved line in Fig. 37 we see that the first two points are slightly low (possibly due to the very small amount of Pa^{231} present and subsequent errors in its counting --- a small uncorrected background could cause this). If

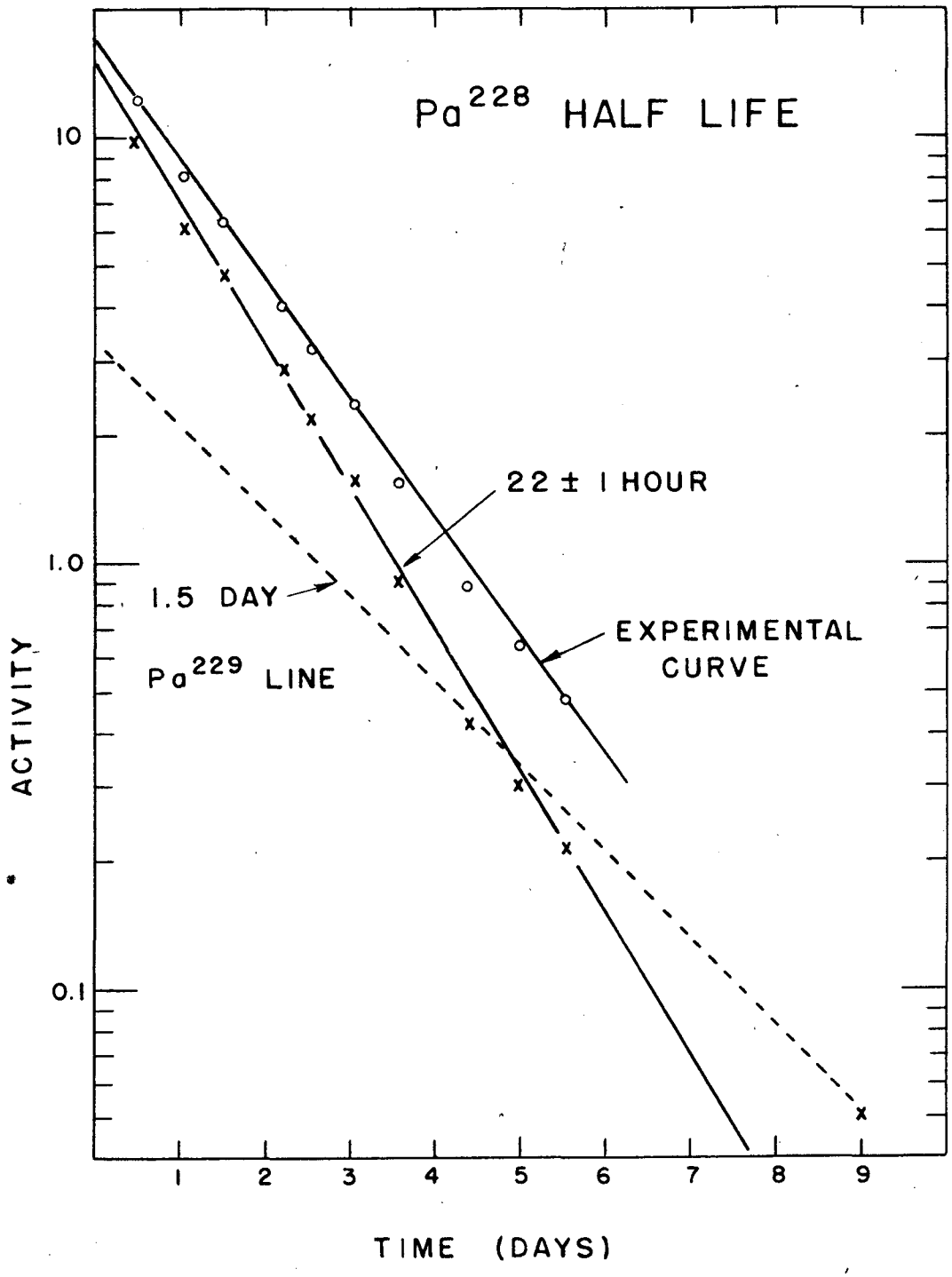

Fig. 37. Determination of the Pa^{228} half-life by resolution of the pulse analysis curves shown in part in Fig. 36.

these points are arbitrarily raised to fall more in line with the next three points the best line through the points now becomes about 21.6 hours.

Hence it can be seen that although various resolutions of our experimental pulse analysis points give different values for the half-life of Pa^{228}, all of these values are consistent with a half-life of 22 ± 1 hours for this isotope.

Chemical milkings of 1.9 year Th^{228} from the decay of a known amount of Pa^{228} prove the mass assignment of this isotope. An aliquot of the original Pa^{228} solution was pulse analyzed to determine the amount of Pa^{228} present, and Th^{230} tracer added to determine chemical yield. The sample was allowed to decay for six days before thorium separation by Procedure 90-3 of Appendix II. The plates of the final thorium separation were pulse analyzed to determine the amount of Th^{228} and Th^{230} present. The value obtained for the K/α ratio for this isotope is $53 \pm 5\%$.

Chemical milkings of a lead-bismuth fraction from an equilibrium mixture of the Pa^{228} series indicated the presence of a long range alpha which decayed with two half-lives, one of approximately one hour and one of about 10 hours. After this long range alpha was identified as Po^{212} by pulse analysis the gross alpha decay of the sample was followed in an ordinary alpha counter. The two half-lives with which the alphas were decaying were due to the 60.5 minute Bi^{212}(ThC) from the main line of decay of the series and the 10.6 hour Pb^{212}(ThB) from the branching decays of the series. Further milkings of a bismuth fraction alone showed a one hour decay of the alphas.

2. Ac^{224}

The energies and half-life of this isotope were determined by milking chemically an actinium-thorium fraction from an equilibrium mixture of Pa^{228} and its daughters. Lanthanum fluoride-hydroxide cycles were used in this chemical separation with barium carrier to hold back the radium. The lanthanum chloride was finally plated and flamed, giving a good plate for pulse analysis.

The half-life value obtained in this way agreed with the value of 2.9 ± 0.2 hours found by following the decay of the At^{216} peak from pulse analysis curves of a recoil sample. The decay obtained with the recoil sample is shown in Fig. 38.

By pulse analyzing recoil samples from Pa^{228} we were able to determine the number of Ac^{224} alpha disintegrations present and later the amount of the orbital electron capture daughter Ra^{224} present after complete decay of the Ac^{224}. Although resolution of the pulse analysis curves was rather difficult we did obtain a value for the K/α branching ratio of Ac^{224} of 10 ± 2 (two determinations gave 8.75 and 11.6). The assumption that a negligible amount of Ra^{224} is present in the sample due to the recoil from the 1.9 year Th^{228} from the original parent sample appears to be a good one.

This isotope has a long enough half-life that considerably more could be done with it in the way of characterizing its radiations, etc.

3. Fr^{220} The energy of this isotope was obtained from the actinium-thorium sample mentioned above since francium was in equilibrium with the Ac^{224} parent in this sample.

A half-life of 27.5 ± 1.5 seconds was found from recoil experiments. From a large sample of Pa^{228} we collected recoil samples for short periods of time and followed these samples for gross decay on an alpha counter. From this gross decay we were able to resolve the half-life for this isotope (see Fig. 39). In these experiments the contribution of the Ra^{222} which was present in low abundance from the U^{230} series was negligible.

4. At^{216} The half-life for this isotope, as measured on the electronic set-up for short half-lives, was found to be about three or four hundred microseconds. It is interesting to note the check between the energy of these At^{216} alpha-particles and the energy reported by Karlik and Bernert[20] for At^{216} as formed by the beta-particle branching decay of Po^{216}(ThA). There does seem to be good reason to doubt the beta instability of ThA however (see Perlman, Ghiorso and Seaborg[15] for a

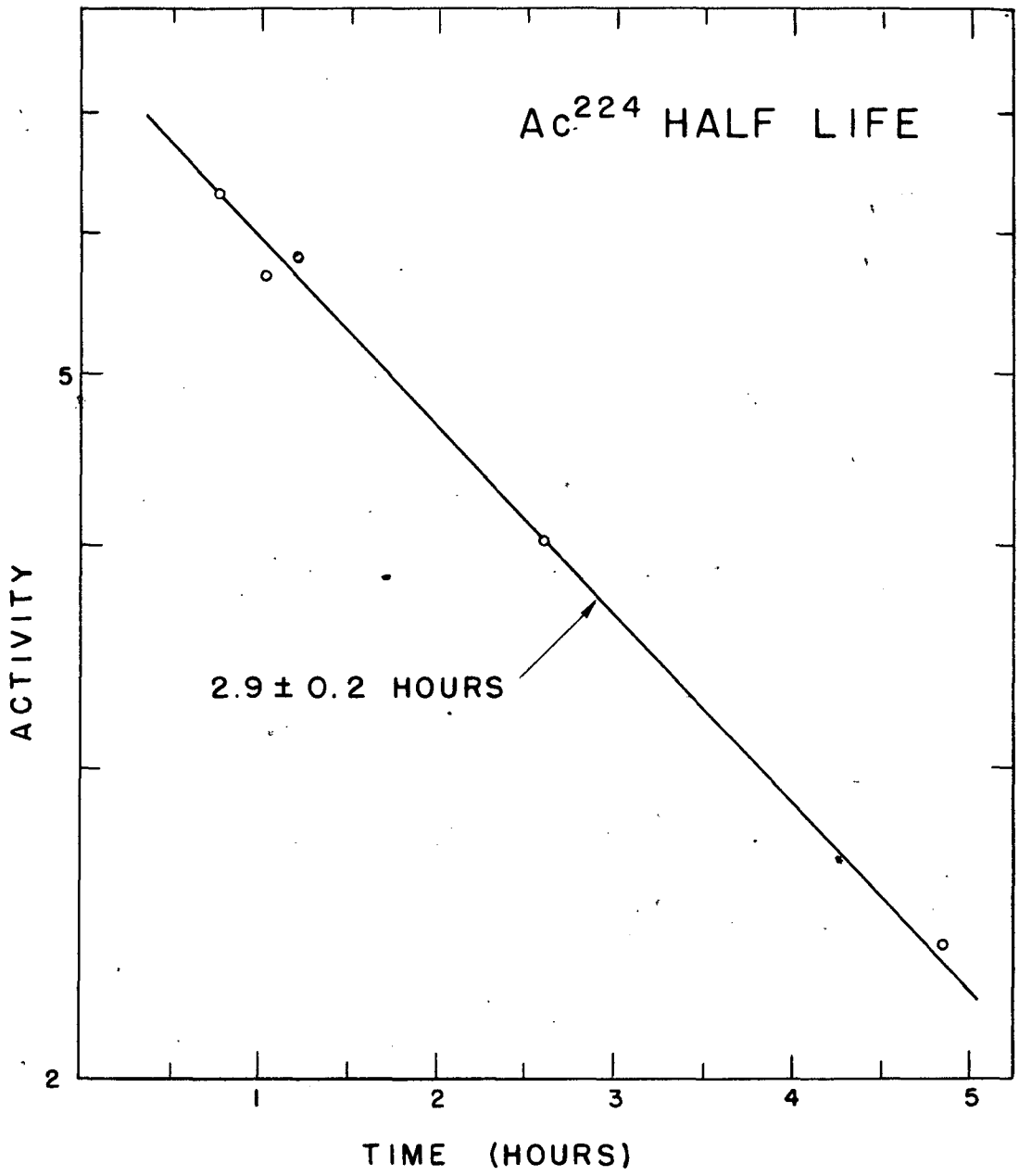

Fig. 38. Determination of the half-life of Ac^{224} from the decay of the At^{216} peak from pulse analysis curves of a recoil sample from Pa^{228}.

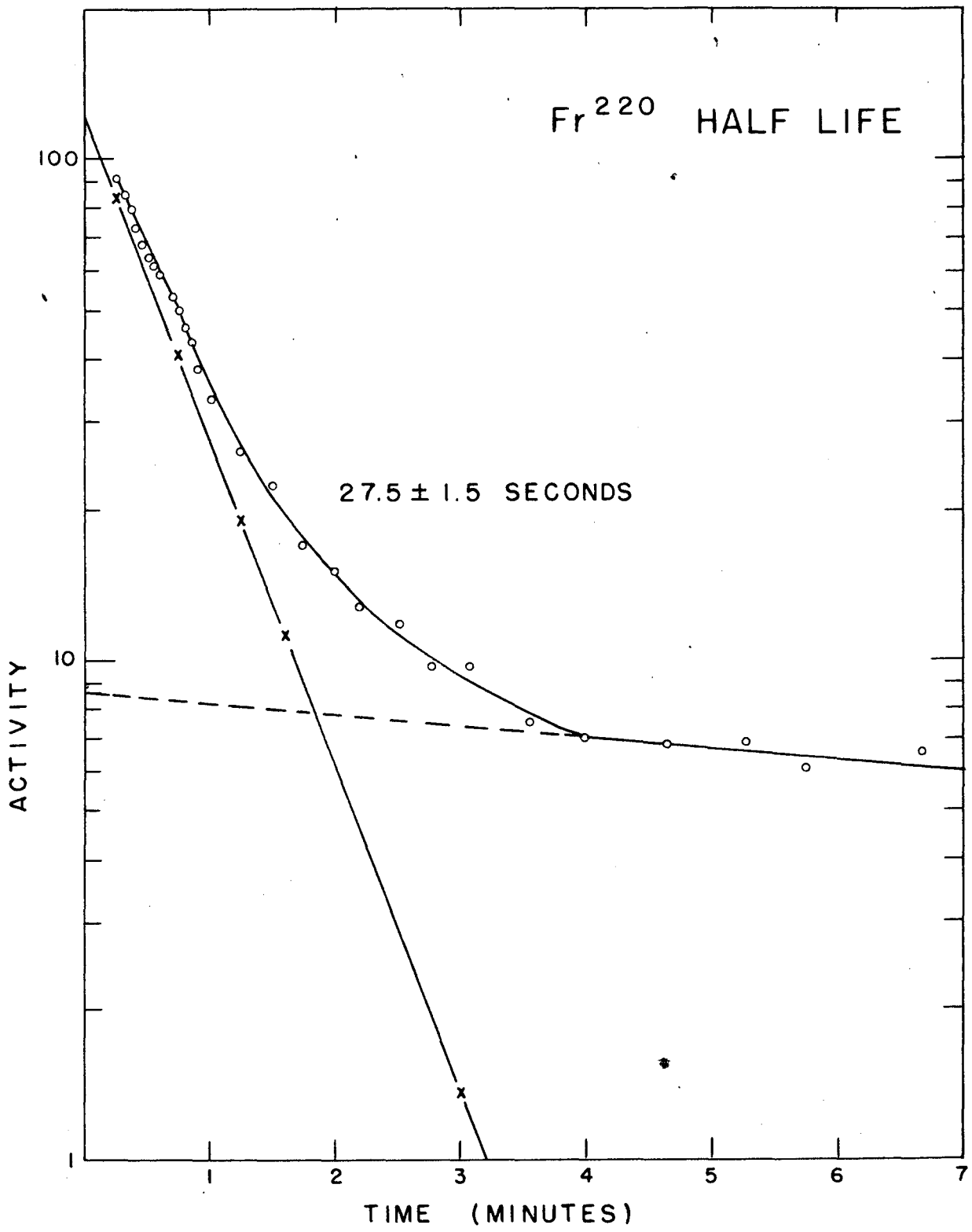

Fig. 39. Determination of the half-life of Fr^{220} from gross decay of recoil samples from a large amount of the Pa^{228} series.

discussion of this point).

D. The U^{227} Series

Although it has eluded us to date, this series figures heavily in our plans for the future. Bombardments of thorium nitrate salt in the jiffy probe and 4.5 minute chemistry from shutdown to counting have served only to give us a brief glimpse of what we think to be this series.

Fig. 40 shows a block diagram of this series which is collateral to the actinium or 4n + 3 family. In Fig. 41 is shown the best evidence we have so far that there is a uranium series shorter lived than the 9.3 minute U^{228} series. The dotted line represents a pulse analysis of the sample taken about 10 minutes after the solid line but extrapolated back along the 9.3 minute decay of U^{228} so as to accurately represent the U^{228} activity at the time of the solid curve. It can be seen that there is some difference between the two curves due possibly to the effect of one alpha group above the Th^{224} peak, two groups above the Ra^{220} peak, one group above the Em^{216} peak, and one group above the Po^{212} peak. This positioning of the peaks is what we would expect from alpha systematics for this series. With the new pneumatic tube-jiffy probe set-up we should be able to find and characterize the members of this series.

A summary of the predicted values for this series is listed in Table 4. The values for Po^{211} have been obtained from the literature.[7]

Table 4

U^{227} Collateral Series Data

Isotope	Type of Radiation	Half-Life	Energy of Radiation(Mev)
U^{227}	α	(pred 30 sec)	(pred 6.9)
Th^{223}	α	(pred 0.1 sec)	(pred 7.5)
Ra^{219}	α	(pred 5×10^{-3} sec)	(pred 7.9)
Em^{215}	α	(pred 5×10^{-6} sec)	(pred 8.6)
Po^{211}(AcC')	α	5×10^{-3} sec	7.434
Pb^{207}	Stable		

ARTIFICIAL COLLATERAL RADIOACTIVE SERIES

PRODUCED BY

$Th^{232}(\alpha, 9n)\, U^{227}(?)$

$Th^{232}(d, 7n)\, Pa^{227}$

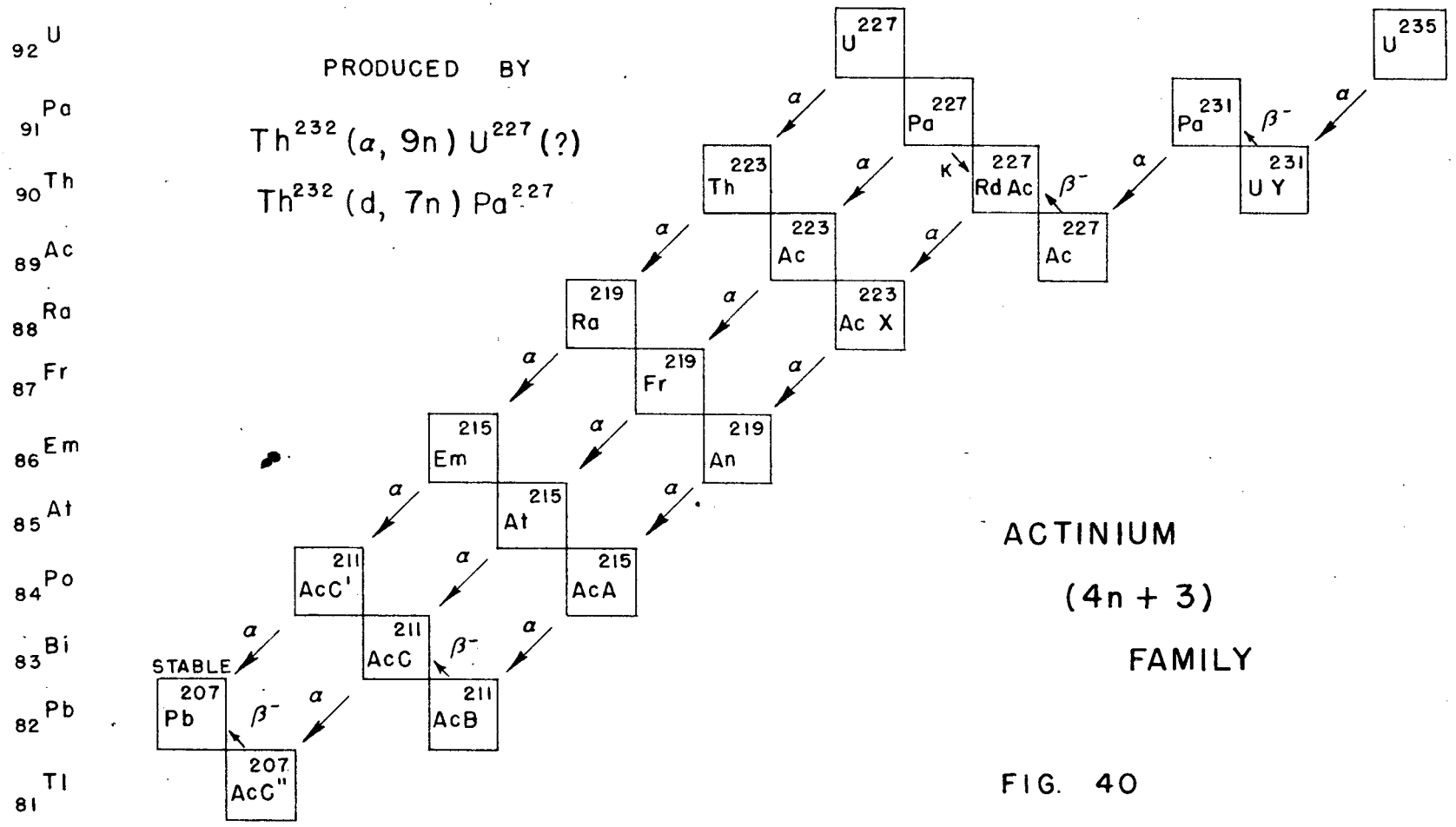

ACTINIUM

(4n + 3)

FAMILY

FIG. 40

14150-I

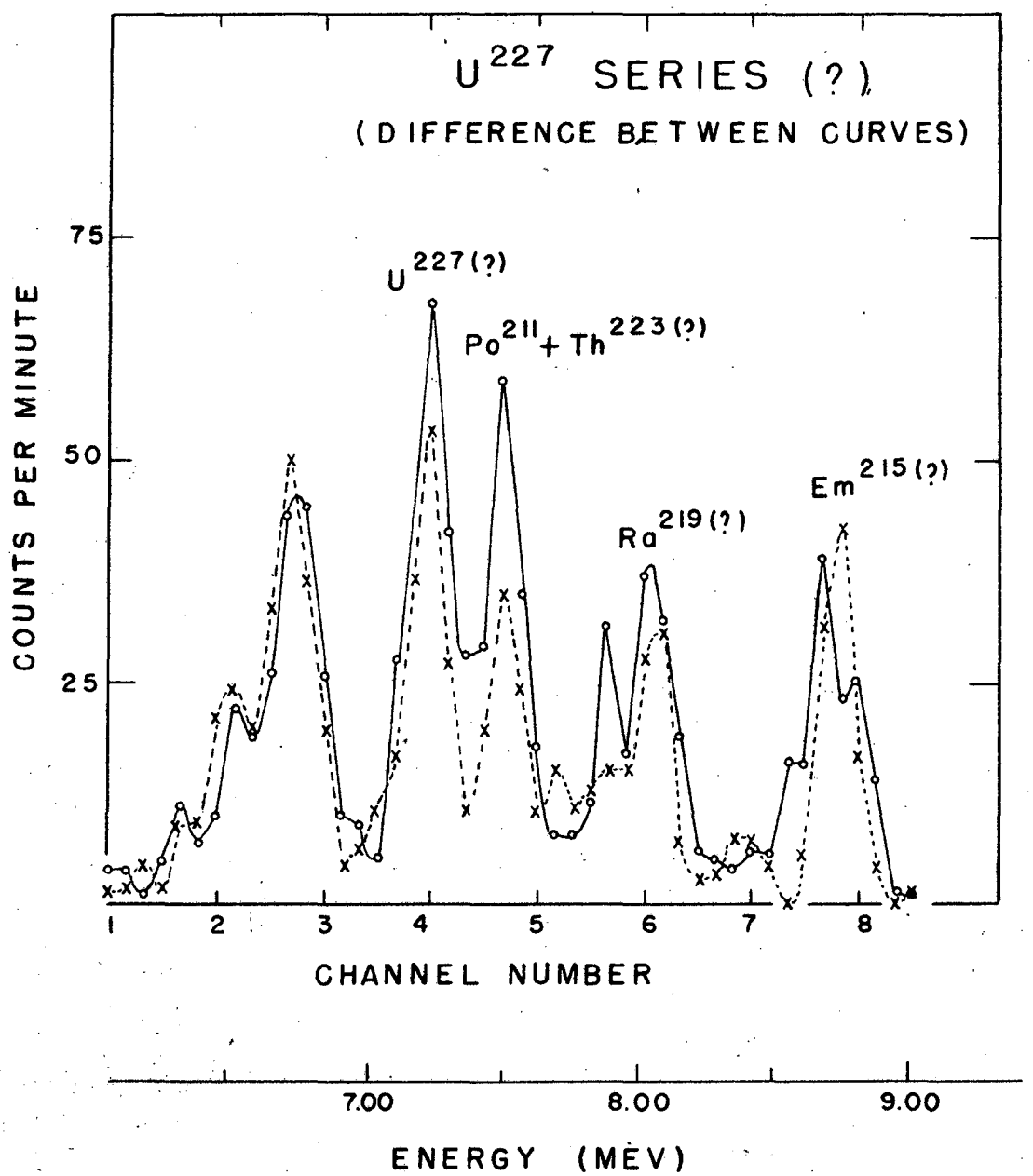

Fig. 41. Alpha-pulse analysis curve of the U^{227} series (?) from a two minute bombardment of thorium nitrate with 160-Mev alpha particles in the jiffy probe. This curve represents a one minute count of the uranium fraction, the count being started 4.5 minutes after shutdown. The dotted line represents the amount of U^{228} series present during this count. A #3 collimator was used.

E. The U^{228} Series

This series, a collateral branch of the thorium or 4n family, is shown in block diagram in Fig. 42. It becomes evident in a uranium fraction immediately after an alpha bombardment of thorium and is most easily followed by its long range alpha peak of Po^{212}. Our early experiments tended to assign to it a shorter half-life than 9.3 minutes because of difficulties in resolution with the pulse analyzer. With careful and fast chemical separations, however, we were able to obtain a good clean pulse analysis curve of the series as shown in Fig. 43. As this series decays, its place is taken over by the 58 minute U^{229} series as shown in Fig. 44.

A summary of data for the isotopes in this series is given in Table 5. The radioactive properties of ThC' are the accepted values from the literature[7].

Table 5

U^{228} Collateral Series Data

Isotope	Type of Radiation	Half-Life	Energy of Radiation (Mev)
U^{228}	α	9.3 ± 0.5 min	6.72
Th^{224}	α	(pred. 0.1 sec)	7.20
Ra^{220}	α	(pred 5×10^{-3} sec)	7.49
Em^{216}	α	(pred 2×10^{-5} sec)	8.07
Po^{212} (ThC')	α	3×10^{-7} sec	8.776
Pb^{208}	Stable		

1. U^{228} The half-life of this isotope was determined by following the decay of the Th^{224} and Ra^{220} peaks resolved from pulse analyses curves. The value obtained is 9.3 ± 0.5 minutes as shown in Fig. 45. By following the decay of the Po^{212} peak we obtained a value which was slightly smaller, but appeared to be more affected by straggling of the alphas in the pulse analysis peak.

ARTIFICIAL COLLATERAL RADIOACTIVE SERIES

PRODUCED BY
Th^{232} $(\alpha,8n)$ U^{228}
AND
Th^{232} $(d,6n)$ Pa^{228}

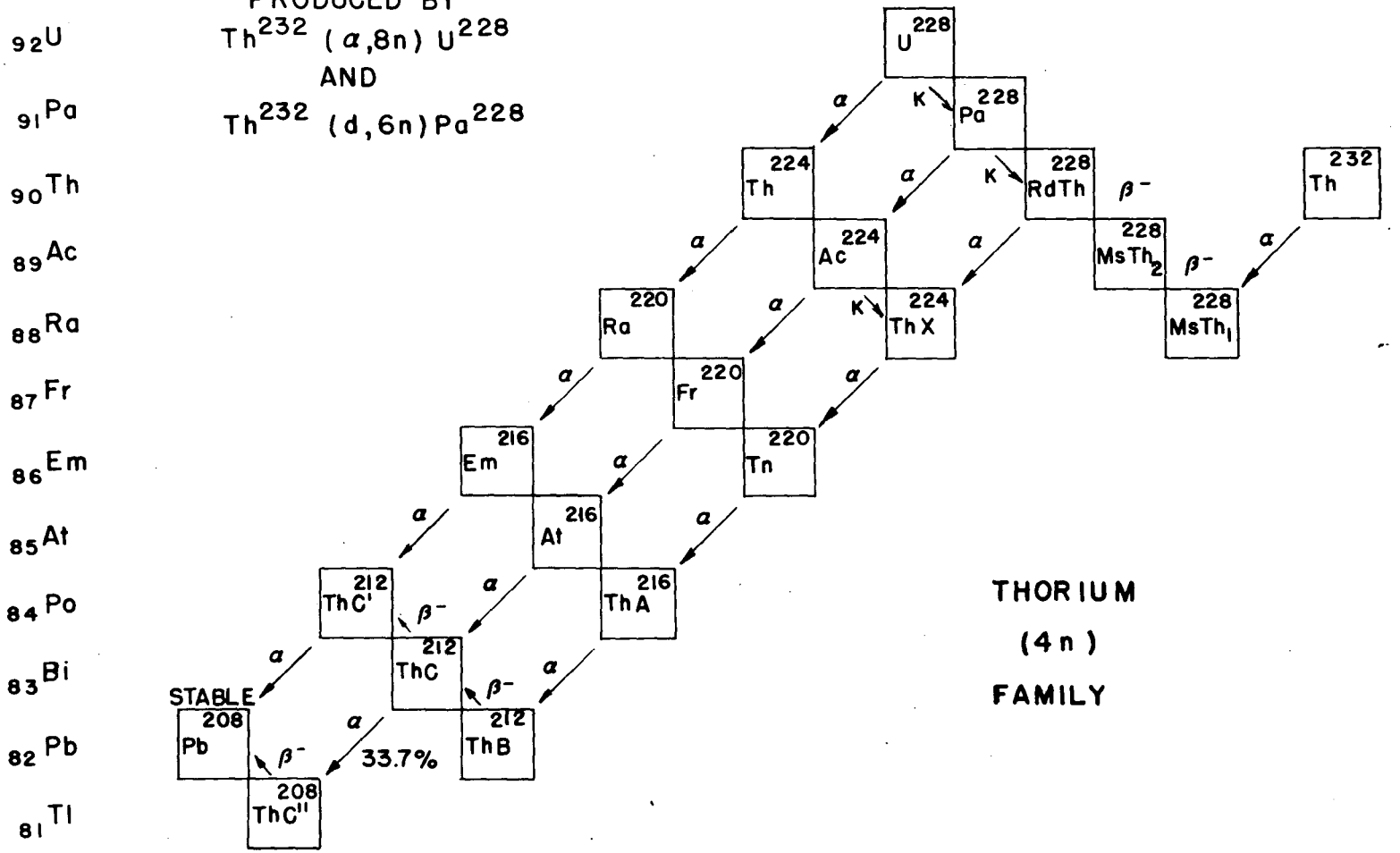

FIG. 42

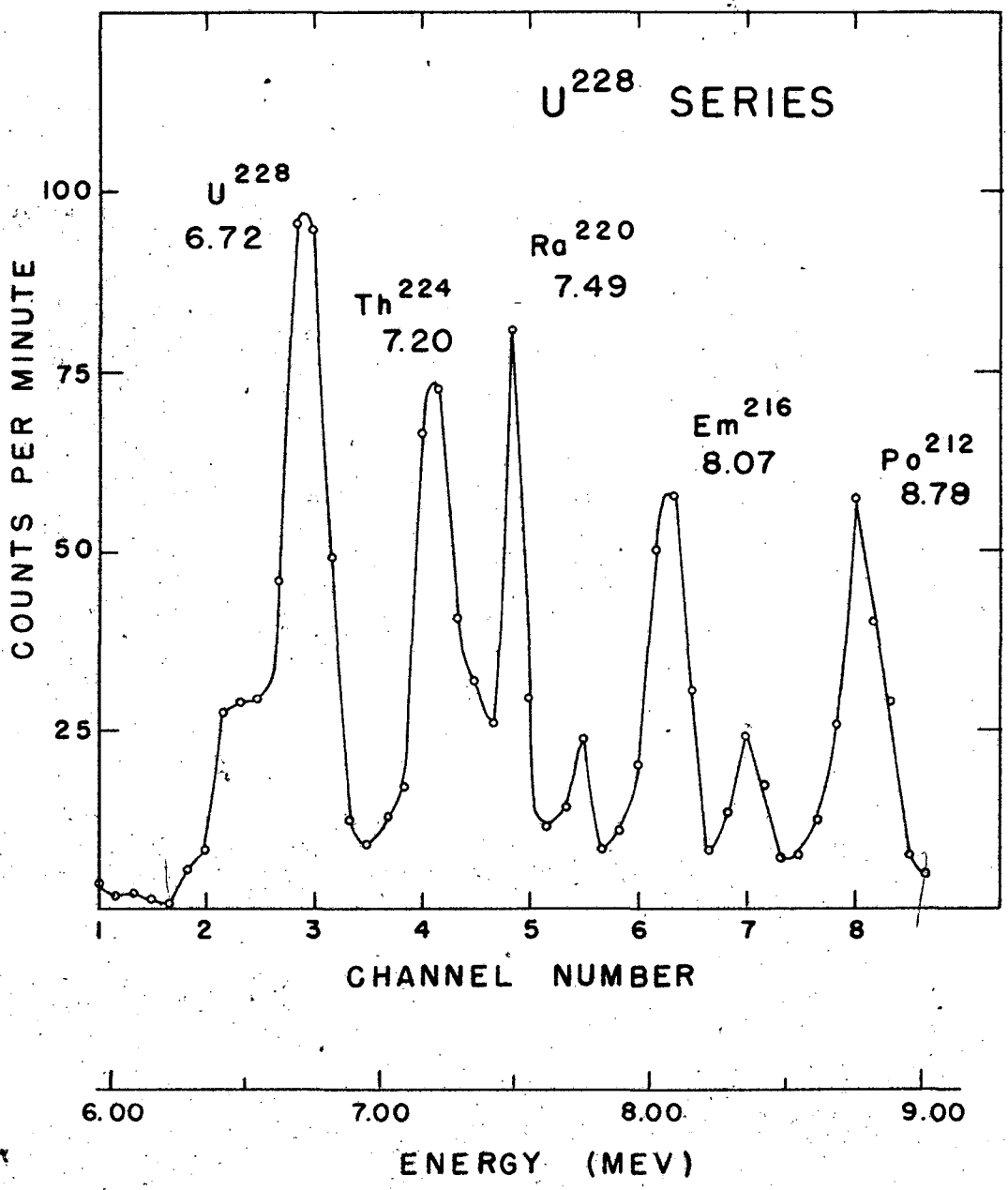

Fig. 43. Alpha-pulse analysis curve of the U^{228} series in the uranium fraction of a seven minute, 120-Mev alpha-particle bombardment of thorium metal. This two minute count started 21 minutes after shutdown and used a #3 collimator with a Zapon coating for collimation. Contaminating peaks are those of the U^{229} series.

Fig. 44 Alpha-pulse analysis curves showing the decay of the U^{228} series, leaving the U^{229} series. Pulse analysis made on the uranium fraction of a seven-minute, 120-Mev alpha particle bombardment of thorium metal.

Sample A was counted for two minutes, starting 21 minutes after shutdown.

Sample B was counted for two minutes, starting 36 minutes after shutdown.

Sample C was counted for four minutes, starting 65 minutes after shutdown.

A #3 collimator with Zapon covering was used for collimation.

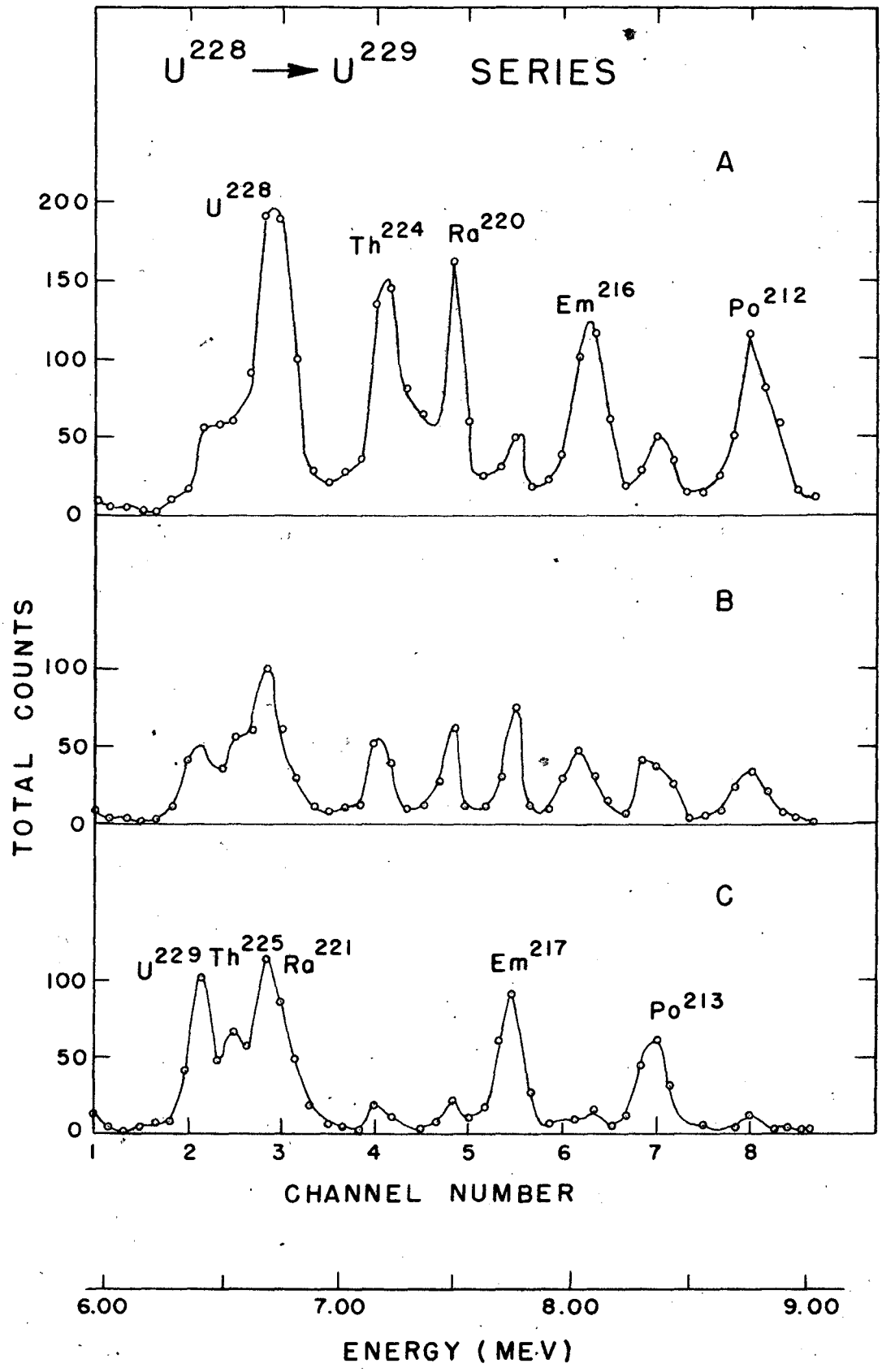
U228 → U229 SERIES
A
B
C
U228
Th224
Ra220
Em216
Po212
U229 Th225 Ra221
Em217
Po213
TOTAL COUNTS
CHANNEL NUMBER
ENERGY (MEV)
6.00
7.00
8.00
9.00

Fig 44

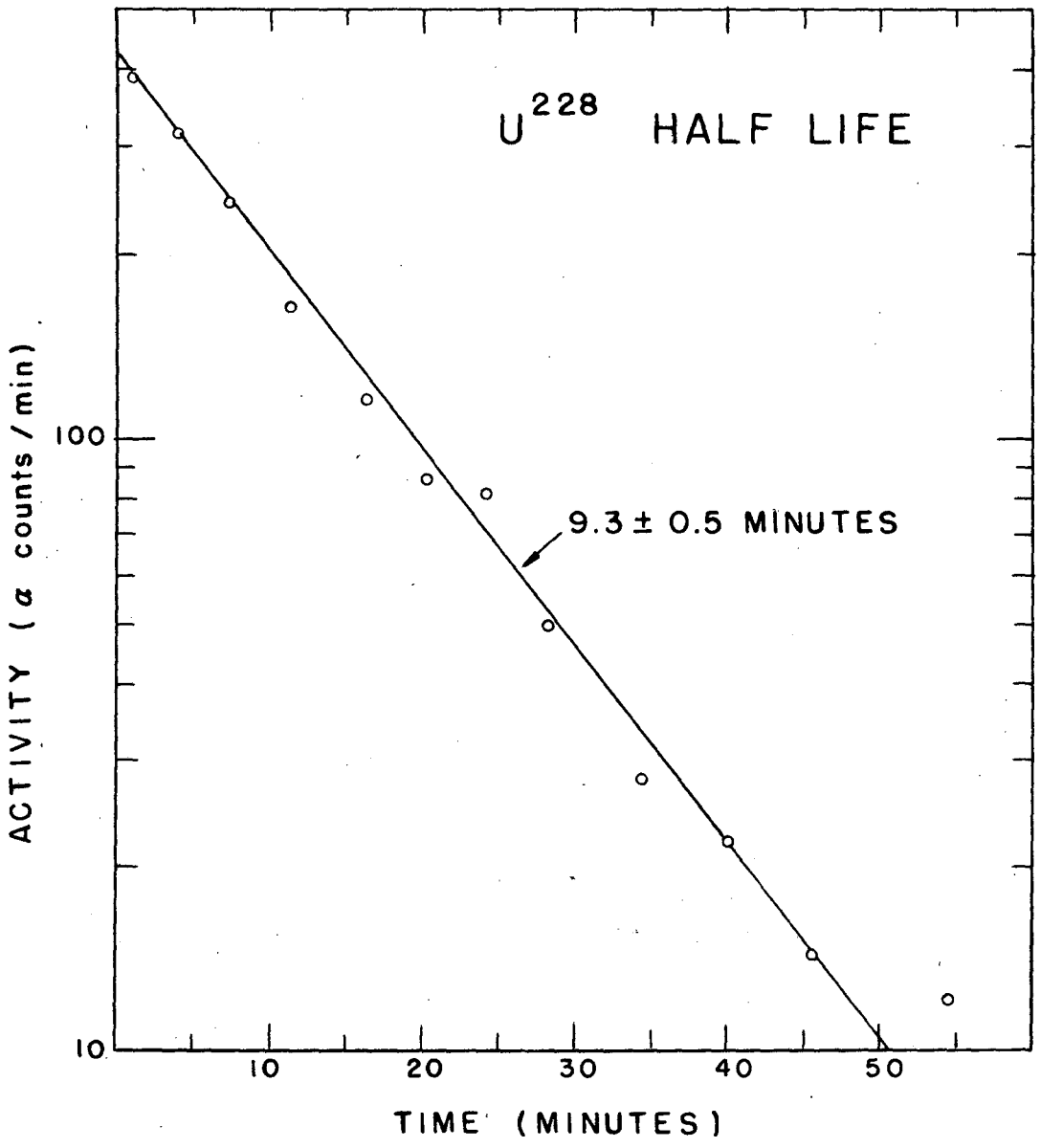

Fig. 45. Determination of the half-life of U^{228} from the decay of the Th^{224} and Ra^{220} peaks from pulse analysis curves shown in part in Fig. 44.

Since this chain decays directly into a stable lead isotope, the longest-lived member of the entire chain being the parent, the only way in which we can positively identify the series chemically is by branching decays of its members. We have been able to chemically milk Pa^{228} from the decay products of a large amount of this series, after first having taken special precautions to remove by TTA-benzene extractions all Pa^{228} formed in the original bombardment.

The chemistry used involved separation of the uranium fraction from a 10-minute thorium metal bombardment by ether extraction from saturated ammonium nitrate solution, washing of the ether with three portions of saturated ammonium hitrate, and finally washing the uranium back into pure water. This water was then made 6 N in nitric acid and was extracted three times with double volumes of TTA-benzene solutions to eliminate any small traces of Pa^{228} which might have come through the ether extraction. Tracer Pa^{231} was then added to check chemical yield and a small aliquot of the water taken for pulse analysis and determination of the U^{228} activity. After standing 20 minutes the solution was again stirred with a TTA-benzene solution, this time to extract the daughter Pa^{228}, and the organic layer was plated and counted.

The results of this milking experiment are very poor and were never repeated although the experiment is not too difficult a one. The pulse analysis of the U^{228} sample was poor in resolution and indefinite in geometry (since a #3 collimator was used and its geometry was not accurately known). The protactinium plate gave only about 0.4 counts per minute of Pa^{228} with 73% recovery of the tracer. The ratio of K/α reported in the table as 0.25 may be very much in error and is presented only as evidence that there is some orbital electron branching. This milking experiment will definitely be repeated.

2. Other members of the U^{228} Series None of the other members of this series have been investigated for half-lives. The alpha energies were all determined by pulse analyses. We intend to investigate these short half-lives with the rotating disc and electronic measuring devices.

F. The U^{229} Series

After the U^{228} series has decayed out of a uranium sample from an alpha bombardment of thorium, this 58 minute series dominates the pulse analyses for a matter of several hours until it gives way to the U^{230} series. This U^{229} series is shown in block diagram in Fig. 46. On pulse analysis we obtain a sample with three poorly resolved short range peaks and the two longer range ones as shown in Fig. 47. The presence and decay of the series can be determined by observing the Po^{213} long range alpha peak. Within a few hours this series in turn gives way to the U^{230} series as shown in Fig. 48. A summary of isotope data for the U^{229} series is given in Table 6. The radioactive properties of Po^{213} and Pb^{209} are the accepted literature values.[7]

Table 6

U^{229} Collateral Series Data

Isotope	Type of Radiation	Half-Life	Energy of Radiation (Mev)
U^{229}	α	58 ± 3 min	6.42
Th^{225}	α	8.0 ± 0.5 min	6.57
Ra^{221}	α	31 ± 1.5 sec	6.71
Em^{217}	α	10^{-3} sec $\pm$ 10%	7.74
Po^{213}	α	4.2×10^{-6} sec	8.336
Pb^{209}	β^-	3.32 hr	0.70
Bi^{209}	Stable		

ARTIFICIAL COLLATERAL RADIOACTIVE SERIES

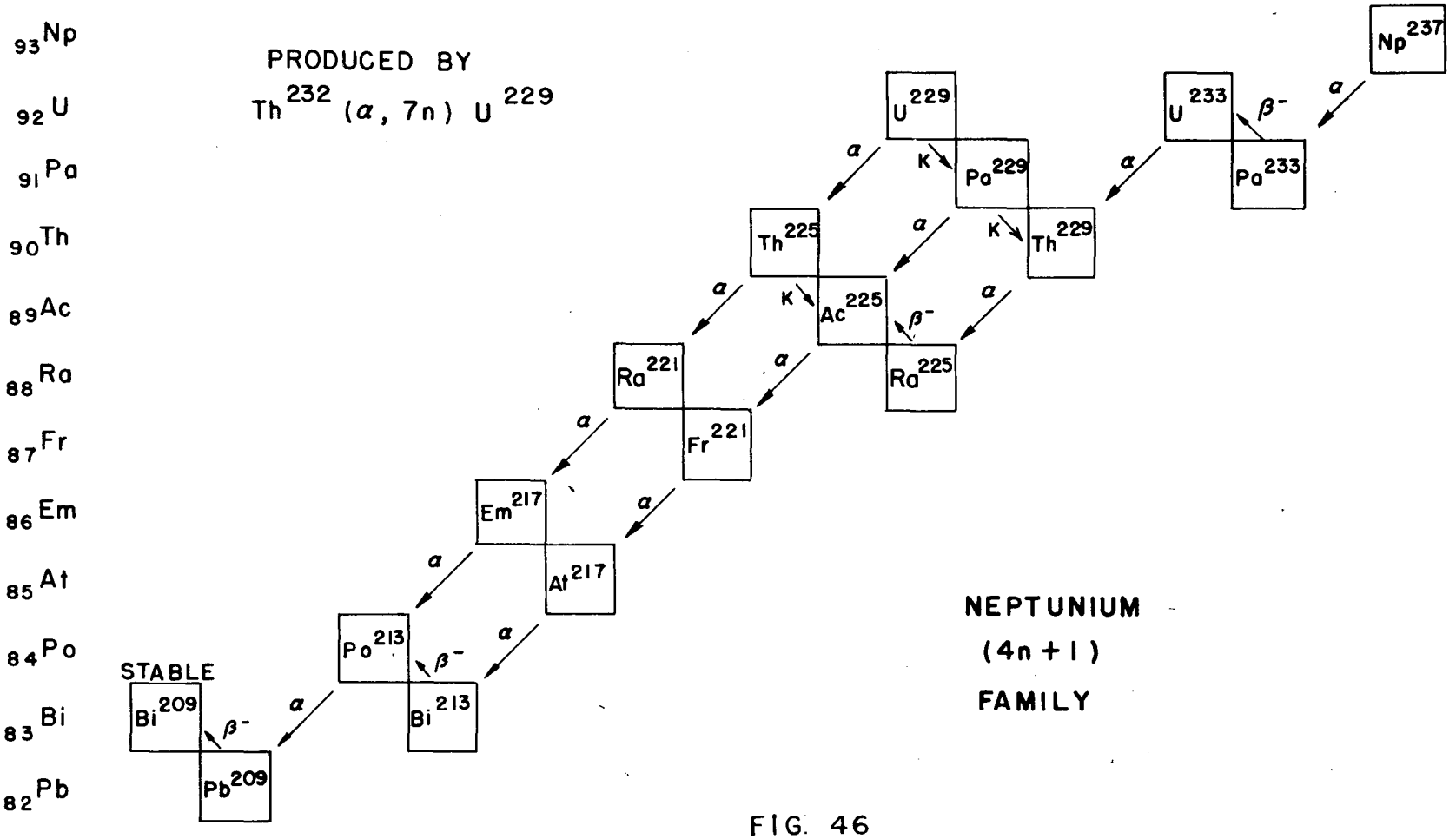

FIG. 46

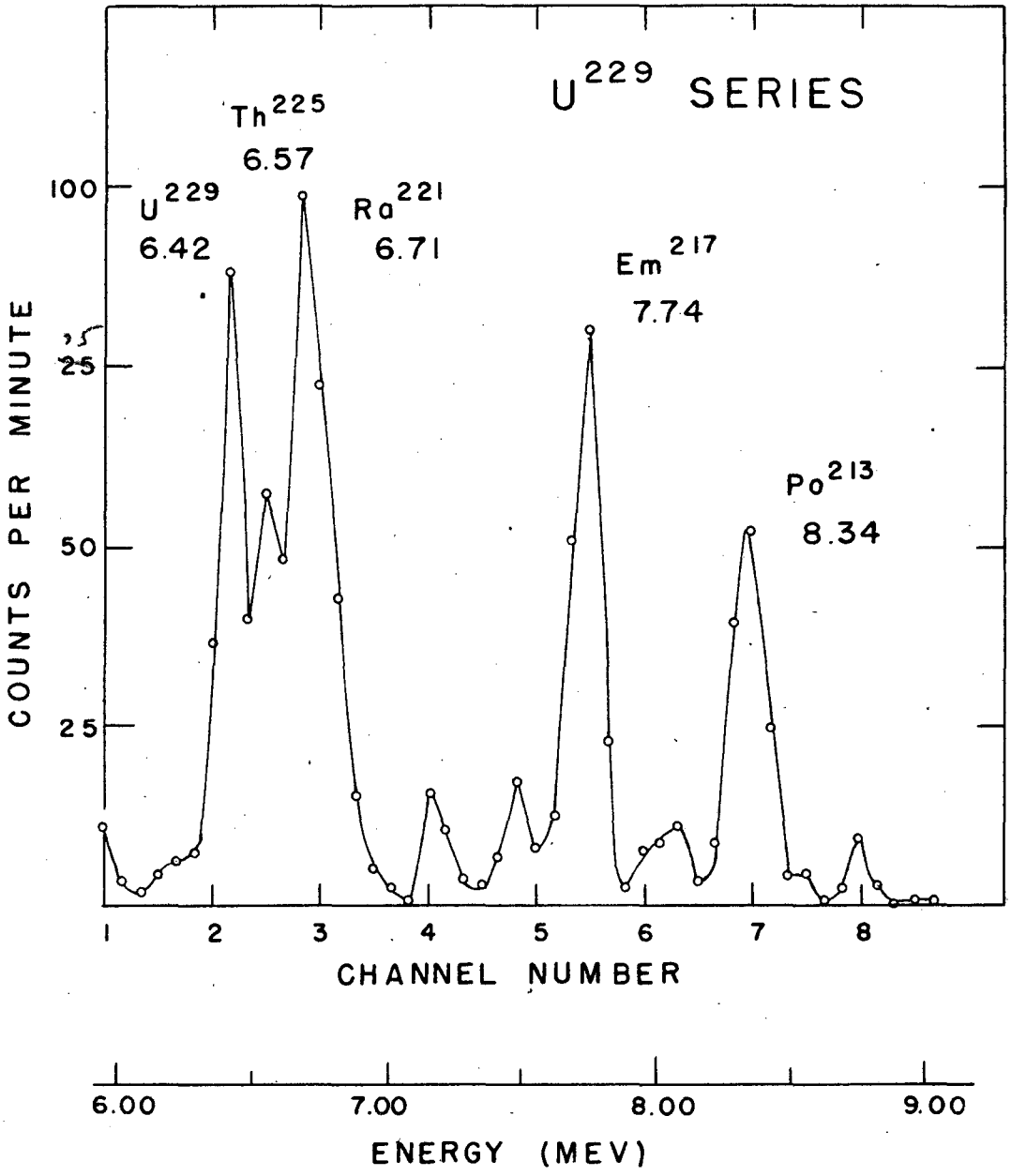

Fig. 47. Alpha-pulse analysis curve of the U^{229} series in the uranium fraction of a seven minute, 120-Mev alpha-particle bombardment of thorium metal. This four minute count started 65 minutes after shutdown and used a #3 collimator with Zapon covering for collimation.

Fig. 48. Alpha-pulse analysis curves showing the decay of the U^{229} series, leaving the U^{230} series. Pulse analysis made on the uranium fraction of a 45-minute, 120-Mev alpha-particle bombardment of thorium metal.

Sample A was counted for 7 minutes, starting one hour after shutdown.

Sample B was counted for 10.4 minutes, starting four hours after shutdown.

Sample C was counted for 10 minutes, starting eight hours after shutdown.

No collimation was used.

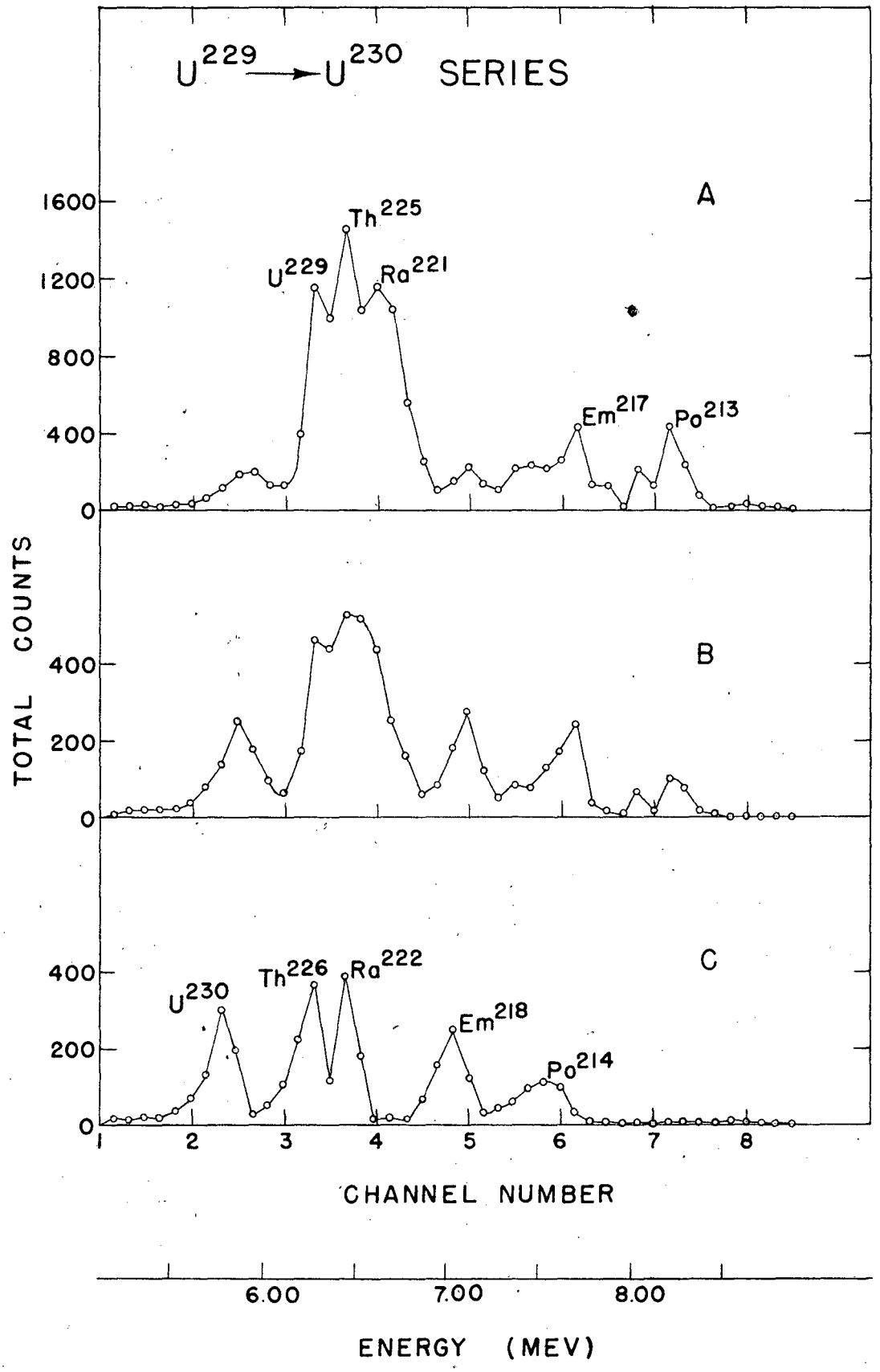
U229 → U230 SERIES
A
B
C
Th225
U229
Ra221
Em217
Po213
U230
Th226
Ra222
Em218
Po214
1600
1200
800
400
0
400
200
0
400
200
0
TOTAL COUNTS
1
2
3
4
5
6
7
8
CHANNEL NUMBER
6.00
7.00
8.00
ENERGY (MEV)

Fig 4'3

1. U^{229} By following the decay of the alpha counts in the U^{229}, Th^{225} and Ra^{221} peaks (as well as the decay of whatever grows into these peaks) on pulse analysis curves we were able to obtain a half-life for this isotope of 58 ± 3 minutes. The decay points and resolution for these peaks are shown in Fig. 49.

In checking the branching ratio of this isotope we patterned our chemistry after that used for U^{228} although time was not such a factor here. To eliminate any influence of U^{228} decay into Pa^{228} in the milking, the target was allowed to stand for one hour after shutdown. It was then worked up for the uranium fraction, purified as usual with three ammonium nitrate washes, and then subjected to further purification from protactinium by four washes of TTA-benzene solutions. The sample was then allowed to decay for 3.5 hours, at the end of which time the protactinium was separated with TTA-benzene, and the Pa^{231} tracer and Pa^{229} daughter pulse analyzed. Pulse analysis of aliquots at the beginning of the milking decay determined the amount of U^{229} present originally. The value for K/α of about 5 (if the K/α ratio of Pa^{229} is 100) is a fair value, the limiting factor being the determination of the initial amount of U^{229} in the sample.

2. Th^{225} By following the decay of the Po^{213} peak on pulse analysis of several recoil samples grown for a short time from a large amount of U^{229}, we were able to determine the half-life of this isotope to be 8.0 ± 0.5 minutes as shown in Fig. 50.

The branching ratio of this isotope was found by a method similar to that used for Ac^{223}. A recoil sample was grown for 3.5 hours from a plate of the U^{229} series. The short-lived activities were allowed to decay out by letting the sample stand for 9.5 days and then pulse analyzing it to determine the amount of Ac^{225} and series present (from the orbital electron capture branching of Th^{225}). The amount of Th^{225} daughter activity recoiling off the U^{229} plate was determined by several short recoil experiments in the same manner as for Ac^{223}.

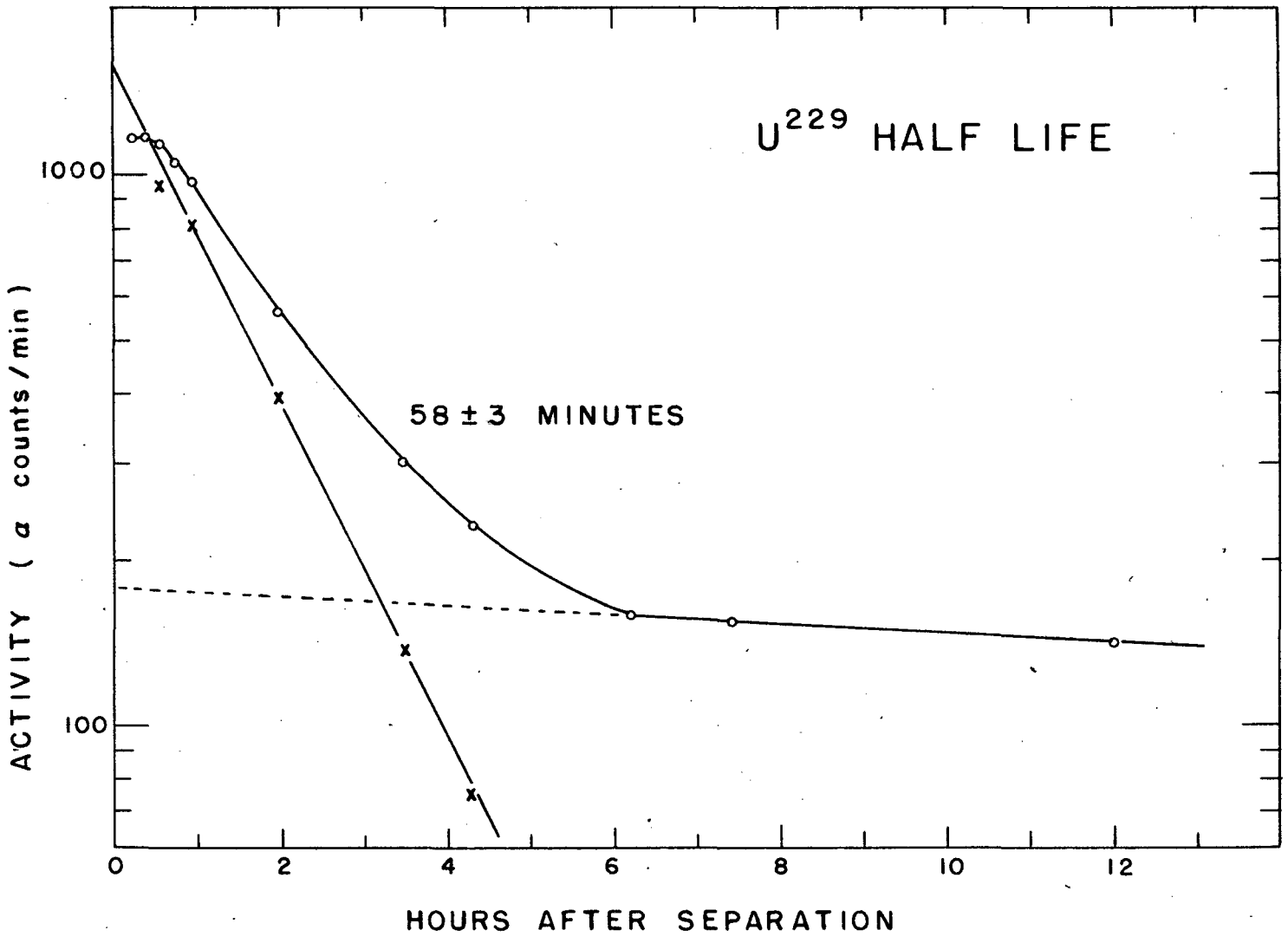

Fig. 49. Determination of the half-life of U^{229} from the decay of the U^{229}, Th^{225}, and Ra^{221} peaks from pulse analysis curves shown in part in Fig. 48.

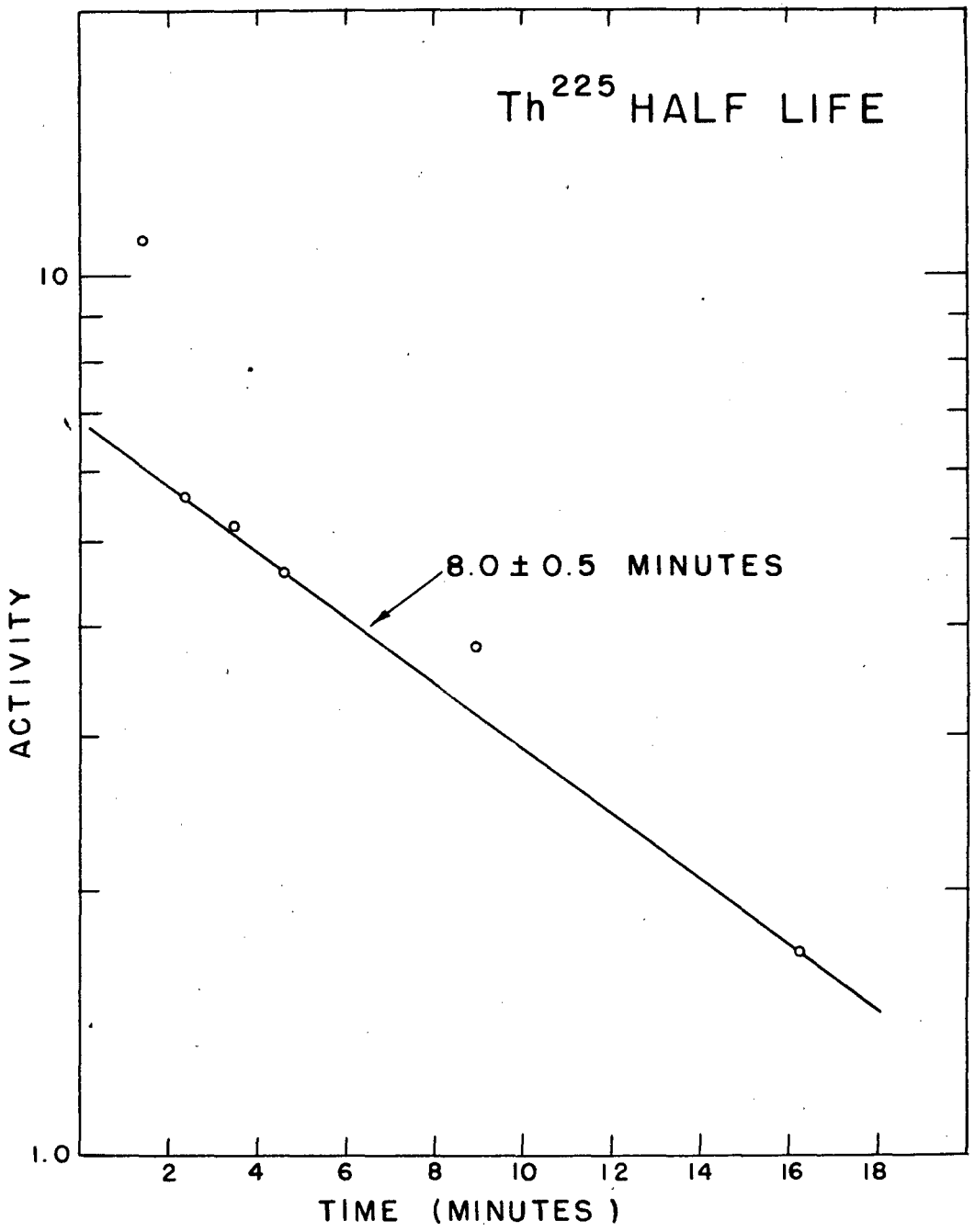

Fig. 50. Determination of the half-life of Th^{225} from the decay of the Po^{213} peak in a U^{229} recoil sample.

The sample of U^{229}, however, was not as active as is desirable for this type of experiment since it was separated from a poor bombardment. Consequently only 0.4 counts per minute of Ac^{225} were found on the recoil plate. It would seem then that our value of 0.12 for the K/α branching ratio of this isotope might be considerably in error. This milking experiment would bear repeating when a good alpha bombardment can be obtained from the 184-inch cyclotron.

3. Ra^{221} Two types of recoil experiments were made to obtain the 30 ± 2 second half-life of this isotope. By using the rotating disc method we obtained a half-life value of 31.7 seconds (Fig. 51). These points have been corrected for the decay of the parent during the time of the experiment and also for the 25% contamination of 38 second Ra^{222} present from the U^{230} series.

The other method involves manual transference of the recoil sample to an alpha counter and following of its decay long enough to resolve any long-lived tail and obtain the required half-life. Fig. 52 shows the result of a run by this method in which the indicated half-life has not yet been corrected for the 10% Ra^{222} contamination present. Only a few representative points have been put on the graph. Actually counts were taken every 0.05 minutes and recorded on a trafficounter. With such a relatively low counting rate and such a short interval between counts, the statistical fluctuations are considerable, as can be seen from the figure. To minimize these fluctuations we have plotted these data on an integral curve in Fig. 53. (This is the same method used by Studier and Hyde in the evaluation of their Ra^{222} data[8].) Each count was corrected for background and these values summed up to a time t. The summed values of counts were plotted against t and the value which they approached was taken as A_∞. In the integral curve, then, we plotted the difference between this A_∞ (the total number of counts observed on complete decay) and A_t (the total number of counts observed to a certain time t). A plot of this value on a logarithmic scale against time determines a half-life of 30 ± 2 seconds for the activity. It can be seen that the statistical variations in the data have been

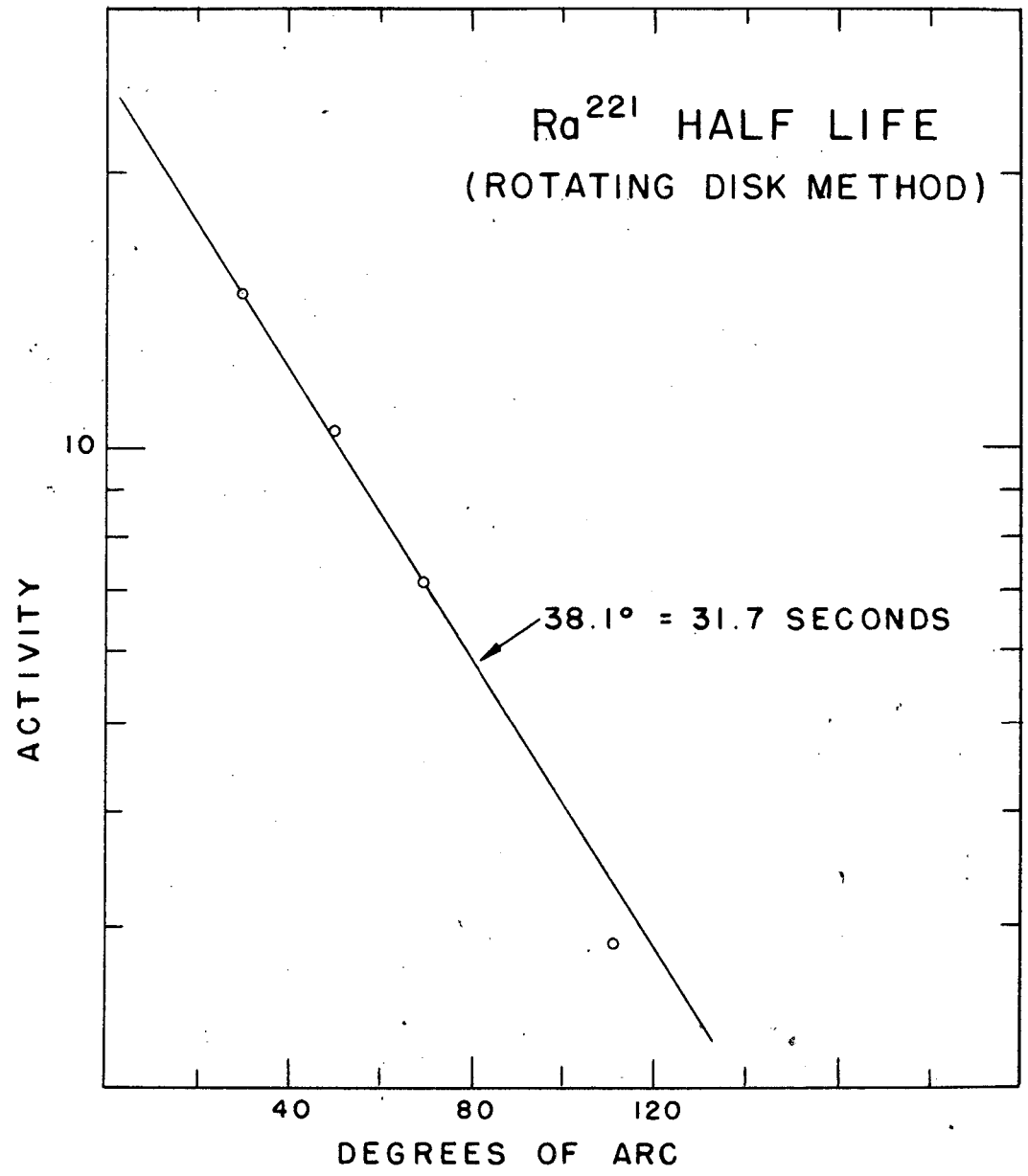

Fig. 51. Determination of the half-life of Ra^{221} by the rotating disc recoil method.

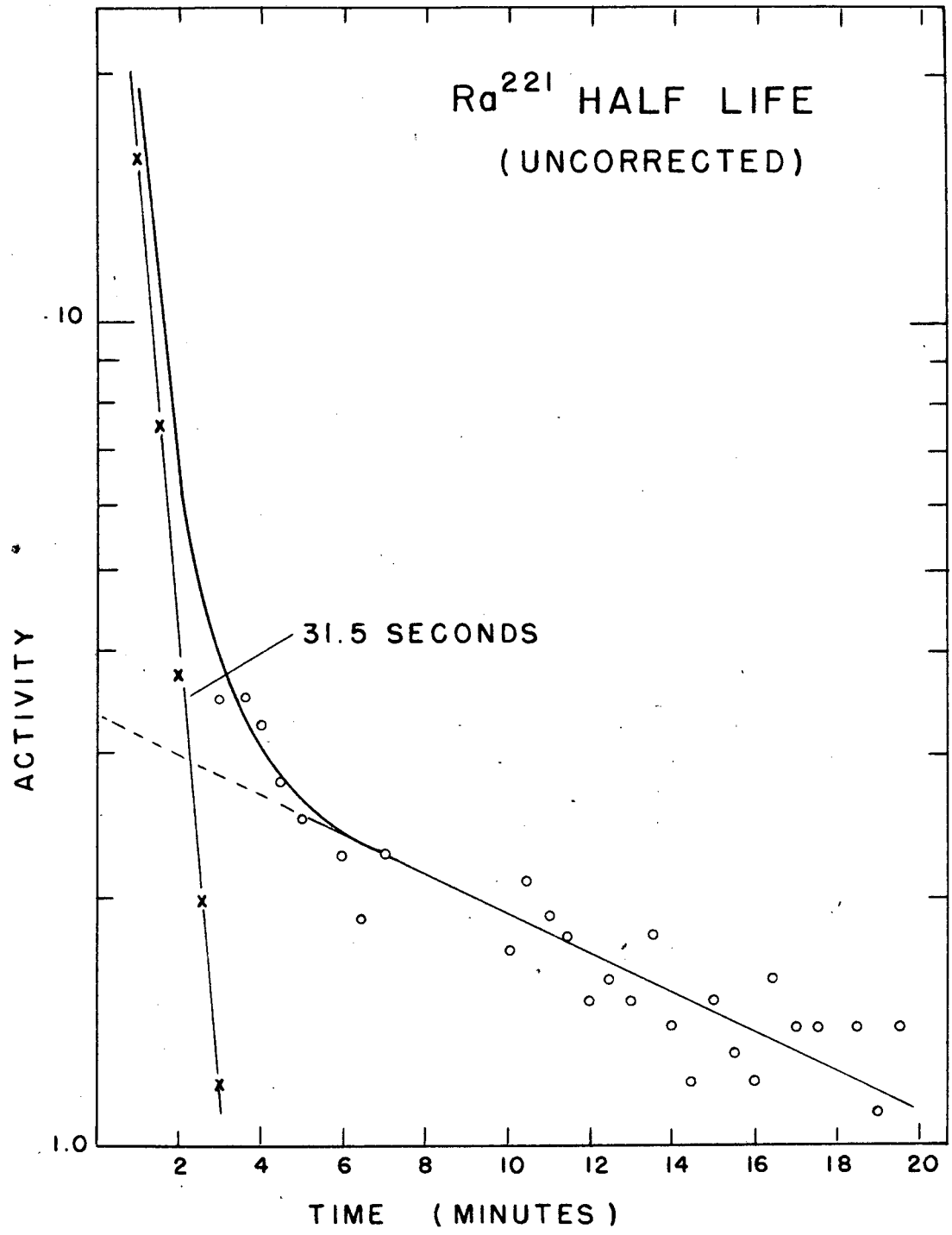

Fig. 52. Determination of the half-life of Ra^{221} by resolution from the gross decay of a recoil sample from a large amount of the U^{229} series.

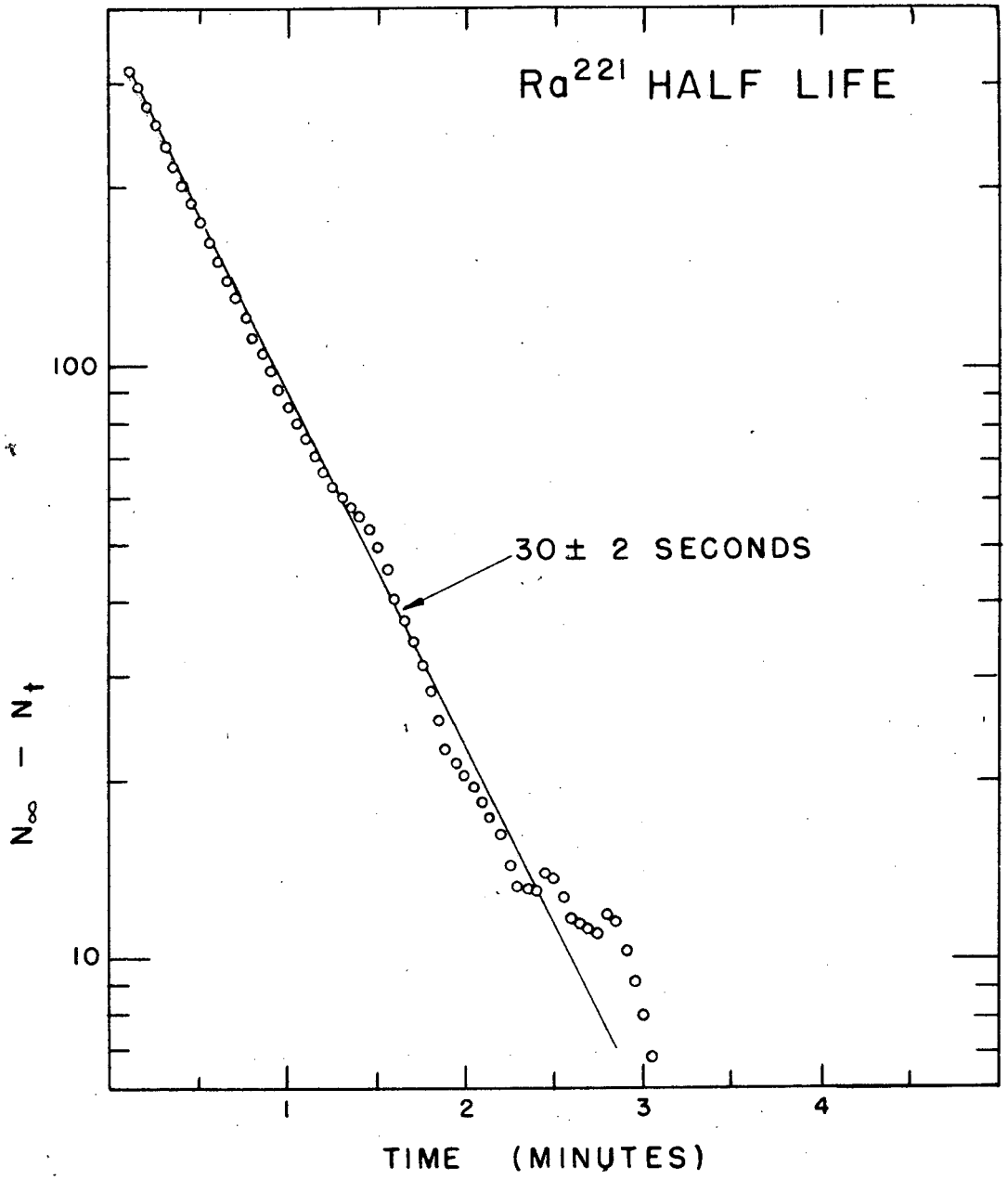

Fig. 53. Decay curve of Ra^{221}. N_∞ = total number of observed counts. N_t = number of observed counts within the time interval t.

greatly reduced. By this method it is also possible to eliminate the usual differential plotting error introduced in counting a sample for an appreciable part of its half-life.

4. Em^{217} By electronic measurements the half-life for this isotope has been determined to be one millisecond within about 10%.

V. Discussion of Results

A study of alpha systematics curves shows the regularity of the energies and half-lives of these collateral series alpha emitters and also serves to point out irregularities which may be the result of experimental error. With the kind permission of Professor I. Perlman, I am including four of the systematics curves which are published in the paper by Perlman, Ghiorso and Seaborg on "Systematics of Alpha-Radioactivity"[15]. Fig. 54 shows a plot of alpha disintegration energy (including the energy of recoil) against mass number for the known alpha emitters. Fig. 55 shows a plot of half-life against alpha disintegration energy for even-even nuclei; Fig. 56 for even-odd nuclei; and Fig. 57 for odd-even and odd-odd nuclei. (Even-odd denotes an even number of protons and an odd number of neutrons, etc.)

Predicted values which are included in the preceeding tables of experimental results were obtained from the above curves. If the particle energy was observed, the disintegration energy was calculated from it and the half-life read off the suitable curve. When both energy and half-life were predicted, the energy was first predicted from Fig. 54, and then used to predict the half-life.

No unambiguous Geiger counting has been done on any of these series. In our first bombardments our chemistry was not clean enough to give good Geiger results. It would now be possible, however, using Procedures 91-1 and 92-1 in Appendix II, to obtain pure protactinium and uranium fractions free from any contaminating Geiger activity. There undoubtedly are gamma rays associated with some of the isotopes of these collateral series and their presence should be investigated now

Fig. 54. Alpha-energy vs. mass number. Relationships of the Heavy Nuclides.
(From Perlman, Ghiorso and Seaborg, Phys. Rev. January 1, 1950, in press.)

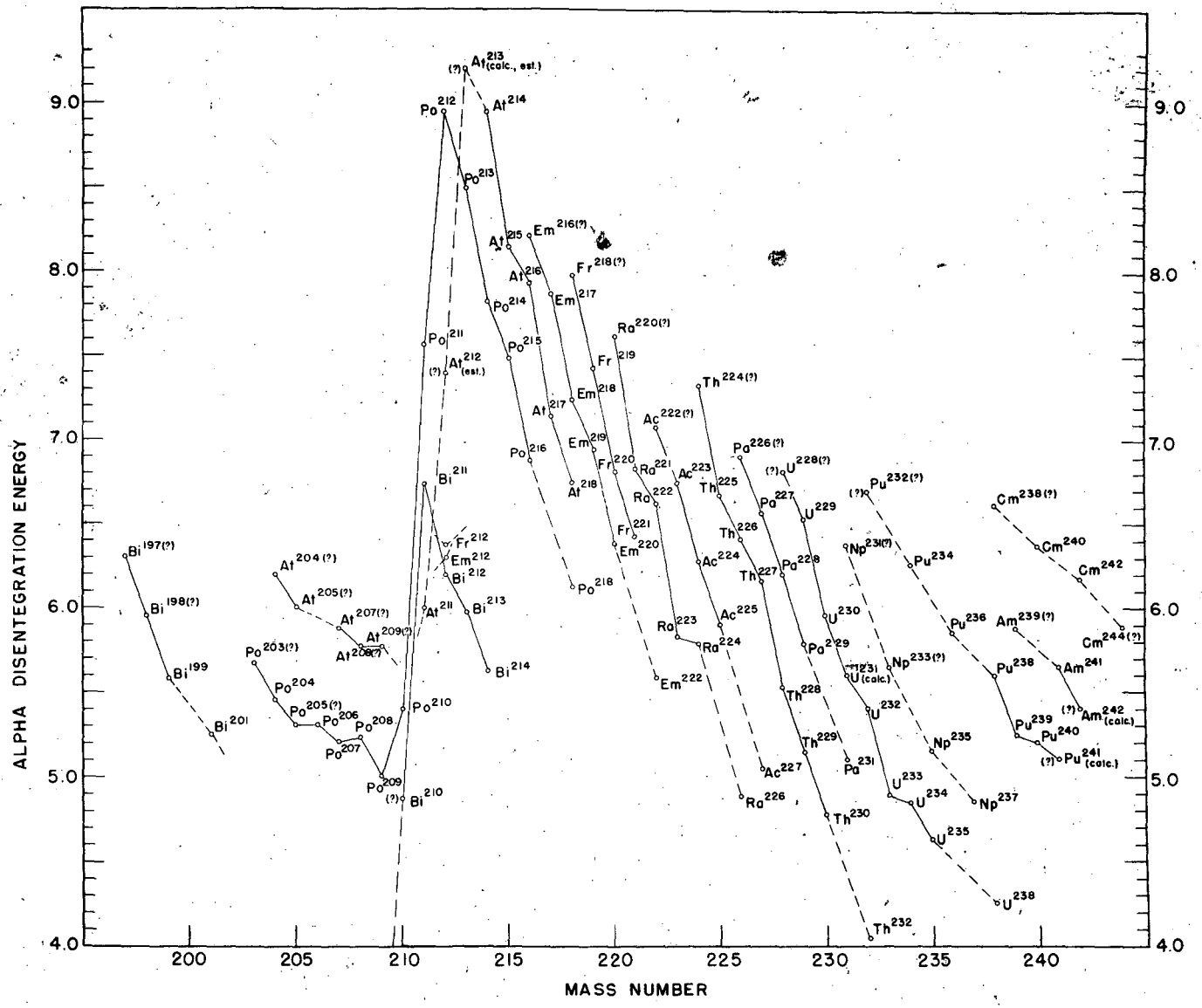
ALPHA DISENTEGRATION ENERGY
MASS NUMBER
9.0
8.0
7.0
6.0
5.0
4.0
200
205
210
215
220
225
230
235
240
Bi197(?)
Bi198(?)
Bi199
Bi201
At204(?)
At205(?)
At207(?)
At209(?)
At208(?)
Po203(?)
Po204
Po205(?)
Po206
Po207
Po208
Po209
Po210
Bi210
At211
Bi211
At212 (est.)
Fr212
Em212
Bi212
Bi213
Bi214
At213 (calc., est.)
Po212
At214
Po213
At215
Em216(?)
At216
Fr218(?)
Em217
Po214
Po215
Ra220(?)
Fr219
Po211
Em218
At217
Th224(?)
Ac222(?)
Em219
Fr220
Po216
Ra221
At218
Pa226(?)
U228(?)
Ra222
Ac223
Th225
Fr221
Em220
Pa227
U229
Po218
Th226
Ac224
Th227
Pa228
Em222
Ra223
Ac225
U230
Ra224
Pa229
Th228
U232
Ac227
Th229
Pa231
U233
Ra226
Th230
U234
U235
U238
Th232
Pu232(?)
Np230(?)
Pu234
U231 (calc.)
Np233(?)
Cm238(?)
Cm240
Cm242
Pu236
Am239(?)
Cm244(?)
Pu238
Am241
Pu239
Am242 (calc.)
Pu240
Pu241 (calc.)
Np235
Np237

Fig. 55. Half-life vs. energy relationship for the even-even nuclides. (Roman numerals indicate short-range groups in fine structure and "0" the ground state transition).

(From Perlman, Ghiorso, and Seaborg, Phys. Rev. January 1, 1950, in press).

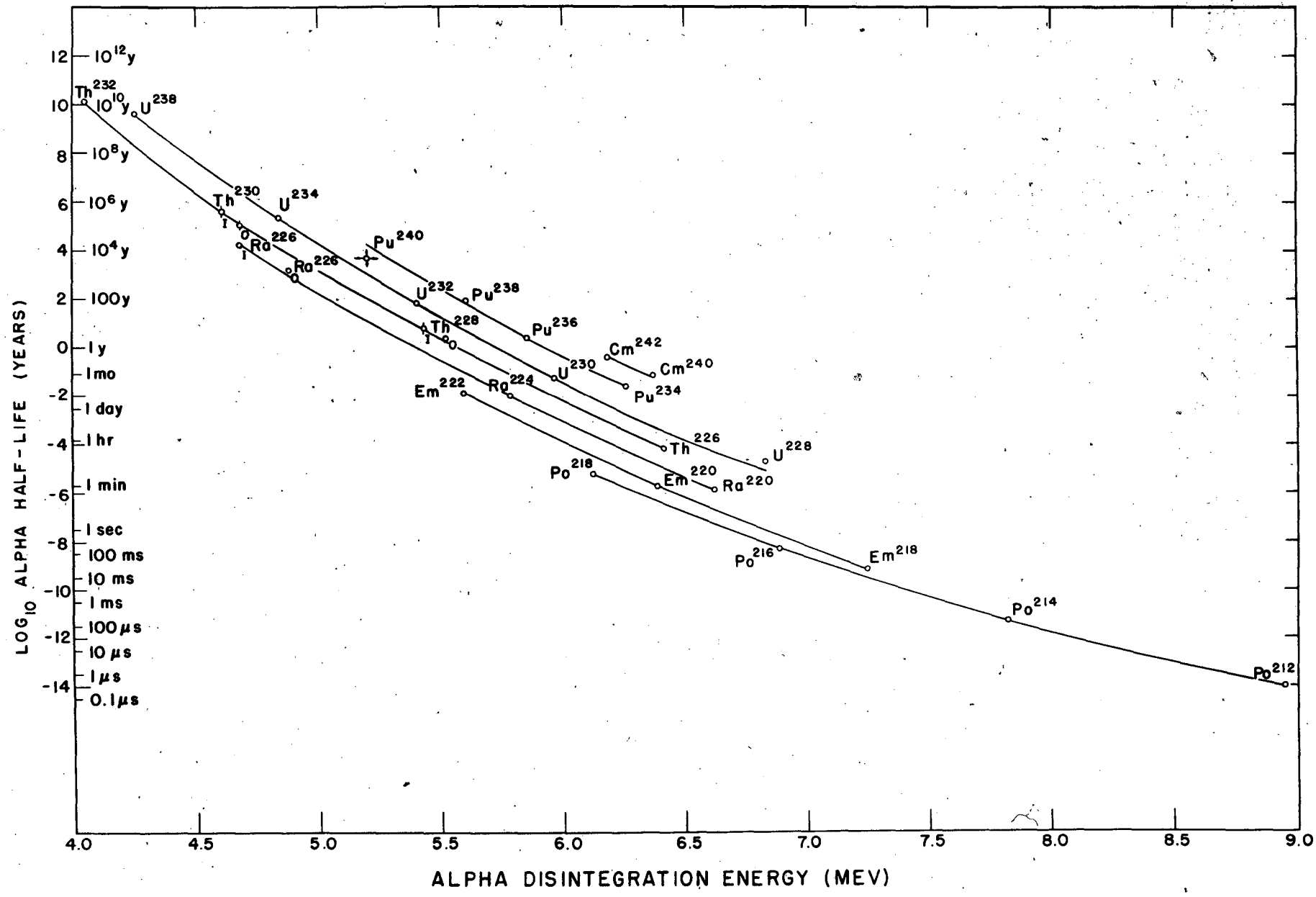
LOG10 ALPHA HALF-LIFE (YEARS)
12
10
8
6
4
2
0
-2
-4
-6
-8
-10
-12
-14
10^12 y
10^10 y
10^8 y
10^6 y
10^4 y
100 y
1 y
1 mo
1 day
1 hr
1 min
1 sec
100 ms
10 ms
1 ms
100 μs
10 μs
1 μs
0.1 μs
Th232
U238
Th230
U234
Ra226
Pu240
Ra226
U232
Pu238
Th228
Pu236
Cm242
Cm240
U230
Pu234
Em222
Ra224
Th226
U228
Po218
Em220
Ra220
Po216
Em218
Po214
Po212
4.0
4.5
5.0
5.5
6.0
6.5
7.0
7.5
8.0
8.5
9.0
ALPHA DISINTEGRATION ENERGY (MEV)

OZ 622

Fig. 56. Half-life vs. energy relationship of the even-odd nuclides. (Roman numerals indicate short-range groups in fine structure and "0" the ground state transition).

(From Perlman, Ghiorso, and Seaborg, Phys. Rev. January 1, 1950, in press.)

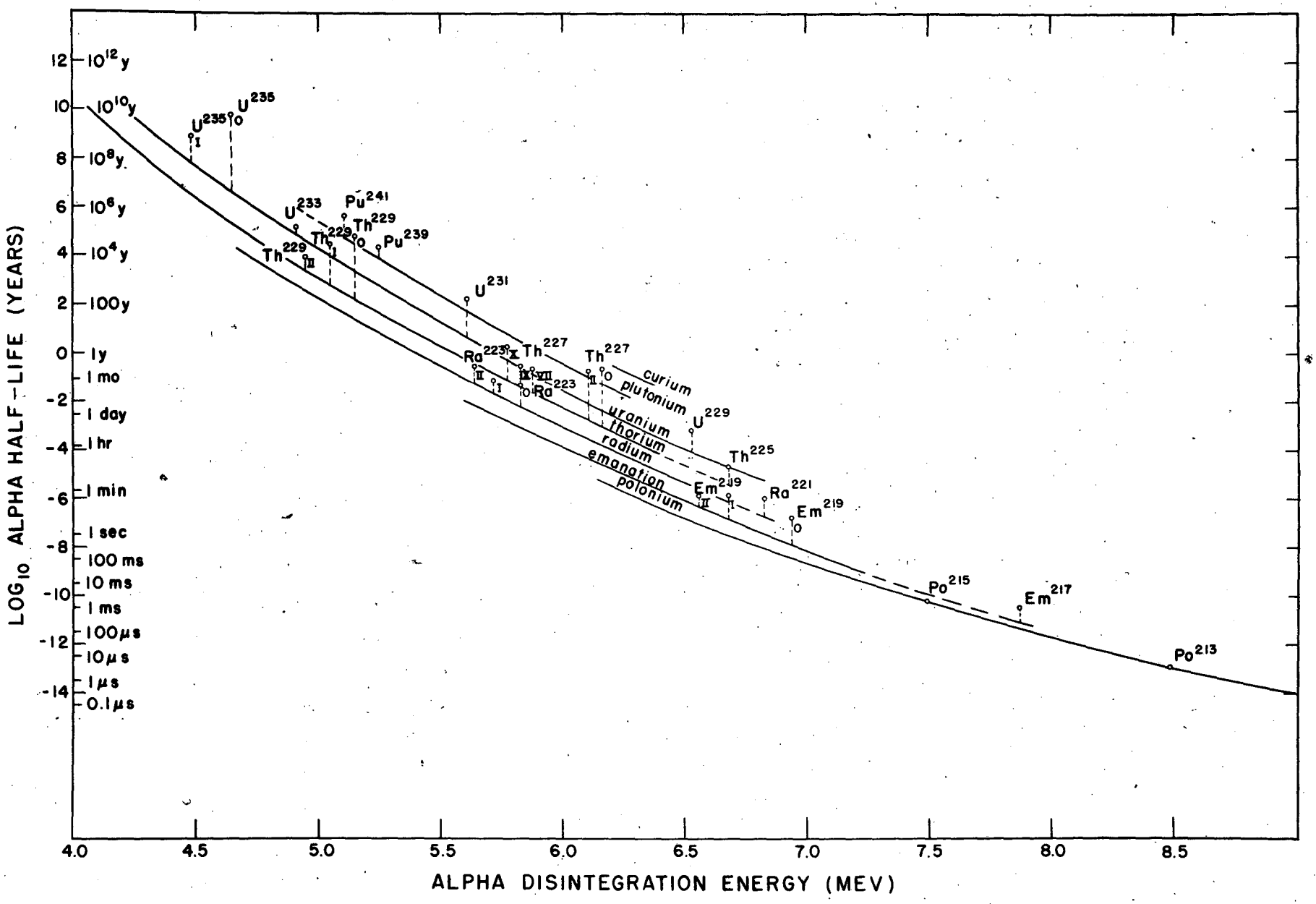
LOG10 ALPHA HALF-LIFE (YEARS)
12 10^12 y
10 10^10 y
8 10^8 y
6 10^6 y
4 10^4 y
2 100 y
0 1 y
-2 1 mo
-4 1 day
-6 1 hr
-8 1 min
-10 1 sec
-12 100 ms
-14 10 ms
1 ms
100 μs
10 μs
1 μs
0.1 μs
4.0
4.5
5.0
5.5
6.0
6.5
7.0
7.5
8.0
8.5
ALPHA DISINTEGRATION ENERGY (MEV)
U235 I
U235 O
U235
U233
Pu241
Th229
Th229 I
Th229 II
Th229
Pu239
U231
Ra223 II
Ra223 I
Ra223
Th227
Th227 II
Th227 O
Th227
curium
plutonium
uranium
thorium
radium
emanation
polonium
U229
Th225
Ra223 O
Ra223
Em219 II
Em219 I
Ra221
Em219 O
Em219
Po215
Em217
Po213

Fig. 57. Half-life vs. energy relationship for the odd-even and odd-odd nuclides. (Roman numerals indicate short-range groups in fine structure and "0" the ground state transition).

(From Perlman, Ghiorso, and Seaborg, Phys. Rev. January 1, 1950, in press.)

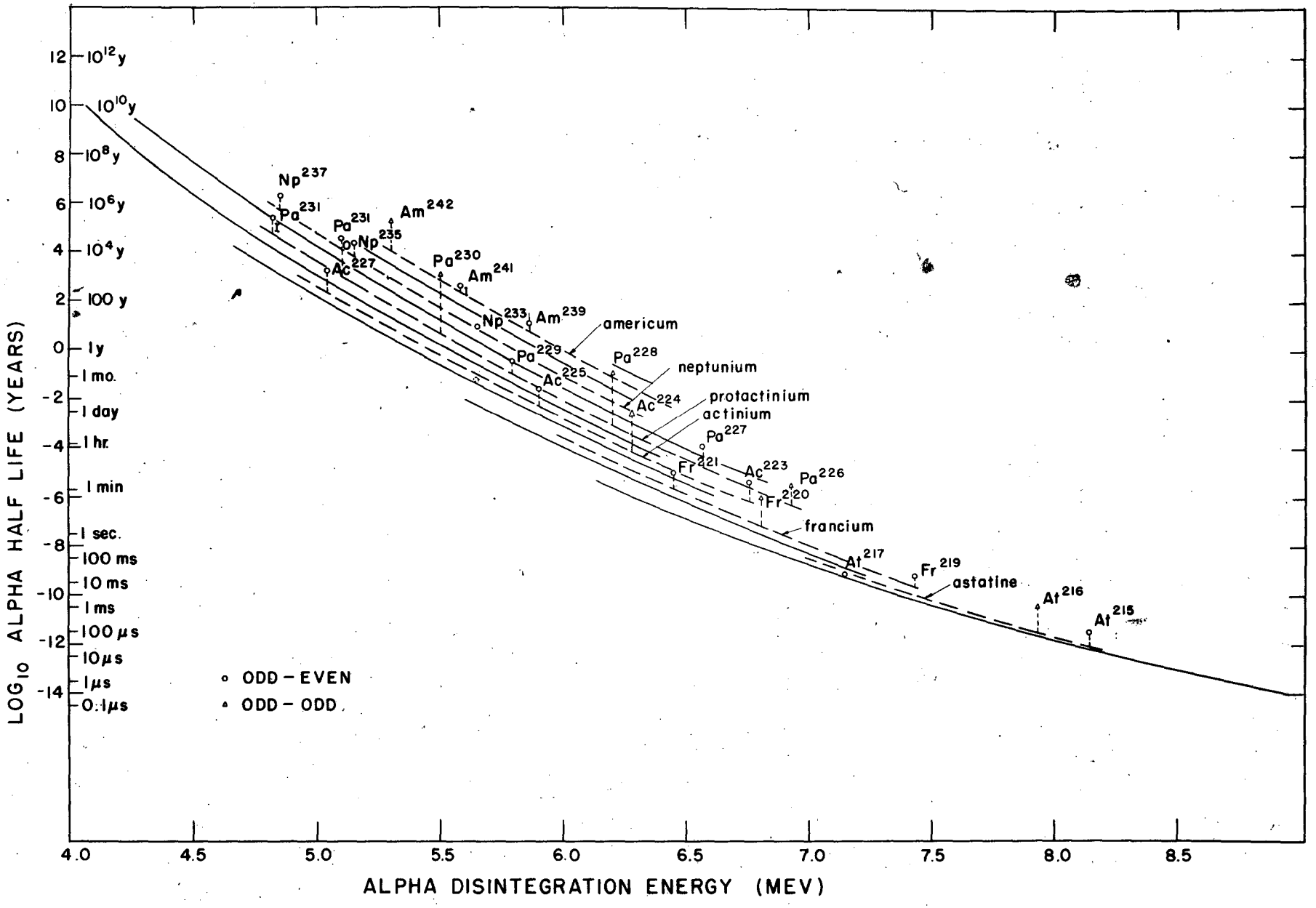
LOG10 ALPHA HALF LIFE (YEARS)
12
10
8
6
4
2
0
-2
-4
-6
-8
-10
-12
-14
10^12 y
10^10 y
10^8 y
10^6 y
10^4 y
100 y
1 y
1 mo.
1 day
1 hr.
1 min
1 sec.
100 ms
10 ms
1 ms
100 μs
10 μs
1 μs
0.1 μs
o ODD – EVEN
▲ ODD – ODD
Np237
Pa231
Pa231
Am242
Np235
Ac227
Pa230
Am241
Np233
Am239
americum
Pa229
Pa228
neptunium
Ac225
Ac224
protactinium
actinium
Pa227
Fr221
Ac223
Pa226
Fr220
francium
At217
Fr219
astatine
At216
At215
4.0
4.5
5.0
5.5
6.0
6.5
7.0
7.5
8.0
8.5
ALPHA DISINTEGRATION ENERGY (MEV)

07621

that clean chemistry has been worked out.

Aside from the fact that this work with the collateral series has resulted in either partial or complete identification and characterization of 18 new isotopes, it has also added important new concepts to our understanding of the heavy elements and alpha radioactivity in particular. The applications of the properties of these isotopes to alpha decay systematics and calculations are lucidly covered in the above mentioned article by Perlman, Ghiorso and Seaborg.[15] Suffice it to say here that with these collateral series we have for the first time been able to explore the neutron deficient side of stability in the heavy element region and to extend the alpha systematics into this region.

At the beginning of this work it was believed that the neutron deficient isotopes in the heavy region, as in the lighter regions, would decay to stability through one or more orbital electron capture steps. We see now, however, that alhtough some of the isotopes above francium with slight neutron excesses do have a large amount of orbital electron capture branching, as this neutron excess becomes larger the isotopes decay primarily by alpha emission. Hence it is our belief that the large yield of isotopes such as At^{211} in high energy bombardments of thorium is due in part to formation of parents such as Pa^{223} which have such a short half-life to alpha emission that they decay immediately down through a series of very short-lived alpha emitters to their daughters, such as 7.5 hour At^{211}.

One further importance of these collateral series should be mentioned. Through their discovery we have obtained Pa^{227}, an isotope ideally suited for excitation function work. With Pa^{227} we have been able to explore the variations of yield with energy for several reactions in which it is produced. This work is discussed in Chapter 2.

Chapter II

Excitation Functions

I. Introduction

The investigation of excitation functions may be instigated by a desire to verify current ideas of the course of nuclear reactions or merely by a desire to obtain information which will allow one to maximize the yield of a particular isotope in a bombardment. The former was the main goal of many careful investigations using low energy accelerators and measuring precisely both the yields and energies involved.[21] This work has led to a better understanding of low energy nuclear reactions.

There has been, however, a great need for some general survey work on the many reactions that are possible with the high energy particles available or soon to be available at several sites. Excitation functions of a few light element reactions with high energy particles have been reported,[22] but those of heavy elements have not been investigated except for one determination by E. L. Kelly on the $Bi^{209}(\alpha,2n)At^{211}$ reaction using an electrostatically deflected beam of 388-Mev alpha-particles.[23]

While working on the collateral series[5,6] found in bombardments of thorium with deuterons and alpha-particles (and more recently protons) from the 184-inch cyclotron of the University of California Radiation Laboratory, we became interested in determining, through excitation functions, the energies for maximum yield of certain isotopes. By the summer of 1948 a few yield values had been determined and it appeared that only for (α,xn) reactions was there any very pronounced peak in the excitation functions where six or more neutrons were knocked out. For deuteron reactions it appeared that in this region of the periodic table the nucleus had become very transparent and was giving the type of excitation function mentioned by Serber[24] for high energy reactions, with

no sharply defined peak and only very slowly varying yields. In addition, it was noticed that there was a definite trend to lower absolute yields as more neutrons were knocked out in the initial reaction.

When the availability of 348-Mev protons became certain, it was decided that excitation functions should be determined for several reactions of thorium and uranium with these high energy particles. The crude equipment that had been used previously was discarded and an entirely new set-up was designed to give excitation functions for all three of the particles that would be available on the 184-inch cyclotron in the spring of 1949: 348-Mev protons, 194-Mev deuterons, and 388-Mev alpha-particles.

The ensuing paper is based on the results of our thorium and uranium foil bombardments made to determine the excitation functions of the simpler reactions encountered.

II. Experimental Methods

In determining excitation functions there are several methods (or variations of methods) which can be used. The most popular, perhaps, is the stacked-foil technique in which the carefully weighed target foils, either alone or with intermediate absorber foils of aluminum or copper, cut down the beam to low energy values. A variation of this method can be applied to a thick target by successively milling off thin layers, weighing these layers and determining the amount of yield per unit mass in each layer. With the area (milled out) and the weight of the material known, the range-energy relationships can be applied and a regular excitation function determined.

When experimental conditions such as small cross section, low beam intensity, or poor beam energy definition make the above methods impractical, it is possible to obtain an excitation function by making bombardments at various radii in the

internal beam of a cyclotron, since the radii and energies are interrelated. This type of bombardment actually does duplicate the conditions used in trying to maximize the yield of one isotope over other isotopes in the characterization of a particular isotope. There is no straggling to contend with and the energy spread of the incident beam has not been exaggerated by passage through a great amount of extraneous material. The principal objection to this method is the fact that in a cyclotron it is very difficult to duplicate conditions of beam current and beam position; consequently conditions of consecutive bombardments may vary considerably. In such bombardments, therefore, some reaction whose excitation function has been previously determined by the stacked foil technique should be determined coincidentally as a monitor to correct for these beam fluctuations.

In several of our early bombardments with the 184-inch cyclotron a rough attempt was made to check the variation of yield with energy of a few of the protactinium isotopes by interposing copper absorbers between several target foils. It was a few months later, however, before it was decided to look for the $Th^{232}(d,7n)Pa^{227}$ reaction using 20 foils scattered through a stack of copper absorbers.

A. Recoil Method

When the target foils are backed up with aluminum foil during a bombardment, the recoil fragments from the initial reaction collect on the aluminum. Since the thorium target foils were scarce at the time we thought it desirable to use this method, which does not require solution of the target. With this method moreover, it is possible to use the same target foils many times.

In this first attempt a one-inch stack (enough to completely stop the deuteron beam) of 1-1/2-inch squares of copper and thorium was used. The thickness of the copper squares was varied to produce the desired reduction in beam energy. The targets consisted of one-mil thorium foils backed up with 1/2-mil aluminum foils. The thorium target foils were not worked up chemically but instead the recoil fragments

that had collected on the aluminum were counted directly for gross alpha activity. As was expected the 38.3-minute Pa^{227} dominated the decay of many of the samples and was evident in all of them.

The bombardment was made in the electrostatically deflected beam of the 184-inch cyclotron in order that a good percentage of the beam could hit the middle of the target. After bombardment the entire piece of aluminum foil was counted in an alpha counter. Since most of the foils were much too active to count immediately after bombardment, they were allowed to decay until countable. Several counts were taken over a period of three hours for 16 of the samples while four samples were followed continually for ca. nine hours to obtain good resolution of the long lived tail and the 38.3-minute line.

The results indicate, as would be expected, that the recoil excitation curve of a particular reaction is not the same as the regular excitation function since a factor for the efficiency of recoil for the reaction at a given energy also enters into the determination.

B. Direct Method

When we found that the recoil method was giving us a different type of function than we wanted, it became necessary to work directly with our targets. It is possible in reactions such as $C^{12}(d,n)N^{13}$ and $Al^{27}(d,\alpha p)Na^{24}$ to count the target foils directly at such times as to minimize other activities present and thus obtain a satisfactory excitation function. When elements higher in the periodic table are bombarded (especially with high energy particles), chemistry is usually required to separate the variety of products formed. Thorium targets present the additional problem of a high alpha background due to the thorium metal itself (ca. 18,000 alpha c/m from a one-inch square of two-mil thorium — a thick source of Th^{232} alpha-particles). For this reason it is impossible to count thorium target foils directly in an alpha chamber.

In work with the Berkeley 184-inch cyclotron there are three types of charged particle beams which can be used for bombardment purposes, the internal beam, the external beam, and the electrostatically deflected beam. The internal beam is used when a target can be inserted into the tank of the cyclotron and intercept the beam at any desired radius. The beam hits the target on its edge only. With the big cyclotron it is usually possible to obtain an internal beam current of about 1/2 to 1-microampere of deuterons or protons, and about one-tenth of this value for alpha-particles.

The external beam affords some distinct advantages over the internal beam. (1) It can be brought out of the tank through thin aluminum windows and led into an external "cave" for use in experiments. (2) Its energy definition is good (1/2 to 1% spread). (3) It can be collimated to any desired shape and is very adaptable to experiments. (4) It can be made to intercept the center of a target foil. (5) It does not require that the targets be in a vacuum and hence the number of possible bombardments is greatly increased. The proton and deuteron beam current is, however, only ca. 3×10^{-5} microamperes which, except in rare cases, is not enough to be very useful for chemical determinations of reactions with cross sections of 10^{-2} barns or less.

There is, however, the third possibility in bombarding with the big cyclotron, namely the electrostatically deflected beam. When this beam is used the target is placed an inch or so beyond the 82-inch maximum radius of the internal beam. As an internal beam pulse reaches its maximum orbit an electrostatic field is applied to the deflector. The particles are bent in the orbit of the electrostatic field as well as the magnetic field and are essentially pulled in from their maximum orbit. When the particles pass the end of the 120° arc of the deflector they again move in an orbit similar to their maximum orbit but with a center displaced so that the beam can now intercept the middle of a target at a radius of

about 83 inches. By adjusting the amount of electrostatic field applied to the deflector the particles can be maximized on a certain portion of the target. The current of the electrostatically deflected beam is less than that of the internal beam by a factor of 50 or more for some bombardment arrangements but often there is still enough activity produced to give significant results.

Target preparation for excitation function experiments varies with the type of beam used in the bombardment. When stacked foils are used, range-energy calculations are necessary to determine the energy at a particular foil. These range-energy data were obtained from W. A. Aron, B. G. Huffman, and F. C. Williams of the Theoretical Physics Group here at the U. C. Radiation Laboratory.[25]

1. Internal beam targets: In this type of stacked foil bombardment, the foils of copper and target material were securely clamped together in a target holder and the leading edge sawed off with a band saw to insure that each foil was flush with every other foil. This precaution was very important. The thickness of each foil (mg/cm^2) was calculated by weighing the foils and measuring their area (approx. 1-1/2" x 3/4"). After bombardment, the foils were separated, the desired product removed chemically and counted.

Another type of internal beam target we have used in this work is the thin target bombarded at different beam radii. These targets should be so positioned as to obtain an accurate measure of the radius of the beam at the leading edge of the foil. The target thickness should be only a few percent of the total range of the incident particles; usually foils of five-mil thickness or less are satisfactory. (See Table 7 for the range (in inches) of beam particles at various energies in aluminum, copper and lead.)

2. External beam targets: For this type of bombardment the target foil is securely suspended behind the beam collimator. If the full energy beam is not wanted, absorbers must be used to decrease the energy to a desired value. Radiation hazards of the target are minimized since the gross induced activity is usually very

Table 7

Approximate Thicknesses of Common Absorbers
Necessary to stop Various Energy Beam Particles

Alpha Energy (Mev)	Al (inches)	Cu (inches)	Pb (inches)
388	1.370	0.500	0.550
350	1.142	0.417	0.461
300	0.908	0.318	0.354
250	0.630	0.231	0.259
200	0.421	0.156	0.176
150	0.252	0.094	0.108
100	0.122	0.046	0.054
50	0.036	0.014	0.017
Deuteron Energy (Mev)			
194	2.73	0.993	1.095
175	2.27	0.829	0.923
150	1.733	0.632	0.710
125	1.254	0.459	0.515
100	0.840	0.310	0.354
75	0.504	0.187	0.215
50	0.224	0.092	0.108
25	0.072	0.028	0.034
Proton Energy (Mev)			
348	12.05	4.31	4.58
300	9.45	3.39	3.61
250	6.98	2.51	2.69
200	4.79	1.725	1.860
150	2.93	1.056	1.148
100	1.437	0.523	0.576
50	0.420	0.155	0.175

low. While this type of bombardment is more versatile than the other two, it does require that the reaction concerned have a sufficiently high cross section and suitable half-life to give measurable activity.

3. Electrostatically deflected beam targets: The previously mentioned bombardment for recoils with this beam showed that beyond the calculated "zero" energy foil in a particular stack of foils there was a considerable "background" of activity which seemed to be produced by beam particles coming in from the side and hitting the rear foils in the stack. Because of this high "zero energy background" we considered the apparatus used inadequate for definite excitation function studies and started thinking about a design which would be satisfactory for use with alpha-particles, deuterons, and the new high energy protons which were to be available within a few months.

It is necessary that this design meet several requirements. The apparatus should be capable of mounting a 4-1/2 inch stack of copper absorbers (enough copper to completely stop the 348-Mev proton beam as well as the other particle beams). The absorbers should be rigidly held in place to provide reproducibility of position and results. The target material should be so placed between the absorbers as to obtain the maximum amount of beam for the minimum amount of target foil used; it should also be readily removable from the bulk of copper absorbers, (and incidentally the bulk of the hazardous activity after bombardment). Most important of all, enough absorber should be imposed on the beam side of the target foils to reduce the beam coming in from the side of the stack by a considerable amount over the previous experiments.

The following apparatus was designed with these requisites in mind and with many helpful suggestions from Herman P. Robinson and A. Ghiorso of this laboratory. In this apparatus, which is shown in exploded assembly in Fig. 58 and pictured in Figs. 59 and 60, the energy is reduced by 2-1/2" x 3" copper sheets of various thicknesses with sides milled parallel to within 0.2 mil and the thickness

EXCITATION FUNCTION APPARATUS

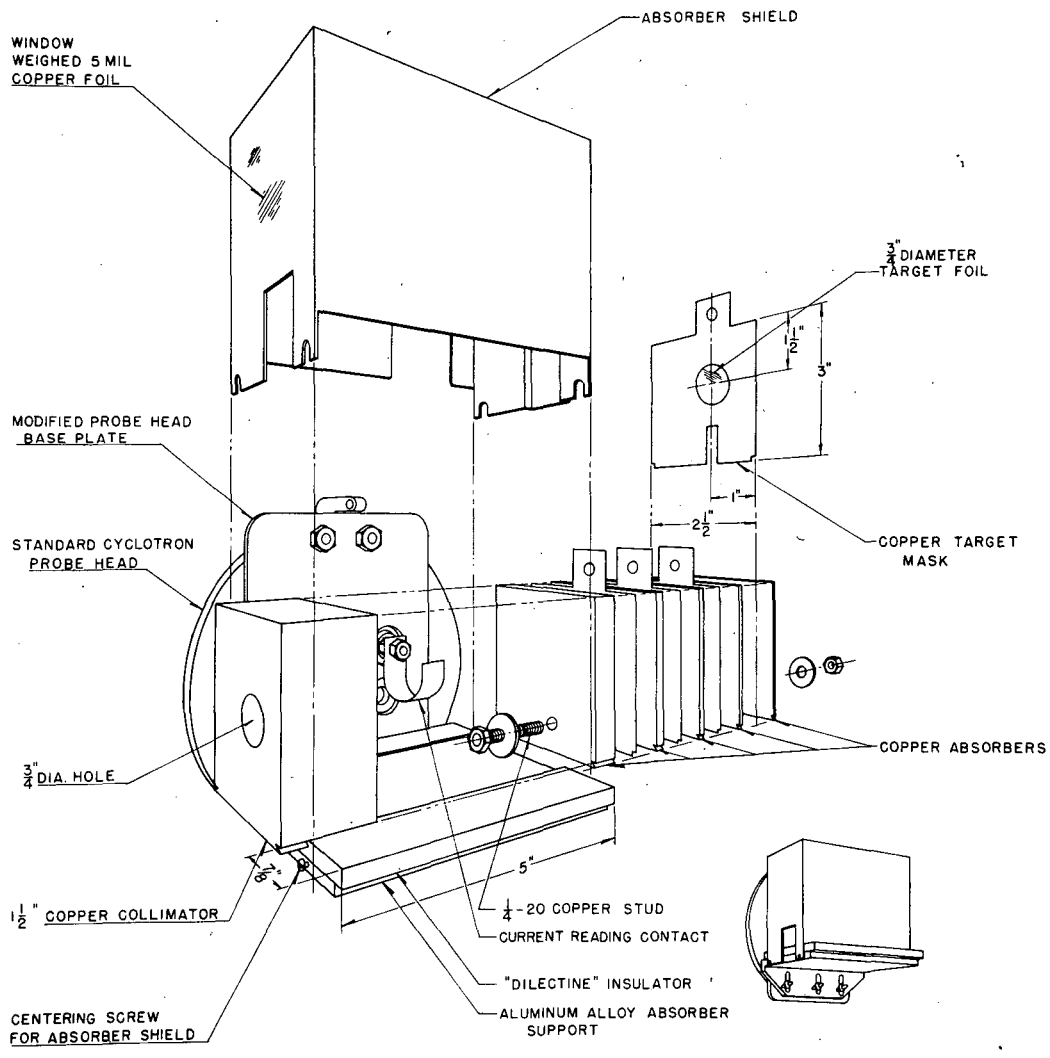

FIG. 58

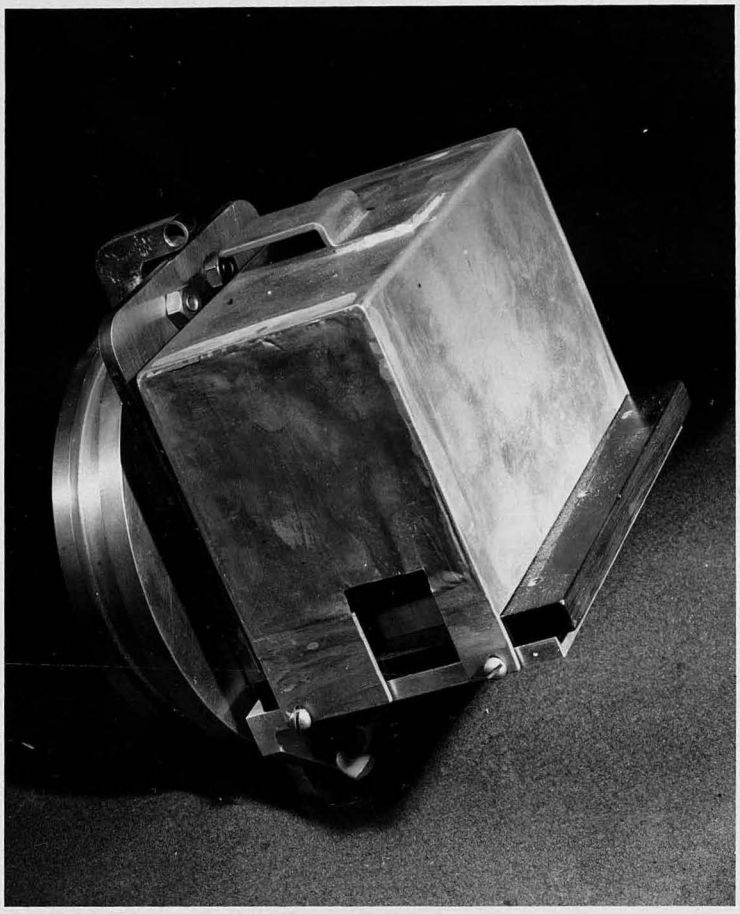

FIG. 59 EXCITATION FUNCTION APPARATUS WITH SHIELD.

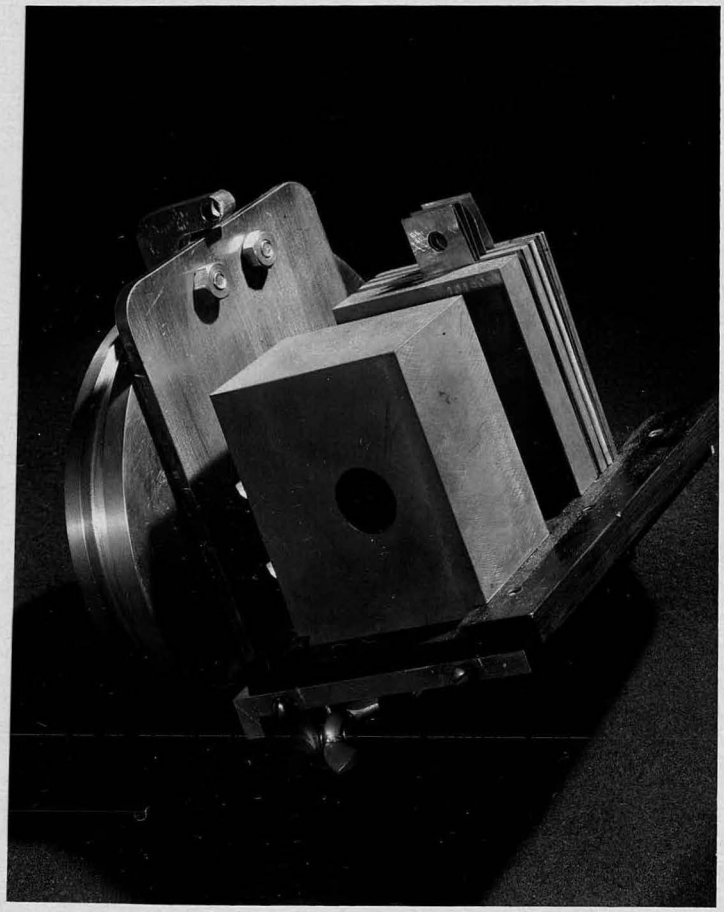

FIG. 60. EXCITATION FUNCTION APPARATUS WITHOUT SHIELD

(in mg/cm^2) determined by weighing. The five-mil target material is in the form of 3/4 inch-diameter metal discs and is held in a mask of five-mil copper, about 3/4 of an inch from the beam side edge and midway between top and bottom of the copper absorbers. (Small pieces of scotch tape on each side suffice to secure the disc to the mask.) The amount of copper on the beam side of the target material lowers the background due to particles coming in from the side of the absorber stack to about one-hundredth (or less in some cases) the maximum activity of the excitation curve. A support ledge is provided on the beam side of the absorber stack to permit the addition of more absorber if it becomes necessary to lower this background even more.

A 1-1/2 inch thick copper collimator is placed in front of the absorber stack for deuteron and alpha-particle bombardments. Its 3/4 inch collimating hole is lined up directly with the target disc holes in the masks. Admittedly, to be most effective, the collimation should present a much smaller area than the targets. In many experiments, however, we were working with rather small amounts of activity and could not afford to reduce the beam size. In addition, the target size was somewhat limited by our efforts to reduce the extraneous beam coming in from the side. Actually the main purpose of the collimation was to enable us to obtain a good bombardment with the electrostatically deflected beam. In proton bombardments we luckily were able to obtain reproducibly good results with this beam without a collimator, but with alpha-particles the use of the collimator increased the yield by a factor of 20. It was impossible to obtain a deuteron bombardment of any kind without the collimator. The latter, being grounded, allows the beam current to be maximized on the target foils themselves rather than just anywhere on the block of absorbers. This insures that the target foils are hit by the beam "hot spot" rather than by scattered radiation from the edge of the beam.

The absorbers and collimator are locked in the insulating tray by the chamfer corners, the absorbers being kept from lateral motion by the copper stud through their lower portion.

When the apparatus is assembled, the copper current-reading contact rests upon the absorber stack which is insulated from the rest of the apparatus by the "Dilectine" insulator tray and by pieces of mica between it and the absorber shield which is grounded to the absorber support. The shield is necessary to electrically shield the absorber stack from the external electrostatic fields which would influence the current readings. The absorber shield is kept in position by two screws on each end of the absorber support. In our experiments it was imperative that the shield be as close to the absorber stack as possible since it is difficult for the deflector system to throw the beam in much farther than the ca. 1 inch of absorber and shield.

Since the absorber shield is imposed all around the target foils it has a weighed front window whose thickness is included in range energy calculations. This entire apparatus fits on the standard cyclotron probe head set-up.

Immediately after bombardment the four centering screws are loosened, the absorber shield lifted off with a pair of tongs by a small hook which is not shown in the drawing, the bolt on the absorber stack loosened, a small rod slipped through the tab holes in the masks, and the masks lifted free. Back at the laboratory the discs are punched out of the masks and are ready for chemistry.

To maximize the beam on the target, it is possible to vary the radius of the probe, and the voltage on the deflector. Furthermore the entire tray of absorbers can be raised or lowered to position the targets vertically in the beam. This adjustment is made by loosening the wing nuts holding the absorber support as shown in the insert in the drawing.

Shop drawings of the parts of the apparatus are given in Figs. 61-66 inclusive. The tolerances required for the absorbers and masks are indicated. Absorbers of many different thicknesses were made up to enable us to determine simultaneously as many as 16 points (with a minimum interval of five Mev) on an excitation curve for protons, deuterons, or alpha-particles.

Even with the electrostatically deflected beam a considerable amount of activity is obtained in a bombardment of 3/4 inch discs of five-mil thorium in the above apparatus. For a half-life proton bombardment of an isotope of 38.3-minute half-life, we obtained ca. 1.5×10^6 alpha disintegrations/minute for a cross section of about 10^{-2} barns.

C. Chemistry

Even though the new apparatus had apparently solved the problem of beam particles coming in from the side there remained the very real problem of determining the chemical yield of the elements separated.

Protactinium is an excellent product to remove chemically in this excitation function work since the 38.3-minute Pa^{227} and its daughters are the only alpha activity in evidence in the protactinium fraction for a matter of at least five hours after shutdown. Moreover, on extraction with a solution of trifluorothenoylacetone(TTA) [16] in benzene the majority of the protactinium, clean from other alpha contamination, is removed from the solution of target material.

When allowed to stand for any length of time at a near neutral pH, protactinium goes into a non-extractable colloidal state and hence the use of Pa^{231} as tracer leaves much to be desired. It was found, however, that a single TTA-benzene extraction after solution of the target foil could give consistent results on a number of foils if the processes were carried out simultaneously on each foil; the same amount of reagents being added, all samples being stirred at the same time, etc.

To facilitate this mass production basis for the chemistry a "bicycle rack" type of stand was built (Fig. 67). Small laboratory stirrers (with glass

SHOWN ON										
ISSUED TO		DATE ISSUED		DELIVER TO 4-103	JOB NO. 118-1	DATE REQ'D		MAKE		
						TOLERANCES WHERE NOT OTHERWISE GIVEN				

RADIATION LABORATORY	DRG. NO. 4D5621
UNIVERSITY OF CALIFORNIA—BERKELEY	
DRAWN J.W.Lilly	CHECK
APPROVED BY	SCALE FULL

DATE 12-23-48

Dwg 4D5621-1
4D5621-2 } See Note 2

Excitation Function Equipment
ABSORBER

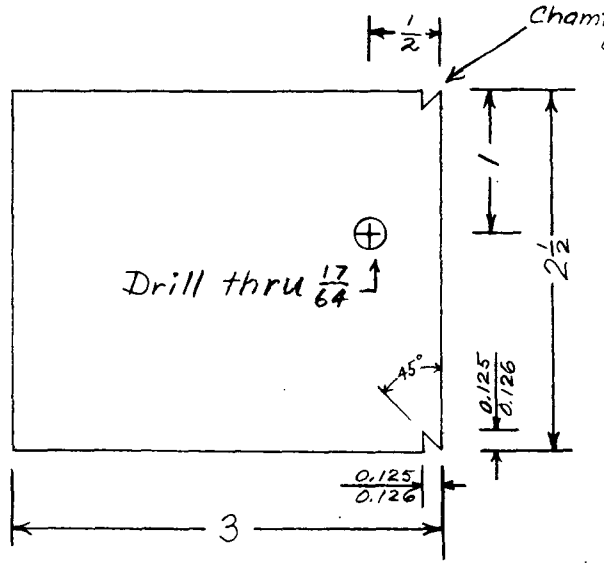

Note: 1. Absorber must slide readily into ways on 4D5631
2. Faces must be parallel within 0.0002 for 4D5621-1 and within 0.001 for 4D5621-2
3. Thickness will be specified.

FIG. 61

MATERIAL COPPER	CHANGE LETTER	DRAWN BY	CHECK BY	DATE	CHANGE

"ALBANENE" 1951 K. & E. CO., N. Y.
REG. U. S. PAT. OFF.

SHOWN ON										
ISSUED TO		DATE ISSUED		DELIVER TO 4-103	JOB NO. 118-1	DATE REQ'D		MAKE		
						TOLERANCES WHERE NOT OTHERWISE GIVEN				

RADIATION LABORATORY	DRG. NO. 4D5611
UNIVERSITY OF CALIFORNIA—BERKELEY	
DRAWN JWLilly / CHECK / DATE 12-27-43	
APPROVED BY / SCALE FULL	

Excitation Function Equipment
COPPER MASK

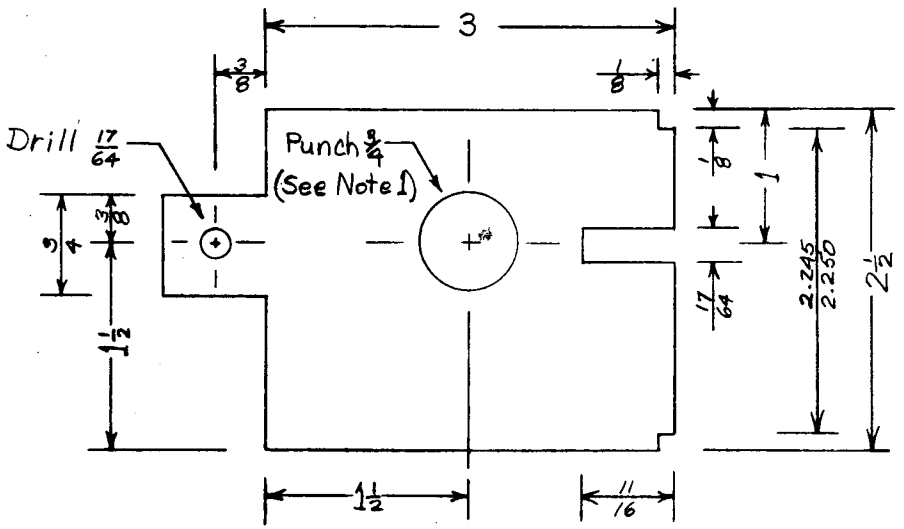

Note:
1. Hole must be punched with same punch as used for ~~3/4~~ thorium discs. Material for latter will be supplied.
2. Thicknesses are nominal but plate must be uniform in thickness within 0.0002.

Thickness (Note 2)

4D5611 -1	.005 ± .0002
4D5611 -2	.004 ± .0002
4D5611 -3	.002 ± .0002

FIG. 62

MATERIAL COPPER	CHANGE LETTER	DRAWN BY	CHECK BY	DATE	CHANGE

"ALBANENE" 195L K. & E. CO., N. Y.
REG. U. S. PAT. OFF.

SHOWN ON										
ISSUED TO		DATE ISSUED		DELIVER TO 4-103	JOB NO. 118-1		DATE REQ'D		MAKE	
							TOLERANCES WHERE NOT OTHERWISE GIVEN			

RADIATION LABORATORY DRG. NO. 4D5631A

UNIVERSITY OF CALIFORNIA—BERKELEY

DRAWN JWLilly	CHECK	DATE 12-27-48
APPROVED BY	SCALE FULL	

Excitation Function Equipment

ABSORBER INSULATOR

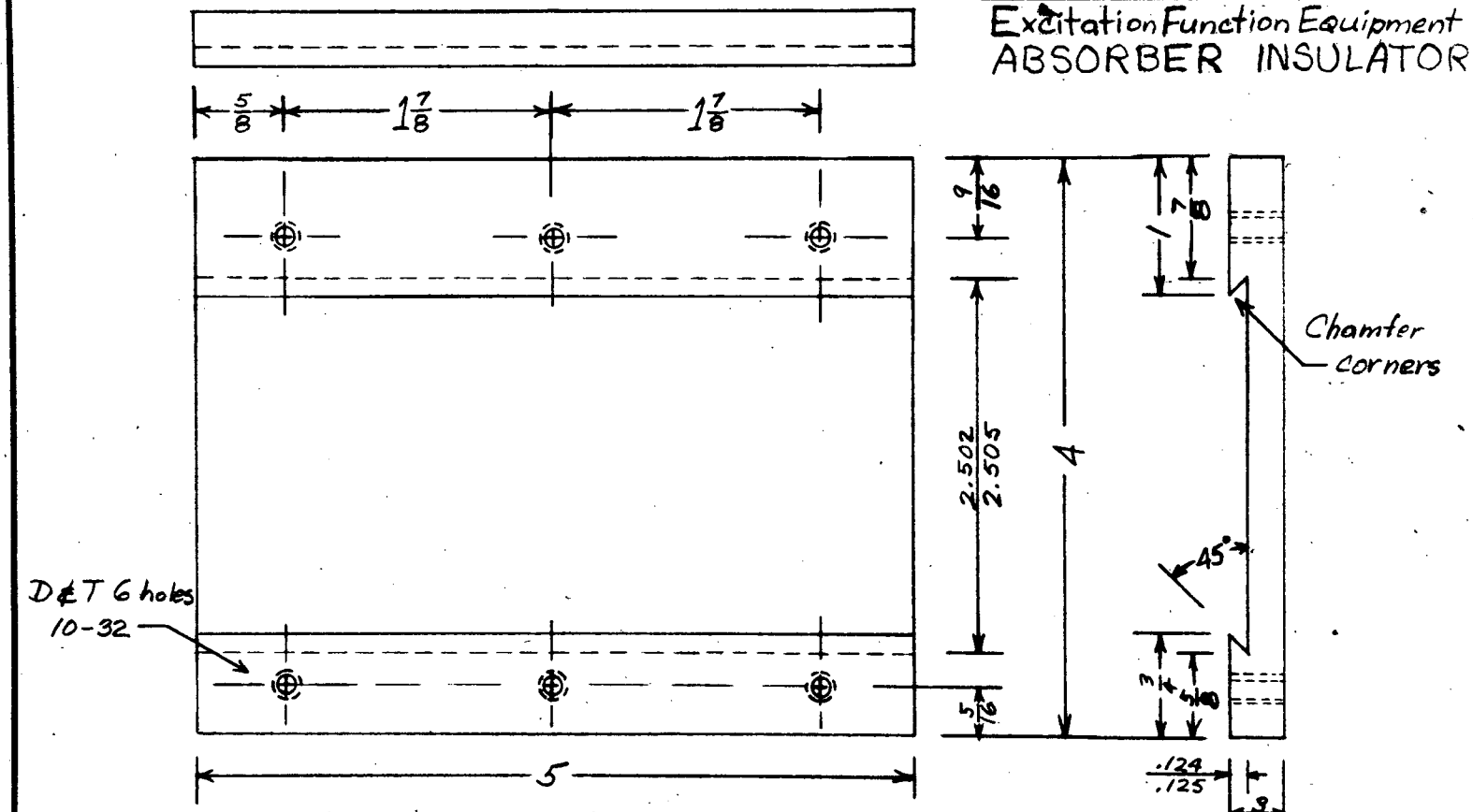

Note: Holes must match those in 4D5652

FIG. 63

MATERIAL 3/8" DIELECTENE OR MICARTA (A)

CHANGE LETTER	DRAWN BY	CHECK BY	DATE	CHANGE
A				ADDED TO MAT'L NOTE "OR MICARTA"

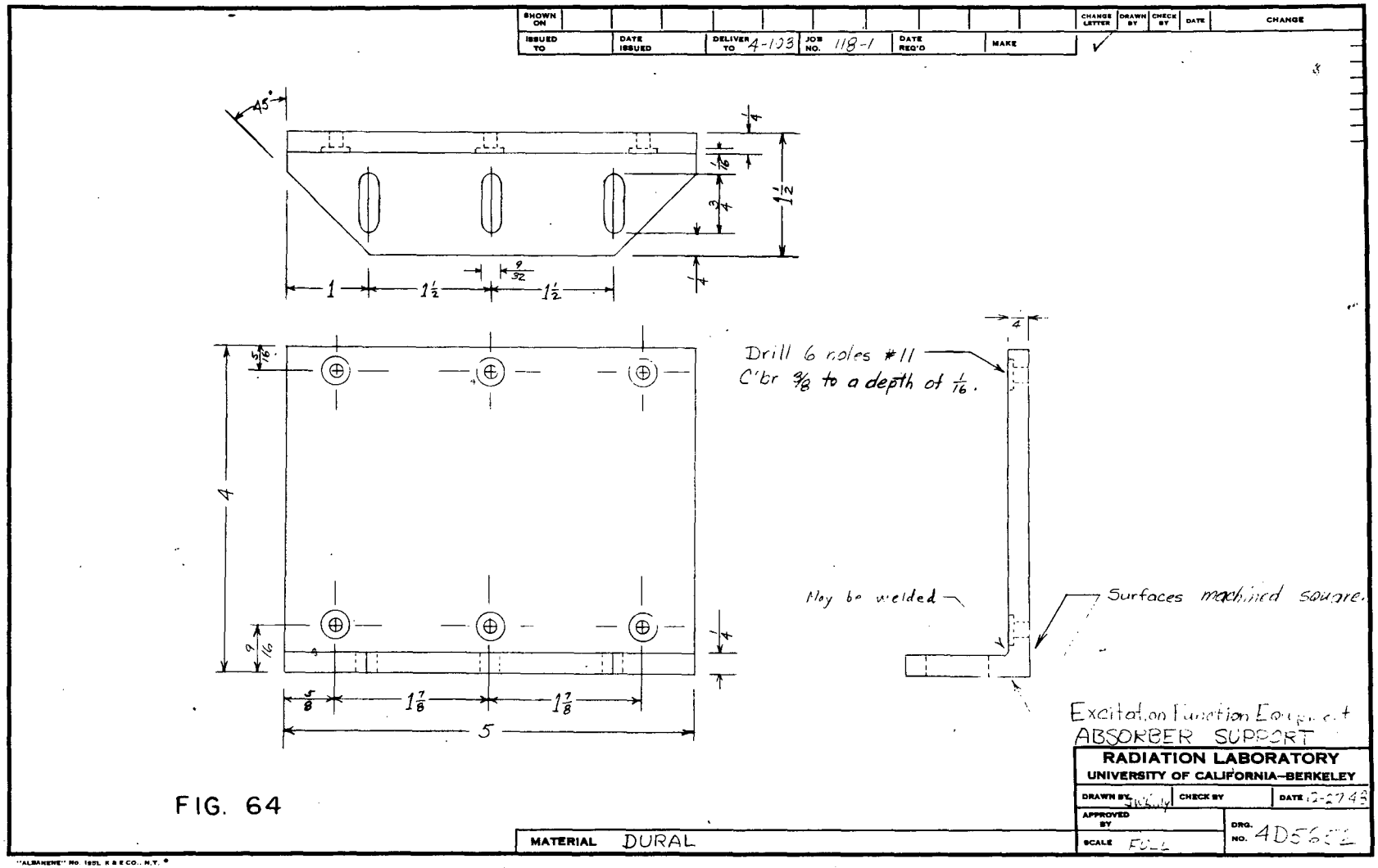

FIG. 64

SHOWN ON									
ISSUED TO	DATE ISSUED	DELIVER TO 4-103	JOB NO. 118-1	DATE REQ'D	MAKE				
				TOLERANCES WHERE NOT OTHERWISE GIVEN					

RADIATION LABORATORY	DRG. NO. 4D5641
UNIVERSITY OF CALIFORNIA—BERKELEY	
DRAWN JWLilly	CHECK	DATE 12-27-48
APPROVED BY	SCALE FULL

Excitation Function Equipment

BOLT

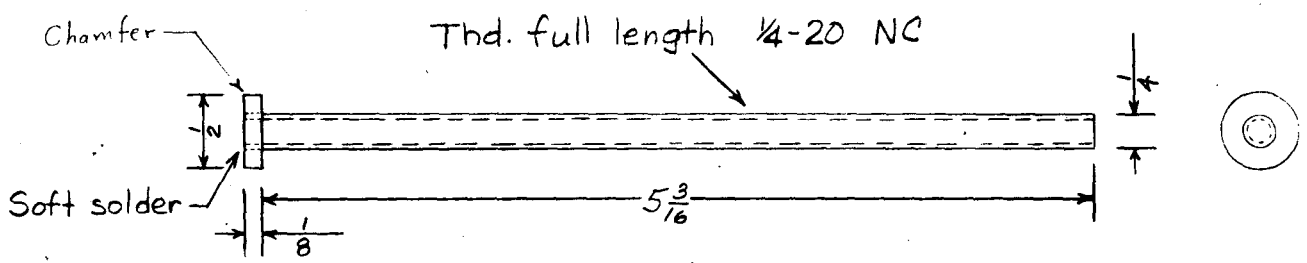

FIG. 65

MATERIAL COPPER	CHANGE LETTER	DRAWN BY	CHECK BY	DATE	CHANGE

"ALBANENE" 1951 K. & E. CO., N. Y.
REG. U. S. PAT. OFF.

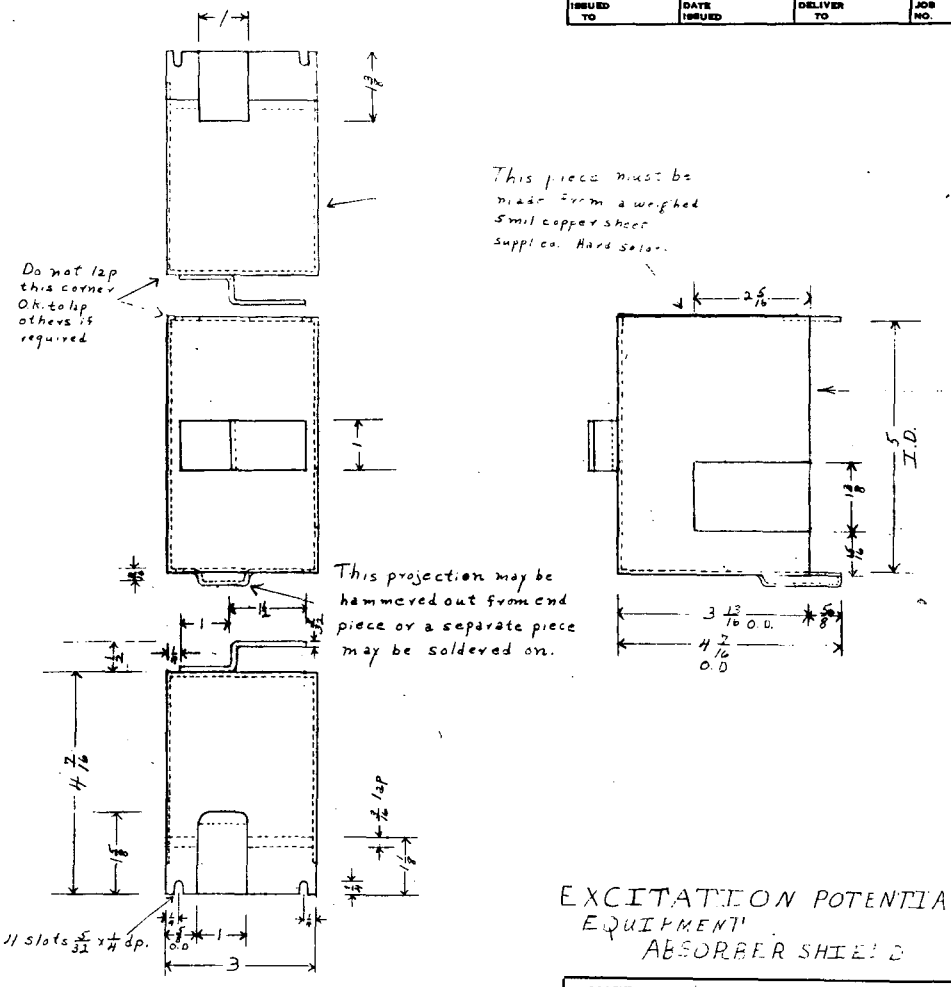

Note: Silver solder all joints
Do not use soft solder

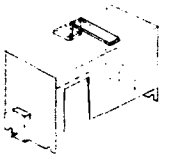

FIG. 66

EXCITATION POTENTIAL EQUIPMENT
ABSORBER SHIELD

FIRST USED ON	118-1
ROUGH FINISH	FINE FINISH
GOOD FINISH	GRIND FINISH
MACHINED DIMENSIONS ± .010 UNLESS OTHERWISE SPECIFIED	
MATERIAL 1/16 copper except as noted	

RADIATION LABORATORY
UNIVERSITY OF CALIFORNIA—BERKELEY

DRAWN BY [illegible] CHECK BY DATE 7-2-[illegible]
APPROVED BY
SCALE 1" = 1"
DRG. NO. 4D 9382

"ALBANENE" 1951 K. & E. CO., N. Y. Reg. U. S. PAT. OFF.

STIRRER FRAME

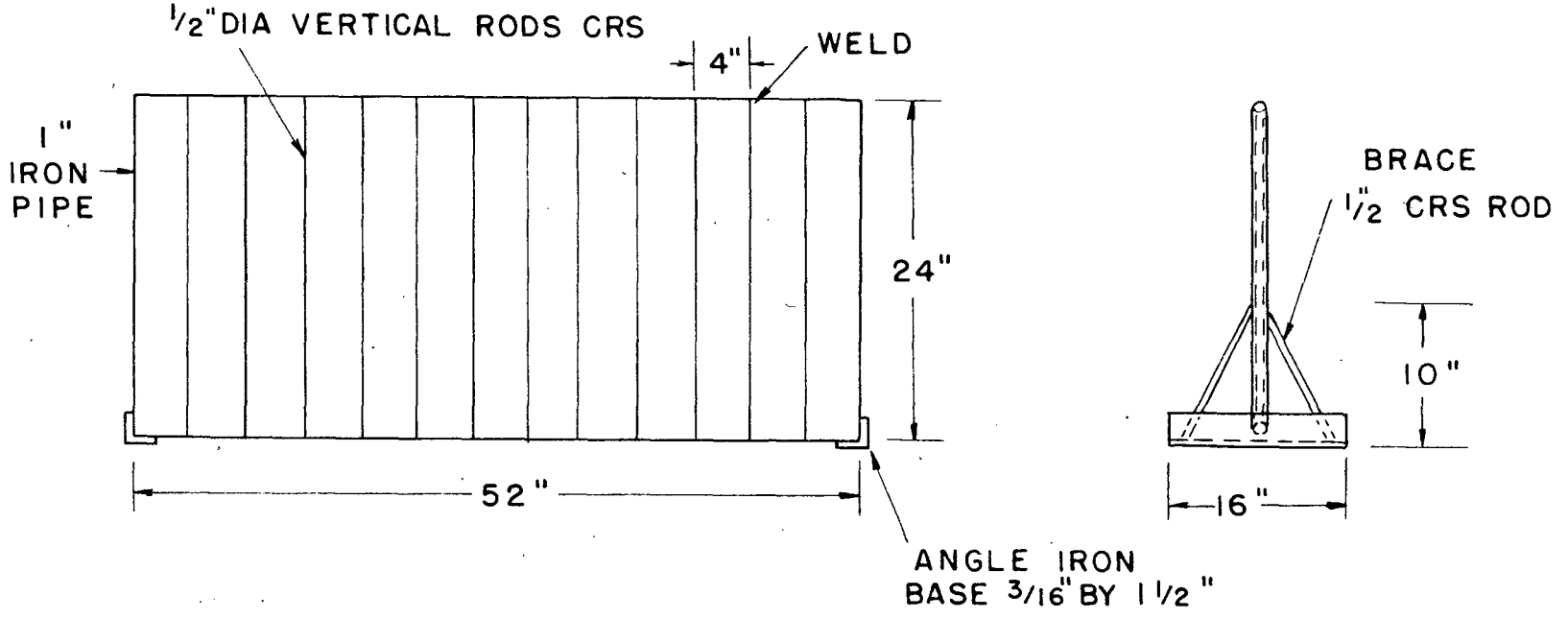

ALL DIMENSIONS MEASURED TO CENTER LINE OF RODS

FIG. 67

stirring rods) and open top 40 ml separatory funnels were clamped to the 12 cross bars. This set-up is pictured in Fig. 68 .

In the chemical procedure [26] (Appendix II, Procedure 91-2) the thorium discs are dissolved in 125 ml Phillips beakers with 10 ml of concentrated nitric acid and one drop of 0.2 M ammonium fluosilicate. The solution is heated gently on a hot plate until the reaction starts. Ten ml of water is added and the solution poured into separatory funnels (40 ml centrifuge cones with stopcocks sealed to the bottom). Ten ml of 0.4 M TTA-benzene solution is added and the mixture stirred for 5 minutes. The aqueous and organic layers are collected in separate tubes and about half of the organic layer (containing the protactinium) is plated on platinum plates, flamed, and counted for gross alpha counts.

Figure 69 pictures the set-up used to simultaneously plate as many as 16 samples. Heat from the hot plates and heat lamps was adjusted to evaporate the benzene rapidly but without spattering. The platinum plates were placed on 1/4-inch washers to raise them above the surface of the hot plate and thus allow loading of as much as one ml of the TTA-benzene solution at a time. By using individual transfer pipettes (with rubber medicine dropper bulbs) for each sample it was possible to evaporate about 6 ml of the organic solution on each of 16 plates and flame these plates within 45 minutes. We encountered no cross contamination between samplesin using this plating technique.

In order to determine purity of the samples, at least two counts were taken of each plate within an interval of about 40 or 80 minutes to compare the decay of the gross alpha activity with the 38.3-minute half-life of Pa^{227}. If necessary, alpha-pulse analyses were made to check any further question of purity. Additional pulse analyses made several weeks after shutdown give an idea of the amount of 17 day Pa^{230} (growing 20.8 day U^{230} and daughters) present in the samples.

The chemical yields of the runs reported in this paper are consistent within themselves to within 5 or 10% but the absolute chemical yield has in most

FIG. 68 STIRRING RACK SET-UP

FIG. 69 PLATING SET-UP

cases been left undetermined. It has been possible to start counting the plates from a run of 16 foils, as early as one hour and 50 minutes after shutdown.

Protactinium procedures have proven very adaptable to a mass production scale. By comparison, uranium procedures, which are required to separate the products of (α,xn) reactions on thorium, do not give satisfactory results when done on such a scale.

The procedure, used by Newton [17] and others, involving ether extraction of the uranium from 10 M ammonium nitrate solutions is satisfactory for bombardments of thorium in which the uranium isotopes are formed in relatively high yields. In these cases we used the following procedure. The thorium foils are dissolved in concentrated nitric acid with the addition of a few drops of 0.2 M ammonium fluosilicate (heating gently on a hot plate until the reaction starts). This solution is evaporated to thorium nitrate crystals, care being taken not to decompose the crystals with excess heat into the difficultly soluble ThO_2. The salts are taken up in 1 N nitric acid saturated with ammonium nitrate and transferred to the open topped separatory funnels. An equal volume of ethyl ether is added. The mixture is stirred for 5 minutes and the aqueous layer drawn off. The ether is washed two or three times with a lightly acidic solution saturated with ammonium nitrate and then plated.

When done simultaneously on 16 samples with enough speed to catch a one-hour half-life, this chemistry did not give very good yields of the uranium (a maximum of 10%). The plates of the ether solution were rather thick (from salting impurities etc.) and did not pulse analyse well. Since pulse analyses were required for each sample, it was not possible to obtain good yield values for the excitation curves.

As the energy of the bombarding particles is increased, moreover, the yield of astatine and polonium isotopes from the spallation process [27] becomes

very pronounced and the astatine, in particular, solvent extracts into the ether in fairly high yield. This chemical contamination at high bombarding energies makes it very difficult to obtain a complete curve for the (α,xn) reactions unless much more involved chemical procedures are used.

The procedure used by Crane [26] (Appendix II, Procedure 92-1) has proven satisfactory in removing all extraneous activities from a uranium fraction. The yield has been found to be rather low (less than 10%) however, unless much time is spent in recovering lost yield by re-extractions and re-precipitations.

This procedure as adapted to our work required that immediately after shutdown, the thorium metal foils be dissolved in concentrated nitric acid containing a few drops of 0.2 M ammonium fluosilicate, to which known amounts of U^{233} tracer had been added for chemical yield determinations. (Heat is required to initiate solution.) The solution is then diluted with an equal volume of water and transferred to open topped separatory funnels. There an equal volume of 0.4 M TTA-benzene solution is added and the mixture stirred for five minutes. The organic layer is discarded and the TTA-benzene extractions repeated three more times to insure fairly complete separation of the Pa^{230} formed in the bombardment both from deuteron contamination of the alpha-particle beam and from the (α,p5n) reaction. Since this protactinium separation can be completed in about 1-1/2 hours after shutdown, only 1/40 of the U^{230} atoms present at the end of that time come from the beta decay of Pa^{230}, if the Pa^{230}/U^{230} atom ratio at end of bombardment is 100.

The acid solutions from these simultaneous separations are then set aside and worked up at our leisure. The actual uranium separation was performed on each sample individually and required between 1-1/2 and 2 hours per sample for completion. The solutions from the protactinium extractions were evaporated to thorium nitrate crystals, redissolved in 1 M nitric acid and saturated with ammonium nitrate. The uranium was extracted with one pass of ether, washed three

times with a slightly acidic solution of saturated ammonium nitrate and finally washed into water. This carrier-free solution of uranium in water was then further purified by precipitating out the uranium on lanthanum hydroxide, dissolving the precipitate in acid, and scavenging with a $ZrO(IO_3)_2$ precipitate. (It is very easy to lose yield in this scavenge step. See Appendix II for other remarks.) The lanthanum hydroxide was again precipitated and then dissolved in 1 N nitric acid. The solution was salted and the uranium extracted from the lanthanum with ether. After three washes with salted solutions, the ether was plated. These plates were finally pulse analyzed to determine the chemical yield of the U^{233} tracer added at the beginning of the procedure and thence to determine the yield of U^{230} from the bombardment.

D. Counting and Pulse Analysis

In measuring the activity for our excitation functions, we counted alpha emitters in an ordinary argon ionization chamber whose pulses were fed into a scale of 512 counting circuit. Tests have indicated that the counter gives negligible coincidences even up to a counting rate of several hundred thousand counts per minute. (The validity of these tests however is in question.) The counting arrangement gives a geometry of about 50%. When only gross counts were taken of a set of samples, at least two rounds of counts were always taken to make sure that the activity decayed with the correct half-life.

When there was some question of the purity of the samples obtained in the bombardments, they were subjected to alpha-pulse analysis with a 48-channel differential pulse analyser.[12] This procedure was especially important in determining the U^{230} and daughter content of the protactinium samples several weeks after shutdown (U^{230} coming from the beta decay of Pa^{230}). In many cases of the Pa^{230} excitation functions, pulse analysis of every sample would have been too time consuming and tedious since most of the samples were relatively slow counting. Hence only a few representative samples were pulse analyzed to determine the

U^{230} content as well as the contamination of astatine and other impurities that made up the total gross alpha count. Usually one pulse analysis of a sample at full energy, one at the peak of the curve, and one below the threshold for a given excitation function were enough to indicate the trend of contamination present. In general, it was found that near the peak of the curve the sample was almost 100% U^{230} series, while at full energy and below the threshold, contamination of 20% or more was usually found. These contamination percentages were interpolated roughly through the intermediate energies to the pure U^{230} samples at the reaction peak to obtain contamination correction values for all samples of the curve.

Geiger counting, when required, was done on an end-window type counter, approximately 4 inches long and 1 inch in diameter. The mica window over one end is about 3 mg/cm^2 thick. The tubes are filled to a pressure of 9 cm argon and 1 cm ethyl alcohol. These tubes operate at about 1200 volts and have a plateau of about 200 volts. The output pulses are fed into a scaling circuit of 64; the counting efficiencies of the tubes are 100%. The Geiger counts presented in the accompanying excitation functions were made on the bottom shelf (shelf five-about 2.9 inches below the window) of a standard five shelf geometry set-up. Coincidence corrections of 1.2% per thousand were made on all counts.

E. Calibration of Sample Discs and Absorbers

All weighings of sample discs and foils were made on a regular analytical type chainomatic balance, which weighs to tenths of a milligram. All weights of target foils listed are probably good only to $\pm$ 0.3 mg.

The absorbers were machined parallel to within 0.2 mil and were then calibrated by weighing on the analytical balance. Absorbers that were too heavy for this balance were weighed on a rough assay balance.

All areas were carefully measured with calipers and the thicknesses in mg/cm^2 found by dividing the weight by the area.

F. Calculation of Yields

All of the yields plotted in the following graphs and listed in the tables have been extrapolated to the end of bombardment and corrected for the number of members in the series counted in gross alpha decays. The yields are given as disintegrations per minute of the activity (except for Geiger activity which is given as counts per minute on the fifth shelf), and are corrected to 0.4 gm thorium, 0.7 gm uranium, 0.1 gm aluminum, or 0.04 gm polystyrene. Where more than one run of a certain reaction has been made, the reaction that is considered most accurate or most consistent is taken as a standard and the yields of the other runs are normalized to it to make as smooth a curve through all the points as possible. In one case, (the (d,7n) reaction on thorium) a mistake in tabulating the absorbers, apparently made, caused the peak of one run to shift 12 Mev to the high energy end. In this case, insertion of a hypothetical absorber in the stack for the calculations, normalized the energies to the other runs to give a smooth curve.

Where the points of inflection of curves (peaks, thresholds, etc.) fall at low energy values, the sensitivity of the energy values to absorber values may cause considerable spreading out of these points (e.g. the threshold of a reaction may fall beyond the "calculated zero energy" and hence not be shown on the curve). In such cases it has been found convenient to plot yields directly against mg/cm^2 of absorber instead of converting the absorber values to energy units.

In proton bombardments, yield values have been corrected for the reduction in beam intensity caused by absorption on passing through the 4.3 inch stack of copper and target foils. These correction factors have been obtained from V. Peterson of the Radiation Laboratory who has experimentally measured the number of particles entering and leaving copper blocks of known thickness. His results are shown in Fig. 70 . As indicated in the figure the points are known to within only about 20% but since this correction term is so important in the proton bombardments it was thought best to use the values available. A more accurate set-up is now

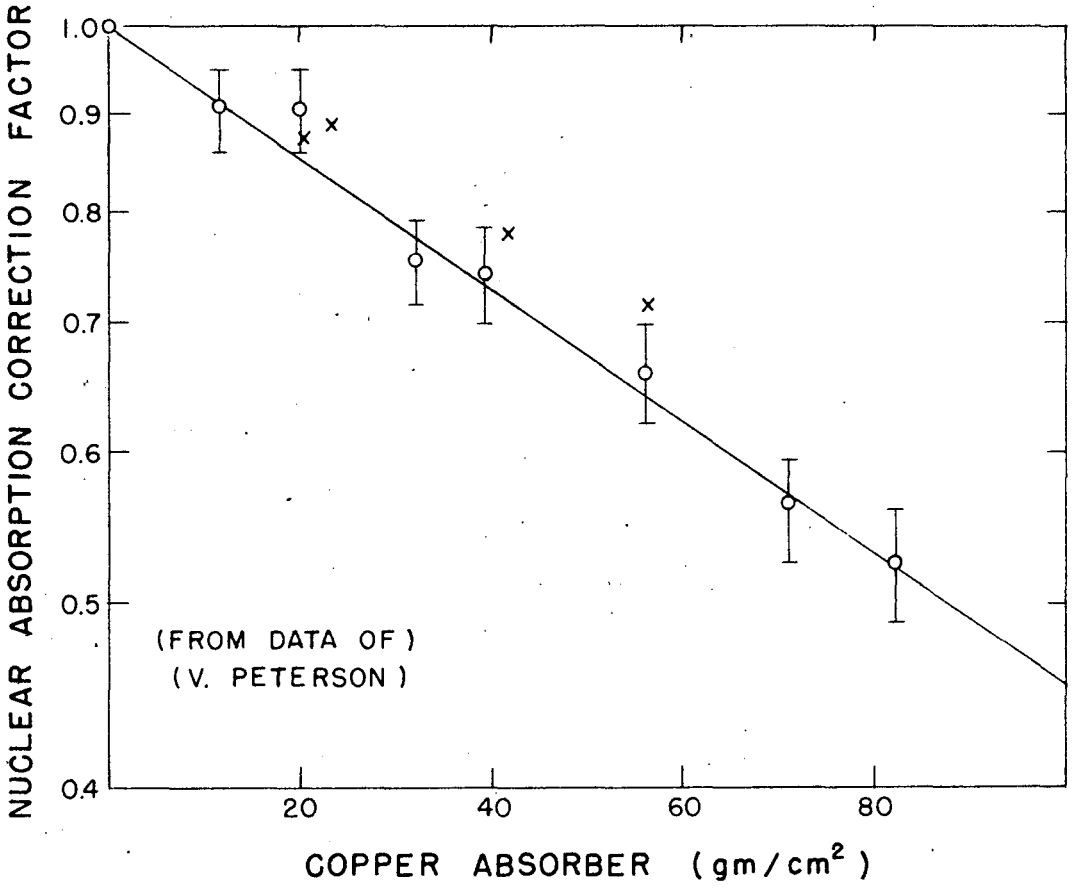

Fig. 70. Determination of the reduction in beam intensity due to nuclear absorption. The line was used in corrections of all yield values presented in this paper for proton bombardments. However more recent measurements also made by Peterson (as plotted by "x" above) indicate this correction may have been too large.

being tested by Peterson and R. Phillips for better measurements of these values.

To our knowledge no measurements have been made of this nuclear absorption for deuterons or alpha particles. Since their ranges are much less (ca. one inch and 1/2-inch of copper respectively) than protons, the correction factor is probably not greater than 20% and may be considerably less. No correction has been made for this effect in the deuteron and alpha-particle bombardments presented in this paper.

The actual experimental yields, corrected as mentioned above, are tabulated in the tables (not the normalized values). In addition, the calculated proton energy at the front and back of the target foil is listed to indicate the energy interval covered by the target foil. The thickness (measured by weighing) of the 3/4 inch diameter discs of target material is given in mg/cm^2. Finally, the total amount of absorber between the front and the back of each target foil is listed. These latter values are included since they and the experimental yield values are the basic data of these experiments and could be used with other modified range-energy relationships and a variety of spreads of the cyclotron beam to give modified forms of the excitation function curves presented here.

In general, the yields given are not corrected for the chemical yield, which is unknown. In only two reactions have the absolute cross sections been determined and then only roughly. The tricky chemistry of protactinium, due to possible colloid formation, makes the use of protactinium tracer a rather unreliable means of determining chemical yield unless the average of many runs is taken.

In the two cases in which the cross section has been determined--- the (p,6n) and (d,7n) reaction on thorium--- the current measurements were made by V. Peterson by using a Faraday cup to collect all the particles that had passed through the piece of target material bombarded in the external cyclotron beam. From these determinations, the values for the cross sections for the (p,3n) and (d,4n) reactions could be obtained since the Pa^{227} is essentially an internal

monitor for the Pa^{230} reactions. In the determinations of Pa^{227} in the external beam however barely enough activity was obtained to make definitive measurements (only a few thousand counts per minute at shutdown from a half-life bombardment of 5-mil thorium at full energy). Hence this method would not be feasible for the other reactions of thorium or uranium reported in the following sections.

The amount of U^{230} in a protactinium sample was determined by alpha-pulse analysis of the sample as mentioned above. From this U^{230} value and the elapsed time since uranium separation, the amount of the Pa^{230} isotope present originally (assuming 10% beta branching of the Pa^{230} as reported by Studier and Bruehlman [32]) can be calculated by the standard growth equation:

$$N_2 = N_{01} \frac{\lambda_1}{\lambda_2 - \lambda_1} \left(e^{-\lambda_1 t} - e^{-\lambda_2 t} \right)$$

where N_2 = number of U^{230} atoms, N_{01} = number of Pa^{230} atoms initially present, t = time, λ_1 = disintegration constant of Pa^{230}, and λ_2 = disintegration constant of U^{230}, (taking the half-life of Pa^{230} as 17 days and that of U^{230} as 20.8 days).[8]

A number of values for disintegrations of U^{230} growing from 10^{10} atoms of Pa^{230} after various periods of time have been calculated from the above formula and are presented in Table 8. These values can be plotted on logarithmic or cross section graph paper to facilitate interpolation of values not listed. Of course for a different number of Pa^{230} atoms present initially, a simple proportion will indicate the dis/min of U^{230} formed.

Table 8

Amount of U^{230} formed from the β^- decay of 10^{10} Atoms Pa^{230}
(assuming 10% β^- branching of Pa^{230})

t	a/m U^{230}	t	a/m U^{230}
1/2 hr	19.68	4 day	3.24×10^3
1 hr	39.4	5 day	3.91×10^3
2 hr	78.8	7.5 day	5.30×10^3
8 hr	312	10 day	6.48×10^3
16 hr	619	20 day	8.98×10^3
24 hr	905	30 day	9.31×10^3
1.5 day	1.332×10^3	40 day	8.59×10^3
2 day	1.748×10^3	50 day	7.44×10^3
3 day	2.513×10^3	78 day	4.15×10^3

III. Range-Energy Calculations

In excitation function work it is necessary to have some basis for assigning energies to the target foils. In our work we have used range-energy relationships calculated by the Theoretical Physics Group here at the Radiation Laboratory and published in graphical form in UCRL-121 Revised, "Collection of Range vs. Energy and Rate of Energy Loss vs. Energy Curves for Heavy Particles in Various Media", by W. A. Aron, B. G. Hoffman and F. C. Williams (2nd Edition November 1948). Part of the introduction to that report should be included here. "The rate of energy loss given by the curves is generally obtained from the theoretical formula given by Bethe and Livingstone, Rev. of Mod. Phys. 9, 263 (1937). A few of the curves at low energies are based on experimental measurements. The range values are determined by numerical integration of the reciprocal of the rate of energy loss with respect to the energy, with low energy values being based on experimental values rather than theoretical.

"The results given here are tentative pending better determination of the average ionization potentials, I, used in the calculation. The value of I used was 11.5 Z ev. Recent experiments indicate a considerably lower value."

Instead of the actual curves given in the report above, however, we used the calculated ranges from which the curves were drawn. These values were obtained from the Theoretical Physics Group in tabular form and are presented in Tables 9 - 17 inclusive. (Values for Tables 10 and 11 were uncluded in UCRL 121, Second Revision by Aron, Huffman and Williams.) In making the energy calculations for the excitation functions, a certain value was taken as the range of the full energy particles from the 184-inch cyclotron (Table 18). From this value was

Table 9

Range of Protons in Carbon

Energy (Mev)	R (mg/cm^2)
0	0
1	2.760
2	8.1130
3	15.9838
4	26.2925
5	38.8859
6	53.5789
7	70.3867
8	89.2378
9	110.106
10	132.935
12	184.374
14	243.321
16	309.577
18	382.973
20	463.358
30	965.798
40	1626.67
50	2436.03
60	3385.80
70	4469.08
80	5679.79
90	7012.42
100	8461.97
150	17311.9
200	28545.0
250	41671.5
300	56553.4
350	72860.7

Table 10

Range of Protons in Copper

Energy(Mev)	R(mg/cm^2)	R_{348}-R(mg/cm^2)	ΔR(mg/cm^2)
4	46.66		
5	68.48		
6	91.70	97158.3	
8	146.95	97103.05	
10	213.45	97036.55	
12	290.71	96959.29	
14	378.36	96871.64	97.72
16	476.08	96773.92	107.53
18	583.61	96666.39	117.10
20	700.71	96549.29	126.46
22	827.17	96422.83	135.64
24	962.81	96287.2	144.63
26	1107.44	96142.6	153.47
28	1260.91	95989.1	162.19
30	1423.1	95826.9	442.5
35	1865.6	95384.4	494.1
40	2359.7	94890.3	544.0
45	2903.7	94346.3	592.2
50	3495.9	93754.1	639.1
55	4135.0	93115.0	684.7
60	4819.7	92430.3	729.1
65	5548.8	91701.2	772.4
70	6321.2	90928.8	814.7
75	7135.9	90114.1	855.9
80	7991.8	89258.2	896.3
85	8888.1	88361.9	935.7
90	9823.8	87426.2	974.2
95	10798	86452	1012
100	11810	85440	2134
110	13944	83306	2276
120	16220	81030	2413
130	18633	78617	2544
140	21177	76073	2670
150	23847	73403	2792
160	26639	70611	2909
170	29548	67702	3023
180	32571	64679	3132
190	35703	61547	3238
200	38941	58309	8536
225	47477	49773	9124
250	56601	40649	9667
275	66268	30982	10169
300	76437	20813	10633
325	87070	10180 / 97,250	11065
350	98135		

Table II

Range of Protons in Lead and Thorium

Energy(Mev)	R_{Pb}(mg/cm^2)	R_{Th}(mg/cm^2)	ΔR_{Th}(mg/cm^2)	$\Delta R_{Th}/\Delta R_{Cu}$
1	7.90			
2	25.05			
3	49.8			
4	81.668	83.353		
6	151.522	154.648		
8	238.252	243.167		
10	340.863	347.895		
12	458.034	467.483		
14	589.509	601.671		
16	734.831	749.991		
18	893.608	912.043	175.434	1.498
20	1065.496	1087.477	188.500	1.491
22	1250.186	1275.977	201.284	1.484
24	1447.401	1477.261	213.810	1.478
26	1656.889	1691.071	226.099	1.473
28	1878.418	1917.170	238.166	1.468
30	2111.770	2155.336	646.900	1.462
35	2745.594	2802.236	718.871	1.455
40	3449.935	3521.107	786.937	1.447
45	4220.965	4308.044	853.223	1.441
50	5056.942	5161.267	917.438	1.436
55	5955.836	6078.705	979.788	1.431
60	6915.820	7058.493	1040.416	1.427
65	7935.206	8098.909	1099.436	1.423
70	9012.419	9198.345	1156.958	1.420
75	10145.991	10355.303	1213.06	1.417
80	11334.53	11568.36	1267.83	1.415
85	12576.73	12836.19	1321.31	1.412
90	13871.33	14157.50	1373.59	1.410
95	15217.16	15531.09	1424.70	1.408
100	16613.06	16955.79	2998	1.405
110	19551	19954	3190	1.402
120	22676	23144	3374	1.398
130	25982	26518	3551	1.396
140	29461	30069	3721	1.394
150	33107	33790	3883	1.391
160	36912	37673	4043	1.390
170	40873	41716	4193	1.387
180	44981	45909	4341	1.386
190	49234	50250	4481	1.384
200	53625	54731	11792	1.381
225	65178	66523	12575	1.378
250	77499	79098	13296	1.375
275	90526	92394	13962	1.373
300	104206	106356	14575	1.371
325	118487	120931	15144	1.369
350	133325	136075		

Table 12
Range of Protons in Lead and Uranium

Energy(Mev)	R_{Pb}(mg/cm^2)	R_U(mg/cm^2)	ΔR_U(mg/cm^2)	$\Delta R_U/\Delta R_{Cu}$
1	7.90			
2	25.05			
3	49.8			
4	81.668	83.630		
6	151.522	155.163		
8	238.252	243.977		
10	340.863	349.053		
12	458.034	469.046		
14	589.509	603.675	148.814	1.523
16	734.831	752.489	162.592	1.512
18	893.608	915.081	175.018	1.503
20	1065.496	1091.099	187.129	1.496
22	1250.186	1280.228	201.954	1.489
24	1447.401	1482.182	214.522	1.483
26	1656.889	1696.704	226.852	1.478
28	1878.418	1923.556	238.96	1.473
30	2111.770	2162.516	649.06	1.467
35	2745.594	2811.571	721.26	1.460
40	3449.935	3532.837	789.56	1.451
45	4220.965	4322.395	856.07	1.446
50	5056.942	5178.460	920.49	1.440
55	5955.836	6098.955	983.05	1.436
60	6915.820	7082.007	1043.88	1.432
65	7935.206	8125.889	1103.10	1.428
70	9012.419	9228.987	1160.81	1.425
75	10145.991	10389.799	1217.10	1.422
80	11334.53	11606.90	1272.05	1.419
85	12576.73	12878.95	1325.71	1.417
90	13871.33	14204.66	1378.17	1.415
95	15217.16	15582.83	1429.44	1.412
100	16613.06	17012.27	3008	1.410
110	19551	20020	3201	1.406
120	22676	23221	3385	1.403
130	25982	26606	3563	1.401
140	29461	30169	3734	1.399
150	33107	33903	3896	1.395
160	36912	37799	4056	1.394
170	40873	41855	4207	1.392
180	44981	46062	4355	1.390
190	49234	50417	4497	1.389
200	53625	54914	11830	1.386
225	65178	66744	12617	1.383
250	77499	79361	13340	1.380
275	90526	92701	14009	1.378
300	104206	106710	14624	1.375
325	118487	121334	15195	1.373
350	133325	136529		

Table 13

Range of Deuterons in Aluminum

Energy(Mev)	R(mg/cm^2)	R_{50}-R(mg/cm^2)	ΔR(mg/cm^2)
0.2	0.192		
0.4	0.503		
0.6	0.917		
0.8	1.42		
1	2.03		
2	6.90		
3	13.38		
4	21.6	1651.4	9.6
5	31.2	1641.8	10.8
6	42.0	1631.0	12.6
7	54.6	1618.4	14.4
8	69.0	1604.0	15.2
9	84.2	1588.8	16.4
10	100.6	1572.4	17.4
11	118.0	1555.0	20.2
12	138.2	1534.8	20.2
13	158.4	1514.6	21.6
14	180.0	1493.0	22.6
15	202.6	1470.4	23.8
16	226.4	1446.6	24.8
17	251.2	1421.8	26.4
18	277.6	1395.4	27.2
19	304.8	1368.2	28.6
20	333.4	1339.6	29.4
21	362.8	1310.2	30.4
22	393.2	1279.8	31.8
23	425.0	1248.0	33.0
24	458.0	1215.0	34.2
25	492.2	1180.8	35.2
26	527.4	1145.6	36.2
27	563.6	1109.4	37.6
28	601.2	1071.8	77.4
30	678.6	994.4	167.0
34	845.6	827.4	183.4
38	1029	644	200
42	1229	444	214
46	1443	230	230
50	1673	0	

Table 14

Range of Deuterons in Copper

Energy(Mev)	R(mg/cm^2)	R_{194}-R(mg/cm^2)	ΔR(mg/cm^2)
8	93.32	22314.7	90.1
12	183.4	22224.6	110.5
16	293.9	22114.1	133.0
20	426.9	21981.1	154.5
24	581.4	21826.6	175.3
28	756.7	21651.3	195.5
32	952.2	21455.8	214.8
36	1167	21241	234
40	1401	21007	253
44	1654	20754	272
48	1926	20482	289
52	2215	20193	307
56	2522	19886	324
60	2846	19562	885
70	3731	18677	988
80	4719	17689	1088
90	5807	16601	1185
100	6992	15416	1278
110	8270	14138	1369
120	9639	12769	1461
130	11100	11308	1540
140	12640	9678	1630
150	14270	8138	1710
160	15980	6428	1800
170	17780	4628	1870
180	19650	2758	1950
190	21600	808	2020
200	23620		

Table 15

Range of Deuterons in Lead and Thorium

Energy(Mev)	R_{Pb}(mg/cm^2)	R_{Th}(mg/cm^2)	ΔR_{Th}(mg/cm^2)	$\Delta R_{Th}/\Delta R_{Cu}$
0.1	.177			
0.2	.460			
0.3	.814			
0.5	1.699			
0.7	2.761	2.818		
1	4.850	4.950		
1.5	9.629	9.828		
2	15.682	16.001		
2.5	22.94	23.41		
3	31.05	31.69		
3.5	40.07	40.90		
4	50.27	51.31		
5	73.28	74.79		
6	99.69	101.75		
7	129.78	132.46		
8	163.19	166.56		
11.9941	302.894	309.14	176.95	1.602
15.9921	476.268	486.09	209.36	1.574
19.9901	681.389	695.45	239.05	1.547
23.9881	915.615	934.50	268.24	1.529
27.9861	1178.43	1202.74	296.49	1.517
31.9842	1468.93	1499.23	323.95	1.508
35.9822	1786.33	1823.18	350.70	1.499
39.9802	2129.94	2173.88	376.81	1.490
43.9782	2499.13	2550.69	402.37	1.479
47.9762	2893.37	2953.06	427.41	1.479
51.9743	3312.14	3380.47	451.98	1.473
55.9723	3754.98	3832.45	476.09	1.468
59.9703	4221.45	4308.54	1293.16	1.462
69.9654	5488.47	5601.70	1437.02	1.453
79.9604	6896.45	7038.72	1573.10	1.445
89.9555	8437.75	8611.82	1705.6	1.439
99.9505	10108.9	10317.4	1834.0	1.435
109.946	11905.8	12151.4	1958.6	1.431
119.941	13824.8	14110.0	2079.8	1.414
129.936	15862.6	16189.8	2197.8	1.427
139.931	18015.9	18387.6	2312.7	1.418
149.926	20281.9	20700.3	2424.9	1.418
159.921	22657.8	23125.2	2534.5	1.408
169.916	25141.0	25659.7	2641.2	1.412
179.911	27728.9	28300.9	2746.0	1.408
189.906	30419.3	31046.9	2847.9	1.410
199.901	33209.7	33894.8		

Table 16

Range of Alphas in Copper

Energy(Mev)	R(mg/cm^2)	R_{388}-R(mg/cm^2)	ΔR(mg/cm^2)
4	5.09		
6	9.52		
8	14.91		
10	21.23		
12	28.44		
14	36.52		
16	45.43		
18	55.16		
20	65.68	11192.3	22.3
23.84	87.95	11170.0	54.8
31.78	142.8	11115.2	66.1
39.73	208.9	11049.1	76.7
47.67	285.6	10972.4	87.0
55.62	372.6	10885.4	97.1
63.56	469.7	10788.3	106.8
71.51	576.5	10681.5	116.3
79.45	692.8	10565.2	125.6
87.40	818.4	10439.6	134.7
95.34	953.1	10304.9	143.6
103.29	1096.7	10161	152.5
111.23	1249.2	10009	160.8
119.2	1410	9848	440
139.0	1850	9408	490
158.9	2340	8918	541
178.8	2881	8377	588
198.6	3469	7789	635
218.5	4104	7154	680
238.4	4784	6474	724
258.2	5508	5750	767
278.1	6275	4983	809
298.0	7084	4174	850
317.8	7934	3324	890
337.7	8824	2434	930
357.5	9754	1504	966
377.4	10720	538	
397.3	11730	--	

Table 17

Range of Alphas in Lead and Thorium

Energy(Mev)	R_{Pb} (mg/cm^2)	R_{Th}(mg/cm^2)	ΔR_{Th}(mg/cm^2)
.1	.4142		
.2	.6337		
.3	.8213		
.5	1.1470		
.7	1.462		
1.0	1.933		
1.5	2.804		
2.0	3.745		
3.0	6.060		
5	12.461		
7	21.017		
10	37.524		
12	50.976	52.028	
14	66.329		
16	81.086		
18	96.974		
20	113.975	116.326	
22	132.069		
24	151.239		
26	171.468		
28	192.741		
30	215.041		
32	238.332		
34	262.596	268.013	
36	287.823	293.761	
38	314.003	320.481	
40	341.124	348.161	
42	369.178	376.794	
44	398.155	406.369	
46	428.047	436.878	
48	458.845	468.311	
50	490.541	500.661	
55	573.574	585.407	
60	662.156	675.816	

Table 17 (cont'd)

Range of Alphas in Lead and Thorium

Energy(Mev)	R_{Pb} (mg/cm^2)	R_{Th} (mg/cm^2)	ΔR_{Th} (mg/cm^2)
65	756.096	771.693	
70	855.299	872.944	101.251
75	959.683	979.481	106.537
80	1069.168	1091.225	111.744
85	1183.681	1208.100	116.875
90	1303.151	1330.035	121.935
95	1427.513	1456.963	126.928
100	1556.706	1588.821	131.858
110	1829.36	1867.10	278.28
120	2120.66	2164.61	297.31
130	2430.22	2480.36	316.95
140	2757.66	2814.55	334.19
150	3102.65	3166.66	352.11
160	3464.87	3536.35	369.69
170	3857.51	3937.09	400.64
180	4239.76	4327.23	390.24
190	4651.80	4747.77	420.54
200	5079.90	5184.70	436.93
218.497	5966.85	6089.95	905.25
238.360	6866.64	7008.30	918.35
258.224	7879.06	8041.61	1033.31
278.087	8949.01	9133.63	1092.02
297.950	10074.8	10282.6	1148.97
317.814	11255.2	11487.4	1204.8
337.677	12488.9	12746.5	1259.1
357.540	13774.6	14058.8	1312.3
377.404	15111.3	15423.0	1364.2
397.267	16497.6	16837.9	1414.9

Table 18

Interpolated Range of Maximum Energy Particles
in Copper from the 184-inch Cyclotron

Particles	Energy	Range(mg/cm^2 Cu)
Protons	348	97,250
Deuterons	194	22,418
Alphas	388	11,258

subtracted the thickness (mg/cm^2) of absorbers interposed in the beam. Finally the energy at the middle of the target foil was obtained and plotted. It is admitted that the accuracy of these range values is not as great as indicated by the number of significant figures included in the tables. However it is believed that more precise results are obtained by using the tabular values indicated rather than rounding off the last decimal places until every figure is significant.

In the work presented herein the materials interposed in the beam include copper, thorium, uranium, aluminum and polystyrene foils. The alpha, deuteron, and proton beams of the 184 inch cyclotron were used. Range values were available for all three particles in copper and aluminum and for protons in carbon (assuming that carbon atoms alone are responsible for the stopping power of the polystyrene).

To obtain values for thorium and uranium, however, it was necessary to extrapolate the values given for lead by some means or other. It can be shown that when the range in mg/cm^2 times the ratio Z/A is plotted vs Z for a particular element at a given energy the resultant curve is fairly linear and can be used for extrapolation and interpolation between known values of the ranges. Since, however, only four actual points are available from aluminum to lead inclusive it is hard to tell just how to extrapolate. Hence the method of extrapolation we used assumed

that near lead the value of Range times Z/A is a constant. While this assumption is not strictly true it should give the range in the thorium and uranium to within at least 2%. Since in each of the experiments the amount of target foil was never more than 16% of the total foil thickness for alpha bombardments, about 8% for deuteron bombardments and about 1.8% for proton bombardments, the overall error through the absorber stack is rather small.

For each bombardment the energy calculations were kept in terms of either copper or aluminum, the former being used in most cases. To find the amount of copper equivalent to a certain amount of thorium, the ratio of differential range between two adjacent energy values of thorium to that same interval value for copper was calculated (ΔR in Tables). The amount of thorium (mg/cm^2) was then divided by this figure to obtain the equivalent amount of copper.

This same method was used whenever mg/cm^2 of one absorber had to be changed into equivalent mg/cm^2 of another absorber.

In the tables are listed the theoretical ranges of various energy particles, as well as the ΔR values (differences in range between two adjacent energy values). In calculations of excitation function energies, the sum of absorber values must be subtracted from the assumed maximum range of the particles in order to determine the range and hence the energy of the particles at a particular foil. To facilitate this process a column has been included in the tables giving $[R(max) - R]$ --- (where R(max) is the value given in Table 18) enabling direct conversion of the amount of absorber already inserted in the beam into energy values. In the tables involving the heavy elements, the ranges of lead are the calculated values of Aron et.al., while the ranges given for thorium and uranium have been interpolated as mentioned above. A factor of 1.0206 was used to multiply range in lead to give range in thorium; a factor of 1.0240 was used for uranium ranges. The ratio of

$\Delta R_{Th}/\Delta R_{Cu}$ and the same ratio for uranium are used to find the amount of copper equivalent to a given amount of the heavy metal.

Tables 10, 11 and 12 give the range of protons in copper, thorium and uranium respectively; Tables 13, 14 and 15 give the ranges of deuterons in aluminum, copper and thorium respectively; while Tables 16 and 17 give the ranges of alpha particles in copper and thorium respectively.

In planning these excitation function experiments we assumed a most probable maximum value of the beam energy for each of the three particles. By linear interpolation of the range-energy tables a range value for this energy was obtained which by definition was then called the maximum range of the particles. These energies and ranges are listed in Table 18 .

The 184 inch cylotron is not however a precision instrument in its energy definition, probably having a spread of up to 3% in its full energy internal beam and 1/2 to 1% in the external beam. If the full energy beam were spread evenly over these intervals, by the time the energy of the particles had been reduced the indicated amounts through copper these spreads would be magnified as shown in Table 19 .

In reality of course the situation is not as bad as this table would seem to indicate since the beam spread probably has a distribution much like that shown in Figure 71, where the maximum values mentioned above and in Table 18 are those for point A in the figure.

When the electrostatically deflected beam is used the energies selected are probably more homogeneous than with the plain internal beam since the field of the cyclotron acts as a crude velocity selector and only a portion of the total area of the deflected beam is allowed to hit the target.

POSSIBLE ENERGY DISTRIBUTION
FOR 184" CYCLOTRON BEAM

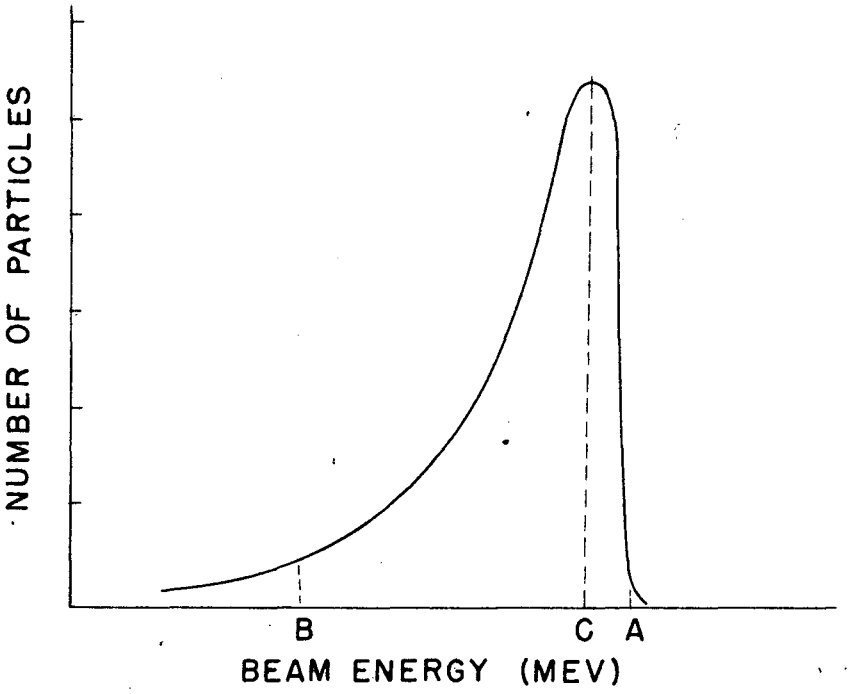

FIG. 71

Table 19

Spread of Particles of Given Initial Spreads at Various Energies

External Beam

Initial Beam Spread	Mev	Approximate Spread (Mev)	
348-346 Mev(~1/2%)	22.8	22.8 -0	(22.8)
	60	60 - 53.5	(6.5)
	120	120 - 116.2	(3.8)
	180	180 - 177.1	(2.9)
348-344.5 Mev(~1%)	31.2	31.2 - 0	(31.2)
	60	60 - 48	(12)
	120	120 - 113	(7)
	180	180 - 175	(5)

Internal Beam

Initial Beam Spread	Mev	Approximate Spread(Mev)	
348-343 Mev (~1-1/2%)	38.6	38.6 - 0	(38.6)
	60	60 - 42.2	(17.8)
	120	120 - 110.3	(9.7)
	180	180 - 172.7	(7.3)
348-338 Mev (~3%)	57.2	57.2 - 0	(57.2)
	60	60 - 14.2	(45.8)
	120	120 - 99.5	(20.5)
	180	180 - 165.2	(14.8)

E. L. Kelley has used the value of 388 Mev for the peak energy (point C, Figure 71) of the initial distribution of the alpha-particle beam and has roughly matched the peak on a $Bi^{209}(\alpha,2n)At^{211}$ excitation curve taken with the electrostatically deflected beam of the 184-inch cyclotron[23] with a curve of the same reaction taken very carefully with the 39 Mev external alpha beam of the 60 inch Berkeley cyclotron.[28]

In Kelley's experiments however the half width of the peak for the electrostatically deflected beam determination is about 500 mg/cm^2 of aluminum compared to about 116 mg/cm^2 of aluminum on the 60 inch cyclotron. Hence it can be seen that there are definite factors causing increasing spread of the beam in the large cyclotron.

There are two principal effects tending to spread out a sharp peak in an excitation function performed with stacked foils on the 184-inch cyclotron. First there is the initial energy distribution of the electrostatically deflected beam (which as mentioned above may be somewhat less than that for the internal beam). A possible distribution for the internal beam is listed very roughly for the various particle beams in Table 20 , where A and B refer to points in Figure 71 .

Table 20

Possible Initial Energy Spread of Internal Cyclotron Beam

Particles	Energy Spread (Mev)	
	A	B
Protons	348	334
Deuterons	194	188
Alphas	388	376

These distributions are probably not much more than guesses. Probably the best way to determine the energy distribution is to take a reaction with a known excitation function at low energies, bombard with minimum errors in calibration and yield, and find what initial distribution (corrected for straggling) could give the

observed peak broadening.

One other effect must be considered in this calculation, -- the straggling of the particle beams. This effect can be calculated and the correction applied to any curve obtained from stacked foil bombardment -- although this correction may be quite involved. Such a calculation has been made by W. Aron of the Theoretical Physics Group of the Radiation Laboratory, indicating the straggling of protons by passage through copper. The values presented in Table 21 are the squares of the "widths" of the Gaussian distribution of the distance in copper traveled by particles (starting at 350 Mev) which have lost the same amount of energy. The values were obtained by Aron by using formula (790) in Bethe's article (Rev. Mod. Phys. 9, 283 (1937)). Similar values for deuterons and alpha-particles can be obtained by applying formula (795a) of Bethe's to the values given in Table 21 . To obtain the "width" of energy corresponding to this range straggling, multiply the square root of the value from the table by the differential value dE/dX included in Tables 22, 23 and 24 . It is seen that at 100 Mev this energy "width" is about 4.3 Mev while at 50 Mev it has increased to about 7.3 Mev.

While trying to establish an absolute energy scale for proton and deuteron reactions we decided to make an excitation function bombardment on some target material whose cross sections and excitation curve were known accurately from low energy bombardments. A literature search for this type of target material resulted in a considerable list of excitation functions. Appendix I includes most of these thin target excitation functions reported in the literature up to May 1948.

Table 21

Range Straggling of 350 Mev Protons on Copper
(From Calculations by W. Aron)

Energy(Mev)	$(R-\bar{R})^2_{av}$ $(mg/cm^{-2})^2$	Energy(Mev)	$(R-\bar{R})^2_{av}$ $(mg/cm^{-2})^2$
4	8.032×10^5	100	7.842×10^5
8	8.032	120	7.693
12	8.032	140	7.483
16	8.032	160	7.204
20	8.031	180	6.846
30	8.029	200	6.405
40	8.022	225	5.726
50	8.012	250	4.899
60	7.996	275	3.917
70	7.972	300	2.774
80	7.939	325	1.470
90	7.896	350	0

Table 22

Rate of Energy Loss for Protons in Copper

Energy(Mev)	$-dE/dx \cdot 10^3$ (Mev/mgcm^{-2})	Energy(Mev)	$-dE/dx \cdot 10^3$ (Mev/mgcm^{-2})
5	46.08	80	5.706
6	40.46	82.5	5.579
7	36.18	85	5.458
8	32.81	87.5	5.344
9	30.07	90	5.235
10	27.80	92.5	5.132
11	25.88	95	5.034
12	24.24	97.5	4.941
13	22.82	100	4.852
14	21.57	105	4.685
15	20.46	110	4.533
16	19.48	115	4.393
17	18.60	120	4.264
18	17.80	125	4.145
19	17.08	130	4.034
20	16.42	135	3.931
21	15.81	140	3.835
22	15.26	145	3.745
23	14.75	150	3.661
24	14.27	155	3.582
25	13.83	160	3.507
26	13.42	165	3.437
27	13.03	170	3.371
28	12.67	175	3.308
29	12.33	180	3.249
30	12.02	185	3.193
32.5	11.30	190	3.139
35	10.67	195	3.088
37.5	10.12	200	3.040
40	9.629	212.5	2.928
42.5	9.192	225	2.829
45	8.798	237.5	2.740
47.5	8.442	250	2.659
50	8.119	262.5	2.586
52.5	7.824	275	2.519
55	7.552	287.5	2.458
57.5	7.302	300	2.402
60	7.072	312.5	2.351
62.5	6.857	325	2.303
65	6.659	337.5	2.259
67.5	6.473	350	2.218
70	6.300	362.5	2.180
72.5	6.137	375	2.145
75	5.985	387.5	2.112
77.5	5.841	400	2.081

Table 23

Rate of Energy Loss for Deuterons in Copper

Energy(Mev)	$-dE/dx$ (Mev/mgcm^{-2})	Energy(Mev)	$-dE/dx$ (Mev/mgcm^{-2})
12	4.046×10^{-2}	80	9.629×10^{-3}
16	3.281	90	8.798
20	2.780	100	8.119
24	2.424	110	7.552
28	2.157	120	7.072
32	1.948	130	6.659
36	1.780	140	6.300
40	1.642	150	5.985
44	1.526	160	5.706
48	1.427	170	5.458
52	1.342	180	5.235
56	1.267	190	5.034
60	1.202	200	4.852
70	1.067		

Table 24

Rate of Energy Loss for Alphas in Copper

Energy(Mev)	$-dE/dx$ (Mev/mgcm^{-2})	Energy(Mev)	$-dE/dx$ (Mev/mgcm^{-2})
4	5.086×10^{-1}	63.56	7.792
5	4.516	71.51	7.120
6	4.068	79.45	6.568
7	3.707	87.40	6.104
8	3.412	95.34	5.708
9	3.164	103.29	5.368
10	2.954	111.23	5.068
11	2.773	119.2	4.808×10^{-2}
12	2.615	139.0	4.268
13	2.476	158.9	3.852
14	2.353	178.8	3.519
15	2.243	198.6	3.248
16	2.144	218.5	3.021
17	2.055	238.4	2.829
18	1.975	258.2	2.664
19	1.902	278.1	2.520
20	1.834	298.0	2.394
23.84	1.618	317.8	2.282
31.78	1.312	337.7	2.183
39.73	1.112	357.5	2.094
47.67	9.696×10^{-2}	377.4	2.014
55.62	8.628	397.3	1.941

Requisite for a reaction was a relatively plentiful target material, available in foil form, which requires a minimum of chemistry before counting (preferably no chemistry). It was also necessary that the reaction approach some transition (preferably a peak) in the energy interval used. The $Al^{27}(d,\alpha p)Na^{24}$ reaction was the first one checked. This reaction has been explored quite exhaustively by Clarke[29] on the MIT cyclotron but unfortunately the 14.5 Mev available from that cyclotron was not enough to peak the reaction (see Fig. 72). Since the other factors were favorable however this reaction was run in the hopes that the threshold values observed with the 184-inch cyclotron might have some meaning in terms of the absolute energy. The $C^{12}(d,n)N^{13}$ reaction has been studied through its peak by Newson[30] (see Fig. 73).

These two reactions were therefore studied with the 184-inch electrostatically deflected beam in an attempt to establish definite energy relationships between the high and low energy bombardments. This attempt has proven rather unsuccessful although the curves do serve to establish the general validity of our other results.

Furthermore it should be possible to obtain a peak for the (p,3n) reaction very easily and perhaps even to get just the threshold for the (p,6n) reaction with the 32 Mev protons of the Berkeley linear accelerator. When these values are established with a beam whose energy variation can be made $\pm$ 0.2 Mev the interpretation of the curves made with the large cyclotron may be facilitated.

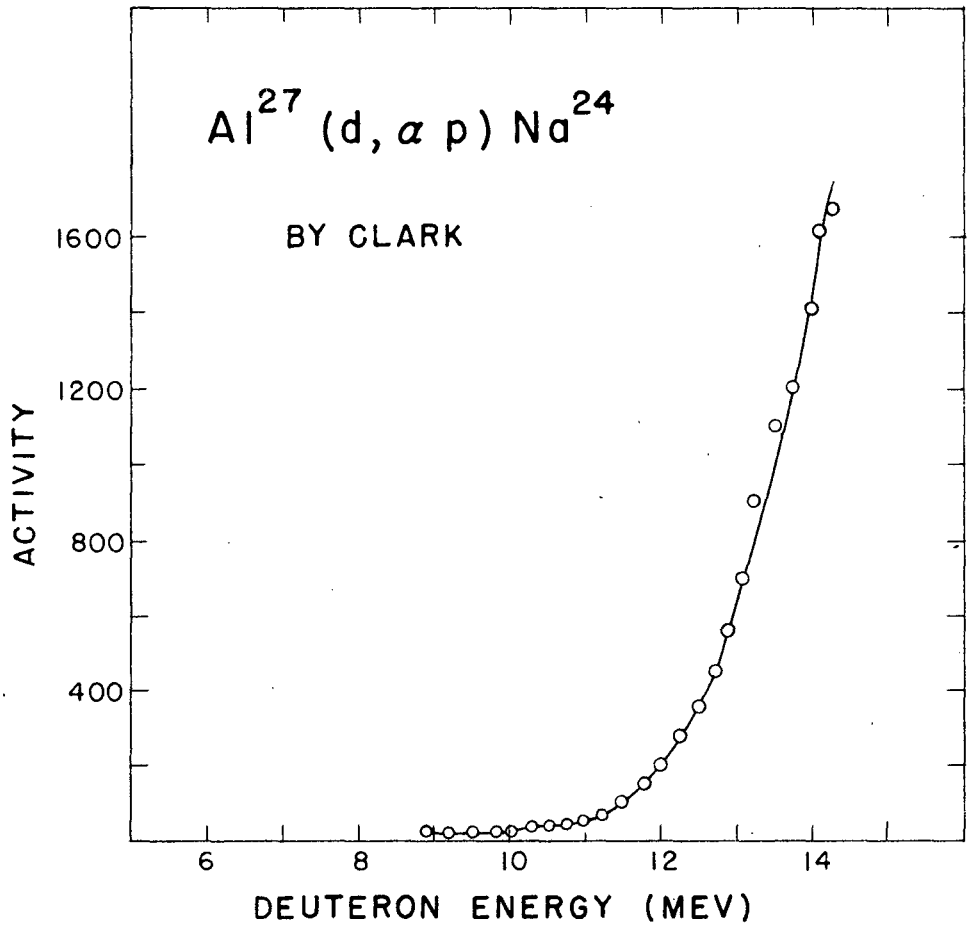

Fig. 72. Excitation function for the $Al^{27}(d,\alpha p)Na^{24}$ reaction as determined by E. T. Clarke, Phys. Rev. 71, 187 (1947).

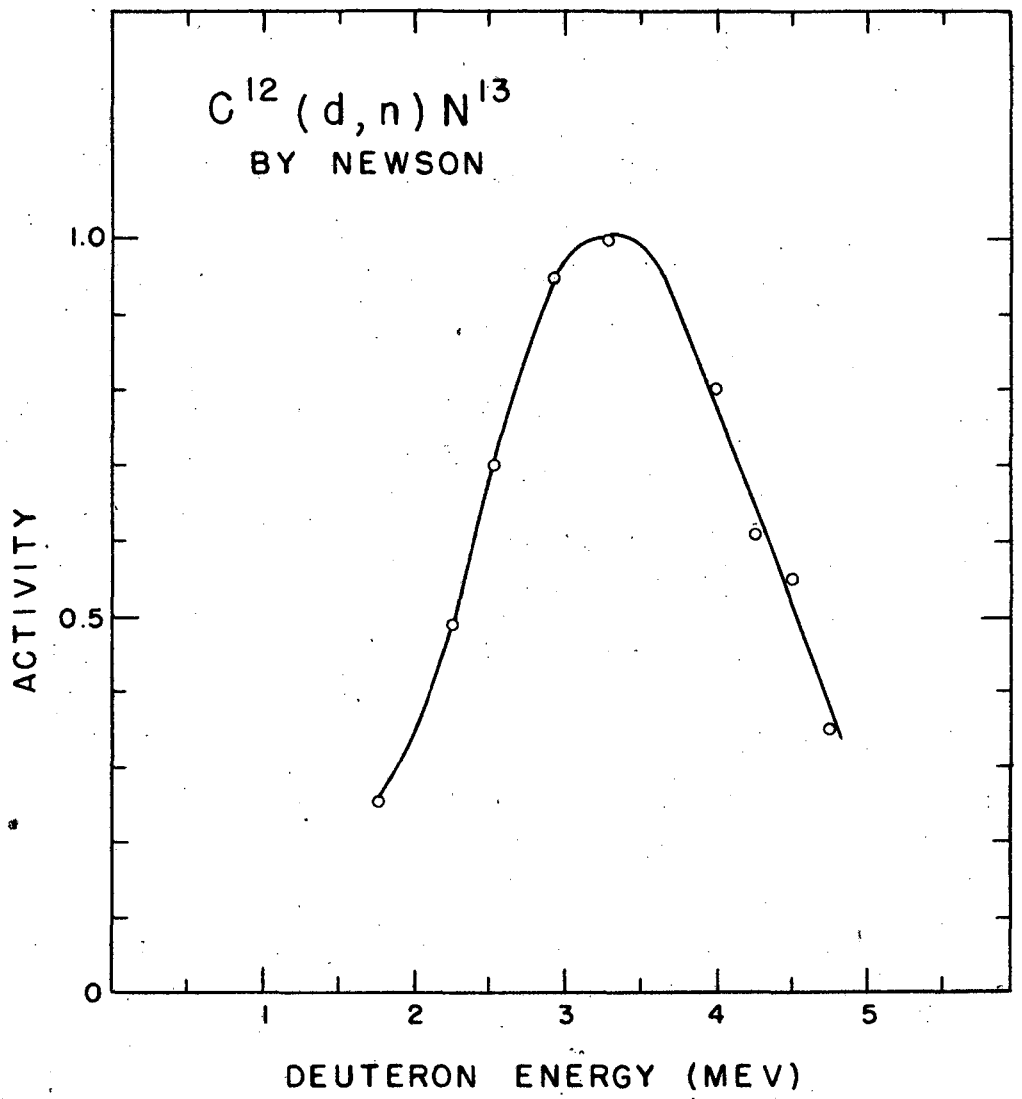

Fig. 73. Excitation function for the $C^{12}(d,n)N^{13}$ reaction as determined by H. W. Newson, Phys. Rev. 51, 620 (1937).

IV. Experimental Excitation Function Determinations

Using the above methods and calculations we have obtained excitation functions for the (d,7n) and (d,4n) reactions on thorium, the (d,αp) reaction on aluminum and the (d,n) reaction on carbon (as polystyrene); the (p,6n) and (p,3n) reactions on thorium, and the (p,α8n) and (p,α5n) reactions on uranium; as well as the (α,p8n) and (α,p5n) reactions on thorium and some rough values for the (α,6n) and (α,8n) reactions on thorium. These reactions will be discussed individually in this section.

A. Deuterons

1. $Th^{232}(d,7n)Pa^{227}$ The results obtained for this reaction with the recoil method are shown in Fig. 74 . The yield distribution is very spread out and gives a false impression of the true excitation function. It is interesting however to compare this curve with Fig. 75 to note how the efficiency of recoil at different energies has affected the shape of the excitation function.

No attempts were made to determine excitation functions for deuterons in the internal beam since the inch or more of copper that the deuteron beam must traverse becomes very unwieldly when clamped in a target holder. Consequently the first yield values obtained with deuterons, aside from the recoils, were a group of absolute cross section values obtained with the help of V. Peterson using the collimated external deuteron beam to bombard 5-mil foils of thorium. The current passing through the target was collected and measured with a Faraday Cup. Pa^{231} tracer was used to determine the chemical yield, pulse analyses being used to obtain the amount of Pa^{231} present in the samples. Values of these absolute cross sections from several experiments are shown in Table 25 .

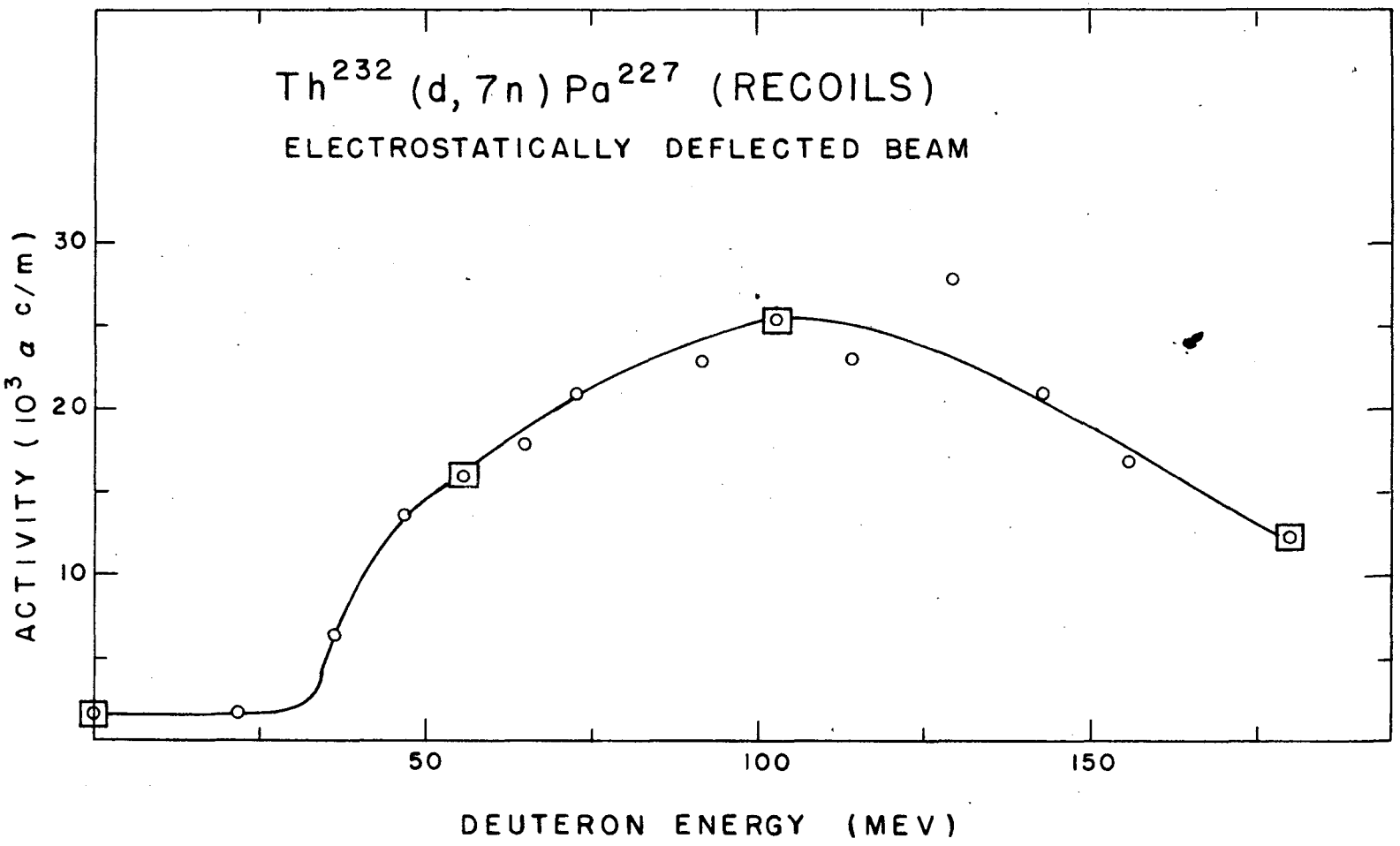

Fig. 74. Recoil excitation function for the $Th^{232}(d,7n)Pa^{227}$ reaction.

Table 25

Absolute Cross Section Values Obtained From the $Th^{232}(d,7n)Pa^{227}$ Reaction

Energy (Mev)	Run	Absolute σ (barns)
194	I	2.31×10^{-3}
194	I	2.38×10^{-3}
194	II	3.28×10^{-3}
134.6	II	5.96×10^{-3}
81.1	II	11.70×10^{-3}
48.2	II	0.78×10^{-3}

Question of the accuracy of these values lies principally in the chemistry. Protactinium has such weird chemistry and tends to go into the colloidal state so readily that one is never quite sure just how non-colloidal the Pa^{231} tracer solution is. Since extraction procedures are used to separate the protactinium, it is absolutely essential that the Pa^{231} tracer be 100% extractable and also be in the same state as the Pa^{227} formed in bombardment, i.e., the two tracers must exchange. The tracer Pa^{231} was stored in a TTA-benzene solution and washed into concentrated nitric acid a few hours before use by diluting the TTA solution with at least a ten-fold volume of benzene. In each case the Pa^{231} tracer was added to the beaker containing the metal target before solution so that the chemical loss was determined from the initial step.

The values presented in Table 25 are probably good to within 15% or better, except for the values for 48.2 and 194 Mev from Run II, which are only upper limits since the observed activity included some contamination that interfered with the pulse analyses.

When the new apparatus for use with the electrostatically deflected beam was completed we checked the general shape of the (d,7n) curve for thorium by taking many more points than the four previously obtained. A summary of the results of three of these bombardments is given in Table 26 and Fig. 75 . In each run the beam was collimated through the 3/4 inch collimator permitting maximizing of the beam on the target foil rather than just somewhere on the large block of absorber area. Run I was rather a poor bombardment as the yields will indicate, while Run II and Run III were more comparable. As mentioned previously, the yield values are given for a 0.4 gm sample of thorium at shutdown. The yields of Runs I and II were normalized to those for Run III by multiplication by 16.75 and 1.41 respectively. The energies of Run II were normalized to the other two runs by inserting 900 mg/cm^2 of copper absorber in the calculations on the low energy side of the "90 Mev" foil. The duration of each bombardment was: Run I, 38 minutes; Run II, 1 hour and 35 minutes; and Run III, 1 hour and 44 minutes.

We can see that the reaction yield rises to a very definite peak which is 8 times the yield value at full energy. The peak energy is 51 Mev on the plotted energy scale while the threshold value is about 30 Mev. The peak "half width" is about 18 Mev. From Table 25 and Fig.75 we obtain a value of about 1.8×10^{-2} barns for the absolute cross section for the reaction at the peak of its excitation function.

Fig. 76 shows the peak of this reaction on an enlarged energy scale while in Fig.77 the same points are plotted on a log scale to show the variation of the low yield points.

2. $\underline{Th^{232}(d,4n)Pa^{230}}$ In Fig.78 and Table 27 we see the companion curves and values to the ones just presented. The same plates that were counted for the yields above were allowed to decay for several weeks and then counted (along with a few alpha pulse analyses) for the U^{230} present. From this, the amount of

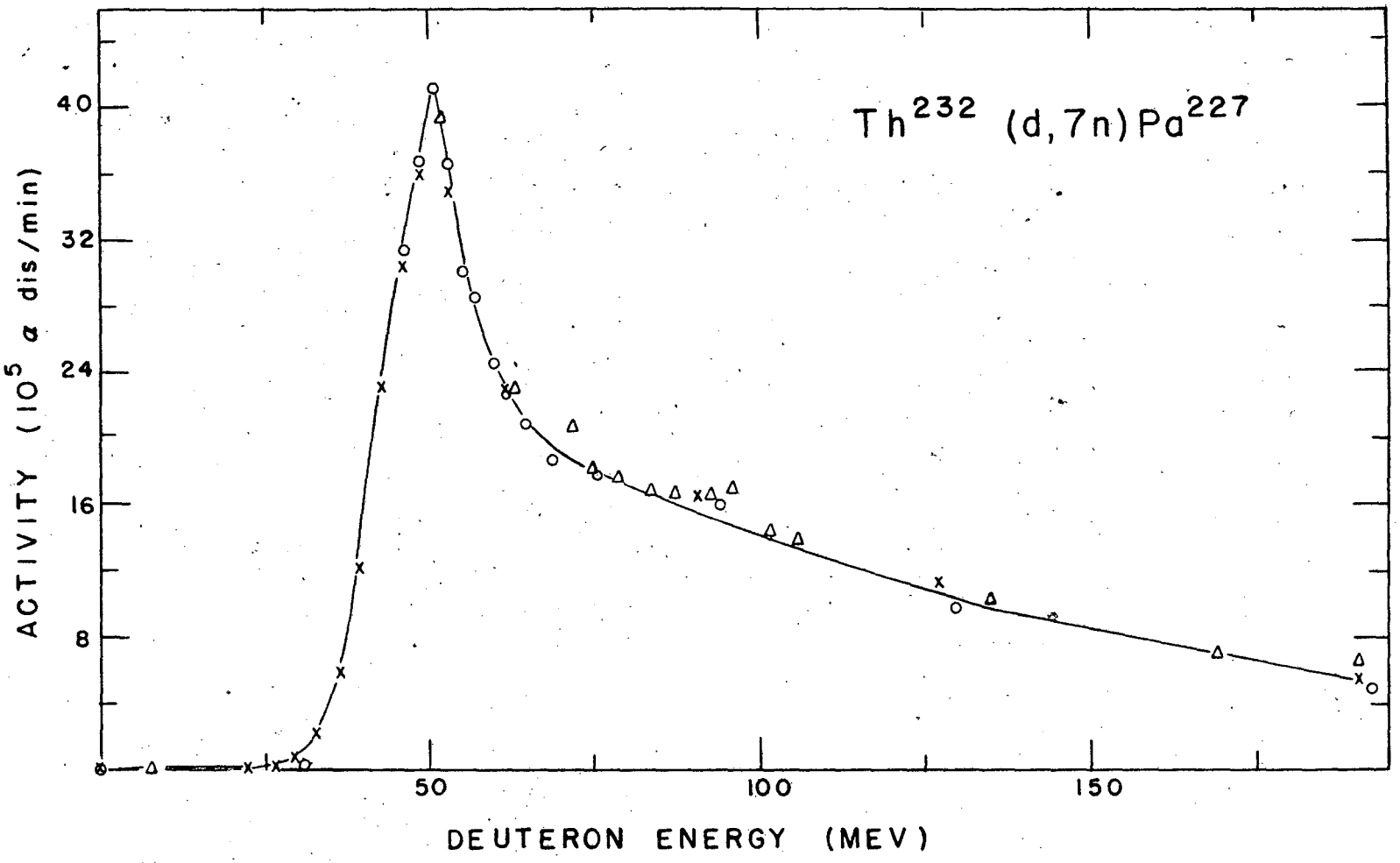

Fig. 75. Excitation function for the $Th^{232}(d,7n)Pa^{227}$ reaction, (Table 26). Circles represent Run III; deltas, Run I; and crosses, Run II. Run I and Run II activity normalized to Run III; Run II energies normalized to Run III.

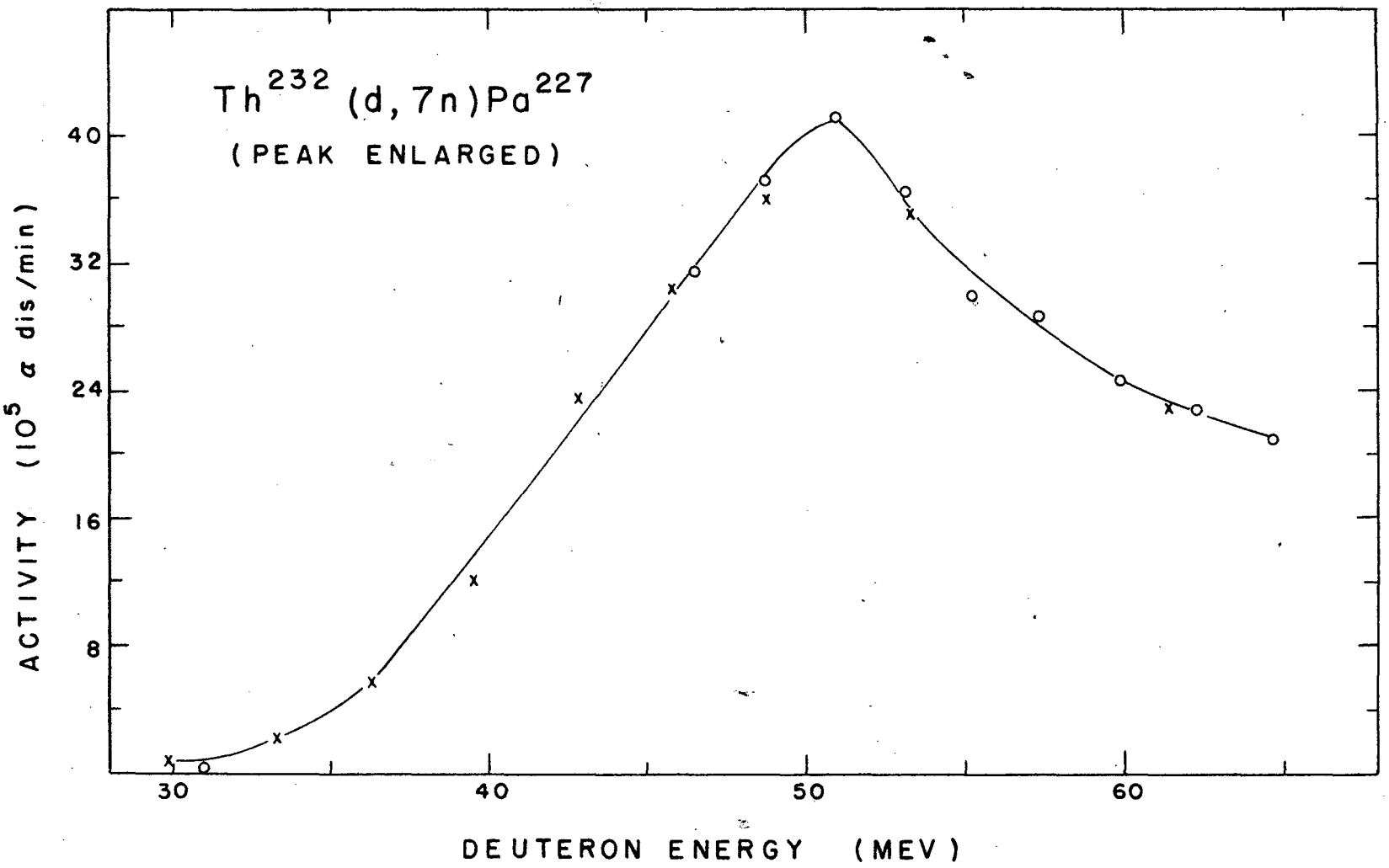

Fig. 76. Enlarged peak of the excitation function for the $Th^{232}(d,7n)Pa^{227}$ reaction, (Table 26). Circles represent Run III; crosses, Run II. Run II activity and energies normalized to Run III.

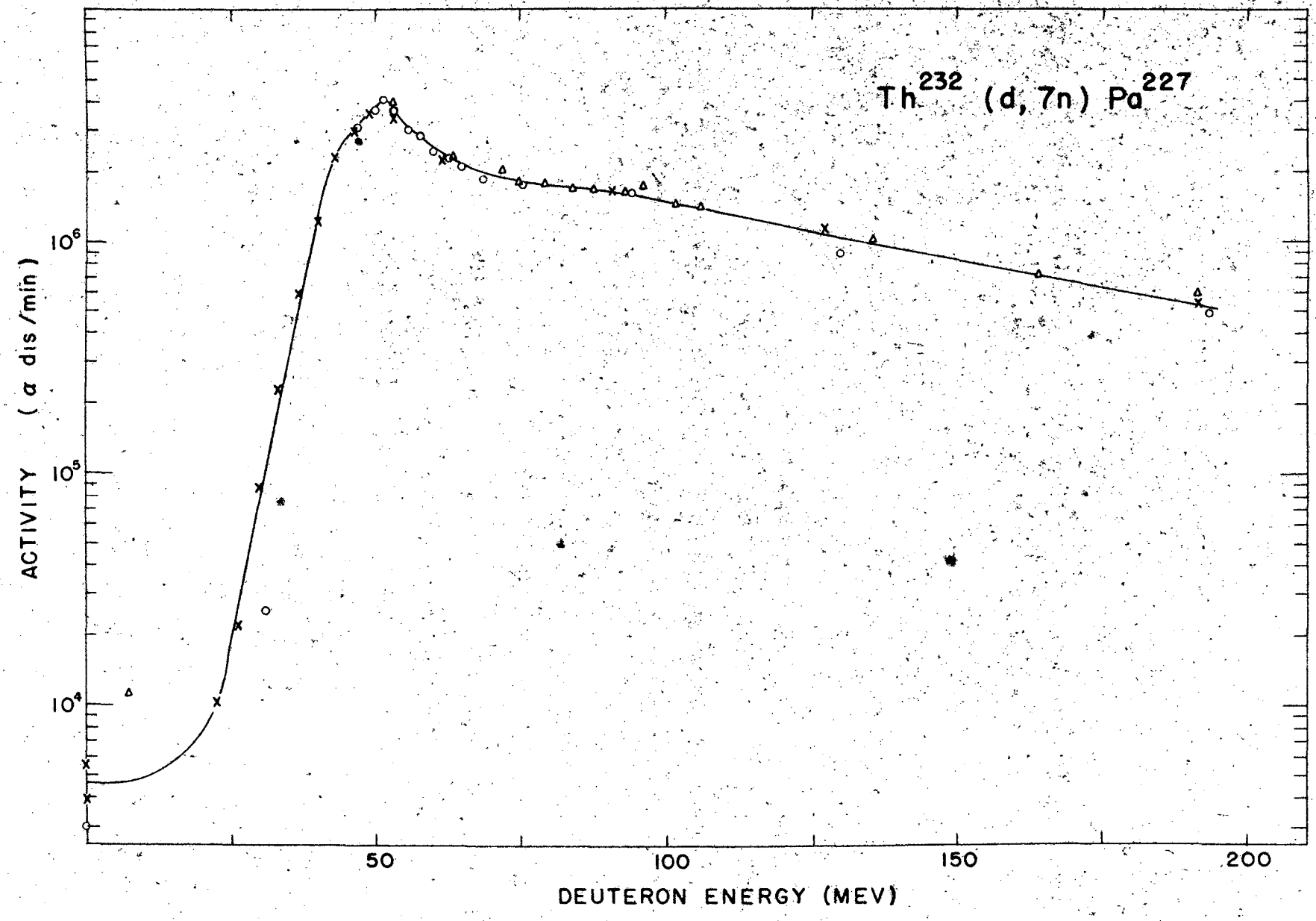

Fig. 77. Excitation function for the $Th^{232}(d,7n)Pa^{227}$ reaction (Table 26). Circles represent Run III; deltas, Run I; and crosses, Run II. Run I and Run II activity normalized to Run III; Run II energies normalized to Run III.

Table 26

Experimental Yields for the $Th^{232}(d,7n)Pa^{227}$ Reaction

Energy(Mev) Front	Energy(Mev) Back	Target Foil (mg/cm^2 Th)	Total absorber in beam(mg/cm^2 Cu) Front	Total absorber in beam(mg/cm^2 Cu) Back	Yield of Pa^{227} (10^4 α dis/min at end of bombardment) Run I	Run II	Run III
193.3	192.7	152.7	151.4	259.7			49.9
191.1	190.6	138.4	591.2	689.3		38.7	
191.0	190.5	140.7	613.1	712.9	3.63		
164.7	164.1	140.5	5589.9	5689.7	4.33		
135.7	135.0	140.9	10432.7	10531.5	6.27		
130.3	129.5	160.8	11269.7	11382.4			89.7
127.5	126.8	137.0	11699.3	11795.3		80.7	
111.7	110.9	139.6	13912.5	14009.9	-		
106.5	105.7	151.9	14583.9	14689.9	8.39		
102.1	101.3	151.4	15147.7	15253.2	8.68		
96.5	95.7	142.5	15828.1	15927.3	10.16		
94.5	93.5	158.6	16071.9	16182.0			160.4
92.8	92.0	138.6	16272.8	16369.0	9.87		
91.0	90.2	138.3	16484.8	16580.8		118.2	
88.0	87.1	152.6	16814.8	16920.6	10.04		
84.0	83.1	141.6	17250.0	17348.0	10.16		
79.5	78.5	139.6	17738.9	17835.4	10.70		
75.9	74.9	142.6	18092.3	18190.6			179.8
75.3	74.3	138.9	18155.9	18251.5	10.83		
72.2	71.3	134.9	18458.5	18551.2	12.42		
71.9	70.9	140.9	18491.1	18588.2		162.2	
69.2	68.0	158.4	18749.9	18858.6			187.2
65.3	64.1	153.3	19095.5	19200.4			210.
64.7	63.6	140.1	19147.5	19243.6		248.	
63.1	62.0	142.7	19287.5	19385.1	13.83		
62.9	61.7	157.8	19306.0	19413.9			228.
60.9	59.8	138.6	19480.5	19575.3		255.	
60.5	59.3	151.3	19518.5	19621.4			247.
58.5	57.2	154.2	19680.9	19786.4		215.	
58.0	56.8	136.2	19726.9	19819.5			286.
55.9	54.7	136.2	19890.7	19983.0			301.
55.9	54.6	151.1	19891.0	19993.7		165.3	
53.8	52.6	137.4	20054.9	20147.8			366.
53.2	52.0	138.4	20099.2	20193.3		85.4	
53.0	51.7	141.6	20115.6	20211.7	23.5		
51.7	50.4	134.7	20218.0	20308.8			411.
51.0	49.6	153.7	20264.5	20368.7		41.3	
49.6	48.1	154.7	20370.4	20475.0			369.
48.6	47.2	143.6	20440.6	20537.7		16.40	
47.2	45.8	140.0	20534.7	20630.1			314.
46.2	44.8	140.0	20607.9	20702.3		6.12	
43.7	42.1	150.1	20774.6	20875.5		1.558	
41.0	39.4	143.4	20945.1	21041.4		0.720	
	31.	142.0	-	-			2.50
30.8	28.9	142.7	21512.6	21606.6		0.400	
10.6	5.0	153.1	22256.7	22350.1	0.067		
0		149.5	22925.4	23015.1		0.276	
0							0.30

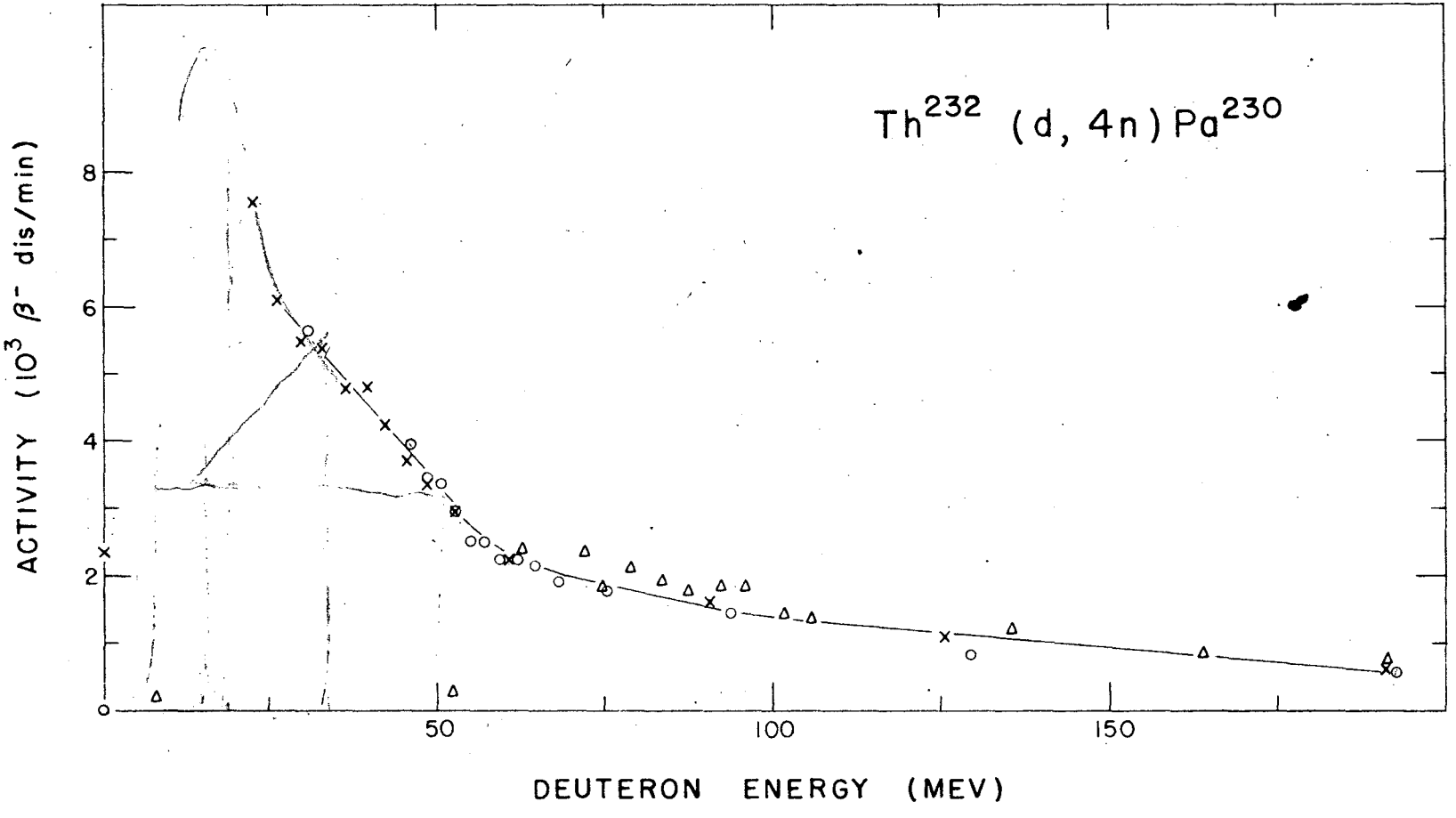

Fig. 78. Excitation function for the $Th^{232}(d,4n)Pa^{230}$ reaction (Table 27). Circles represent Run III; deltas, Run I; and crosses, Run II. Run I and Run II activities normalized to Run III; Run II energies normalized to Run III.

Table 27

Experimental Yields for the $Th^{232}(d,4n)Pa^{230}$ Reaction

Energy (Mev)		Target Foil	Total absorber in		Yield of Pa^{230} (β dis/min. at end of bombardment)		
		mg/cm^2 Th	beam (mg/cm^2 Cu)				
Front	Back		Front	Back	Run I	Run II	Run III
193.3	192.7	152.7	151.4	259.7			545.
191.1	190.6	138.4	591.2	689.3		716.	
191.0	190.5	140.7	613.1	712.9	41.5		
164.7	164.1	140.5	5589.9	5689.7	51.6		
135.7	135.0	140.9	10432.7	10531.5	71.2		
130.3	129.5	160.8	11269.7	11382.4			863.
127.5	126.8	137.0	11699.3	11795.3		1256.	
111.7	110.9	139.6	13912.5	14009.9	-		
106.5	105.7	151.9	14583.9	14689.9	83.5		
102.1	101.3	151.4	15147.7	15253.2	87.6		
96.5	95.7	142.5	15828.1	15927.3	109.9		
94.5	93.5	158.6	16071.9	16182.0			1450.
92.8	92.0	138.6	16272.8	16369.0	110.1		
91.0	90.2	138.3	16484.8	16580.8		1816.	
88.0	87.1	152.6	16814.8	16920.6	106.0		
84.0	83.1	141.6	17250.0	17348.0	118.0		
79.5	78.5	139.6	17738.9	17835.4	127.2		
75.9	74.9	142.6	18092.3	18190.6			1785.
75.3	74.3	138.9	18155.9	18251.5	107.0		
72.2	71.3	134.9	18458.5	18551.2	141.3		
71.9	70.9	140.9	18491.1	18588.2		2520.	
69.2	68.0	158.4	18749.9	18858.6			1922.
65.3	64.1	153.3	19095.5	19200.4			2200.
64.7	63.6	140.1	19147.5	19243.6		3280.	
63.1	62.0	142.7	19287.5	19385.1	145.3		
62.9	61.7	157.8	19306.0	19413.9			2240.
60.9	59.8	138.6	19480.5	19575.3		3744.	
60.5	59.3	151.3	19518.5	19621.4			2260.
58.5	57.2	154.2	19680.9	19786.4		4152.	
58.0	56.8	136.2	19726.9	19819.5			2540.
55.9	54.7	136.2	19890.7	19983.0			2530.
55.9	54.6	151.1	19891.0	19993.7		4728.	
53.8	52.6	137.4	20054.9	20147.8			2950.
53.2	52.0	138.4	20099.2	20193.3		5347.	
53.0	51.7	141.6	20115.6	20211.7	205.1		
51.7	50.4	134.7	20218.0	20308.8			3370.
51.0	49.6	153.7	20264.5	20368.7		5294.	
49.6	48.1	154.7	20370.4	20475.0			3470.
48.6	47.2	143.6	20440.6	20537.7		5971.	
47.2	45.8	140.0	20534.7	20630.1			3960.
46.2	44.8	140.0	20607.9	20702.3		6103.	
43.7	42.1	150.1	20774.6	20875.5		6793.	
41.0	39.4	143.4	20945.1	21041.4		8395.	
31.		142.0	-	-			5670.
30.8	28.9	142.7	21512.6	21606.6		2629.	
10.6	5.0	153.1	22256.7	22350.1	136.8		
0		149.5	22925.4	23015.1		5.5	
0							15.2

Pa^{230} (dis/min at end of bombardment) was calculated. Runs I and II were normalized to Run III by factors of 16.75 and 0.9 respectively. The same energy normalization as for the (d,7n) reaction was used for Run II.

Unfortunately the peak was not outlined by the three runs made on this reaction, but it does seem to come at about 25 Mev. This value is undoubtedly low since the threshold should be around 20 Mev. The energy scale at these low values however is quite sensitive to small errors in calibration and hence is quite unreliable.

If we assume that the point at 23 Mev is near the peak, the ratio of peak values for the (d,4n)/(d,7n) reactions is about 9. Run III which was taken as the standard for the curves, was 104 minutes or 2.7 half-lives of Pa^{227} long. After correction for this factor has been made we find that the ratio of total dis/min of Pa^{230}/Pa^{227} formed in the bombardment is 4.2 for a lower limit, or higher if the peak of Fig. 78 is higher than the 23 Mev point.

The data for these (d,xn) reactions on thorium are summarized in Table 28.

Table 28

Summary of Data from $Th^{232}(d,4n)Pa^{230}$ and $Th^{232}(d,7n)Pa^{227}$ Excitation Function Curves

	(d,4n)	(d,7n)
Maximum deuteron energy used in calculation	194 Mev	194 Mev
Threshold energy	--	30 Mev
Peak energy	--	51 Mev
"Distance" between peak and threshold	--	21 Mev
Peak "half width"	--	18 Mev
Yield at peak(dis/min)	$\geq 7.5 \times 10^3$ β	41×10^5 α
Factor in yield between peak and maximum energy	$\geq$ 12	8

3. $Al^{27}(d,ap)Na^{24}$ In an attempt to better define the energy of the deuteron beam in the low energy range after it has passed through considerable copper absorber, we obtained an excitation curve for this reaction, shown in Fig. 79 and Table 29 . (An excitation function for this reaction using high energy particles has been reported by Helmholz and Peterson. [31]) After an 88 minute bombardment the discs of aluminum were allowed to stand for about 24 hours to allow shorter lived activities to decay out completely. The samples were then counted on shelf 5 of a standard Geiger counter set-up for the 14.8 hour Na^{24} activity. The counts were taken at three successive times each interval greater than one half life of the activity. These counts were extrapolated back to the end of bombardment and corrected to 0.1 gm of aluminum.

The excitation function becomes very sensitive to small changes in absorber thickness at very low energy and consequently does not show a threshold. However the curve can be considered a fairly good representation of the true excitation function since one would expect the peak of the reaction to come at around 20 Mev or so, with the threshold coming as Clarke[29] has reported at around 12.5 Mev. No correction has been made for nuclear absorption in this curve; correction would probably bring up the dip at 50 Mev but would serve to make the peak even more pronounced. Hence the peak in this reaction is at about 20 Mev and rises at least a factor of two above the value at full energy. Beyond the peak the curve returns to a gradually varying function that decreases slowly as higher energies are approached.

A very good comparison of the curve determined by Clarke (see Fig. 72) at low energies and our curve with the 184 inch cyclotron energies can be made by plotting both curves on a mg/cm^2 scale. The energy values determined by Clarke were converted into mg/cm^2 values with the help of Table 13 . The two plots are made in Fig. 80 . Calculations for curve B transformed all absorber values

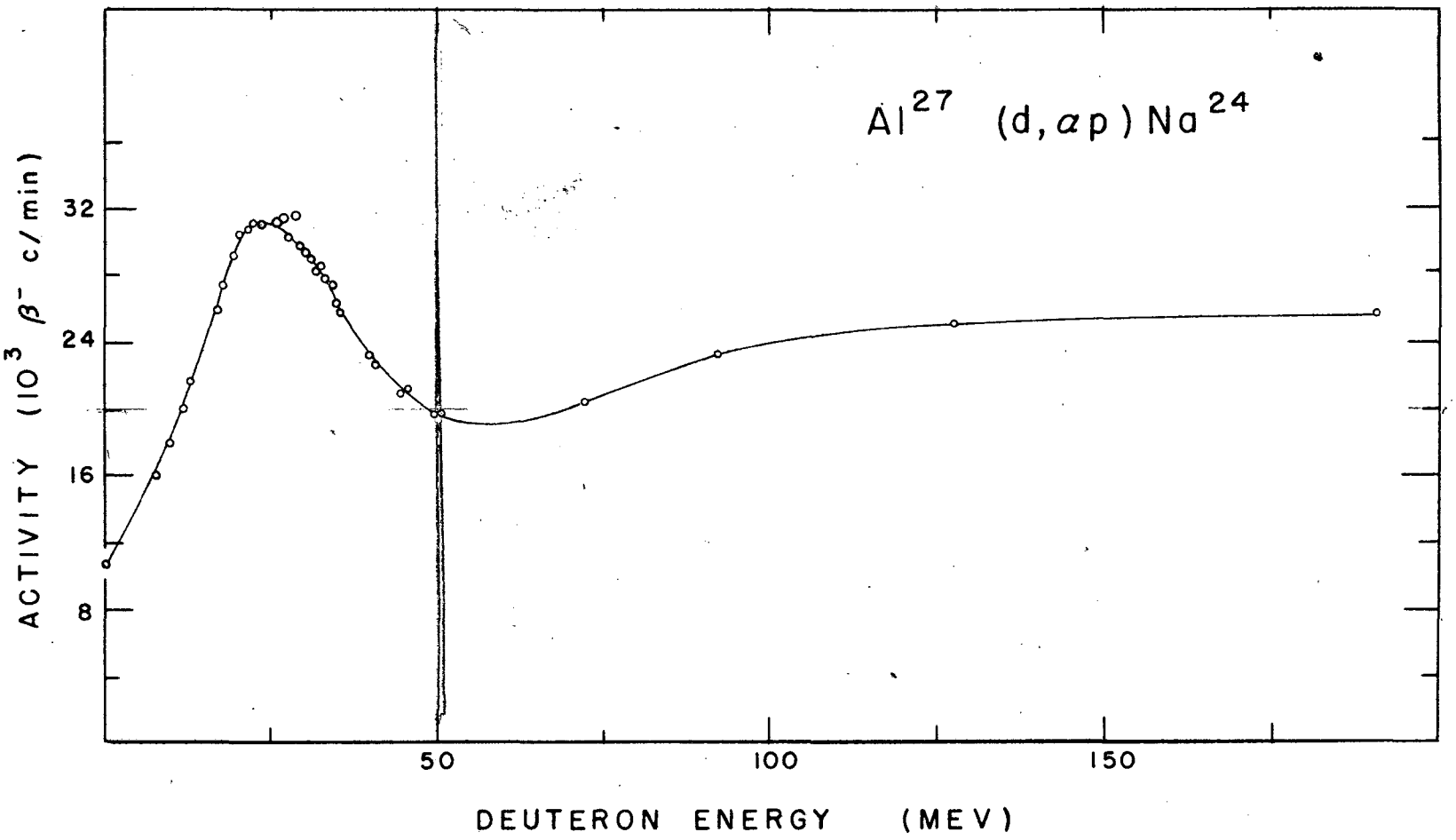

Fig. 79. Excitation function for the $Al^{27}(d,\alpha p)Na^{24}$ reaction, (Table 29).

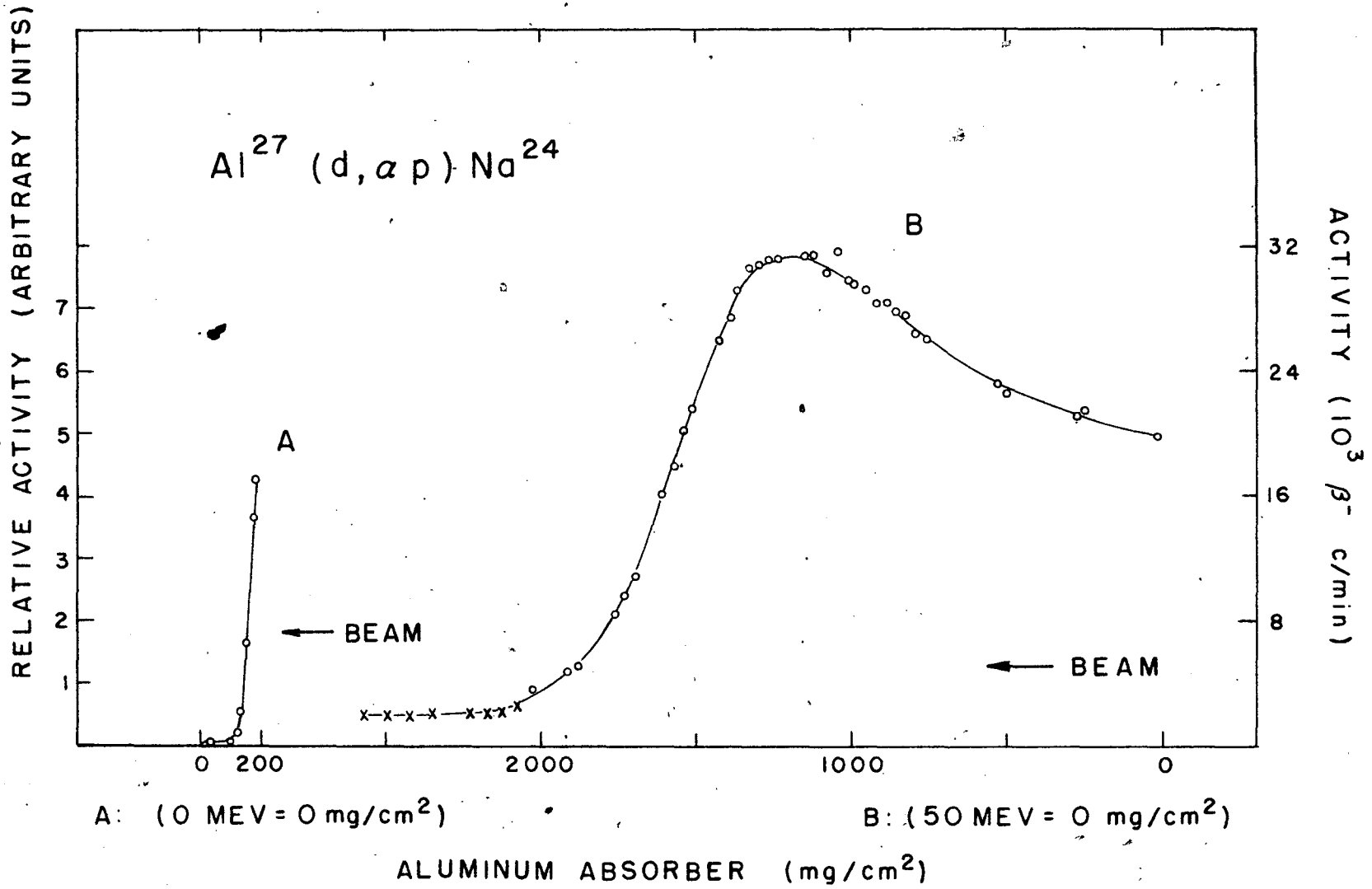

Fig. 80. Excitation function for the $Al^{27}(d,\alpha p)Na^{24}$ reaction. Curve A plotted from data given by E. T. Clarke using 14.5-Mev deuterons, (Phys. Rev. 71, 187 (1947); Curve B from data using 194-Mev deuterons (Table 29).

Table 29

Experimental Yields for the $Al^{27}(d,\alpha p)Na^{24}$ Reaction

Energy(Mev) Front	Energy(Mev) Back	Target Foil mg/cm² Al	Total absorber in beam (mg/cm² Cu) Front	Total absorber in beam (mg/cm² Cu) Back	Yield of Na^{24} (10^2 β^- c/min shelf 5 at end of bombardment Run I
191.1	190.9	32.8	590.7	629.6	257.
127.7	127.5	32.7	11639.6	11678.6	252.
92.0	91.6	32.7	16368.1	16407.4	224.
73.6	73.2	32.7	18317.7	18357.1	207.
50.5	50.0	32.7	20295.0	20334.9	197.
		mg/cm² Al			
50.0	49.5	32.6	0	30.2	198.
46.2	45.6	32.7	221.4	254.1	212.
45.6	44.9	32.7	254.1	286.8	211.
41.3	40.6	32.8	480.0	512.8	226.
40.6	40.0	31.4	512.8	544.2	232.
35.9	35.2	32.6	739.6	772.2	260.
35.2	34.5	32.7	772.2	804.9	265.
34.5	33.8	31.7	804.9	836.6	277.
33.8	33.0	31.3	836.6	867.9	278.
33.0	32.3	31.7	867.9	899.6	284.
32.3	31.5	31.5	899.6	931.1	283.
31.5	30.7	32.6	931.1	963.7	292.
30.7	29.8	31.6	963.7	995.3	296.
29.8	29.1	32.7	995.3	1028.0	298.
29.1	28.3	31.3	1028.0	1059.3	317.
28.3	27.5	32.6	1059.3	1091.1	303.
27.5	26.6	31.8	1091.9	1123.7	315.
26.6	25.8	31.6	1123.7	1155.3	313.
24.0	23.1	31.6	1214.5	1246.1	311.
23.1	22.1	31.3	1246.1	1277.4	311.
22.1	21.0	31.6	1277.4	1309.0	308.
21.0	20.0	31.6	1309.0	1340.6	305.
20.0	18.9	31.4	1340.6	1372.0	291.
18.9	17.7	31.7	1372.0	1403.7	274.
17.7	16.5	31.7	1403.7	1435.4	260.
14.0	12.5	31.6	1492.3	1523.9	217.
12.5	11.0	31.6	1523.9	1555.5	201.
11.0	9.1	32.5	1555.5	1588.0	180.
9.1	6.8	32.8	1588.0	1620.8	161.
0		32.6	1676.6	1709.2	107.8
0		31.6	1709.2	1740.8	97.2
0		31.7	1740.8	1772.5	84.4
0		31.7	1856.1	1887.8	52.4
0		31.8	1887.8	1919.6	47.6
0		31.4	2003.2	2034.6	36.4

to equivalent copper absorber values down to 50 Mev and then aluminum was used as the absorber for calculating purposes. Hence the zero absorber in B is actually at 50 Mev.

The height of curve A is purely arbitrary since from Clarke's work it was not known how far the function was from a peak at its final 14.5 Mev point. It would be interesting to check this reaction on a more powerful cyclotron to determine this peak energy more closely. The Berkeley 60-inch cyclotron might put out enough energy to do the trick.

By comparing the two curves (especially the slope of the leading edge of the curves) in Fig. 80 we can see just how much effect the straggling and initial energy distribution of the beam have in spreading out the energy of the particles which cause reactions in this low energy region.

4. $\underline{C^{12}(d,n)N^{13}}$ Fig. 81 and Table 30 show the results of placing polystyrene foils in the electrostatically deflected beam during a 1 hour and 45 minute bombardment and counting the 10 minute N^{13} activity produced. (Curve A in the figure has been plotted from data by Newson [30] (see Fig. 73.) Unfortunately the N^{13} is not the only activity present. Decays must be followed on all samples and the 10 minute line resolved out from a large amount of 20-minute C^{11} formed from the $C^{12}(d,dn)C^{11}$ reaction. Because of this resolution problem the excitation function is not as accurate as the one for Na^{24} but does give an idea of the tremendous spreading of a peak at 3 Mev by the beam of the 184-inch cyclotron.

5. $\underline{Th^{232}(d,7n)Pa^{227}}$, $\underline{Al^{27}(d,\alpha p)Na^{24}}$, and $\underline{C^{12}(d,n)N^{13}}$ Having been able to obtain excitation functions for these reactions in separate bombardments it was desirable to obtain excitation functions for all three from the same bombardment, thus eliminating effects of minor beam changes etc. Fig. 82 and Table 30 present the results of this one hour and 45 minute bombardment. The carbon was counted first and followed for two hours after shutdown. By this time it had decayed into enough of the 20 minute C^{11} to permit resolution of the curves. There still

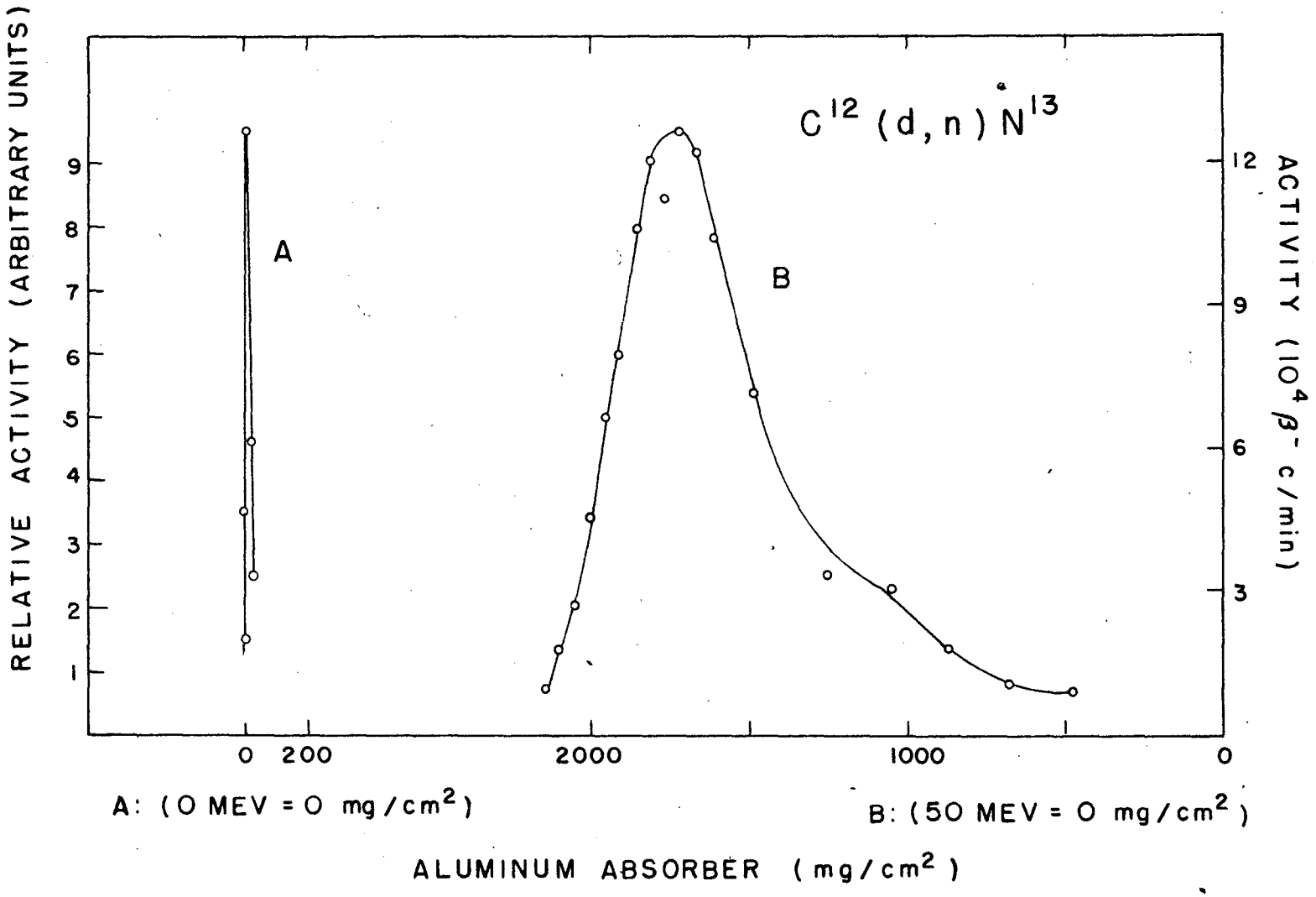

Fig. 81. Excitation function for the $C^{12}(d,n)N^{13}$ reaction. Curve A plotted from data given by H. W. Newson using 5-Mev deuterons (Phys. Rev. 51, 620 (1937)); Curve B from data using 194-Mev deuterons (Table 30).

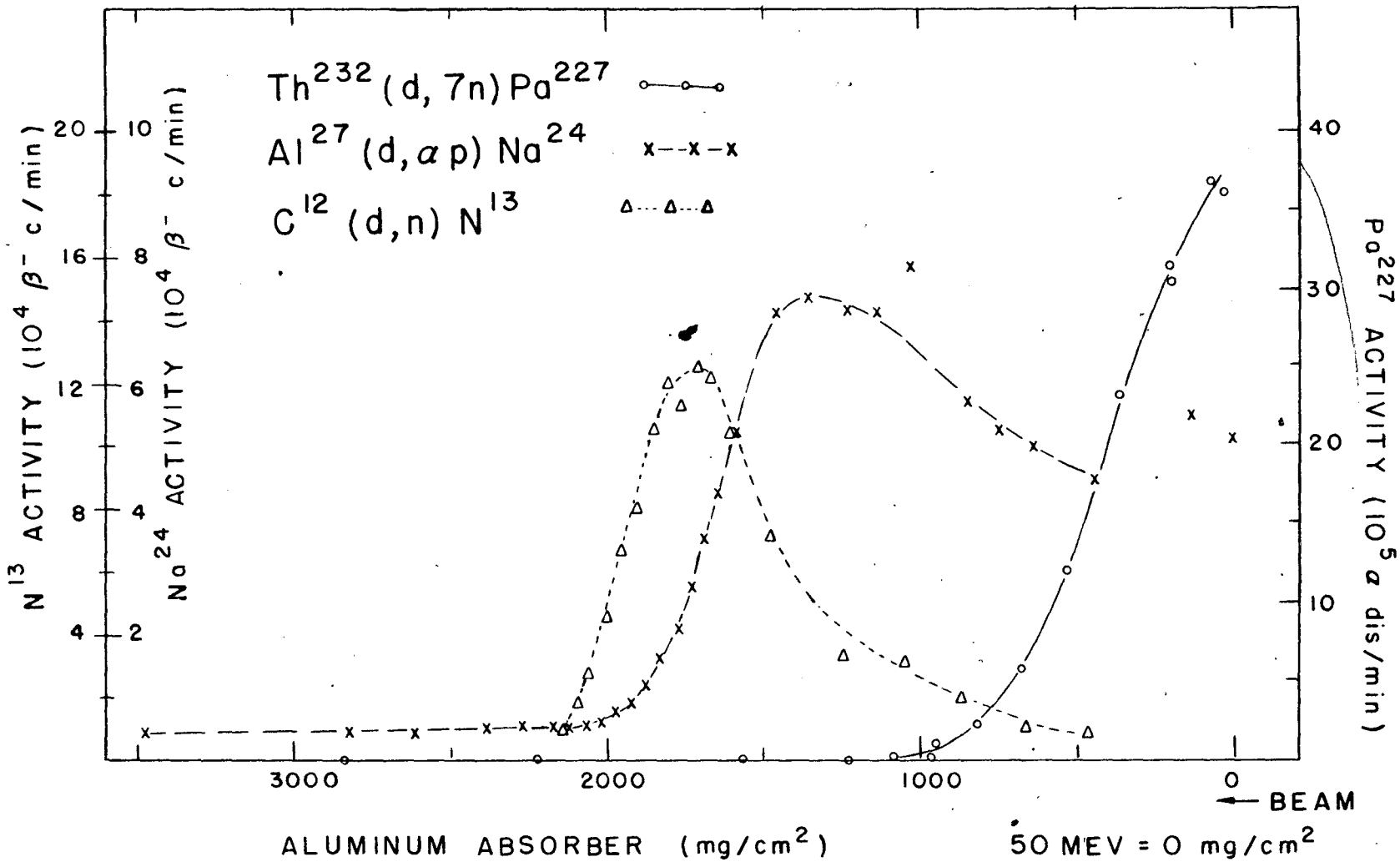

Fig. 82. Excitation functions for the $Th^{232}(d,7n)Pa^{227}$, $Al^{27}(d,\alpha p)Na^{24}$, and $C^{12}(d,n)N^{13}$ reactions (Table 30).

Table 30

Experimental Yields for $Al^{27}(d,\alpha p)Na^{24}$, $Th^{232}(d,7n)Pa^{227}$, and $C^{12}(d,n)N^{13}$ Reactions
(0 mg Al equal to 50.0 Mev Incident Protons)

Target foil mg/cm^2	Foil	Total absorber in beam (mg/cm^2 Al) Front	Back	Na^{24}(10^3 β^- c/min end bbdt.)	Pa^{227}(10^3 α dis/min end bbdt.)	Poly (10^3 β^- c/min end bbdt.)
32.8	Al	0.0	8.8	51.3		
14.8	Poly	8.8	26.5			-
154.7	Th	26.5	112.3		3693.	
32.7	Al	112.3	145.0	54.9		
13.5	Poly	145.0	161.2			-
140.0	Th	161.2	238.8		3137.	
32.7	Al	430.0	462.7	44.2		
14.6	Poly	462.7	480.3			8.64
32.7	Al	539.1	571.8	44.5		
32.7	Al	628.5	661.2	49.7		
14.0	Poly	661.2	678.0			10.53
32.6	Al	735.0	767.6	52.4		
32.7	Al	825.1	857.8	57.5		
15.4	Poly	857.8	876.3			18.21
142.0	Th	936.5	1011.5		25.0	
32.7	Al	1011.5	1044.2	78.7		
15.4	Poly	1044.2	1062.7			31.0
32.8	Al	1120.5	1153.3	71.2		
31.4	Al	1213.2	1244.6	72.0		
14.5	Poly	1244.6	1262.0	-		33.4
32.6	Al	1346.5	1379.1	73.6		
32.7	Al	1438.3	1471.0	71.4		
17.6	Poly	1471.0	1489.1			71.8
31.7	Al	1575.0	1606.7	52.0		
13.8	Poly	1606.7	1623.2			104.1
31.3	Al	1623.2	1654.5	42.3		
13.2	Poly	1654.5	1670.4			122.0
31.7	Al	1670.4	1702.1	34.8		
13.3	Poly	1702.1	1718.0			125.9
31.5	Al	1718.0	1749.5	27.4		
13.1	Poly	1749.5	1765.2			113.4
32.6	Al	1765.2	1797.8	20.4		
14.4	Poly	1797.8	1815.1			120.1
31.6	Al	1815.1	1846.7	16.4		
13.5	Poly	1846.7	1862.9			105.9

Table 30(cont'd)

Experimental Yields for $Al^{27}(d,\alpha p)Na^{24}$, $Th^{232}(d,7n)Pa^{227}$, and $C^{12}(d,n)N^{13}$ Reactions
(0 mg Al equal to 50.0 Mev Incident Protons)

Target foil mg/cm^2	Foil	Total absorber in beam (mg/cm^2 Al) Front	Back	Na^{24}(10^3 β^- c/min end bbdt.)	Pa^{227}($10^3\alpha$ dis/min end bbdt.)	Poly(10^3 β^- c/min end bbdt.)
32.7	Al	1862.9	1895.6	11.80		
14.8	Poly	1895.6	1913.3			79.6
31.3	Al	1913.3	1944.6	9.30		
17.8	Poly	1944.6	1962.8			66.6
32.6	Al	1962.8	1995.4	7.82		
13.3	Poly	1995.4	2011.4			45.8
31.8	Al	2011.4	2043.2	5.98		
13.1	Poly	2043.2	2058.9			27.7
31.6	Al	2058.9	2090.5	5.75		
13.1	Poly	2090.5	2106.2			18.18
31.6	Al	2106.2	2137.8	5.58		
13.0	Poly	2137.8	2153.4			9.73
31.3	Al	2153.4	2184.7	5.82		
135.5	Th	2184.7	2254.6		3.00	
31.6	Al	2254.6	2286.2	5.53		
31.6	Al	2371.7	2403.3	5.01		
31.4	Al	2594.4	2625.8	4.76		
31.7	Al	2817.3	2849.0	4.43		
31.7	Al	3463.3	3495.0	4.21		

remained about three hours in which to work up and count the protactinium fraction before other activities grew in. The Na^{24} was counted the next day and checked the following day for the right decay.

The scales of each curve in the figure are indicated on the graph. It is interesting to note that the leading edge of the N^{13} and Na^{24} curves have the same slope while that of Pa^{227} is somewhat more shallow. This would seem to indicate that the peak for the Pa^{227} reaction is considerably more broad than that for the other two reactions --- which would of course be expected. The three "x" points that fall above the curve in the high energy part of the figure were faced against thorium foils in the bombardment and consequently have abnormally high activity because of recoils kicked out from the thorium. Points of the Pa^{227} yield plotted in the figure, but not listed in the table, were read directly from the graph of Fig. 75 .

B. Protons

1. $Th^{232}(p,6n)Pa^{227}$ When the 184-inch cyclotron was finally converted to enable the acceleration of protons to 348 Mev, we decided to determine whether this reaction peaked as the corresponding deuteron reaction had and also to see just how much it resembled the deuteron reaction.

The results of three runs are shown in Table 31. Run I was just a "shakedown" for the apparatus and consequently the target foils were not weighed separately but were assigned a weight representing the average weight of some foils chosen at random. In this run the points were far enough apart that the curve seemed to have a very broad peak gradually decreasing to about half maximum at full energy. Runs II and III however did show a very definite peak where the yield value is greater than the value at maximum energy by at least a factor of 20. Runs II and III are plotted in Fig. 83 without normalization. Run I is not plotted since its values were not as precise as the other two. The bombardments in Runs I, II and III were

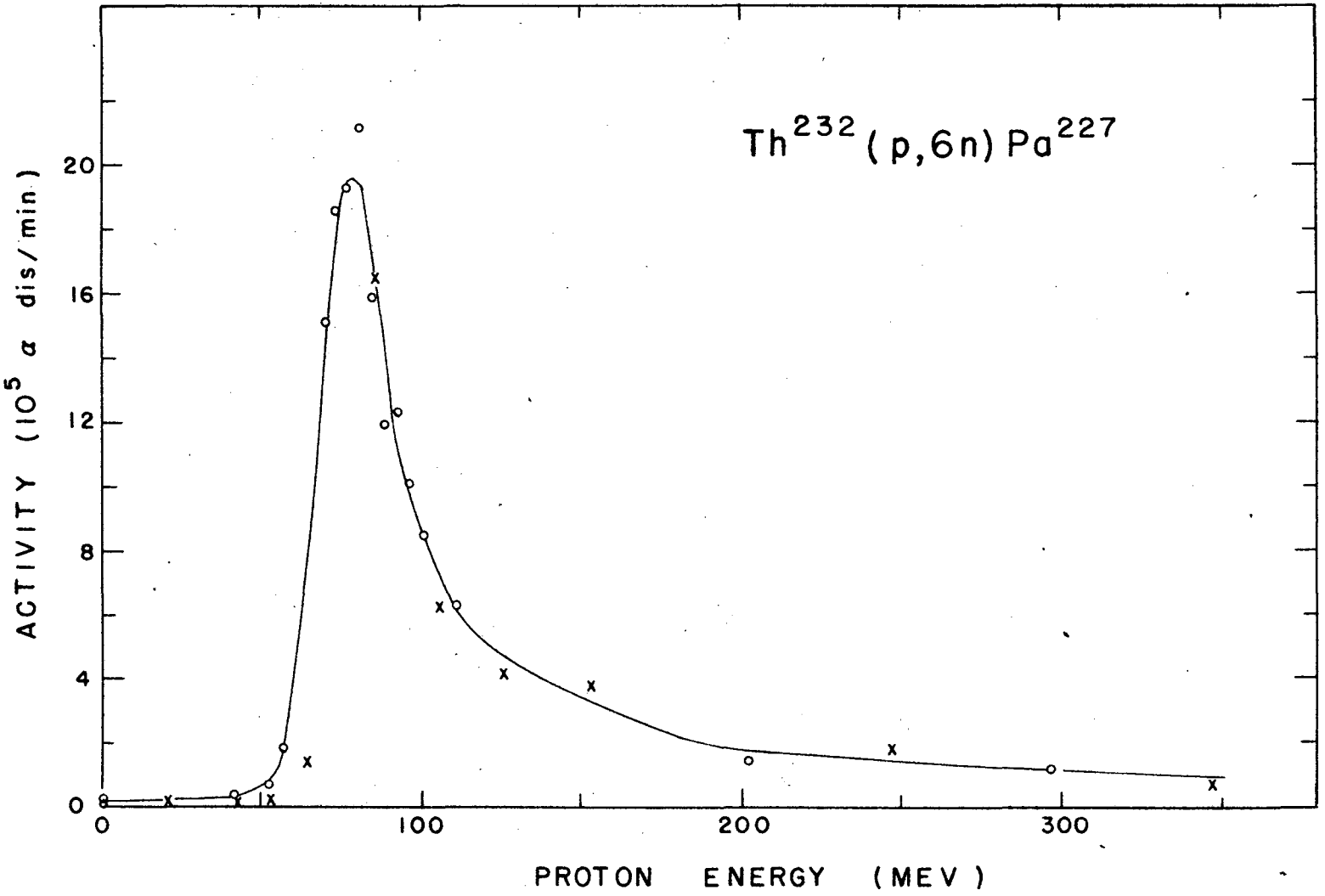

Fig. 83. Excitation function for the $Th^{232}(p,6n)Pa^{227}$ reaction (Table 31). Circles represent Run III; crosses, Run II.

Table 31

Experimental Yields for the $Th^{232}(p,6n)Pa^{227}$ Reaction

Proton Energy(Mev) Front	Back	Target foil mg/cm^2	Total absorber in beam (mg/cm^2 Cu) Front	Back	Yield of Pa^{227} (10^4 α dis/min at end of bombardment) Run I	Run II	Run III
347		141.8	693.5	797.2	12.15		
346.4	346.2	139.4	711.8	813.7		7.60	
297.3	297.1	151.4	21895.0	22003.7			12.18
247.2	246.9	138.1	41683.7	41784.1		18.00	
247		141.8	41685.1	41788.2	30.9		
203.3	203.0	134.8	57193.7	57291.2			14.70
153.6	153.3	139.6	72394.1	72494.5		37.5	
153.5		141.8	72416.1	72518.0	57.0		
125.9	125.5	148.8	79597.5	79704.0		41.9	
111.9	111.4	143.3	82886.0	82988.1			63.7
105.8	105.4	132.7	84198.0	84292.6		63.2	
101.4	100.9	152.7	85146.1	85254.7			85.4
96.4	95.9	153.0	86160.0	86268.6			100.4
93.0	92.4	152.0	86843.5	86951.3			122.5
88.6	88.1	138.1	87681.8	87779.6			119.5
85.7	85.1	152.4	88240.2	88348.1			158.8
85.4	84.8	137.3	88295.6	88392.8		165.3	
81.0	80.4	138.6	89084.4	89182.3			211.5
77.8	77.2	151.1	89640.1	89746.7			192.8
74.1	73.5	152.2	90256.4	90363.7			186.0
70.7	70.1	150.9	90814.9	90921.1			150.8
67.3		141.8	91300.0	91399.9	62.2		
64.5	63.8	141.0	91773.8	91872.7		14.05	
57.7	57.0	153.4	92741.1	92848.3			17.90
53.1	52.3	143.2	93362.7	93462.4		2.22	
51.9	51.2	138.8	93508.8	93605.5			7.13
42.6	41.8	138.8	94604.4	94700.3		1.686	
41.4	40.5	138.2	94743.5	94838.8			3.15
20.5		141.8	96473.9	96570.9	0.198		
20.5	18.9	139.1	96520.3	96613.3		1.401	
0		149.3	98573.8	98673.3			2.59
0		151.5	98660.3	98761.3		1.469	
0		141.8	98906.9	99001.4	0.155		
0		151.5	100809.3	100910.3		1.570	
0		141.8	102736.4	102830.9	0.171		

94.5

of 1-3/4 hours, 68 minute, and 1-3/4 hours duration respectively.

The curve is not drawn through the point at 81 Mev even though this point would appear to be the peak for this reaction. This sample, when counted later for U^{230}, gave a yield value which was very definitely displaced from the curve for the (p,3n) reaction (see Fig. 86). Although no known error had been made on this sample there might have been some error in aliquot etc., to cause the discrepancy.

Fig. 84 shows this same curve drawn on a log scale to better illustrate the spread of the low yield points. In Fig. 85 the peak of the curve has been enlarged to show the extent of the symmetry involved. It can be seen that on the high energy side of the peak another mode of reaction starts to take over around 90 Mev and breaks up the symmetry of the peak.

In a single experiment to determine the absolute cross section for this reaction at full energy, a value of about 2.5×10^{-3} barns was obtained. V. Peterson's apparatus was used to measure the total amount of beam passing through the target. These current values, together with a chemical yield determination, established the absolute cross section. Again in this determination the greatest potential source of error is the exchange or non-exchange of the tracer Pa^{231} with the Pa^{227} formed in the bombardment. The Pa^{231} was washed out of a TTA-benzene solution just a few hours before the bombardment and was kept in concentrated nitric acid, precautions one would think would prevent colloid formation. However a tracer yield of only 39% was obtained through the chemistry, whereas the simple extraction procedure used would be expected to give a higher yield.

From the full energy cross section value we can see that the cross section at the peak of the curve would be about 5×10^{-2} barns. Because of the questionable chemical yield, however, this can only be called the maximum value for the cross section, further experiments being necessary to establish whether it can be reduced

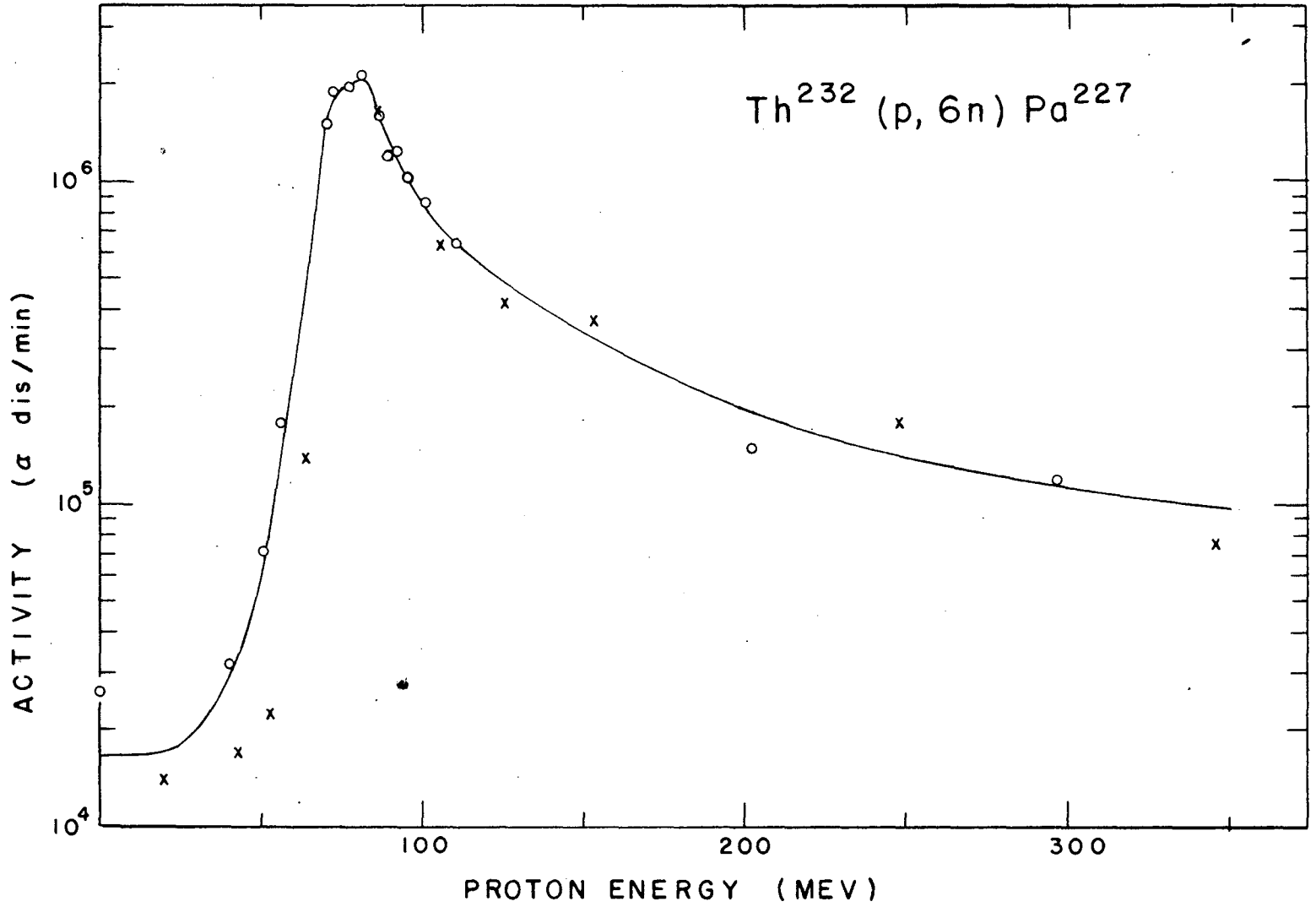

Fig. 84. Excitation function for the $Th^{232}(p,6n)Pa^{227}$ reaction (Table 31). Circles represent Run III; crosses, Run II.

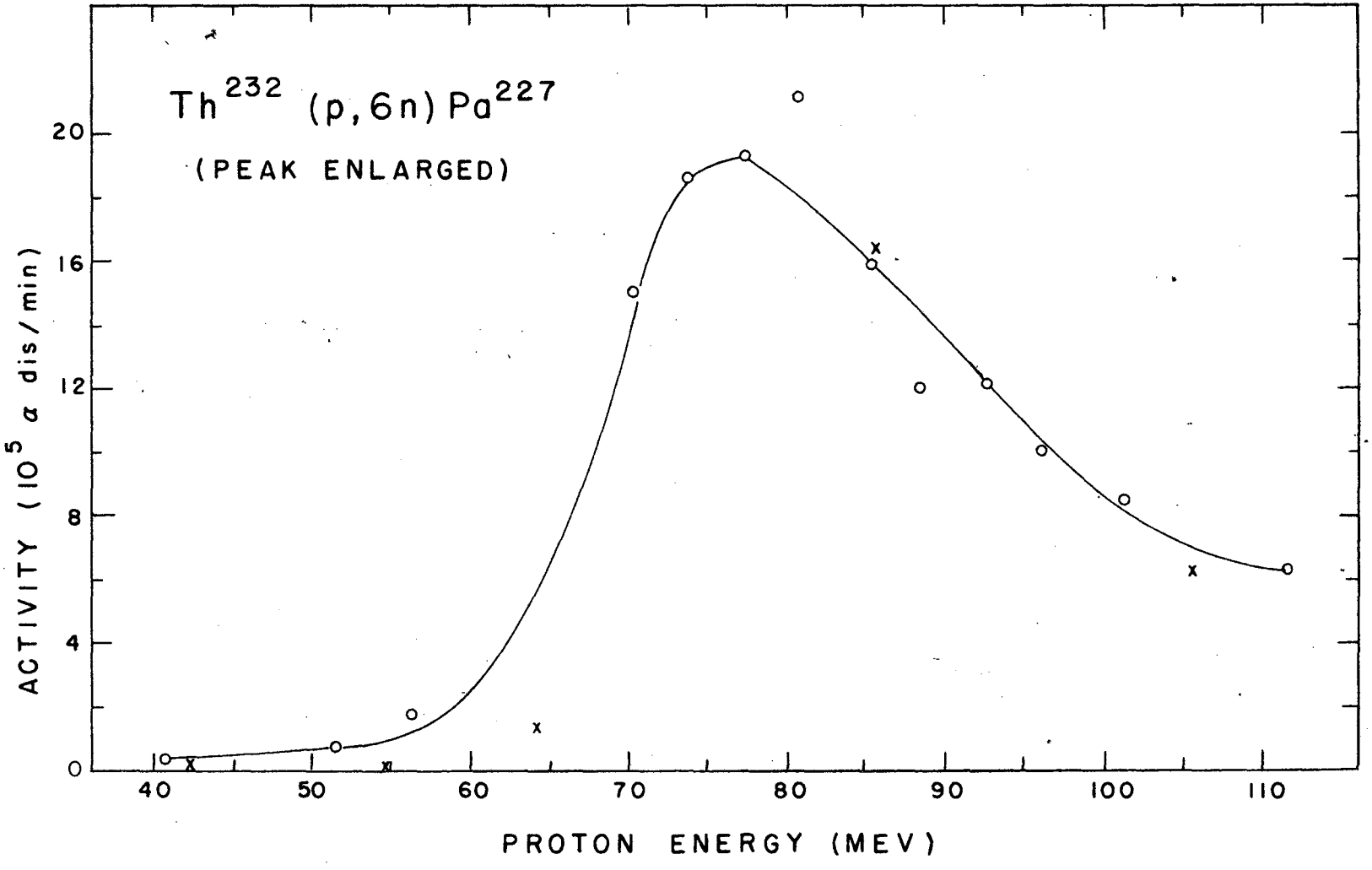

Fig. 85. Enlarged peak of the excitation function for the $Th^{232}(p,6n)Pa^{227}$ reaction (Table 31). Circles represent Run III; crosses, Run II.

a factor of two or so. If this reduction can be made, the absolute cross section for the (d,7n) and (p,6n) reactions on thorium are much the same at the peaks of their excitation curves.

2. $Th^{232}(p,3n)Pa^{230}$ In Figs. 86 and 87 and Table 32 we have the companion values and graphs for this reaction. Again the points from Run I are not plotted. This time Run II is multiplied by a factor of 1.35 to normalize to Run III. This normalization of the Pa^{230} values (and not the Pa^{227} values) is readily explainable by the fact that the Run III bombardment was for 2-3/4 half lives of the 38.3 minute Pa^{227} while Run II was for 1-3/4 half lives. Correction of the Pa^{227} yields for these factors could require normalization in Fig. 83 if atoms formed in bombardment were plotted instead of dis/min at shutdown. As in the case of the (p,6n) reaction, the factor between the yield at the peak and at full energy is about 20.

A very interesting observation can be made from the curves for the (p,6n) and (p,3n) reactions on thorium. Although the two reactions have much the same shape and ratio of peak yield to full energy yield, there is an absolute yield difference of about 5.4 between the two in favor of the (p,3n) reaction. This difference was found by determination of the number of atoms formed by each reaction at the peak of the excitation function. The branching ratios of 10% beta for Pa^{230} (32) and 80% alpha for Pa^{227} were considered in the calculations although these ratios are rather rough.

By using the values of range straggling listed in Table 21 and calculating the energy straggling by the method mentioned in an earlier section we find that the straggling "width" is 4-1/4 Mev for a 100 Mev particle and 7-1/4 Mev for a 50 Mev proton, whose energy has been reduced from 348 Mev by passage through copper.

We see however that this straggling effect, while significant, is not the

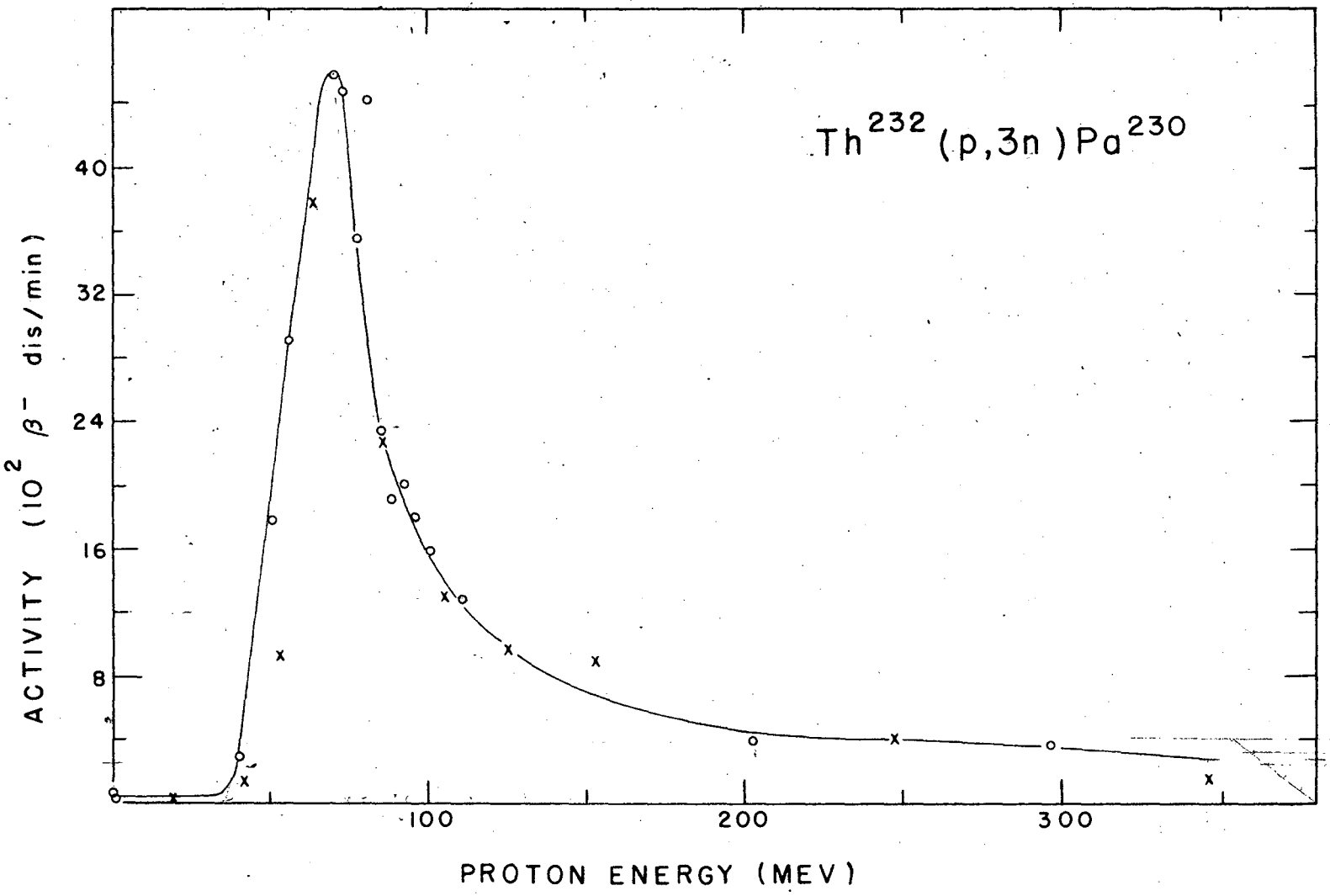

Fig. 86. Excitation function for the $Th^{232}(p,3n)Pa^{230}$ reaction (Table 32). Circles represent Run III; crosses, Run II. Run II activity normalized to Run III.

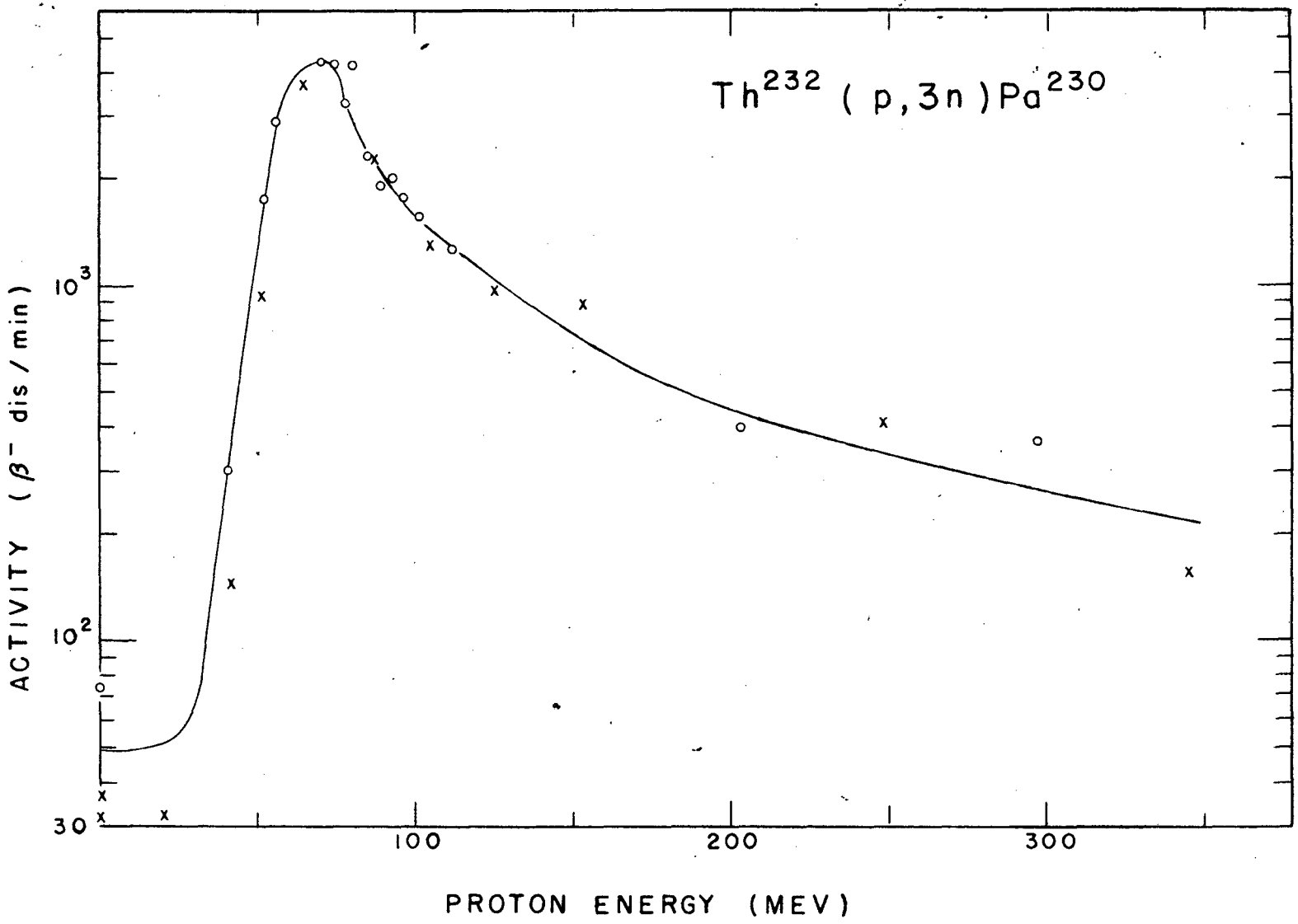

Fig. 87. Excitation function for the $Th^{232}(p,3n)Pa^{230}$ reaction(Table 32). Circles represent Run III; crosses, Run II. Run II activity normalized to Run III.

Table 32

Experimental Values for the $Th^{232}(p,3n)Pa^{230}$ Reaction

Proton Energy(Mev) Front	Back	Target foil mg/cm^2	Total absorber in beam (mg/cm^2 Cu) Front	Back	Yield of Pa^{230} (β^- dis/min at end of bombardment) Run I	Run II	Run III
347		141.8	693.5	797.2	353.		
346.4	346.2	139.4	711.8	813.7		119.9	
297.3	297.1	151.4	21895.0	22003.7			373.
247.2	246.9	138.1	41683.7	41784.1		313.	
247		141.8	41685.1	41788.2	841.		
203.3	203.0	134.8	57193.7	57291.2			402.
153.6	153.3	139.6	72394.1	72494.5		673.	
153.5		141.8	72416.1	72518.0	1472.		
125.9	125.5	148.8	79597.5	79704.0		729.	
111.9	111.4	143.3	82886.0	82988.1			1292.
105.8	105.4	132.7	84198.0	84292.6		980.	
101.4	100.9	152.7	85146.1	85254.7			1586.
96.4	95.9	153.0	86160.0	86268.6			1804.
93.0	92.4	152.0	86843.5	86951.3			2015.
88.6	88.1	138.1	87681.8	87779.6			1916.
85.7	85.1	152.4	88240.2	88348.1			2330.
85.4	84.8	137.3	88295.6	88392.8		1698.	
81.0	80.4	138.6	89084.4	89182.3			4420.
77.8	77.2	151.1	89640.1	89746.7			3540.
74.1	73.5	152.2	90256.4	90363.7			4480.
70.7	70.1	150.9	90814.9	90921.1			4580.
67.3		141.8	91300.0	91399.9	6130.		
64.5	63.8	141.0	91773.8	91872.7		2800.	
57.7	57.0	153.4	92741.1	92848.3			2920.
53.1	52.3	143.2	93362.7	93462.4		691.	
51.9	51.2	138.8	93508.8	93605.5			1771.
42.6	41.8	138.8	94604.4	94700.3		108.1	
41.4	40.5	138.2	94743.5	94838.8			303.
20.5		141.8	96473.9	96570.9	9.5		
20.5	18.9	139.1	96520.3	96613.3		23.9	
0		149.3	98573.8	98673.3			74.0
0		151.5	98660.3	98761.3		26.9	
0		141.8	98906.9	99001.4	-		
0		151.5	100809.3	100910.3		23.1	
0		141.8	102736.4	102830.9	-		

principal cause for the 30 Mev half width of the experimentally determined peak.

Table 33 summarizes data obtained from the (p,3n) and (p,6n) excitation curves.

Table 33

Summary of Data from $Th^{232}(p,3n)Pa^{230}$ and $Th^{232}(p,6n)Pa^{227}$ Excitation Function Curves.

	(p,3n)	(p,6n)
Maximum proton energy used in calculations	348 Mev	348 Mev
Threshold energy	36 Mev	56 Mev
Peak energy	70 Mev	80 Mev
"Distance" between peak and threshold	34 Mev	24 Mev
Peak "half width"	34 Mev	28 Mev
Yield at peak(dis/min)	4.6×10^3 β^-	$1.9 \times 10^6 \alpha$
Factor in yield between peak and maximum energy	20	20

3. $U^{238}(p,\alpha 8n)Pa^{227}$ Since uranium as well as thorium foil was available, we decided to try our luck with this reaction and to characterize its excitation function. The chemical procedure used was modified from the thorium procedure in that the ammonium fluosilicate was not needed to aid the solution of the metal. The extractions appeared successful but difficulties did arise in the final plating step of the procedure. In the thorium procedure it was possible to plate between 5 and 10 ml of the TTA-benzene solution on one platinum plate -- and then to flame most of the organic material off the plate leaving an essentially weightless sample of protactinium. In the uranium separation however, as little as two

ml of the TTA-benzene solution evaporated down to a dark mass on the plate. When the plate was subsequently flamed the TTA carbonized (much like the Pharoah's Serpents of lecture table experiments) into large pieces of ash which tended to blow off the plate, apparently carrying much of the activity with them.

This carbonization of samples caused considerable trouble in the determination of this particular excitation function. The results of the first run (a one hour and 10 minute bombardment) shown in Fig. 88 and tabulated in Run I, Table 34 , seemed to indicate a peculiar but interesting type of reaction was taking place. In this graph the points all fall along a smooth curve -- a situation one would think improbable if variance in yields were due to chemical yield alone. Hence it was temporarily assumed that this yield variance expressed the true excitation function for the reaction.

A second try at establishing the validity of the dip in this curve happened to be made on an unusually hot day (for Berkeley) with the temperature about 100° F in the laboratory. This hot weather (being probably 30° F higher than the normal laboratory temperature) seemed only to aggravate the carbonization of the TTA upon evaporation and flaming, and the results of this run gave a group of very scattered points showing no continuity whatsoever.

It appeared that the excess carbonization was due to a temperature dependent effect that was caused by some difference in the extraction chemistry of uranium and thorium. Professor Melvin Calvin pointed out the possibility that since uranium is considerably more extractable in the TTA-benzene solution than is thorium, the organic phase might be extracting a small amount of the original 0.7 grams of uranium target foil which then catalyzed the carbonization reaction of the TTA. He suggested that after the original extraction had been made an acid wash of the organic layer would rid it of most of the uranium that had been brought along in the first

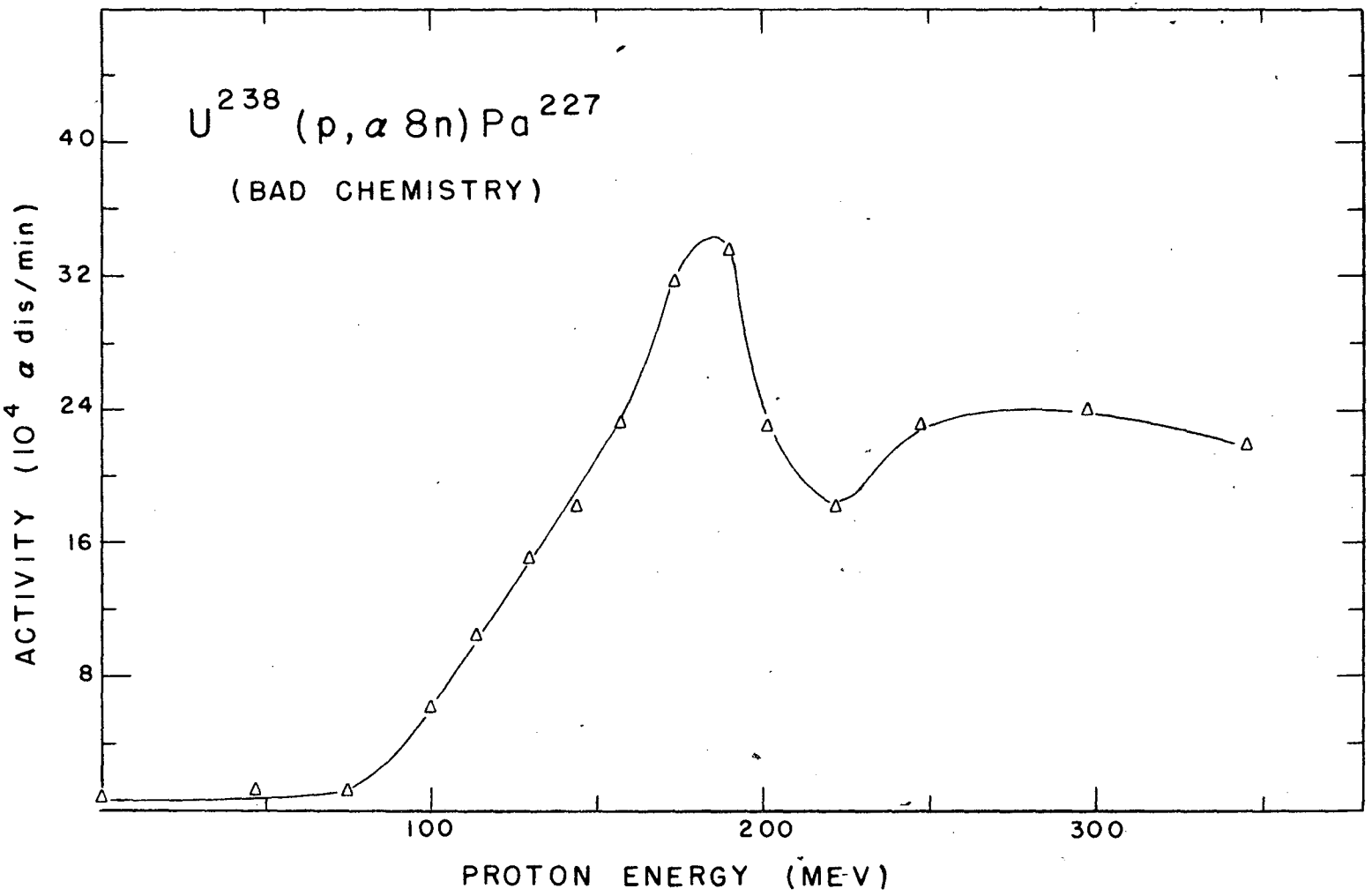

Fig. 38. Effect of bad chemistry on the $U^{238}(p,\alpha 8n)Pa^{227}$ excitation function (Table 34, Run I).

Table 34

Experimental Yields for the $U^{238}(p,\alpha 8n)Pa^{227}$ Reaction

Energy(Mev) Front	Energy(Mev) Back	Target foil gm/cm^{2}U	Total absorber in beam (mg/cm^2 Cu) Front	Total absorber in beam (mg/cm^2 Cu) Back	Yield of Pa^{227} (10^4 α dis/m at end of bombardment) Run I	Run IIA	Run IIB
346.		270.8	730.4	927.7	22.0		
346.3	345.9	266.1	741.7	935.7		42.7	46.2
298.		234.6	21536.7	21707.0	24.1		
298.2	297.7	268.8	21544.7	21739.9		48.0	51.5
272.6	272.1	242.0	31929.9	32105.4		50.0	48.6
248.6	248.4	264.6	41156.4	41347.9		46.7	51.7
248.		233.2	41377.0	41545.7	23.3		
238.8	238.3	241.1	44728.9	44903.2		30.3	46.6
227.1	226.6	235.5	49024.2	49194.4		22.5	46.2
222.		263.0	50596.7	50786.7	18.00		
217.7	217.2	230.6	52265.4	52431.9		48.8	47.1
207.9	207.4	251.8	55606.9	55788.6		43.1	50.9
202.		265.0	57535.7	57726.7	23.0		
198.0	197.5	235.1	58962.6	59131.9		40.5	42.8
190.		266.1	61461.7	61653.3	33.6		
189.5	188.9	270.2	61711.9	61906.4		36.6	37.8
184.5	183.9	270.9	63264.4	63459.3		33.4	39.2
177.3	176.7	236.1	65504.3	65673.9		32.5	36.0
174.		232.8	66391.3	66558.4	31.8		
167.3	166.6	264.1	68498.9	68688.4		26.0	40.9
158.		240.7	71097.4	71269.9	23.4		
143.5		266.8	75047.9	75238.6	18.26		
129.6		267.4	78413.6	78604.3	15.00		
129.0	128.3	266.5	78848.4	79038.5		11.92	11.93
114.3		270.1	82226.1	82418.2	10.40		
100.0		234.3	85356.2	85522.3	6.20		
75.0		239.2	90056.3	90224.5	1.00		
69.0	67.8	265.6	91088.5	91274.0		2.22	1.80
47.5		265.4	93762.5	93946.3	1.20		
0		264.3	97665.3	97839.5	0.67		
0		238.7	99678.0	99832.0		1.22	1.47
0		236.2	99887.5	100123.7	0.65		

extraction. Tracer runs of this procedure gave inconclusive results in eliminating this carbonization.

In a final 1-3/4 hour bombardment each sample was washed with equal volumes of 1 N nitric acid after the original extraction with TTA-benzene solution. Several ml of the organic layer was then plated and the plates flamed. The resulting yields (plotted as crosses in Fig. 89 and tabulated as Run IIA in Table 34) showed that the TTA was still carbonizing, causing loss of yield in some cases.

One further attempt was then made to obtain a good curve for this reaction. After the determination above, one half of the organic portion remained from the extraction. This TTA-benzene solution was plated out in several hundred lambda portions with flaming after each addition. In this manner we were able to reduce yield loss through carbonization. The yields obtained are indicated by circles in Fig. 89 and tabulated in Run IIB in Table 34. Although they scatter considerably they do indicate that the curve has a very broad peak at around 250 Mev which rounds off slightly at full energy. The triangular points in Fig. 89 are points from Run I, Table 34 (also plotted in Fig. 88) normalized by a factor of 2. Run I points above 160 Mev were not used however since they scattered too much. Fig. 90 shows Fig. 89 points plotted on log paper.

All values have been corrected for the absorption of the proton beam upon traversing the stack of the copper absorbers. (See Fig. 70).

4. $U^{238}(p,\alpha 5n)Pa^{230}$ Fig. 91 and Table 35 show the results of total alpha counting of the plates of Runs IIA and IIB after they had decayed for 2-1/2 months. Although these points scatter considerably more than the $(p,\alpha 8n)$ yields, one can make out a broad peak roughly comparable to the $(p,\alpha 8n)$ peak, but shifted to a lower energy by some ten or twenty Mev. Contamination of the samples may account for much of the scattering of points, since no correction (from pulse analyses) was made for this effect.

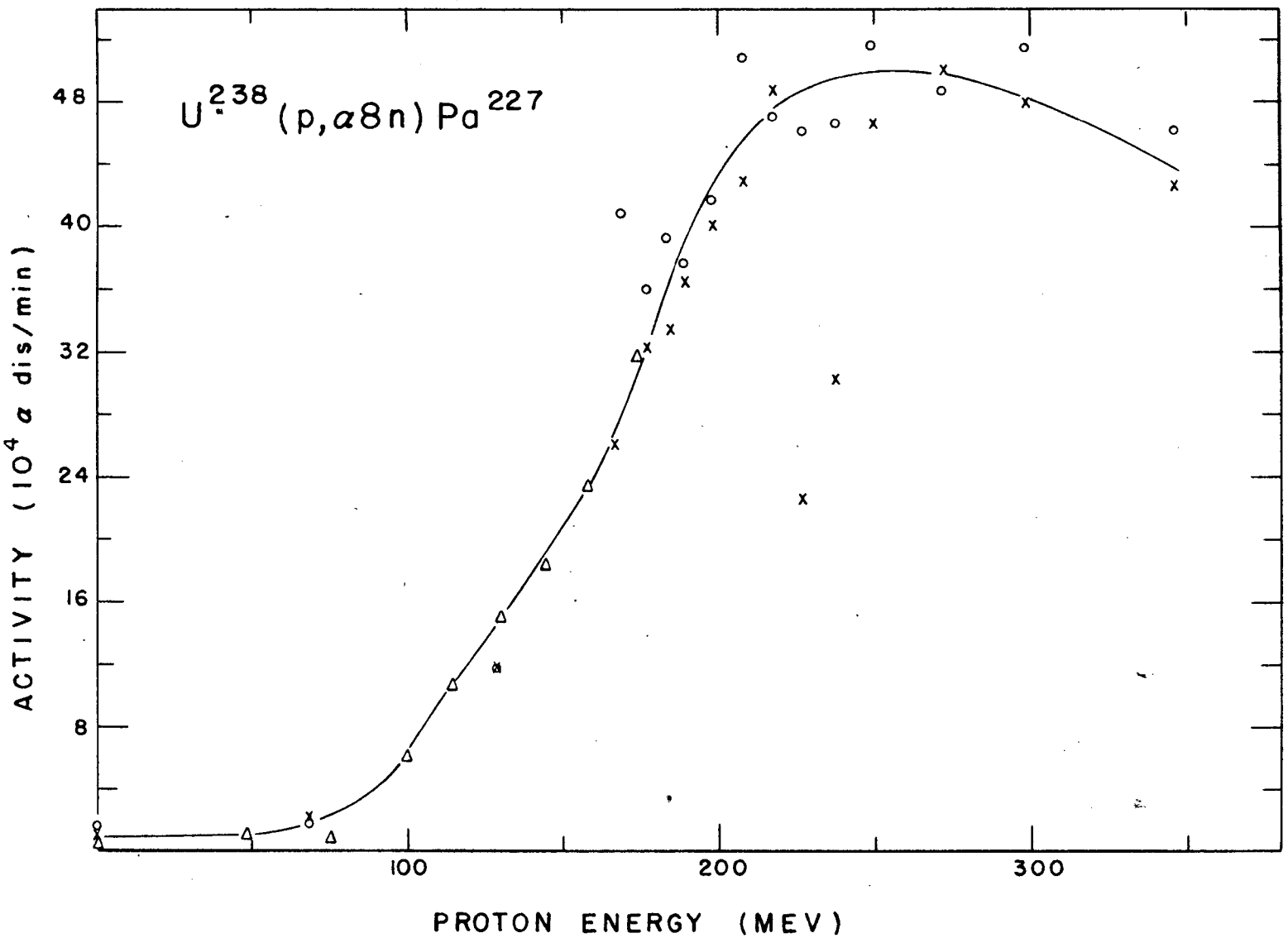

Fig. 89. Excitation function for the $U^{238}(p,\alpha 8n)Pa^{227}$ reaction (Table 34). Circles represent Run IIB; crosses, Run IIA; and deltas, part of Run I. Run I activity normalized to Run II A&B.

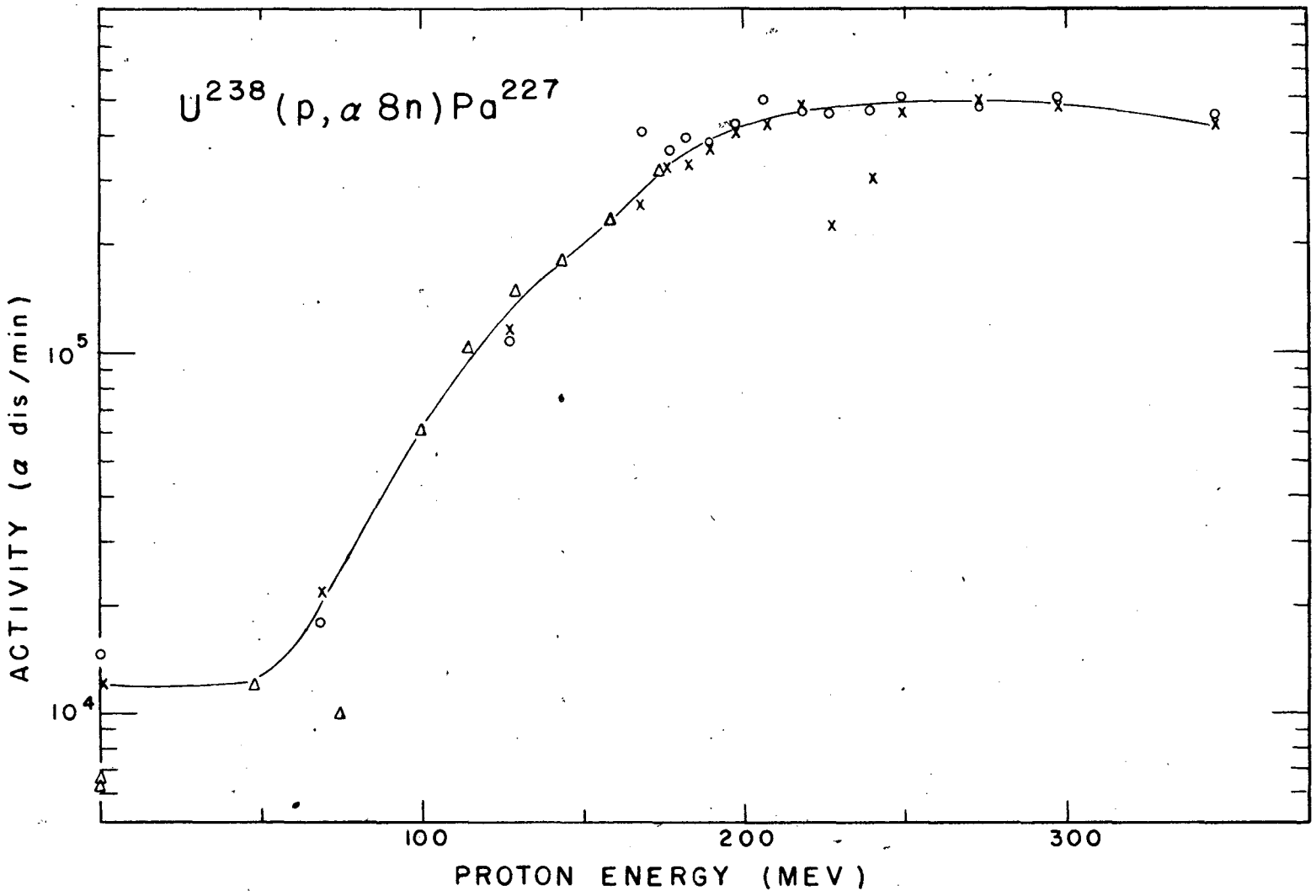

Fig. 90. Excitation function for the $U^{238}(p,\alpha 8n)Pa^{227}$ reaction (Table 34). Circles represent Run IIB; crosses, Run IIA; and deltas, part of Run I. Run I activity normalized to Run II A&B.

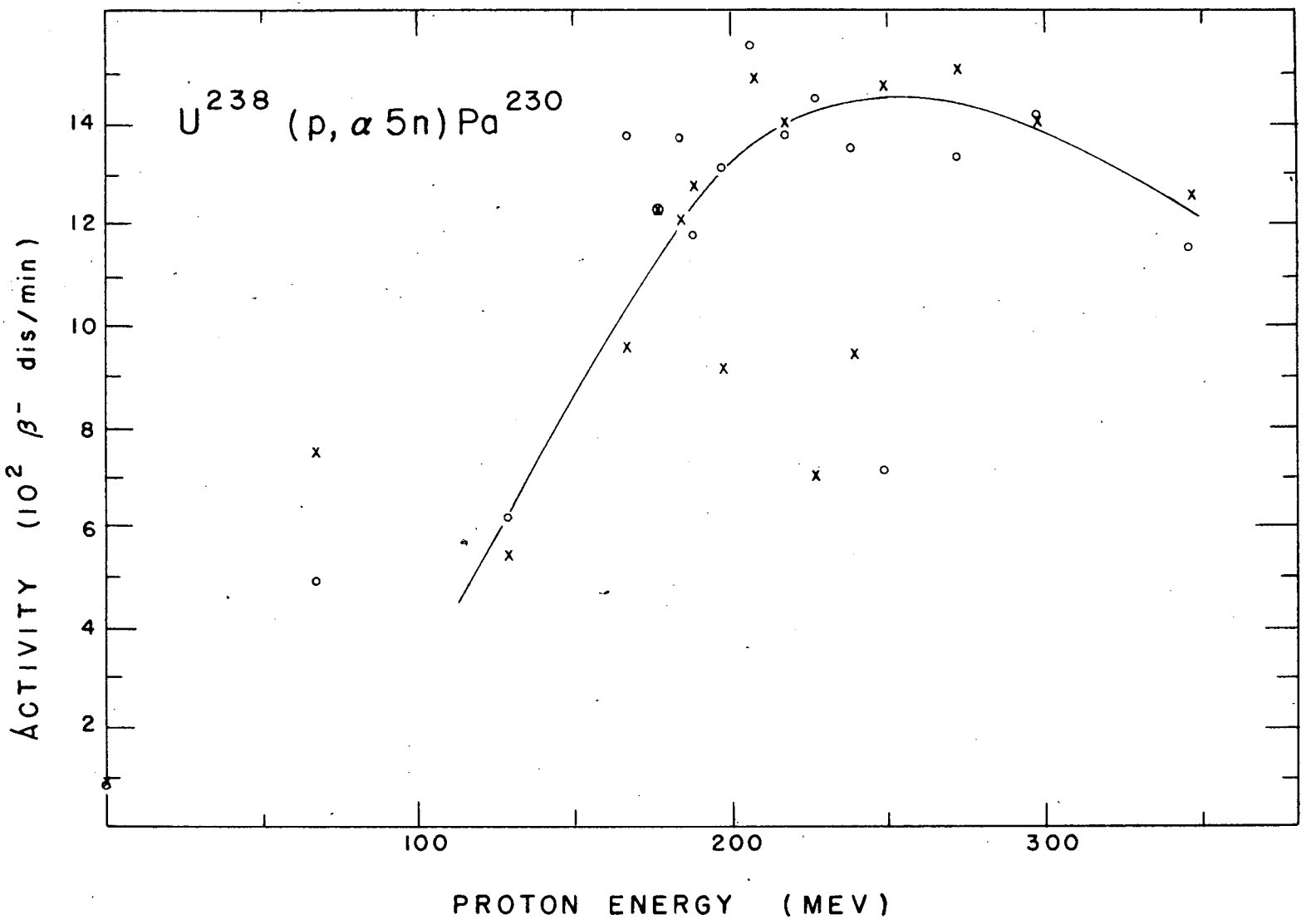

Fig. 91. Excitation function for the $U^{238}(p,\alpha 5n)Pa^{230}$ reaction (Table 35). Circles represent Run IIB; crosses, Run IIA.

Table 35

Experimental Yields for the $U^{238}(p,\alpha 5n)Pa^{230}$ Reaction

Energy(Mev) Front	Energy(Mev) Back	Target foil gm/cm^2 U	Total absorber in beam (mg/cm^2 Cu) Front	Total absorber in beam (mg/cm^2 Cu) Back	Yield of Pa^{230}(β^- dis/min. at end of bombardment) Run IIA	Yield of Pa^{230}(β^- dis/min. at end of bombardment) Run IIB
346.		270.8	730.4	927.7		
246.3	345.9	266.1	741.7	935.7	1254.	1152.
298.		234.6	21536.7	21707.0		
298.2	297.7	268.8	21544.7	21739.9	1406.	1418.
272.6	272.1	242.0	31929.9	32105.4	1508.	1329.
248.6	248.4	264.6	41156.4	41347.9	1476.	710.
248.		233.2	41377.0	41545.7		
238.8	238.3	241.1	44728.9	44903.2	945.	1351.
227.1	226.6	235.5	49024.2	49194.4	703.	1451.
222.		263.0	50596.7	50786.7		
217.7	217.2	230.6	52265.4	52431.9	1402.	1380.
207.9	207.4	251.8	55606.9	55788.6	1494.	1556.
202		265.0	57535.7	57726.7		
198.0	197.5	235.1	58962.6	59131.9	916.	1312.
190		266.1	61461.7	61653.3		
189.5	188.9	270.2	61711.9	61906.4	1279	1176.
184.5	183.9	270.9	63264.4	63459.3	1207	1378.
177.3	176.7	236.1	65504.3	65673.9	1232.	1232.
174		232.8	66391.3	66558.4		
167.3	166.6	264.1	68498.9	68688.4	958.	1380.
158		240.7	71097.4	71269.9		
143.5		266.8	75047.9	75238.6		
129.6		267.4	78413.6	78604.3		
129.0	128.3	266.5	78848.4	79038.5	542.	618.
114.3		270.1	82226.1	82418.2		
100.0		234.3	85356.2	85522.3		
75.0		239.2	90056.3	90224.5		
69.0	67.8	265.6	91088.5	91274.0	749.	492.
47.5		265.4	93762.5	93946.3		
0		264.3	97665.3	97839.5		
0		238.7	99678.0	99832.0	94.5	85.0
0		236.2	99887.5	100123.7		

A rough comparison of the peak values for the (p,α8n) and (p,α5n) curves indicates a factor of about 6.7 in favor of the (p,α5n) reaction. A summary of other comparisons of the two curves is given in Table 36.

Table 36

Summary of Data from $Th^{232}(p,\alpha 5n)Pa^{230}$ and $Th^{232}(p,\alpha 8n)Pa^{227}$ Excitation Function Curves

	(p,α5n)	(p,α8n)
Maximum proton energy used in calculations	348 Mev	348 Mev
Threshold energy	- - -	70 Mev
Peak energy	~ 250 Mev	~ 260 Mev
"Distance" between peak and threshold		~ 190 Mev
Yield at peak (dis/min)	1.5×10^3 β^-	5.0×10^5 α
Factor in yield between peak and maximum energy	1.2	1.1

C. Alpha Particles

1. $Th^{232}(\alpha,p8n)Pa^{227}$ Stacked foils were used to study this reaction in the internal beam of the cyclotron before the new apparatus for use in the electrostatically deflected beam had been developed. A very rough curve had been obtained indicating that the excitation function curve had a threshold about 60 Mev, rising rather steeply to about 120 Mev and then falling slowly to about 2/3 maximum at full energy.

Determinations of this reaction with the new apparatus essentially corroborate our original ideas. The one bombardment (1-1/2 hour) made before a collimator was placed in front of the target is shown in Fig. 92 and in Table 37 (Run I). Evidently

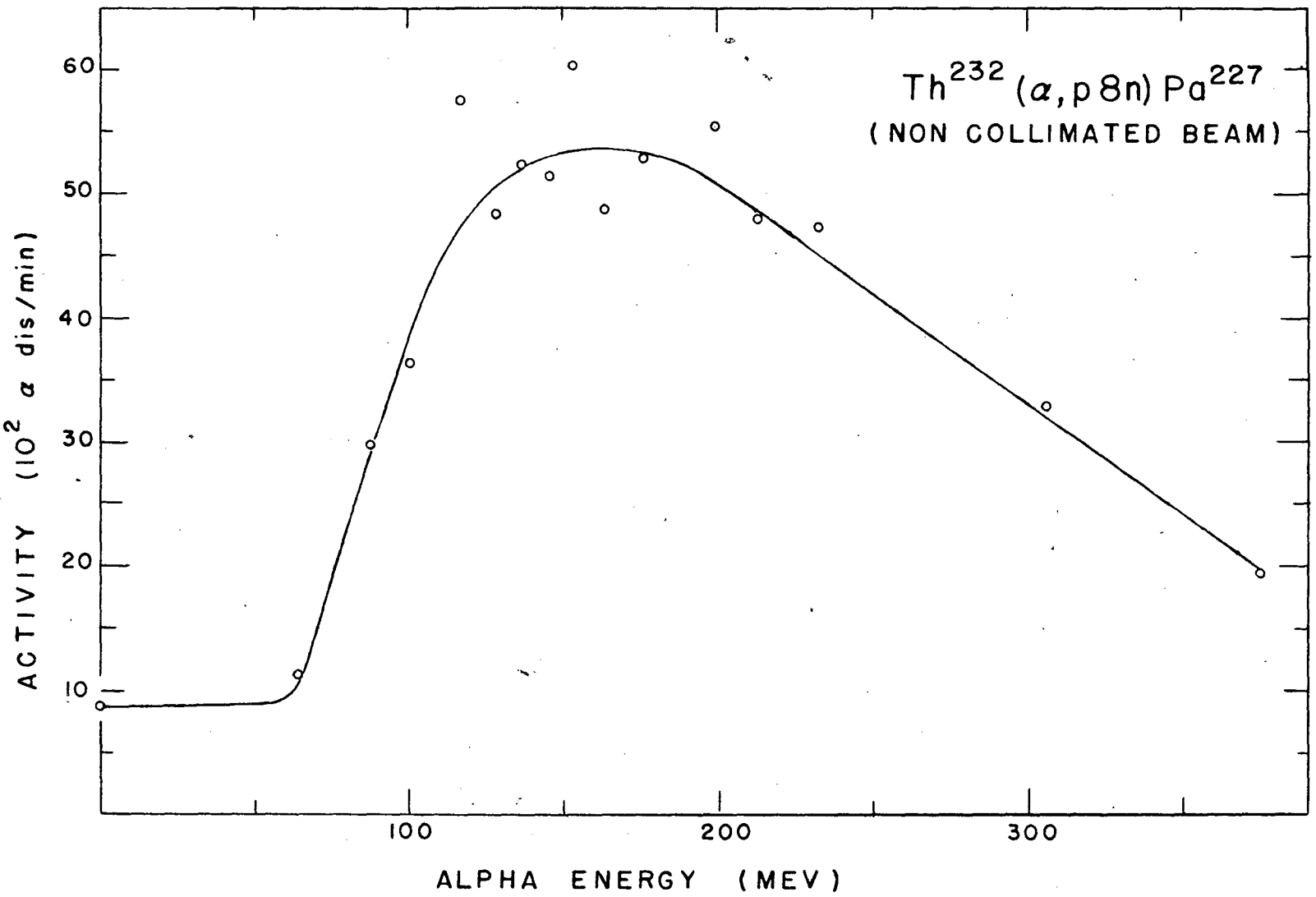

Fig. 92. Excitation function for the $Th^{232}(\alpha,p8n)Pa^{227}$ reaction using a non-collimated beam of bombarding alpha particles, (Run I, Table 37).

Table 37

Experimental Yields for the $Th^{232}(\alpha, p8n)Pa^{227}$ Reaction

Energy (Mev)		Target foil	Total absorber in beam (mg/cm^2 Cu)		Yield of Pa^{227} (10^3 α dis/min at end of bombardment)	
Front	Back	gm/cm^2	Front	Back	Run I	Run II
375.7	373.4	158.6	619.6	732.2		52.6
375.5	373.5	141.6	628.3	728.8	1.95	
307.3	304.8	150.4	3775.1	3881.1	3.29	
292.2	289.5	153.3	4406.5	4515.5		69.7
234.8	231.7	150.5	6597.1	6702.8	4.74	
216.1	212.7	153.8	7231.5	7339.0		78.9
215.0	211.9	140.0	7266.7	7364.4	4.81	
201.1	197.7	152.8	7709.9	7816.2	5.54	
198.3	194.8	149.7	7796.8	7901.1		72.9
184.2	181.2	138.7	8246.6	8342.4		78.6
178.6	174.4	152.1	8391.1	8496.5	5.29	
166.1	162.6	139.1	8721.0	8817.1	4.88	
158.9	154.7	149.5	8917.3	9020.9		85.7
156.3	152.4	140.7	8981.3	9078.4	6.01	
148.1	143.9	150.5	9183.1	9286.8	5.15	
145.6	141.7	138.1	9245.4	9340.4		86.0
139.7	135.2	138.4	9391.7	9486.6	5.24	
134.6	129.9	155.5	9504.6	9611.3		80.5
130.7	126.3	143.3	9592.4	9690.4	4.85	
125.2	120.9	139.0	9714.4	9809.5		85.9
119.2	114.4	143.3	9846.9	9944.5	5.74	
115.9	111.2	142.0	9914.4	10011.2		63.4
105.6	99.9	153.7	10117.0	10221.5		43.9
102.7	97.1	151.3	10171.2	10273.5	3.65	
91.1	85.6	133.7	10377.3	10467.7	2.97	
91.0	84.2	141.6	10378.0	10473.7		18.60
70.1	62.9	144.2	10700.4	10796.9		11.97
67.5	60.6	135.9	10734.9	10824.6	1.11	
54.2	45.7	137.5	10900.7	10991.3		11.44
0		154.3	11258.5	11357.3		10.48
0		151.9	11262.0	11353.1	0.89	
0		138.2	12263.1	12348.8		7.38

only the fringe of the electrostatically deflected beam hit the target foils. The rest of the beam probably hit near the edge of the absorbers and was scattered in some cases into the rear target foils to cause a yield maximum that is somewhat more elevated than the one obtained with a collimated beam from a 1-1/2 hour bombardment (Fig. 93 and Run II, Table 37). With the collimated beam (using the collimator illustrated in Fig. 58) this situation is reversed. Since the collimating hole is the same area as the target discs, a given amount of beam hits the front target and then is reduced by scattering on passage through the target foils and absorbers. This latter effect, although probably small, would tend to reduce the height of the peak in the excitation function.

2. $Th^{232}(\alpha,p5n)Pa^{230}$ In Fig. 94 and Table 38 are presented the curves and values for this reaction. The run made with the collimated beam is given since only in it was there enough activity to give any U^{230} alpha counts.

In these (α,pxn) curves we find that the peak yield of the $(\alpha,p5n)$ reaction is higher by a factor of 6.9 than the peak yield for the $(\alpha,p8n)$ reaction. A summary of other comparisons of these two curves is given in Table 39 .

Table 39

Summary of Data from $Th^{232}(\alpha,p5n)Pa^{230}$ and $Th^{232}(\alpha,p8n)Pa^{227}$ Excitation Function Curves

	$(\alpha,p5n)$	$(\alpha,p8n)$
Maximum alpha energy used in calculations	388	388
Threshold energy	55 Mev	78 Mev
Peak energy	125 Mev	145 Mev
"Distance" between peak and threshold	70 Mev	67 Mev
Yield at peak (dis/min)	2.3×10^{2} β^-	8.5×10^{4} α
Factor in yield between peak and maximum energy	2.6	1.6

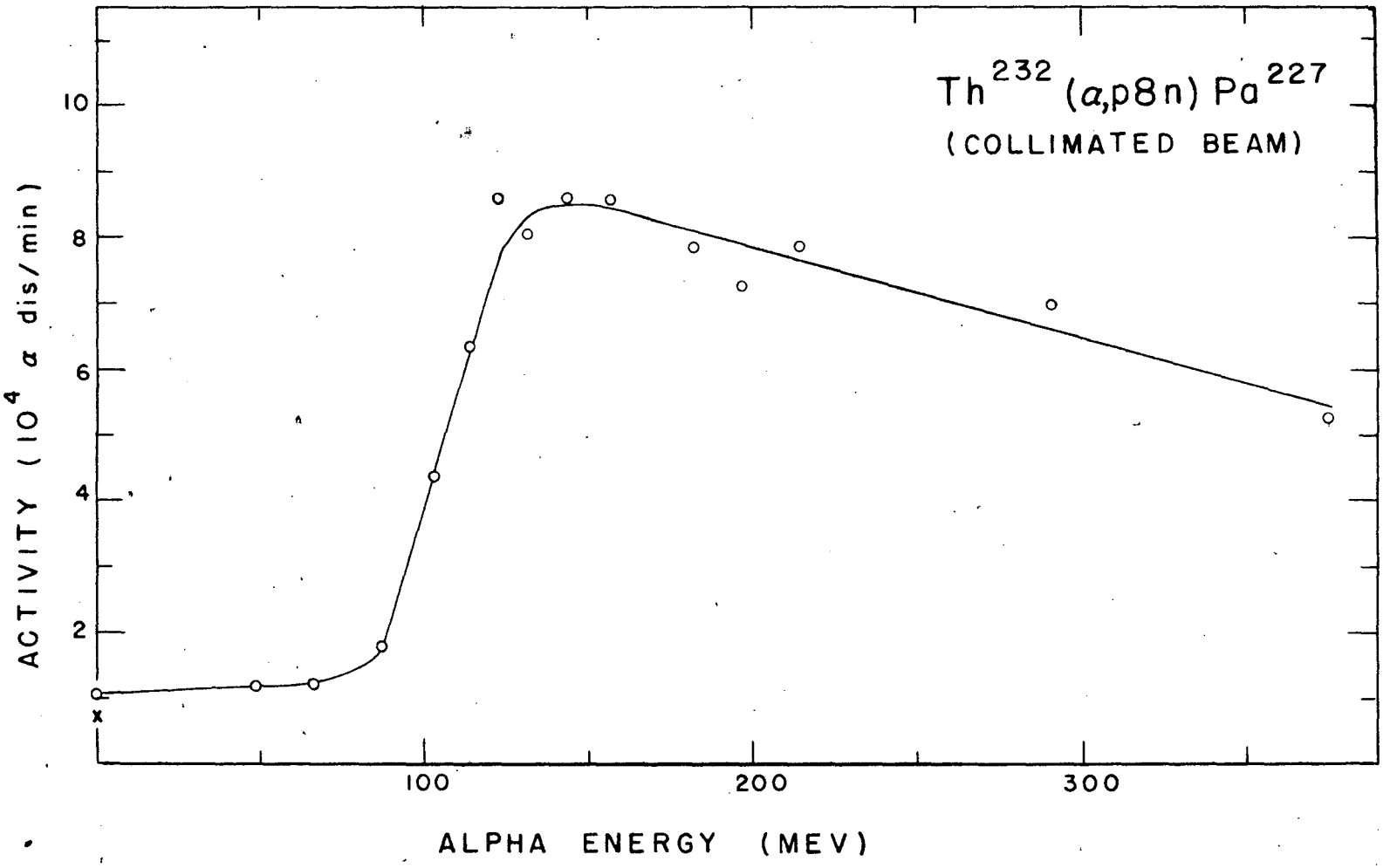

Fig. 93. Excitation function for the $Th^{232}(\alpha,p8n)Pa^{227}$ reaction using a well collimated beam of bombarding alpha particles (Run II, Table 37).

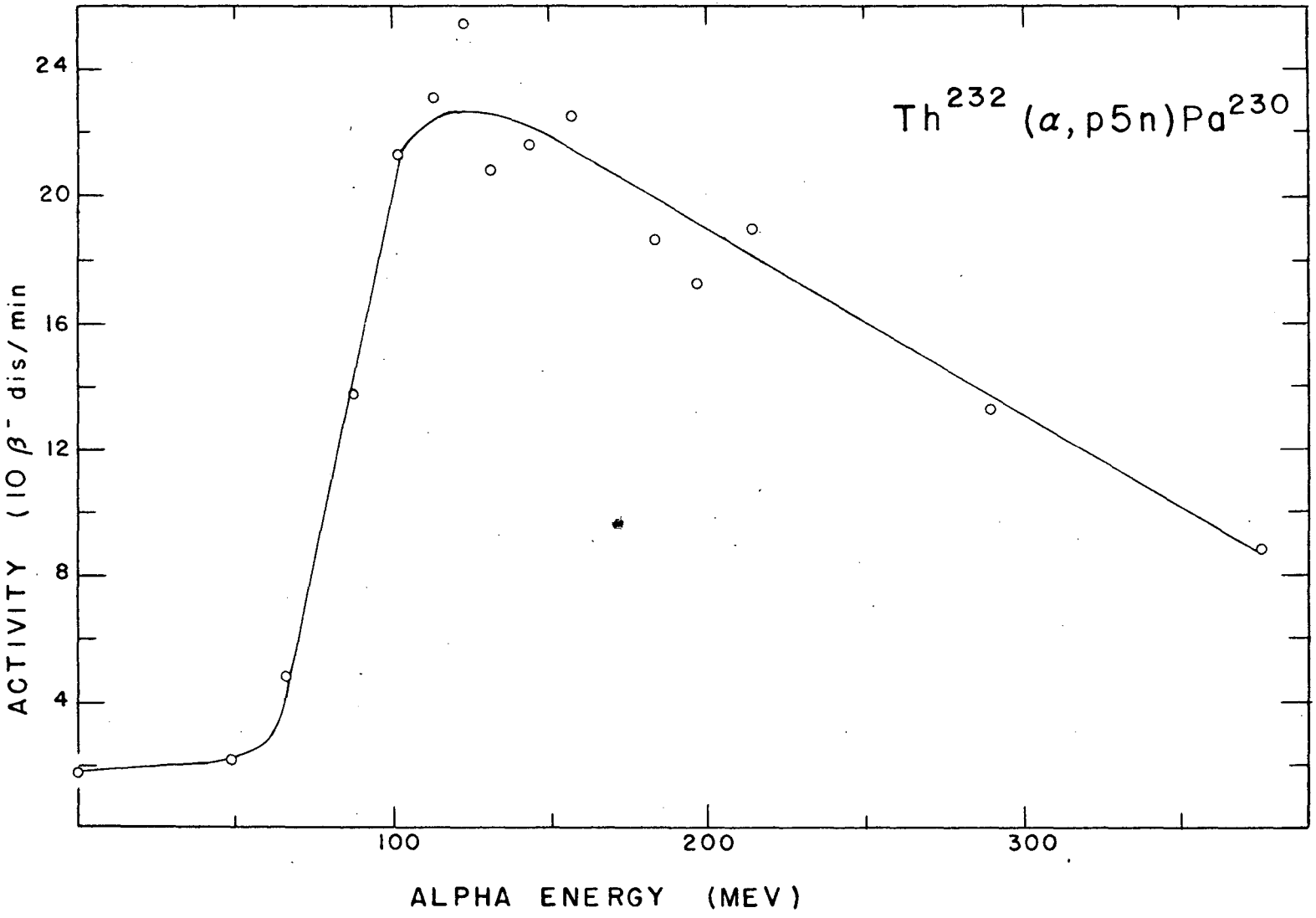

Fig. 94. Excitation function for the $Th^{232}(\alpha,p5n)Pa^{230}$ reaction (Run II, Table 38).

Table 38

Experimental Yields for the $Th^{232}(\alpha,p5n)Pa^{230}$ Reaction

Energy (Mev)		Target foil	Total absorber in beam (mg/cm^2 Cu)		Yield of Pa^{230}(β^- dis/min. at end of bombardment)	
Front	Back	gm/cm^2	Front	Back	Run I	Run II
375.7	373.4	158.6	619.6	732.2		88.2
375.5	373.5	141.6	628.3	728.8		
307.3	304.8	150.4	3775.1	3881.1		
292.2	289.5	153.3	4406.5	4515.5		133.3
234.8	231.7	150.5	6597.1	6702.8		
216.1	212.7	153.8	7231.5	7339.0		190.3
215.0	211.9	140.0	7266.7	7364.4		
201.1	197.7	152.8	7709.9	7816.2		
198.3	194.8	149.7	7796.8	7901.1		171.6
184.2	181.2	138.7	8246.6	8342.4		186.1
178.6	174.4	152.1	8391.1	8496.5		
166.1	162.6	139.1	8721.0	8817.1		
158.9	154.7	149.5	8917.3	9020.9		226.
156.3	152.4	140.7	8981.3	9078.4		
148.1	143.9	150.5	9183.1	9286.8		
145.6	141.7	138.1	9245.4	9340.4		217.
139.7	135.2	138.4	9391.7	9486.6		
134.6	129.9	155.5	9504.6	9611.3		208.
130.7	126.3	143.3	9592.4	9690.4		
125.2	120.9	139.0	9714.4	9809.5		255.
119.2	114.4	143.3	9846.9	9944.5		
115.9	111.2	142.0	9914.4	10011.2		231.
105.6	99.9	153.7	10117.0	10221.5		213.
102.7	97.1	151.3	10171.2	10273.5		
91.1	85.6	133.7	10377.3	10467.7		
91.0	84.2	141.6	10378.0	10473.7		137.4
70.1	62.9	144.2	10700.4	10796.9		48.5
67.5	60.6	135.9	10734.9	10824.6		
54.2	45.7	137.5	10900.7	10991.3		21.8
0		154.3	11258.5	11357.3		18.07
0		151.9	11262.0	11353.1		
0		138.2	12263.1	12348.8		16.97

The high background (below the thresholds) for these (α,pxn) reactions is due at least partially to deuteron contamination of the alpha-particle beam. An α/D_2 ratio of 20/1 is considered very good under ordinary operating conditions. This 5% of deuteron contamination produces Pa^{230} and Pa^{227} from thorium with much higher cross sections than the alpha-particles can.

Deuterons however are slowed down much less than alpha particles in traversing a given thickness of absorber. Figure 95 shows the corresponding deuteron and alpha-particle energies when both particles have been slowed from full energy by passage through copper.

Hence if the amount of background due to deuteron contamination is estimated, the excitation function can be corrected since the (d,xn) excitation functions on thorium are known.

3. $Th^{232}(\alpha,6n)U^{230}$ and other (α,xn) Reactions Results obtained when we attempted to separate a uranium fraction from alpha bombardments of thorium were poor. Early experiments in the internal beam had indicated that we could expect a peaked excitation function reducing to very low values at high energies -- a reduction of perhaps a factor of 50 or more. However in working with this reaction one is never sure that the U^{230} present is really there from the bombardment or has just decayed from Pa^{230} present in high yield. The ideal way to check an (α,xn) reaction would be to separate U^{229} (a 58 minute alpha emitter) formed in the bombardment, using tracer if necessary to determine the chemical yield. The chemistry however has not been clean enough or fast enough to do this.

By using the alpha beam we have already suffered a reduction of a factor of about 10 in beam intensity from the deuteron and proton beams. In addition, the cross section values for the (α,xn) reactions seem to be much lower than the cross sections for the corresponding (p,xn) and (d,xn) reactions. The combination of these two factors reduces the yield from (α,xn) reactions to such a point that it is no

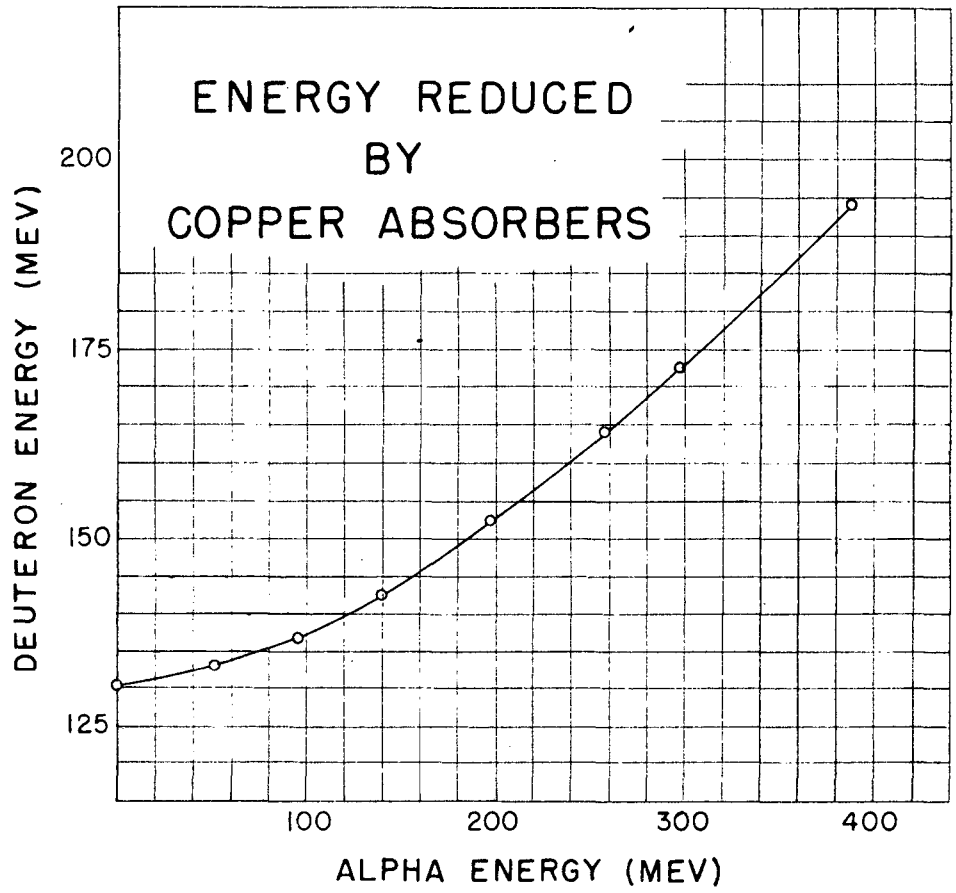

Fig. 95. The energy of deuteron contamination in an alpha beam of given energy, both alpha-particles and deuterons having been reduced from 388 Mev and 194 Mev respectively by passage through copper.

longer possible to obtain their excitation function with the electrostatically deflected beam. Several attempts were made with this beam but too little activity was obtained and the chemistry was too inadequate for definitive results.

A final attempt was made to obtain a good curve with a one half hour internal beam bombardment of stacked foils followed by immediate separation of the Pa^{230} formed. A few counts of U^{233} tracer were added before solution of the weighed foils to give a true picture of the chemical yield. Procedure 92-1 of Appendix II was used after the TTA-benzene separation of the Pa^{230}. The results, shown in Fig. 96 indicate that the peak has been spread out by the angular variation of the cyclotron beam.

This effect is illustrated in Fig. 97. Particles coming in from B traverse more copper than those coming along A, and hence for a given target foil induce a higher energy reaction than the perpendicular beam. Particles coming in along C however induce a higher energy reaction than the perpendicular beam. The angle indicated in the figure was merely assumed for the argument. This effect can however spread reaction peaks considerably. Fig. 96 then is not a true excitation curve. The only reason for its inclusion in this paper is to indicate how a person can err if he works with the internal beam of the cyclotron without taking into consideration the angular variation of the beam.

Hence it appears that unless a much larger alpha beam becomes available from the 184-inch cyclotron the only method remaining for determining these excitation functions would be to make numerous bombardments at different radii in the cyclotron and relate them to each other with a monitor of some sort which is sensitive to alpha particles only (e.g. the At^{211} formation from Bi^{209} would probably work fairly well as an alpha monitor.)

One exploratory set of four bombardments was made without the benefit of a monitor but with care to keep the conditions of the bombardments as nearly identical as possible. The results for the $(\alpha,6n)$ and the $(\alpha,8n)$ reactions on thorium are shown in Fig. 98, as well as the $(\alpha,6n)$ being superimposed on the stacked foil

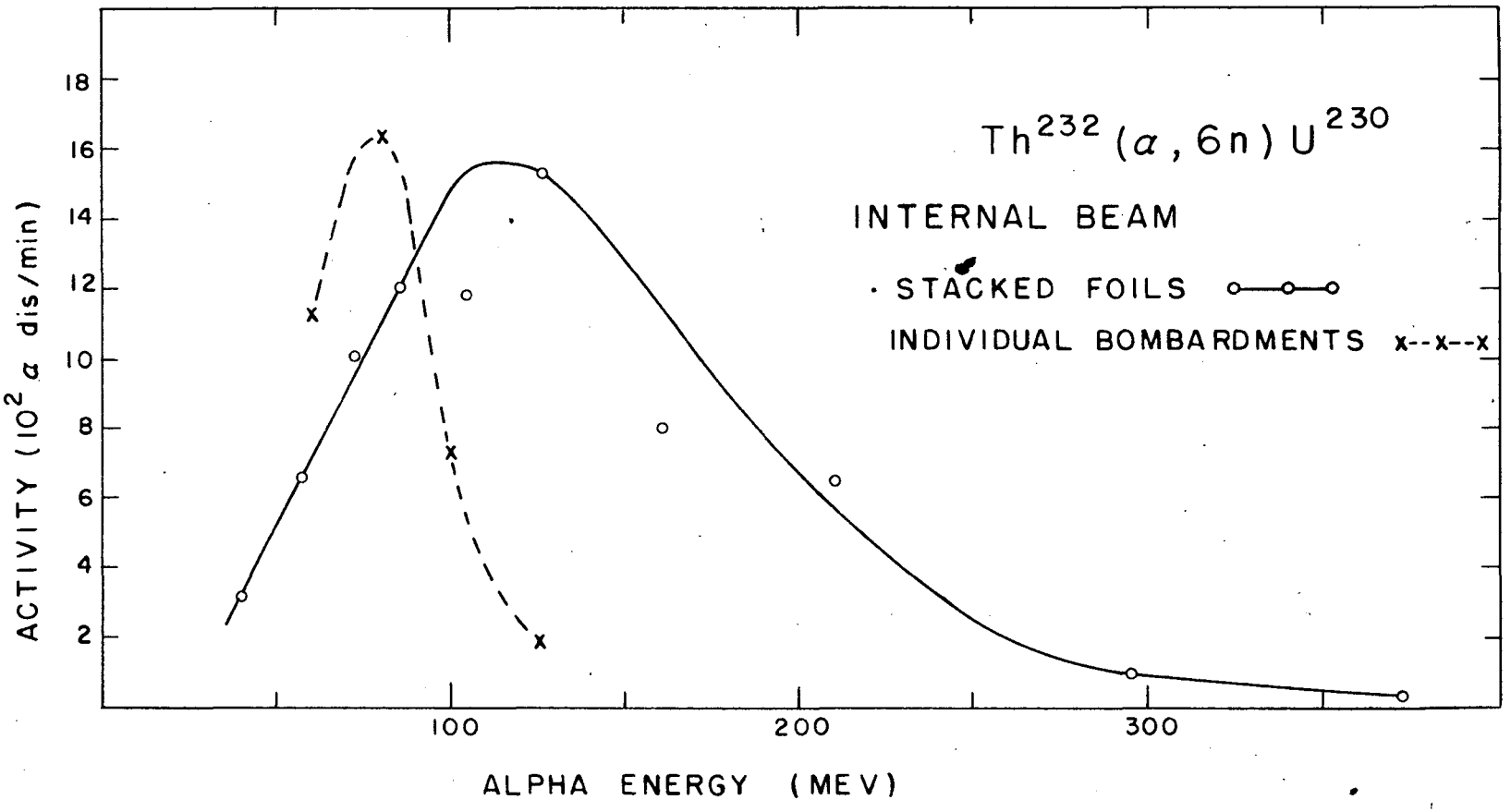

Fig. 96. Excitation function for the $Th^{232}(\alpha,6n)U^{230}$ reaction in the internal cyclotron beam for both stacked foils and different radii bombardments of thin targets.

EFFECT OF ANGULAR VARIATION OF CYCLOTRON INTERNAL BEAM

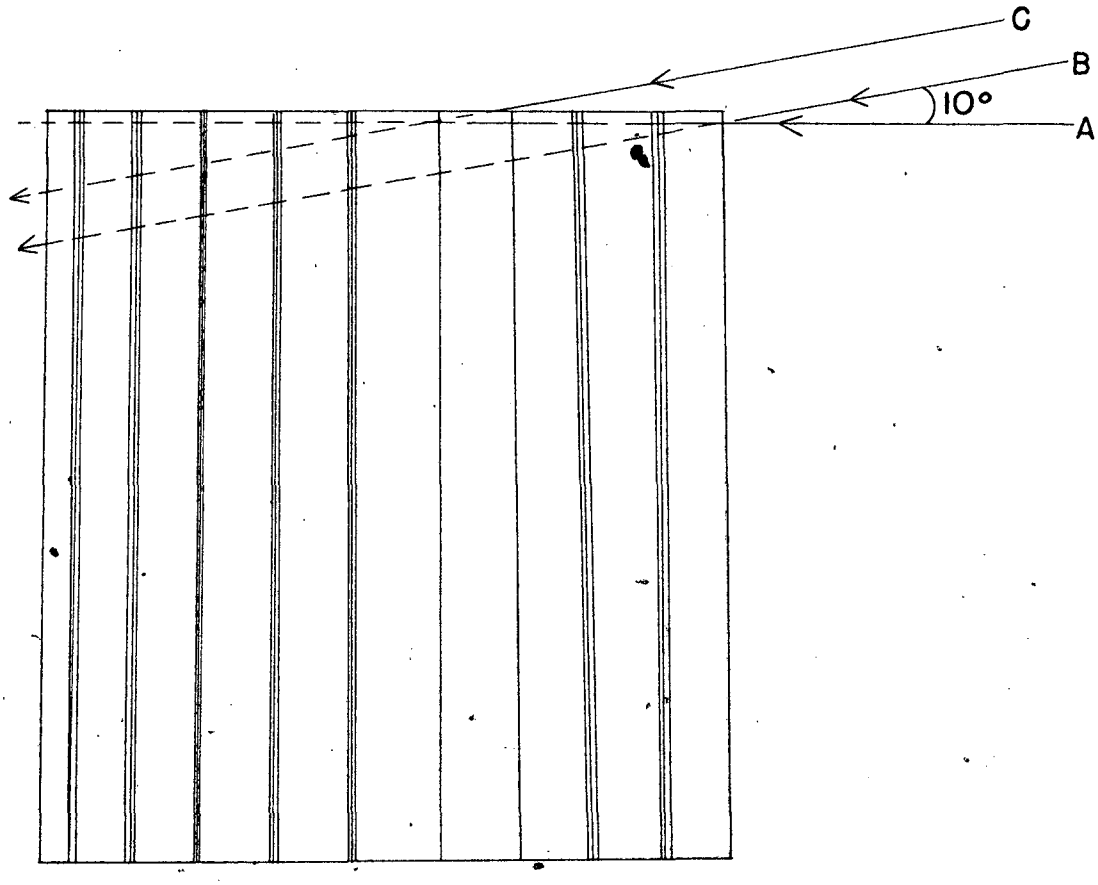

FIG. 97

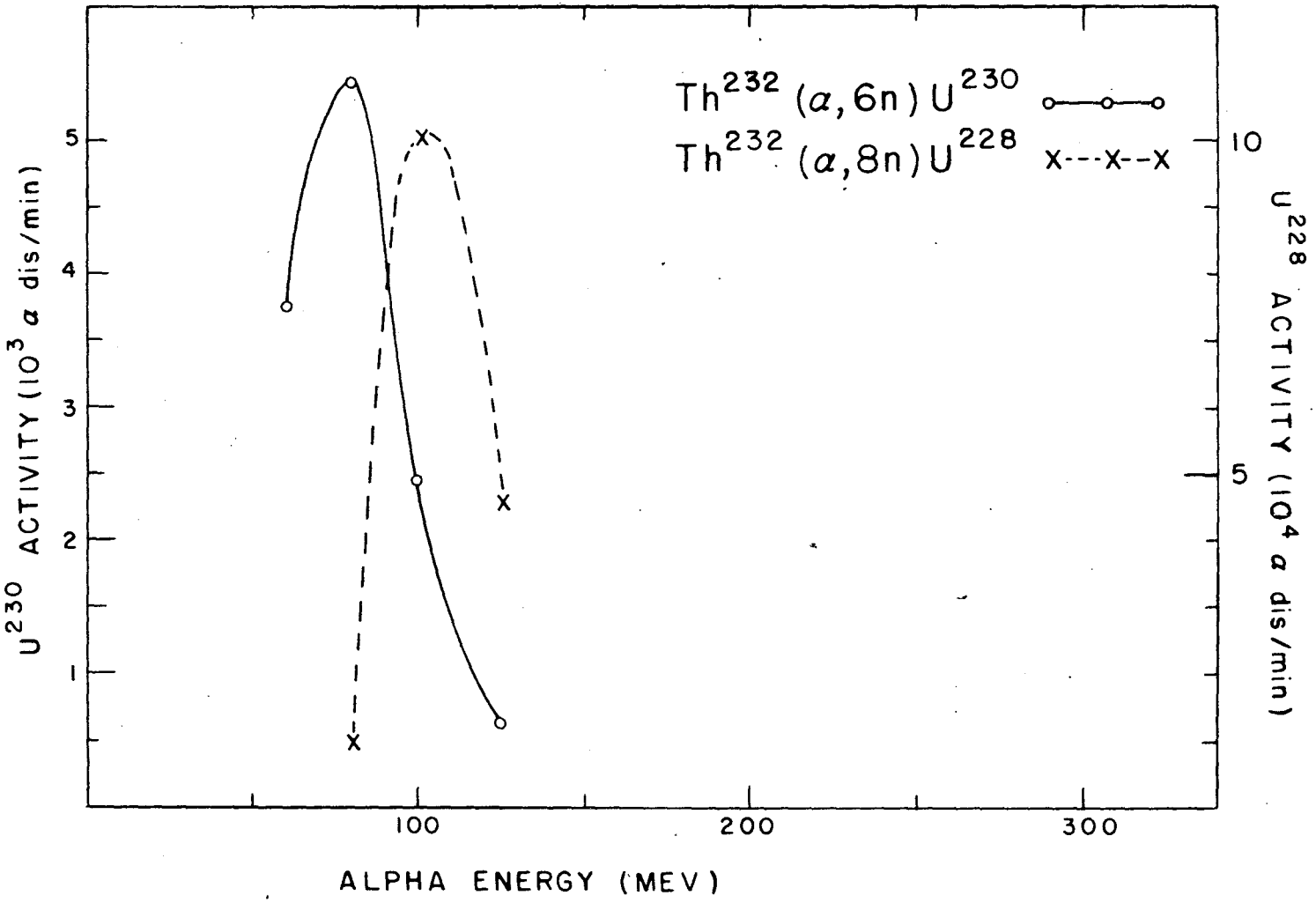

Fig. 93. Excitation functions for the $Th^{232}(\alpha,6n)U^{230}$ and $Th^{232}(\alpha,8n)U^{228}$ reactions from different radii bombardments of thin targets.

internal target of Fig. 96 . Each target was the same size and presented the same amount of surface to the internal beam. Each was bombarded for a period of 15 minutes.

Shown in Fig. 99 are the results for the 58 minute activity resolved from the same pulse analyses as were used for the above values. There undoubtedly was some other activity (probably astatine) that was coming through the simple chemistry used and was being pulse analyzed along with the U^{229}. Hence the results of this curve are undoubtedly false.

Tracer U^{233} was used in the chemistry for the above samples so that the yield values quoted have been corrected for chemical yield. The ratio of peak yields U^{230}/U^{228} appears to be about 20 although this value must be considered quite rough.

V. Discussion of Results

Probably the most important basic fact illustrated in this work is that even up in the so-called higher energy range (above 20 or 30 Mev) the (d,xn) and (p,xn) reactions peak very definitely, extending the pattern of behavior from the case when x = 3, up to when x = 6 or 7. The (p,α8n) and (p,α5n) reactions on uranium, on the contrary, have a very broad peak in the high energy range around 300 Mev and begin to decrease only at full energy of the beam. The (α,p8n) and the (α,p5n) reactions, on the other hand, rise rather rapidly to a peak at around 100 Mev and then fall off gradually to half maximum at full energy.

In the d and p,xn reactions we see two different reaction mechanisms at work. In the peak we have the reaction still proceeding by the same compound nucleus type of reaction that is valid for the (d,2n) reaction type. However instead of a completely symmetrical peak going down to almost zero on the high energy end, a high energy tail takes off about 4/5ths of the way down the peak and gradually decreases until the full energy is reached. This slowly varying curve can be explained by the picture of the transparent nucleus given by Serber.[24] Instead of the

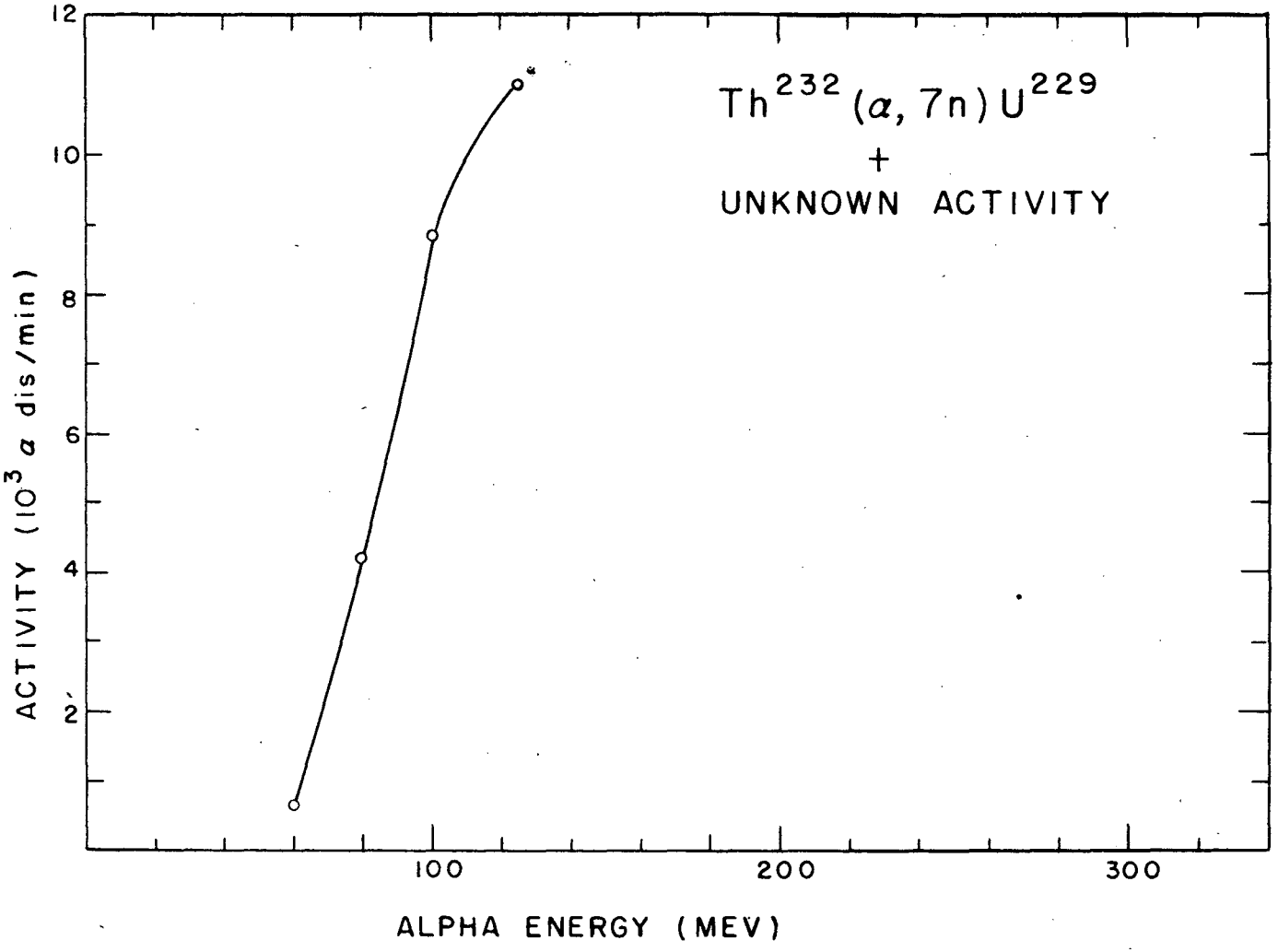

Fig. 99. Excitation function for the $Th^{232}(\alpha,7n)U^{229}$ reaction plus some unknown activity from different radii bombardments of thin targets.

projectile either hitting the target nucleus to form a compound nucleus, or missing the target nucleus completely, the possibility arises that a whole spectrum of energies can be imparted to the target nucleus depending upon just how much of the energy of the incident particle is imparted to the target. These cases may range from a near miss, where the target nucleus is excited by only a few Mev, to the case where the entire energy of the incident particle is absorbed in the target nucleus, highly exciting it and causing many particles to be boiled out. At high energies therefore, because of the transparency of the nucleus, cross sections should vary rather slowly with energy.

This same type of transparency picture can be applied to the other reactions studied, the (p,αxn) and the (α,pxn) reactions, to explain their slowly varying curves and peaks.

Another mechanism for the (α,pxn) reactions involves the splitting of the bombarding alpha particle upon hitting the target nucleus, leaving one proton and one neutron in the nucleus while the other proton and neutron proceed away from the nucleus. The two particles that remain can impart enough energy to boil out neutrons much the same as the xn reactions.

The peaking of the (α,xn) reactions, on the other hand, indicates that the entire alpha particle amalgamates with the target nucleus to form a compound nucleus before these xn reaction products can be produced.

It is interesting to note that for the four general types of reactions giving Pa^{230} and Pa^{227} which we have investigated, the ratios of yields of these two isotopes at the excitation function peaks is in each case about 6. This is logical since the difference between the reactions is always the same three neutrons. The (α,pxn) and (p,αxn) ratios are even closer to each other than to the other two reactions, possibly explainable by the fact that they both require the emission of a charged particle before the neutrons are emitted.

It should be born in mind while considering the summaries of data from curves presented above that the assignment of absolute energies to any of the yield values is very difficult. In most cases, calculation of threshold values by assuming a binding energy of about 6.5 or 7 Mev per neutron is more reliable than reading values off the curves. Other energy values have a corresponding variation.

When a reaction such as the (p,6n) on thorium is finally characterized as to energy and yield it will make a very good monitor of beam current for bombardments of other materials. The chemistry for the separation is easy, although work will have to be done to determine what precautions should be taken to prevent formation of the colloidal state of the Pa^{231} tracer used to check chemical yield.

It might even be possible to make a suspension of thorium salt in a thin plastic sheet which could then be counted directly without chemical separation. Since the Pa^{227} is such a sensitive detector of even microgram amounts of thorium, it would make a very good monitor.

Aside from arousing theoretical interest in the general shape of the excitation functions for several heavy element reactions, this work definitely indicates the need for using a maximum yield energy in (deuteron or proton, xn) bombardments if maximum yields are desired.

Chapter 3

Alpha Half-Lives of the Protactinium Isotopes

I. Introduction

While investigating the members of the artificial collateral alpha-decay chains we had occasion to determine the branching ratios (orbital electron capture decay/alpha decay) of the three lightest protactinium isotopes known to date (Pa^{226}, Pa^{227}, and Pa^{228}). With this information we were able to determine the partial alpha half-lives for these isotopes and the regularities of these half-lives when plotted against mass number or alpha energy. Since there still remained two other isotopes between the above isotopes and the long-lived Pa^{231}, we decided to determine the branching ratios of both the Pa^{229} and Pa^{230} isotopes, and to check the feasibility of milking alpha daughters from the Pa^{232} and Pa^{233} activities.

In all cases alpha-pulse analysis of samples established the amounts of parents and daughters, Th^{230} and Ac^{225} tracers being used in chemical procedures to determine chemical yield.

II. Chemistry

The chemistry used in determining the branching ratios of course varies from isotope to isotope. For the light isotopes, Pa^{227}, Pa^{228}, and Pa^{229} whose alpha decay is observable, thorium is removed to check the amount of branching by orbital electron capture. For isotopes whose chief mode of decay is by beta particle emission, however, the actinium alpha daughter must be removed to determine the alpha half-life.

The thorium separation given in Procedure 90-3, Appendix II, was used for the Pa^{227} and Pa^{228} determinations. Since the 7000 year Th^{229} must be milked from Pa^{229}, however, much greater purification from other activities is needed and a procedure such as 90-1 in the appendix must be used. For Pa^{230} the actinium separation given in Procedure 89-2, Appendix II was used.

III. Experimental Results

The branching ratio determinations will be discussed individually for each of the protactinium isotopes.

A. Pa^{226}

When, in pulse analysis of this series, we were unable to detect any alpha peaks of Th^{226} and daughters once the Pa^{226} had decayed out, we set a limit of ~ 1 for the K/α branching ratio. Since the half-life determined for this isotope was 1.7 minutes, this branching determination would mean that the alpha half-life must be between 1.7 and 3.4 minutes.

Chemical separation of the thorium would be possible if a large amount of Pa^{226} were separated and allowed to decay. It would be necessary, however, to determine whether any Th^{226} from the original solution were present. Even small amounts of the thorium metal target material coming through the TTA-benzene extraction of the protactinium could be easily detected, however. Several successive milkings after a period of 20 minutes would determine whether the Th^{226} had actually come from the 1.7 minute Pa^{226} or was being constantly formed from a small amount of U^{230} or Pa^{230} present in the solution. Perhaps when the new jiffy probe-pneumatic tube set-up is ready for use we will be able to obtain enough Pa^{226} to better bracket this branching ratio.

B. Pa^{227}

The results of the milkings of this isotope have been mentioned in Chapter 1. The K/α ratio obtained by milking 18.6 day Th^{227} from the decay of Pa^{227} was 0.18 with an error of $\pm$ 0.02. This ratio then serves to increase the 38.3 minute total half-life of this isotope to 45.3 minutes. This alpha half-life is quite accurate and rather easily determined from the amount of Pa^{227} formed in a half-hour bombardment of thorium with 60-Mev deuterons or protons.

C. Pa^{228}

The branching ratio determination for this isotope is also discussed in Chapter 1. The value of 53 ± 5% for the K/α ratio was determined by separating the 1.9 year Th^{228} from a solution of Pa^{228} which had decayed for six days. This branching ratio then determines an alpha half-life of about 1190 hours for this isotope. This value is quite easily obtained from the Pa^{228} produced in a one hour bombardment of thorium with 60-Mev deuterons or protons.

D. Pa^{229}

The determination of this branching ratio presents a very definite problem. From systematics one would guess that this K/α ratio should be somewhere between 100 and 1000. The thorium daughter from orbital electron capture decay is, however, the 7000 year Th^{229}. Hence while the orbital electron capture branching is more than for Pa^{228} by a factor of from two to twenty, the half-life of the daughter is greater by a factor of 3500. This means that in order to determine this branching ratio, the sample of Pa^{229} which is to be milked must contain very little Pa^{228} contamination, so that the Th^{229} will not be completely masked by the Th^{228} peak in pulse analysis.

We have tried many methods of obtaining the Pa^{229} for this experiment and have succeeded only in being able to choose the most desirable of a group of undesirable methods. A resume of these methods is given in the following paragraphs in the hope that they might save someone considerable time and effort with a similar problem.

Pa^{229} had been discovered by a (d,3n) reaction on Th^{230} (ionium) using the 20-Mev deuteron beam of the Berkeley 60-inch cyclotron.[34] Since the ionium is so messy to work with because of its high specific alpha activity we explored other methods of making this isotope.

The high energy particles produced by the large cyclotron can of course easily make the isotope. Once we had found Pa^{228} with these particles, however, we ran

into the trouble mentioned above in trying to obtain Pa^{229} comparatively free from Pa^{228}. Several careful bombardments using small radii (low energies) and further cutting the energy of the beam down with stacked thorium foils indicated that the best ratio of Pa^{229}/Pa^{228} alphas one can expect from deuteron bombardments with the large cyclotron is about 10/1. Undoubtedly the initial energy distribution as well as the overlapping of adjacent excitation functions causes this low upper limit. Since a Pa^{229}/Pa^{228} ratio of at least several hundred was required to see the Th^{229} we tried other methods.

With the discovery of U^{229}, with a 58 minute half-life and a branching decay partially by orbital electron capture to Pa^{229}, it appeared that we might make enough pure Pa^{229} from milkings of U^{229} for our branching experiments. U^{228} of course also has some orbital electron branching decay but its shorter half-life enables one to allow most of it to decay before one collects the protactinium daughters of U^{229}. The U^{228} was allowed to decay for at least eight half-lives after shut-down, the Pa^{228} being washed out several times during this decay. The remaining U^{229} was then allowed to almost completely decay and the protactinium fraction separated.

Although this procedure does give very pure Pa^{229}, a total of only 300 alpha counts per minute was obtained in two consecutive hour and a half bombardments designed to give a maximum amount of U^{229} ($\sim 10^7$ alpha c/m per bombardment). This low yield is due largely to the small alpha beam current (at least a factor of 10 below that for deuterons and protons) available from the large cyclotron. In order to obtain as high a yield as mentioned above it was found necessary to have a new filament installed just before bombardment to increase the alpha beam current.

Although the 300 alpha counts separated in this set of experiments was not pure from contaminating Geiger activities, Procedure 91-1 (Appendix II), which has been worked out since the completion of these experiments, does insure complete radioactive purity. At any rate there was not enough activity to determine the

branching ratio -- and unless the alpha beam of the large cyclotron is increased in intensity by a factor of 10 or so, this type of experiment is of no use for our problem.

Another type of experiment sought to take advantage of the larger proton beam intensity, and the relatively large cross section for the (p,pxn) reaction. Uranium foil was bombarded with full energy protons of the 184-inch cyclotron and the uranium separated from contaminating protactinium isotopes by TTA-benzene extractions. The U^{229} was allowed to decay and the protactinium again separated.

After the two hour bombardment the target was very active, giving a reading of about 800 mr at 20 feet soon after shutdown. Consequently the chemistry was quite difficult to perform even though it consisted mostly of simple extractions performed in the lead shielded Berkeley box. Eleven TTA-benzene extractions were required to completely separate the original protactinium from the target material.

It was found, however, that in spite of the extra beam current with protons, only four times the amount of U^{229} formed in the alpha bombardments was formed here. Apparently fission and spallation takes a much larger percentage of the reaction products at these high energies than in lower energy alpha-particle bombardments where one bombards near the peak of the (α,xn) reaction excitation function. Consequently this method is not satisfactory for making Pa^{229} for branching ratio determinations.

For a time it was thought possible to obtain a very high yield of activity from a small amount of material mounted on quarter mil aluminum foil for bombardments. If the foil plus target material is thin enough, the beam, in passing through the target, will not lose enough of its energy to cause it to leave its path. Hence the beam will circulate through the target again and again. This type of bombardment is very good for target materials which are scarce but it does not give the yields which can be obtained from large amounts of thorium.

Finally, therefore, as a last resort, we decided to make a bombardment of ionium on the 60-inch cyclotron to produce the required amount of Pa^{229}. About 100 milligrams of an ionium-thorium mixture (13% ionium) was bombarded in a small platinum boat on the interceptor of the 60-inch cyclotron. The platinum boat was silver soldered to the end of the interceptor which is shown in Fig. 100-102. This boat was 1" x 1/2" x 1/8" O.D. with a wall thickness of 10 mils. Grooves were cut in the bottom of the boat to help secure the target material. The ionium (as the dioxide) was cemented in the boat with sodium silicate to insure against flaking off during the course of the bombardment.

The entire interceptor was then sealed into a target lock to prevent escape of the ionium during bombardment. Two mils of tantalum foil was placed in the window of this lock to cut down the beam energy enough to sufficiently reduce the yield of Pa^{228}. Assuming the full energy deuteron beam delivered externally by the 60-inch cyclotron is 18.5 Mev, this tantalum foil cut the energy down to 16.7 Mev.

The interceptor was bombarded for about 1-1/2 days, allowed to cool overnight and then worked up chemically. Procedure 90-4 in Appendix II describes the preparation and solution of the target. Once the target is dissolved, protactinium was separated from the solution by four MnO_2 precipitations, and two di-isopropyl ketone extractions with four washings apiece (as given in Procedure 91-1 in the appendix). The protactinium was washed into acid and the Pa^{229} allowed to decay. We obtained about 8×10^5 alpha counts per minute of purified Pa^{229} in this bombardment.

The same type thorium separation as done for Pa^{227} and Pa^{228}, with many cycles to effect the required purification, was made on part of the solution. Unfortunately, because of this chemistry, (Procedure 90-3, Appendix II) only about one per cent yield, not enough for our purposes, was obtained through the entire procedure. For

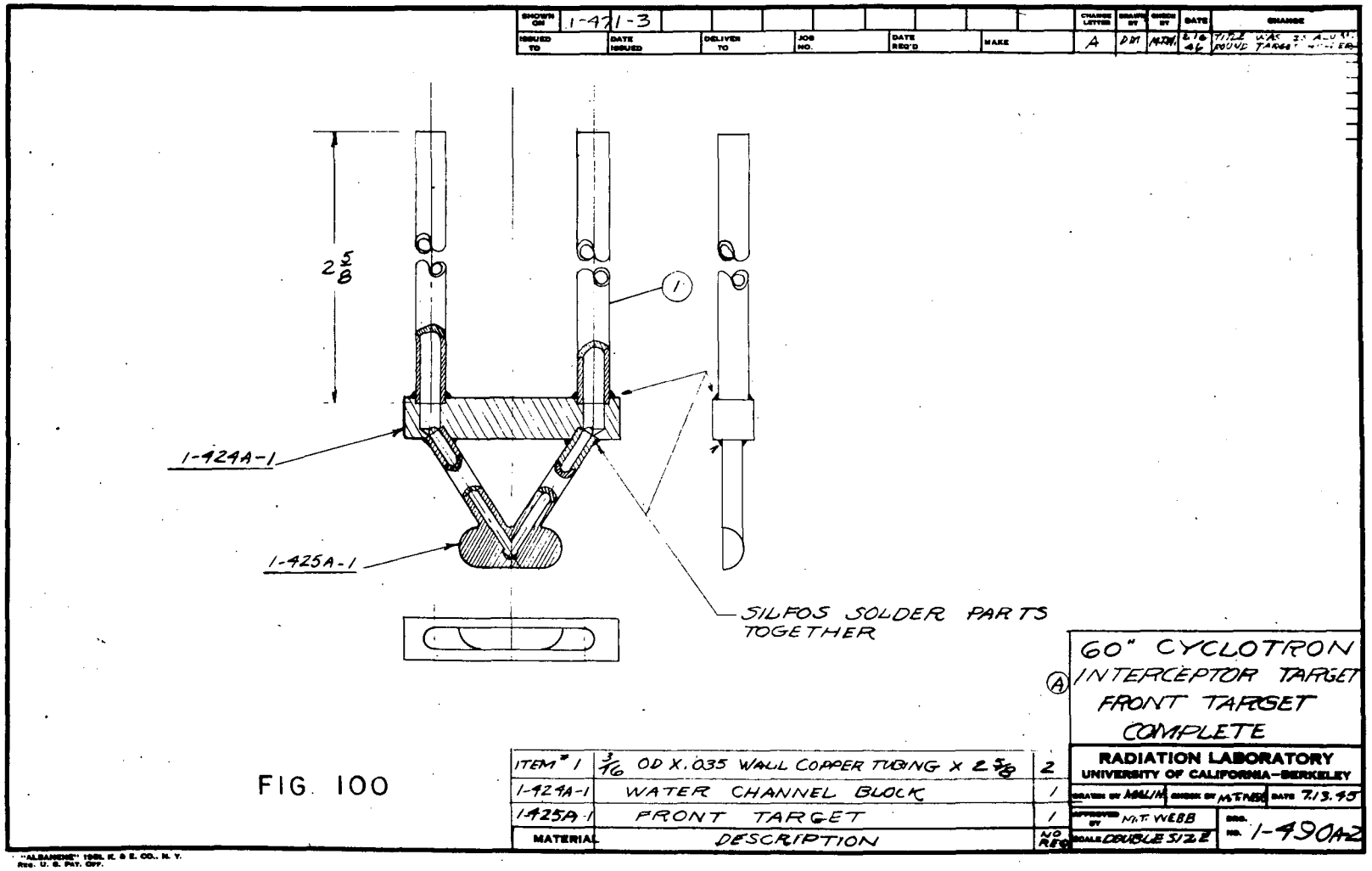

FIG. 100

SHOWN ON	1-417 A-3	1-419 C-2							
ISSUED TO	DATE ISSUED	DELIVER TO	JOB NO.	DATE REQ'D	MAKE				
				TOLERANCES WHERE NOT OTHERWISE GIVEN					

RADIATION LABORATORY DRG. NO. 1-424C-1

UNIVERSITY OF CALIFORNIA—BERKELEY

DRAWN BY	CHECK BY	DATE
MALIM	M.T. WEBB	6.16.45

APPROVED BY	SCALE
M.T. WEBB	DOUBLE SIZE

60" CYCLOTRON INTERCEPTOR TARGET WATER CHANNEL BLOCK

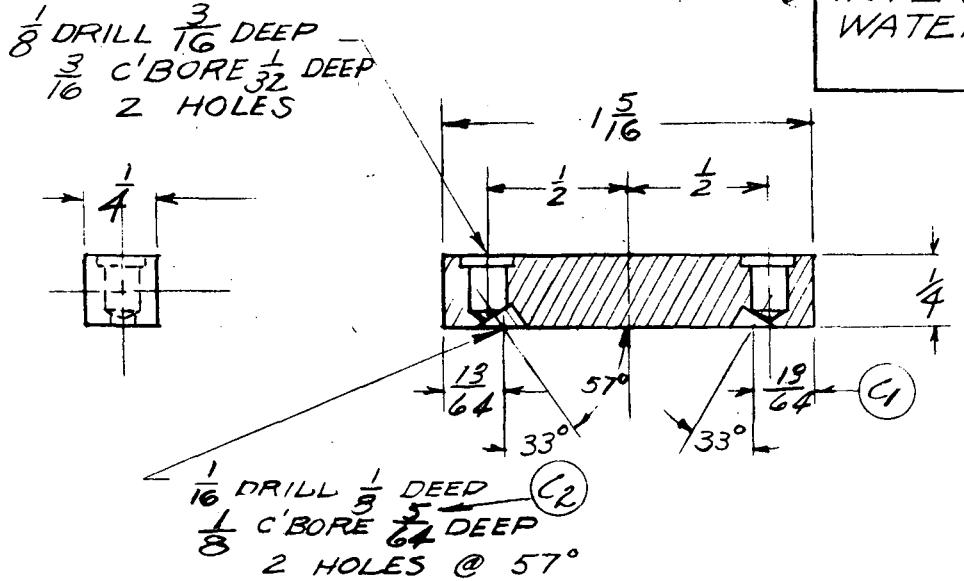

FIG. 101

CHANGE LETTER	DRAWN BY	CHECK BY	DATE	CHANGE
C2	W	M.T.W.	8.1.46	WAS 1/16
C1	V.M.C.	M.T.W.	8.1.46	WAS 7/32
B	"	M.T.W.	2.15.46	TITLE WAS 2.5 ALUM POUND TARGET HOLDER
A	MALIM	M.T.W.	6.16.45	REDESIGNED & REDRAWN

MATERIAL 1/4 X 1/4 COPPER BAR X 1 5/16

SHOWN ON	1-417A-3	1-400-2	3-444-1						
ISSUED TO	DATE ISSUED	DELIVER TO	JOB NO.	DATE REQ'D	MAKE				
				TOLERANCES WHERE NOT OTHERWISE GIVEN					

RADIATION LABORATORY — DRG. NO. 1-425.C-1

UNIVERSITY OF CALIFORNIA—BERKELEY

DRAWN BY	CHECK BY	DATE
MALIH	M.T.WEBB	6.16.45

APPROVED BY	SCALE
M.T.WEBB	DOUBLE SIZE

(B) 60" CYCLOTRON INTERCEPTOR TARGET FRONT TARGET

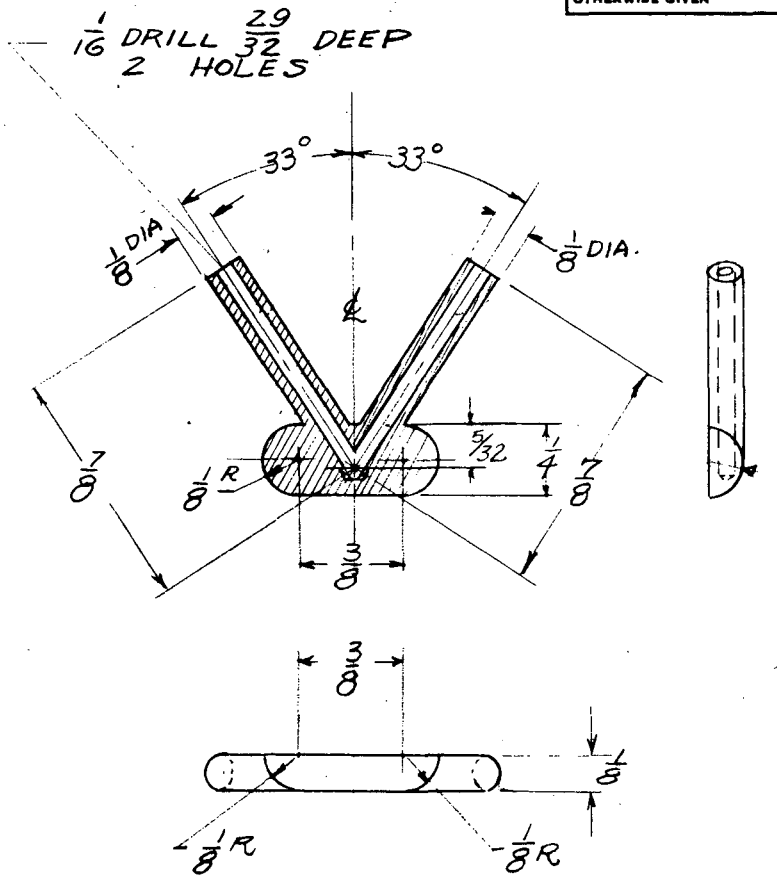

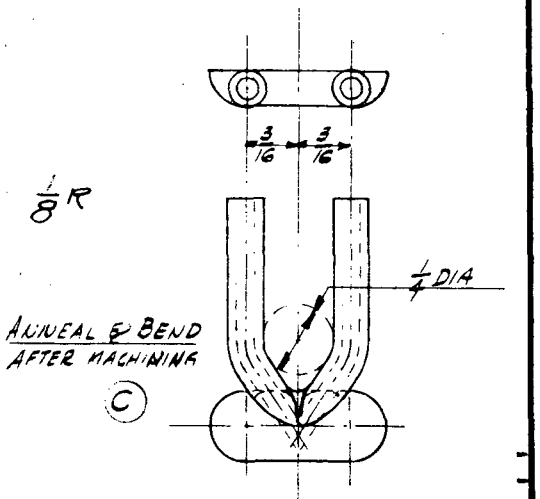

ANNEAL & BEND AFTER MACHINING

(C)

FIG. 102

MATERIAL 1/8 COPPER X 1 3/4 X 2 1/4

CHANGE LETTER	DRAWN BY	CHECK BY	DATE	CHANGE
C	W		7-23-49	BENDING NOTE ADDED
B	D M	M.T.W.	2.15.46	TITLE WAS 25 AL. FND. TARGET HOLDER
A	MALIH	M.T.W.	6.16.45	REDESIGNED & REDRAWN

this reason, the separation listed in Procedure 90-1, Appendix II was finally worked out as satisfactory for this type of milking. In samples made up using this last procedure it was found that considerable Th^{228} was present despite our care in the bombardment energy selection. Further chemical work and pulse analyses however should give us definite results for this alpha half-life. In the meantime we are using a K/α branching ratio of 100 as the approximate value, giving an alpha half-life of about 150 days. In any future bombardments, the energy of the bombarding deuterons should be lowered at least another Mev to reduce the amount of Pa^{228} produced.

E. Pa^{230}

We have also been interested in determining the alpha half-life of this isotope. From systematics it was predicted that this half-life should be a few thousand years. Actinium was separated from a large amount of Pa^{230} and the Ac^{226} from alpha decay of Pa^{230} identified through alpha-pulse analysis by the alpha energy of its beta daughter, 30-minute Th^{226} decaying with the one day half-life of the Ac^{226} parent.

We obtained about 3×10^7 β^- dis/min of pure Pa^{230} (plus probably an equal amount of Pa^{233}) from a 10 microampere hour bombardment of a thick thorium target with 60-Mev deuterons. From the protactinium fraction (after equilibrium had been reached) we were able to obtain about 300 alpha c/m of Th^{226} decaying with the half-life of the Ac^{226} parent.

The actinium was separated by La^{+++} and Ce^{+++} fluoride precipitations and purified from thorium by repeated zirconium phosphate precipitations. At the end of the procedure the Ce^{+++} was oxidized to Ce^{++++} by a bismuthate oxidation and the activity precipitated as a fluoride on the remaining small amount of La^{+++} carrier. The soluble chloride of the carrier gave a thin plate suitable for alpha-pulse analysis. This procedure is described in 89-2, Appendix II.

Rough chemical yields checked with Th^{230} tracer, coupled with the value for the electron capture branching of Pa^{230}, $K/\beta^- = 10$, reported by Studier and Bruehlman,[32] give an alpha half-life for Pa^{230} of 1410 years $\pm$ 20%.

F. Pa^{231}

The value for the alpha (and also of course the total) half-life of this isotope has been determined by VanWinkle, Larson and Katzin, as reported by Seaborg and Perlman,[35] to be 3.43×10^4 years.

IV. Discussion of Results

The alpha half-lives of the protactinium isotopes reported above are summarized in Table 40.

Table 40

Summary of Alpha Half-Lives of Protactinium Isotopes

Isotope	Alpha Half-Life
Pa^{226}	$\geq$ 3.4 min. = 6.5×10^{-6} yr.
Pa^{227}	45.3 min. = 8.9×10^{-5} yr.
Pa^{228}	1190 hr. = 0.133 yr.
Pa^{229}	150 day(?) = 0.410 yr.
Pa^{230}	1415 yr.
Pa^{231}	3.43×10^4 yr.

A good way to systematize alpha half-life data is to plot half-life against mass number. This has been done in Fig. 104. It can be seen that these six isotopes fall on or near two lines (for the odd-even and the odd-odd isotopes) which appear to have a slight curve. If we assume a branching ratio of 100 for Pa^{229}, its alpha half-life falls considerably below the odd-odd line, indicating that perhaps the true branching ratio should be closer to 1000 than 100.

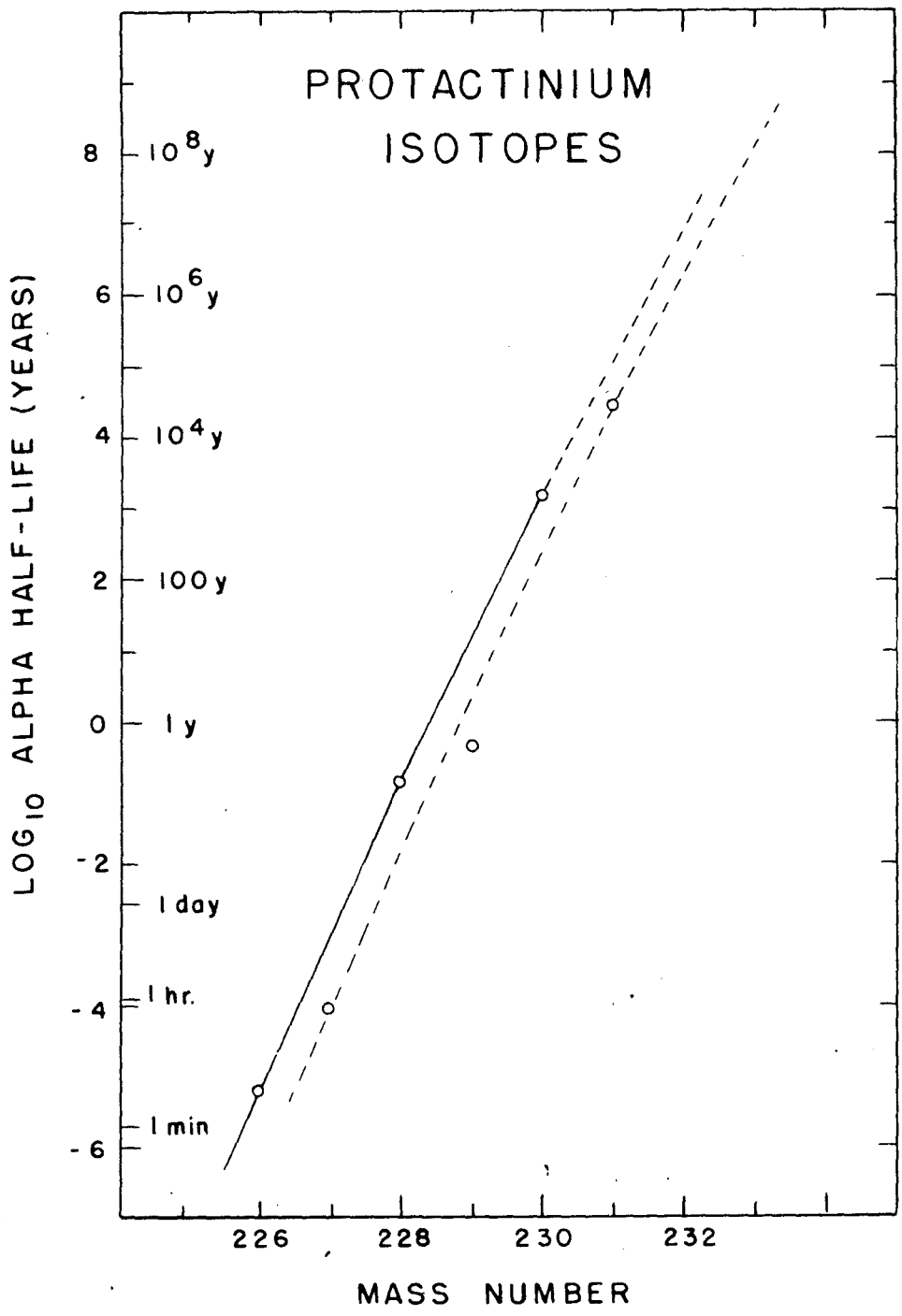

Fig. 104. Half-life vs. mass number relationship for the protactinium isotopes.

By extending these lines to intercept the mass numbers 232 and 233 we find that the alpha half-life for Pa^{232} should be about 10^7 years, while that for Pa^{233} should be about 10^8 years.

Alpha half-lives for these neutron excess isotopes of any elements of the heavy region have not as yet been determined. Hence we have made some calculations as to the feasibility of milking the actinium daughters from the Pa^{232} and Pa^{233}.

The Pa^{233} is the easier to work with since its radiations require less shielding during the processing. Its alpha decay daughter Ac^{229}, however, is so far unknown. Plans for producing and characterizing it have been made and are discussed in Chapter 5. If we assume a half-life of 17 hours for the Ac^{229} and an alpha half-life of 10^8 years for the Pa^{233}, about 1700 dis/min of the Ac^{229} could be milked from one curie of Pa^{233} (100% chemistry). A pile bombardment of thorium metal could probably produce the required Pa^{233} quite easily. The same chemical procedures used for the Pa^{230} milking would be used again in this case, modified of course to rid the final actinium sample of the additional protactinium contaminant present. Although this milking experiment seems feasible, considerable care must be taken in working with the activity since 1.6 inches of lead shielding are required to reduce the radiations from one curie of Pa^{233} to a tolerable level.

An actinium milking of Pa^{232} would be considerably more difficult. The 1.32 day Pa^{232} would have to be made on the 60-inch cyclotron and worked up quite soon after shutdown to take full advantage of the activity formed. The radiations from this isotope are quite intense and would require complete remote control set-ups operating behind a thick lead wall if a curie were to be worked up. Calculations assuming the alpha half-life for Pa^{232} to be 10^7 years indicate that about 1000 dis/min of Ac^{228} could be separated from one curie of Pa^{232}. Preliminary bombardments on the 60-inch cyclotron show that the internal beam (with as high as 200 microamperes current) would have to be used in the bombardment in order to produce

the required amount of Pa^{232}. This problem then would also involve the design of cooling apparatus so that a thorium target could be bombarded in the internal beam without burning up. This experiment is strictly a borderline case and would require considerable extra equipment.

Considering then the two milkings proposed above, it would appear that it would be well worth while to attempt the milking of Pa^{233}, once the Ac^{229} daughter has been produced and characterized. When this established beyond doubt the trend on the neutron excess side of stability of the curves shown in Fig. 104, this trend could then be extrapolated to other elements.

Chapter 4

Emanation Isotopes

The isotope chart at the beginning of this report shows few gaps between the lightest and heaviest known isotopes in the heavy element region. One striking exception however is the series of three isotopes beginning with the mass 221 isotope of emanation. Several years ago an unsuccessful attempt was made at Chicago to milk this Em^{221} from the Ra^{225} then available. It seemed plausible to us however that with the high energy particles available from the 184-inch cyclotron we could now build up a much larger supply of Ra^{225} by spallation than had been available at Chicago and should be able to milk the Em^{221} from it.

Before making a long bombardment to build up yield of Ra^{225}, however, it seemed reasonable to check the yield of emanation isotopes themselves from the spallation of thorium. Several short bombardments indicated that we were obtaining not the heavy mass emanation isotopes but others of lighter mass.

I. New Low Mass Isotopes of Emanation[36]

Among the spallation products obtained from the 350-Mev proton bombardment of Th^{232} we identified two gaseous alpha-emitters which apparently do not decay into any presently known alpha-decay chains. The half-lives observed for the decay of the alpha-activities are 23 minutes (Fig. 105) and 2.1 hours (Fig. 106). These half-lives may be principally determined by an unknown amount of orbital electron capture. At least one alpha-emitting daughter (about 4 hours half-life) was observed to grow from a gaseous parent, but it was not determined whether it arises from alpha-decay or electron-capture.

Since these gaseous atoms emit alpha-particles it is assumed that they are isotopes of element 86 (emanation or radon) rather than a lighter rare gas. If they were heavy isotopes such as Em^{221} or Em^{223}, both unknown, they would decay into known alpha-decay series, the neptunium and actinium series, respectively, and so would grow known short-lived alpha-emitters which would have been detected. It

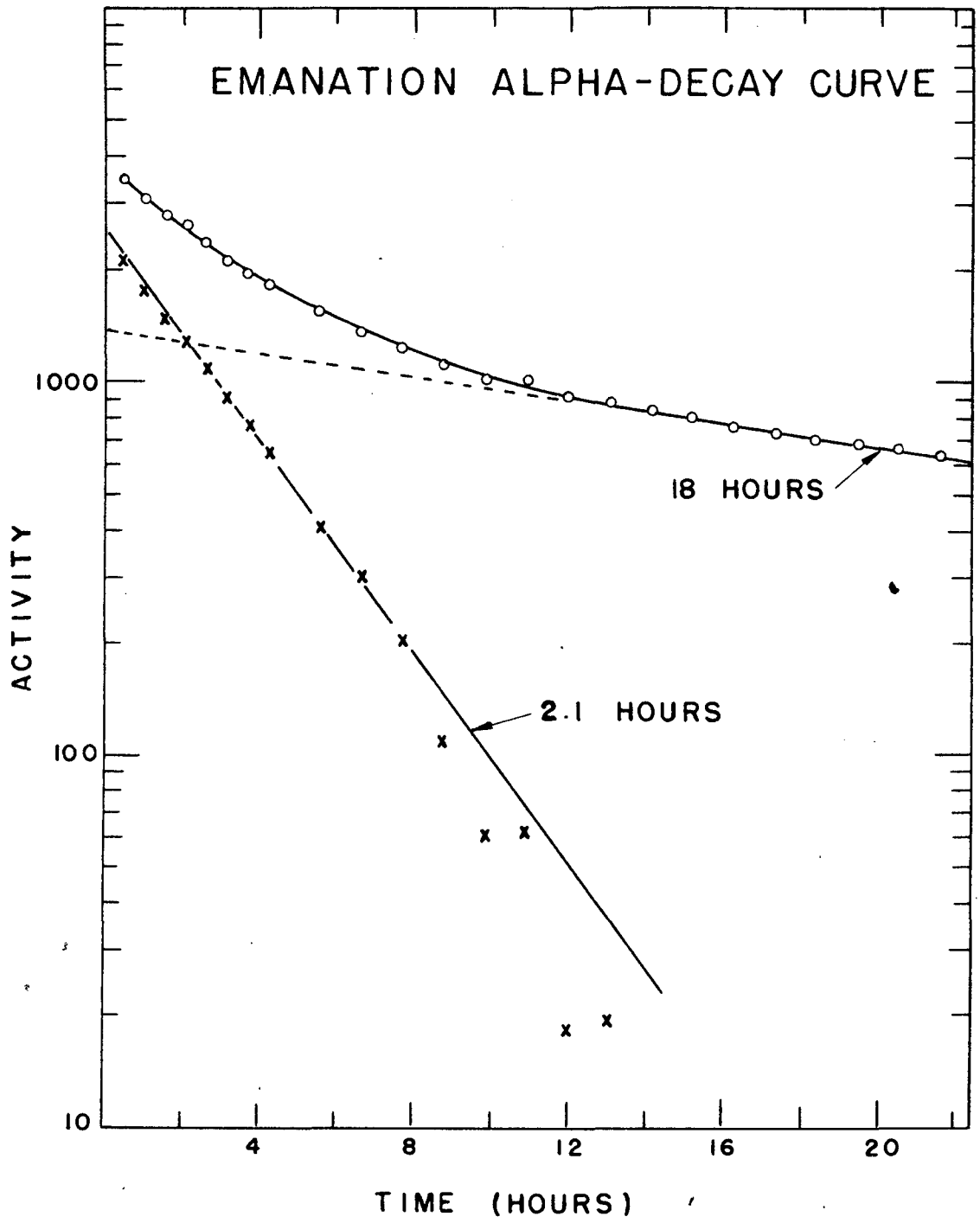

Fig. 106. Determination of the half-life of an alpha-emitting emanation isotope < 212 from a rare gas sample flamed out of thorium metal shortly after 348-Mev proton bombardment.

thus appears reasonable that they must be lighter than the known emanation isotopes.

The lightest isotope of emanation observed prior to these experiments was Em^{216}, which arises from the U^{228} alpha-decay series[6] and which should have a half-life of approximately 20 microseconds as predicted by means of the new alpha-decay systematics[13-15]. The reappearance of longer half-lives, such as 23 minutes and 2.1 hours, with lower mass numbers is apparently due to the stable configuration of 126 neutrons. Thus these activities are to be assigned to the mass numbers 212 and lower (that is, Em^{212} and $Em^{<212}$). It appears therefore that the plot of alpha-energy versus mass number for the isotopes of emanation goes through the same type of maximum and minimum as is observed for bismuth, polonium and astatine.[14,15]

The method used to measure the emanation alpha-activities was very simple but designed to separate the emanation from tremendous amounts of other alpha-emitters, from bismuth to protactinium. The cyclotron target consisted of thin thorium metal strips sandwiched with thin aluminum foils to act as catchers for the transmuted atoms which were able to recoil out of the surface of the thorium. These aluminum foils were then heated at a very low temperature in a vacuum system shown in Fig. 107. They were heated in a small "wash bottle" connected to the system where the "U tube" is in the figure. A slow stream of argon "carried" the emanation through two cold traps (1 and 2) at -50° C and into a final trap (not shown) at -90° C where the emanation should freeze out. From this storage trap it was possible to fill a cylindrical ion chamber in which alpha-pulses could be detected. The pressure guages indicated the gas pressure in different parts of the system. In order to prove that a gas was involved it was shown that the activity could be quantitatively transferred back and forth many times by varying the temperature of the cold trap. After an emanation sample had been allowed to decay for some hours the gas was thoroughly pumped out of the chamber and the alpha-activity left behind (presumably due to the daughters) was followed for decay. It was not possible to measure alpha-energies in these first experiments and Geiger counter measurements

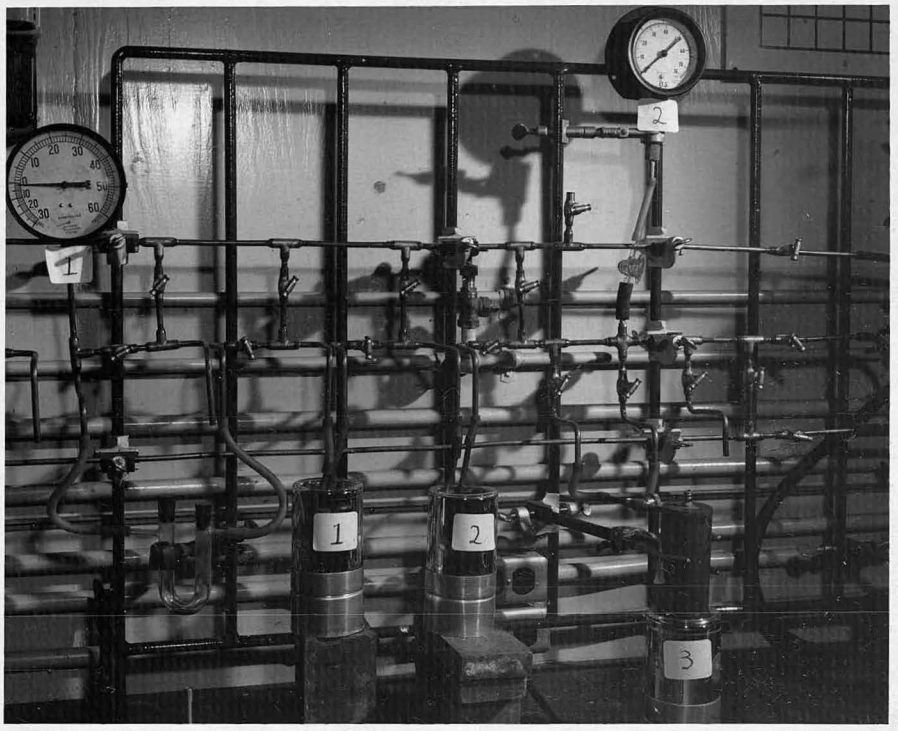

FIG. 107

were clouded by the probability of xenon and krypton fission product contaminants from which no careful separation had been made.

New equipment is now being built with which it should be possible to measure alpha-energies for these emanation isotopes and their daughters and to determine the proper mass assignments.

(Note added in proof: Recently, low mass isotopes of francium have been found[33], one of which decays partially by orbital electron capture to a 23 minute emanation isotope which in turn decays by alpha emission to Po^{208}. This 3 year polonium isotope has been milked chemically from the emanation. Since this 23 minute emanation isotope is most probably the same one as found by spallation of thorium, the mass assignment of the latter to 212 is established.)

II. Em^{221} and Daughters

When it was evident that spallation of thorium gave primarily light mass emanation isotopes, we decided to make a long bombardment for Ra^{225}. About 50 grams of thorium metal (five 10-gram foils of 25-mil metal) was bombarded with full energy protons from the large cyclotron for about 50 hours over a period of 17 days. The target was allowed to stand for about 15 days to allow shorter-lived activities to decay out and was then worked up in parts chemically. Since it was very active it had to be worked up in the lead shielded box shown in Figs. 15-17. Although the large bulk of thorium salt made chemical separations difficult, we finally worked out a good radium separation which was used on the last 10-gram foil from the bombardment. This separation and its difficulties are described in Procedure 88-1, Appendix II.

By the time the radium sample was ready about 45 days had elapsed after shutdown and only a fraction of the activity had been separated into useable form.

The radium sample in solution, containing possibly as much as 10^7 dis/min Ra^{225}, was heated in the U tube and passed through the set-up shown in the Fig. 107. Unfortunately we did not obtain definitive results and concluded that too much of the sample had decayed before our measurements were made.

With the improvements in the chemical procedure, a somewhat shorter bombardment of about 10 hours which is completely worked up within a week after shutdown, can be expected to give positive results. We intend to make such a bombardment in the near future.

Chapter 5

New Neutron Excess Isotopes in the Heavy Region

As can be seen from the isotope chart at the beginning of this paper, information about the neutron excess isotopes of elements from lead to uranium has been obtained primarily from decays of the natural radioactive families.

By closing energy cycles in this region[15] one can calculate decay energies and hence rough half-lives for some of the neutron excess isotopes which might be found in cyclotron bombardments. In so doing it appeared to us that the Pa^{235} and Ac^{229} isotopes in particular would have reasonable half-lives to work with and could also be easily made by (d,αxn) reactions on uranium and thorium metal respectively.

These (d,αxn) reaction products, however, are formed with a rather small cross section and since they are beta-particle emitters must be separated very cleanly from the multitude of products which are formed in large yield by the fission of the target materials.

I. Pa^{235}

Twenty-microampere-hour bombardments of uranium foil in the Berkeley 60-inch cyclotron with 18-Mev deuterons gave a 23.7 minute (Fig. 108) and a 27 day Geiger activity in a highly purified protactinium fraction. A small amount of two intermediate periods of from 15.5 - 18.5 hours and from 2.5 - 2.8 days were present but these most probably can be attributed to a small amount of zirconium and columbium fission products which came through the chemistry. The targets were extreme active after bombardment and were worked up in the lead shielded Berkeley Box shown in Figs. 15-17.

The chemistry, which followed the outline of Procedure 91-1 in Appendix II, took two hours to complete and involved four manganese dioxide cycles, two solvent extractions with di-isopropyl ketone and two extractions with TTA in benzene. The

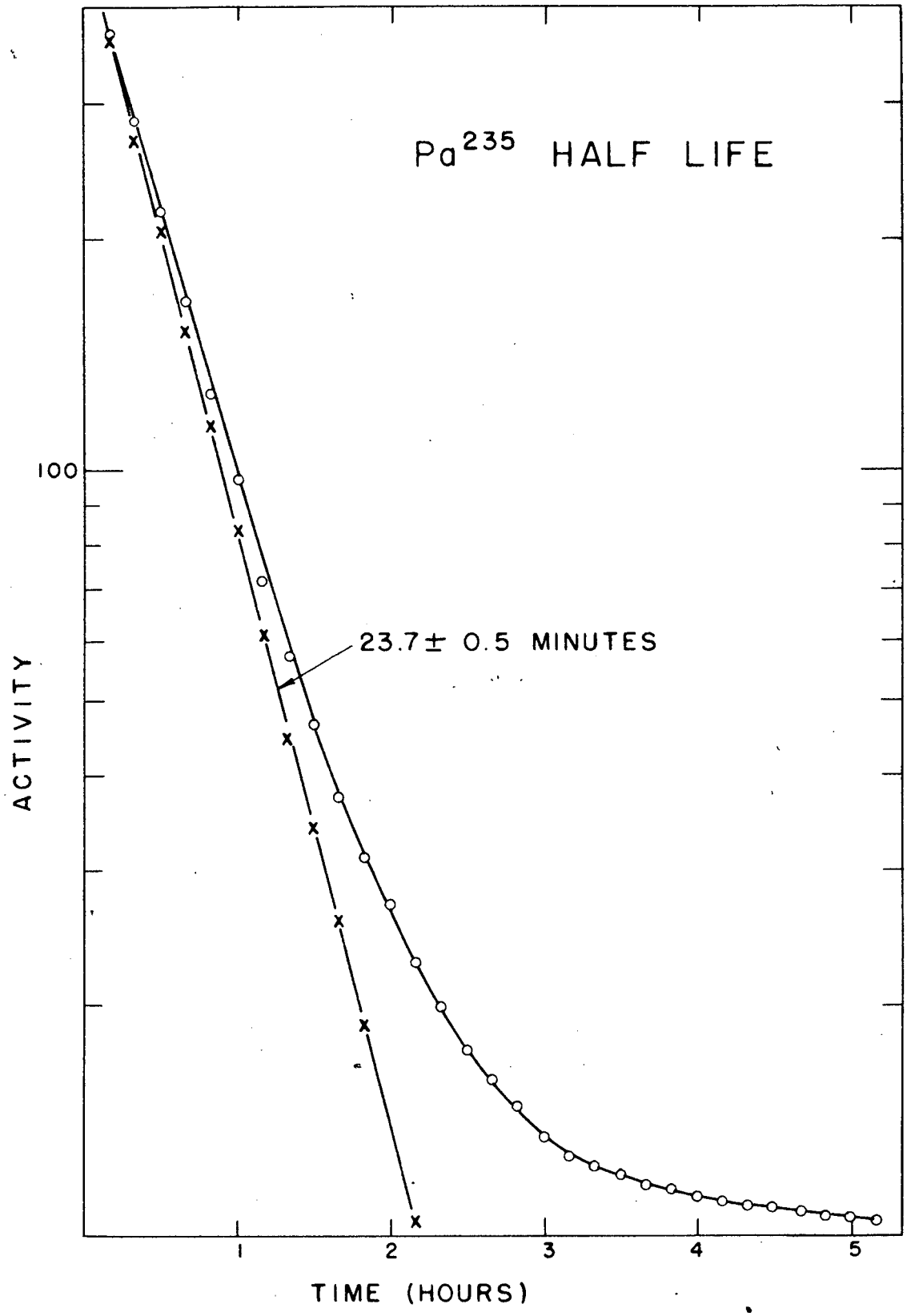

Fig. 108. Determination of the half-life of Pa^{235} by gross Geiger decay.

manganese dioxide cycles consisted of precipitating the MnO_2 from the solution of uranium in nitric acid, centrifuging, dissolving in hydroxylamine, diluting and reprecipitating. The dissolved precipitate from the last cycle was acidified and the protactinium extracted with di-isopropyl ketone, several washings with salted solutions being made to insure good separation from fission products. The protactinium, washed back into a pH 1 solution from the organic solvent, was acidified, extracted into TTA-benzene solution and washed once with acid. The TTA-benzene solution was then evaporated on a platinum plate and flamed, leaving a weightless deposit of protactinium.

The cross section for formation of the 23.7 minute period is about 2×10^{-3} barns, a reasonable value for the (d,α) or (d,αn) reactions on U^{238} which give Pa^{236} or Pa^{235}. The 27-day period is formed with a cross section of about 4×10^{-3} barns (corrected for abundance), reasonable for a (d,α) reaction on the U^{235} present naturally in the uranium foil, giving Pa^{233}.

The 23.7 minute activity was checked in a 9-Mev proton bombardment of U^{238} foil and found to be present in a yield corresponding to a cross section of about 3×10^{-5} barns. This cross section has already been corrected for yield due to deuteron contamination (about 1%) in the proton beam. This correction was determined by counting the U^{239} formed in the bombardment by the (d,p) reaction on U^{238}, assuming the cross section for this reaction to be 0.05 barns, which is probably low. The small but definite yield with protons appears to rule out the possibility that the isotope is Pa^{236} and is consistent with the yield one would expect for a (p,α) reaction at such low proton energies.

An aluminum absorption curve of the 23.7 minute period shows a beta particle whose Feather range is about 610 mg/cm^2, corresponding to an energy of about 1.4 Mev(Fig. 109). All counting was done on the Geiger counting apparatus described in Chapter 2.

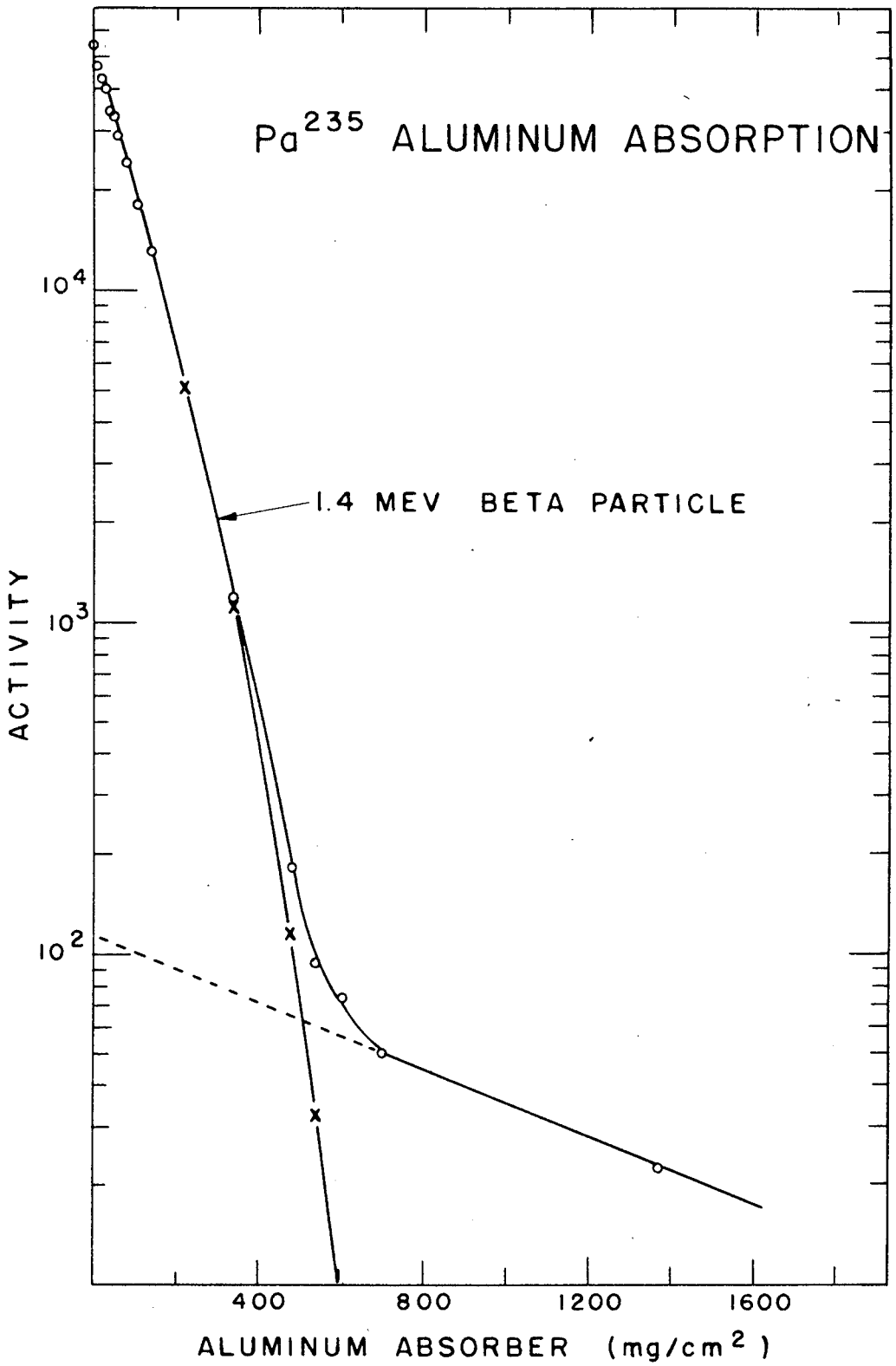

Fig. 109. Determination of the aluminum half-thickness and beta energy of Pa^{235}.

It is interesting to note that by closing energy cycles in the heavy region one calculates a decay energy of 1.24 Mev for Pa^{235} while an energy of 2.09 Mev is calculated for Pa^{236}.

Hence it would seem that the most likely assignment for this new protactinium isotope of 23.7 minutes half-life is to Pa^{235}.

The cross section values mentioned above are quite accurate relatively. In none of the bombardments, however, was the chemical yield determined. To obtain an absolute cross section, a chemical yield value of 20% was arbitrarily taken and is probably not too far from correct. The same chemical procedure was used on all the three bombardments made.

The middle two activities correspond approximately to isotopes of zirconium (Zr^{97} -- 17 hours) and columbium (Cb^{96} -- 2.8 days) which would come through both the manganese dioxide and TTA-benzene steps of the chemistry. Further credence is added to the claim that they are fission products since they can not be detected in the proton bombardment. At that energy of proton bombardment the amount of uranium fission produced is reduced by as much as a factor of 100 from that produced with 19 Mev deuterons.

Several questions are raised by the results of the bombardments however. A large amount of 26-day activity (presumably Pa^{233}) was found in the proton bombardment (a factor of 40 more than in the deuteron bombardment). The most logical explanation is that it was contamination picked up somewhere in the chemical procedure. We have been unable to check this point since the 60-inch cyclotron has not been available for bombardments recently.

In addition we did not observe any 1.4 day Pa^{232} beta particles from the (d,an) reaction on the U^{235} present in the deuteron bombardment. This is hard to understand if the 26-day activity found in the bombardment is really Pa^{233} from a (d,a) reaction on the U^{235} and if the 23.7 minute activity is Pa^{235} from a (d,an) reaction on U^{238}.

II. Ac^{229}

From closed energy cycles it would appear that this isotope would have a half-life of about 17 hours and a beta energy of about 0.83 Mev. We have made one attempt to find this isotope, working up a thorium backing plate which had been inserted in the 60-inch cyclotron in conjunction with a deuteron bombardment of ionium on the interceptor. By the time the ionium was worked up several days had elapsed. In addition, a mix-up in the chemistry caused the loss of much of whatever actinium activity was left. Consequently the run was unsuccessful.

When the 60-inch cyclotron is again available for bombardments however, we intend to make a several hour bombardment of thorium metal and separate the actinium fraction by Procedure 89-2 in Appendix II. Column separation will of course have to be used as the final purification step, with Ac^{225} tracer to tell just when the actinium peak comes off the column.

Acknowledgements

It is a sincere pleasure to thank Professor G. T. Seaborg for his continued advice and encouragement during the course of this work. Discussions with Professor I. Perlman and other members of the Radiation Laboratory staff have been of great value. The interest and ingenuity of Mr. A. Ghiorso, my co-worker on much of this work, is especially appreciated. I would like to express my appreciation to Mr. Herman Robinson for his help in the design and procurement of equipment; to the entire Health Chemistry Group for their assistance in delivering and monitoring active targets, and in designing protective equipment; to Mr. George Edwards for the design of the pneumatic tube-jiffy probe set-up; to Mr. C. M. Gordon for his design of the original jiffy-probe target holders; to Mr. W. A. Aron, Mr. B. G. Hoffman and Mr. F. C. Williams, and to Mr. V. Peterson for permission to include material not published elsewhere; to Professor R. L. Thornton, Mr. J. T. Vale, Mr. R. Watt and the entire 184-inch cyclotron group for their cooperation in making the bombardments; and to Dr. J. G. Hamilton, Mr. T. Putnam, Mr. B. Rossi, and the crew of the 60-inch cyclotron for making the 60-inch bombardments. I would also like to thank Mrs. Marilynn Meinke for her invaluable assistance in the preparation of the graphs and manuscript, Mrs. Lorraine Petch for her careful typing of the manuscript, and Miss Betty Summers and Miss Claire Lynch for their painstaking work in tracing the figures.

This dissertation is based on work performed under the auspices of the Atomic Energy Comission.

Bibliography

1. G. T. Seaborg, Chem. and Eng. News 25, 2819 (1947).

2. D. R. Miller, R. C. Thompson and B. B. Cunningham, Phys. Rev. 74, 347 (1948).

3. R. H. Goeckermann and I. Perlman, Phys. Rev. 76, 628 (1949).

4. I. Perlman, R. H. Goeckermann, D. H. Templeton and J. J. Howland, Phys. Rev. 72, 352 (1947).

5. A. Ghiorso, W. W. Meinke and G. T. Seaborg, Phys. Rev. 74, 695 (1948).

6. W. W. Meinke, A. Ghiorso and G. T. Seaborg, Phys. Rev. 75, 314 (1949).

7. See G. T. Seaborg and I. Perlman, Rev. Mod. Phys. 20, 585 (1948).

8. M. H. Studier and E. K. Hyde, Phys. Rev. 74, 591 (1948).

9. A. C. English, T. E. Cranshaw, P. Demers, J. A. Harvey, E. P. Hincks, J. V. Jelley and A. N. May, Phys. Rev. 72, 253 (1947).

10. F. Hagemann, L. I. Katzin, M. H. Studier, A. Ghiorso and G. T. Seaborg, Phys. Rev. 72, 252 (1947).

11. G. T. Seaborg, Chem. and Eng. News 26, 1902 (1948).

12. See, A. Ghiorso, A. H. Jaffey, H. P. Robinson and B. Weissbourd, "An Alpha-Pulse Analyzer Apparatus", Plutonium Project Record 14B, No. 17.3 (1948) (to be issued).

13. I. Perlman, A. Ghiorso and G. T. Seaborg, Phys. Rev. 74, 1730 (1948).

14. I. Perlman, A. Ghiorso and G. T. Seaborg, Phys. Rev. 75, 1096 (1949).

15. I. Perlman, A. Ghiorso and G. T. Seaborg, Phys. Rev. (Jan. 1, 1950, in press).

16. J. C. Reid and M. Calvin, BC-75 (Revised)(July 1949).

17. A. S. Newton, Phys. Rev. 75, 209 (1949).

18. E. Rutherford, J. Chadwick and C. J. Ellis, "Radiations from Radioactive Substances", p. 557 (1930).

19. B. Karlik and T. Bernert, Naturwiss. 32, 44 (1944).

20. B. Karlik and T. Bernert, Naturwiss. 31, 492 (1943).

21. See for example: E. T. Clarke and J. W. Irvine, Jr., Phys. Rev. 69, 680 (1946); E. L. Kelley and E. Segre, Phys. Rev. 75, 999 (1949); See also Appendix I.

22. See: A. C. Helmholz and J. W. Peterson, Phys. Rev. 73, 541 (1948)abstr.;
R. L. Thornton and R. W. Senseman, Phys. Rev. 72, 872 (1947);
R. W. Chupp and E. M. McMillan, Phys. Rev. 72, 873 (1947);
D. Bockhop, A. C. Helmholz, S. D. Softky, J. W. Rose and T. Breakey, Phys. Rev. 75, 1469 (1949) abstr.

23. E. L. Kelley, UCRL-277 (Jan. 1949).

24. R. Serber, Phys. Rev. 72, 1114 (1947).

25. W. A. Aron, B. G. Hoffman and F. C. Williams, UCRL-121, 1st and 2nd revision.

26. W. W. Meinke, UCRL-432 and Addenda I.

27. See for example: P. R. O'Connor and G. T. Seaborg, Phys. Rev. 74, 1189 (1948).

28. E. L. Kelley, and E. Segre, Phys. Rev. 75, 999 (1949).

29. E. T. Clarke, Phys. Rev. 71, 187 (1947).

30. H. W. Newson, Phys. Rev. 51, 620 (1937).

31. A. C. Helmholz and J. M. Peterson, Phys. Rev. 73, 541 (1948)abstr.

32. M. H. Studier and R. J. Bruehlman, as listed by G. T. Seaborg and I. Perlman, Rev. Mod. Phys. 20, 585 (1948).

33. E. K. Hyde, A. Ghiorso and G. T. Seaborg, (to be published in Phys. Rev.).

34. E. K. Hyde, M. H. Studier, H. H. Hopkins and A. Ghiorso, as listed by G. T. Seaborg and I. Perlman, Rev. Mod. Phys. 20, 585 (1948).

35. Q. Van Winkle, R. G. Larson and L. I. Katzin, as listed by G. T. Seaborg and I. Perlman, Rev. Mod. Phys. 20, 585 (1948).

36. A. Ghiorso, W. W. Meinke and G. T. Seaborg, Phys. Rev. (November 1, 1949 in press).

Appendix I

Bibliography of Excitation Functions for Charged Particle Reactions

APPENDIX I

Bibliography of excitation functions for charged particle reactions

1.9 Mev:

$Na^{23}(d,p)Na^{24}$ — E. O. Lawrence, Phys. Rev. 47, 17 (1935).

$Al^{27}(d,p)Al^{28}$ — E. McMillan and E. O. Lawrence, Phys. Rev. 47, 343 (1935).

2.8 Mev:

$C^{12}(d,n)N^{13}$ — C. L. Bailey, M. Phillips, and J. H. Williams, Phys. Rev. 62, 80 (1942).

3.5 Mev:

$Mg^{26}(d,p)Mg^{27}$; $Mg^{26}(d,\alpha)Na^{24}$ — M. C. Henderson, Phys. Rev. 48, 855 (1935).

$Na^{23}(d,p)Na^{24}$; $Al^{27}(d,p)Al^{28}$; $Si^{30}(d,p)Si^{31}$; $Cu^{63}(d,p)Cu^{64}$ — E. O. Lawrence, E. McMillan, and R. L. Thornton, Phys. Rev. 48, 493 (1935).

$C^{12}(d,n)N^{13}$; $N^{14}(d,n)O^{15}$; $O^{16}(d,n)F^{17}$ — H. W. Newson, Phys. Rev. 48, 790 (1935).

5 Mev:

$Pt^{192}(d,p)Pt^{193}$; $Pt^{196}(d,p)Pt^{197}$ — J. M. Cork and E. O. Lawrence, Phys. Rev. 49, 788 (1936).

$C^{12}(d,n)N^{13}$; $N^{14}(d,n)O^{15}$; $O^{16}(d,n)F^{17}$ — H. W. Newson, Phys. Rev. 51, 620 (1937).

$A^{40}(d,p)A^{41}$ — A. H. Snell, Phys. Rev. 49, 555 (1936).

$Ni^{60}(d,n)Cu^{61}$ — R. L. Thornton, Phys. Rev. 51, 893 (1937).

$Cu^{63}(d,p)Cu^{64}$ — S. N. Van Voorhis, Phys. Rev. 50, 895 (1936).

6 Mev:

$Pd^{108}?(d,p)Pd^{109}?$ (13 hr); $Pd^{110}(d,n)Ag^{111}$ — J. D. Kraus and J. M. Cork, Phys. Rev. 52, 763 (1937).

9 Mev:

$Fe^{54}(d,n)Co^{55}$ — J. M. Cork and B. R. Curtis, Phys. Rev. 55, 1264 (1939).

$Pb^{206}(d,n)Bi^{207}$; $Pb^{208}(d,p)Pb^{209}$ — K. Fajans and A. F. Voigt, Phys. Rev. 60, 619 (1941).

$U^{238}(d,p)U^{239}$ — N. Feather and R. S. Krishnan, Proc. Camb. Phil. Soc. 43, 267 (1947).

9 Mev (cont'd):

$Th^{232}(d,fiss)$; $U^{238}(d,fiss)$ — D. H. T. Gant and R. S. Krishnan, Proc. Roy. Soc. London A178, 474 (1941).

$Bi^{209}(d,n)Po^{210}$; $Bi^{209}(d,p)Bi^{210}$ — D. G. Hurst, R. Latham, and W. B. Lewis, Proc. Roy. Soc. London A174, 126 (1940).

$Th^{232}(d,fiss)$; $U^{238}(d,fiss)$ — I. C. Jacobsen and N. O. Lassen, Phys. Rev. 58, 867 (1940).

$Ag^{107}(d,p2n)Ag^{106}$ — R. S. Krishnan and T. E. Banks, Nature 145, 777 (1940).

$F^{19}(d,H^3)F^{18}$ — R. S. Krishnan, Nature 148, 407 (1941).

$Ag^{107}(d,p)Ag^{108}$; $Ag^{107}(d,H^3)Ag^{106}$; $Ag(d,2n)Cd^{107,109}$ (6.7 h); $Ag(d,2n)Cd^{107,109}$(1 yr)— R. S. Krishnan, Proc. Camb. Phil. Soc. 36, 500 (1940).

$Au^{197}(d,p)Au^{198}$; $Au^{197}(d,2n)Hg^{197}$ — R. S. Krishnan, Proc. Camb. Phil. Soc. 37, 186 (1941).

$Cu^{63}(d,p)Cu^{64}$; $Cu^{63}(d,H^3)Cu^{62}$; $Sb^{121}(d,p)Sb^{122}$; $Sb^{121}(d,H^3)Sb^{120}$ — R. S. Krishnan and T. E. Banks, Proc. Camb. Phil. Soc. 37, 317 (1941).

$Pt^{196}(d,p)Pt^{197}$; $Pt^{198}(d,p)Pt^{199}$ — R. S. Krishnan and E. A. Nahum, Proc. Camb. Phil. Soc. 37, 422 (1941).

$Au^{197}(d,p)Au^{198}$; $Au^{197}(d,2n)Hg^{197}$; $Tl^{205}(d,p)Tl^{206}$; $Tl^{205}(d,2n)Pb^{205}$; $Pb^{208}(d,p)Pb^{209}$; $Bi^{209}(d,p)Bi^{210}$; $Bi^{209}(d,n)Po^{210}$; $Th^{232}(d,p)Th^{233}$ — R. S. Krishnan and E. A. Nahum, Proc. Roy. Soc. London A180, 333 (1942).

$Bi^{209}(d,p)Bi^{210}$; $Bi^{209}(d,n)Po^{210}$ — H. E. Tatel and J. M. Cork, Phys. Rev. 71, 159 (1947).

10 Mev:

$Bi^{209}(d,p)Bi^{210}$; $Bi^{209}(d,n)Po^{210}$ — J. M. Cork, J. Halpern, and H. Tatel, Phys. Rev. 57, 371 (1940).

$Fe^{54}(d,n)Co^{55}$; $Fe^{54}(d,\alpha)Mn^{52}$ — J. M. Cork and J. Halpern, Phys. Rev. 57, 667 (1940).

11 Mev:

$Be^{9}(d,p)Be^{10}$ — E. M. McMillan, Phys. Rev. 72, 591 (1947).

14 Mev:

$Na^{23}(d,p)Na^{24}$; $Br^{81}(d,p)Br^{82}$; $Br(d,2n)Kr$ (34 hr) — E. T. Clarke and J. W. Irvine, Jr., Phys. Rev. 66, 231 (1944).

14 Mev (cont'd):

$Mg^{24}(d,\alpha)Na^{22}$; $Mg^{26}(d,\alpha)Na^{24}$; $Cu^{63}(d,p)Cu^{64}$; $Cu^{65}(d,\alpha)Ni^{63}$; $Cu^{63}(d,2n)Zn^{63}$; $Cu^{65}(d,2n)Zn^{65}$ --- E. T. Clarke and J. W. Irvine, Jr., Phys. Rev. 69, 680 (1946).

$Al^{27}(d,p\alpha)Na^{24}$ --- E. T. Clarke, Phys. Rev. 71, 187 (1947).

15 Mev:

$Bi^{209}(d,p)Bi^{210}$; $Bi^{209}(d,n)Po^{210}$ --- J. M. Cork, Phys. Rev. 70, 563 (1946).

$Cu^{63}(d,p)Cu^{64}$; $Cu^{63}(d,2n)Zn^{63}$ --- R. S. Livingston and B. T. Wright, Phys. Rev. 58, 656 (1940).

20 Mev:

$Th^{232}(d,fiss)$; $U^{238}(d,fiss)$ --- J. Jungerman and S. C. Wright, MDDC 1679

190 Mev:

$Al^{27}(d,\alpha p)Na^{24}$; $Al^{27}(d,\alpha p2n)Na^{22}$ --- A. C. Helmholz and J. M. Peterson, Phys. Rev. 73, 541 (1948). (Abstract).

195 Mev:

$C^{12}(d,dn)C^{11}$ --- R. L. Thornton and R. W. Senseman, Phys. Rev. 72, 872 (1947).

5.3 Mev:

$F^{19}(\alpha,p)Ne^{22}$, $F^{19}(\alpha,n)Na^{22}$ --- N. K. Saha, Z. Physik 110, 473 (1938).

$Al^{27}(\alpha,n)P^{30}$ --- A. Szalay, Nature 141, 972 (1938).

$Al^{27}(\alpha,n)P^{30}$ --- A. Szalay, Z. Physik 112, 29 (1939).

7 Mev:

$Na^{23}(\alpha,n)Al^{26}$; $P^{31}(\alpha,n)Cl^{34}$ --- H. Brandt, Z. Physik 108, 726 (1938).

9 Mev:

$Li^{7}(\alpha,n)B^{10}$ --- O. Haxel and E. Stuhlinger, Z. Physik 114, 178 (1939).

$B(\alpha,n)N$; $Be^{9}(\alpha,n)C^{12}$ --- E. Stuhlinger, Z. Physik 114, 185 (1939).

11 Mev:

$Cu^{63}(\alpha,n)Ga^{66}$; $Cu^{65}(\alpha,n)Ga^{68}$ — W. B. Mann, Phys. Rev. 52, 405 (1937).

20 Mev:

$Rh^{103}(\alpha,n)Ag^{106}$(25m); $Rh^{103}(\alpha,n)Ag^{106}$(8.2 d); $Rh^{103}(\alpha,2n)Ag^{105}$ — H. L. Bradt and D. J. Tendam, Phys. Rev. 72, 1117 (1947).

$Ag^{109}(\alpha,n)In^{112}$; $Ag^{109}(\alpha,2n)In^{111}$ — D. J. Tendam and H. L. Bradt, Phys. Rev. 72, 1118 (1947).

32 Mev:

$Bi^{209}(\alpha,2n)At^{211}$ — D. R. Corson, K. R. MacKenzie and E. Segre, Phys. Rev. 58, 672 (1940).

37 Mev:

$Ag^{107}(\alpha,n)In^{110}$; $Ag^{107}(\alpha,2n)In^{109}$; $Ag^{109}(\alpha,2n)In^{111}$ + $Ag^{109}(\alpha,3n)In^{110}$ — S. N. Ghoshal, Phys. Rev. 73, 417 (1948).

40 Mev:

$Th^{232}(\alpha,$fiss$)$; $U^{238}(\alpha,$ fiss$)$ — J. Jungerman and S. C. Wright, MDDC-1679.

380 Mev:

$Al^{27}(\alpha,\alpha 2pn)Na^{24}$; $Al^{27}(\alpha,2\alpha n)Na^{22}$ — A. C. Helmholz and J. M. Peterson, Phys. Rev. 73, 541 (1948).

390 Mev:

$C^{12}(\alpha,\alpha n)C^{11}$ — R. L. Thornton and R. W. Senseman, Phys. Rev. 72, 872 (1947).

. . . . . .

4 Mev:

$O^{18}(p,n)F^{18}$ — L. A. DuBridge, S. W. Barnes, J. H. Buck and C. V. Strain, Phys. Rev. 53, 447 (1938).

5.7 Mev:

$N^{14}(p,\alpha)C^{11}$ — W. H. Barkas, Phys. Rev. 56, 287 (1939).

6.6 Mev:

$Cr^{52}(p,n)Mn^{52}$ --- A. Hemmendinger, Phys. Rev. 58, 929 (1940).

7 Mev:

$Pd^{106}(p,n)Ag^{106}$; Pd(p,n)Ag (8d + 45d) --- T. Enns, Phys. Rev. 56, 872 (1939).

$Ni^{61}(p,n)Cu^{61}$; $Ni^{64}(p,n)Cu^{64}$; $Cu^{63}(p,n)Zn^{63}$; $Zn^{68}(p,n)Ga^{68}$; $Pd^{106}(p,n)Ag^{106}$; Ag(p,n)Cd (6.5h); $Cd^{114}(p,n)In^{114}$ --- V. F. Weisskopf and D. H. Ewing, Phys. Rev. 57, 472 (1940).

16 Mev:

$Cu^{65}(p,pn)Cu^{64}$ --- J. R. Richardson and B. T. Wright, Phys. Rev. 70, 445 (1946).

140 Mev:

Boric acid(p,)C^{11}; $C^{12}(p,pn)C^{11}$ --- W. W. Chupp and E. M. McMillan, Phys. Rev. 72, 873 (1947).

Appendix II

Chemical Procedures Used in the Bombardment Work[26]

83-3

CHEMICAL SEPARATIONS

Element separated: Bismuth

Procedure by: Meinke

Parent material: Tracer Pa^{228} and daughters

Time for sep'n: 1-1/2 hours

Milking experiment

Equipment required: Centrifuge, stirrers, tank H_2S

Yield: 60%

Degree of purification: Factor of at least 10^3 from Pa and at least 100 from other activities. Factor of at least 5 from Pb.

Disadvantages: Gives a thick plate - rather bad for alpha pulse analysis.

Procedure: Purified tracer Pa in benzene - TTA solution (procedure 91-1 with DIPK and TTA extractions only).

(1) Stir organic layer 10 min with equal volume 6N HCl (daughter into acid layer - most of Pa remains with organic layer).

(2) Wash the acid layer three times with double volume .4 M TTA in benzene, stirring 5 min each. (Removes Pa).

(3) Dilute acid layer to ~ 2 N and add ~ 1/2 mg Bi carrier. Bubble in H_2S gas to ppt Bi and Pb sulfides. Centrifuge.

(4) Again add 1/2 mg Bi carrier and repeat sulfide pptn. Centrifuge and combine ppts of (3) and (4).

(5) Dissolve sulfide ppts in few drops hot conc. HCl. Dilute to at least 1 N acid and reppt sulfides by bubbling in H_2S. Centrifuge.

(6) Repeat step (5), four times.

(7) Dissolve sulfide ppt in few drops conc HCl, dilute to ~ 6 cc and boil to rid solution of H_2S.

(8) Add 1 mg Pb carrier and ppt $PbSO_4$ by adding some SO_4^{-2} (H_2SO_4, $(NH_4)_2SO_4$, etc.) Discard precipitate.

(9) Repeat step (8) three times.

(10) Add H_2S to supn from last pptn and centrifuge out the Bi_2S_3 formed.

(11) Dissolve the Bi_2S_3 in hot conc. HCl, dilute to known volume and plate aliquot for counting. Caution: Do not flame the $BiCl_3$ plate or much of the activity may be lost.

83-3 (cont'd)

Remarks:

In step (3) if the acidity is greater than 2N the Bi will not ppt.

See Prescott and Johnson's Qualitative Chemical Analysis (1933) p. 157 for notes on $PbSO_4$.

In some experiments no Bi - Pb sepn is required and the solution of step (7) can be plated directly.

CHEMICAL SEPARATIONS

Element separated: Emanation

Procedure by: Ghiorso, Meinke

Target material: Thorium metal (1 mil)

Time for sep'n: 5-15 min.

Type of bbdt: 184 inch protons

Equipment required: special emanation closed system with traps

Yield: Small from metal; up to 50% from solutions

Degree of purification: Free from other α activity - does not separate from other rare gases.

Procedure:

(1) Metallic strips of Th which have been bombarded with the full energy proton beam are placed in a small closed flask and heated to red heat with an induction heater for a period of one or two minutes.

(2) Argon carrier is then passed through the flask and through a trap cooled with an ice bath.

(3) The carrier and Em are then frozen out in another trap cooled with a liquid N_2 bath.

(4) The activity can be then introduced into a sealed counting chamber and counted for alpha activity.

(5) The activity can be shown to be a rare gas by transferring it back and forth from counter to trap using the liquid N_2 bath to freeze out the activity and carrier.

Remarks:

The procedure described is simple but effective in purifying the Em. If further purification is required additional traps may be used.

The same type of apparatus may be used when: (a) separating Em from a solution or (b) milking Em isotopes from other elements, e.g., Fr and At.

Care should be taken to check separation from At in these separations since in many cases, at least a small fraction of the At present acts much like a gas and may pass through the traps. A special trap to specifically remove At may be necessary in some cases.

88-1

CHEMICAL SEPARATIONS

Element separated: Radium

Procedure by: Meinke

Target materials: Thorium (~10 gm metal)

Time for sep'n: ~ 8 hrs.

Type of bbdt: 184" full energy particles

Equipment required: Standard plus centrifuges of:
250 ml capacity
50 ml capacity
15 ml capacity
Tank HCl

Yield: 25-50%

Degree of purification: At least 10^7 from thorium, and at least 10^4 from other alpha activities present in high yield.

Advantages: Can be used to separate Ra with Ba carrier from large amounts of target material and (if coupled with column separation) to give weightless fraction of Ra.

Procedure:

(1) Dissolve the thorium metal target in concentrated HNO_3 with drops of .2 M $(NH_4)_2SiF_6$ soln added to make the sol'n ~.01 M SiF_6^{-2}. (A large beaker should be used to prevent bubbling over in the vigorous reaction. The solution needs to be heated to start the reaction but once started the reaction proceeds vigorously.) Continue adding conc. HNO_3 and $(NH_4)_2SiF_6$ solution until target completely dissolves (may be an hour or two for 25 mil pieces of Th.)

(2) Evaporate off most of HNO_3 leaving $Th(NO_3)_4$ crystals. Caution: Do not evaporate to dryness or the nitrate will turn to ThO_2 which is harder than the original Th metal to dissolve. If some ThO_2 is accidentally formed use the same combination of conc. HNO_3, $(NH_4)_2SiF_6$ and heat to dissolve it. ThO_2 is considerably easier to dissolve immediately after forming than after prolonged heating and standing. (See 90-4).

(3) Add 6 mg Ba^{++} carrier to the crystals and dilute with water to ~30 cc. Transfer to 250 ml centrifuge bottle.

(4) Add ~ 16 cc conc. NH_4OH (precipitating $Th(OH)_4$) dilute to 200 cc with water and digest for several minutes.

(5) Centrifuge and pour off supn (containing Ba and Ra plus other activities).

(6) Dissolve ppt (amounting to ~125 cc volume) in ~16 cc conc. HNO_3.

(7) Add 3 mg Ba^{++} carrier, dilute to ~ 30 cc.

(8) Add ~ 20 cc conc. NH_4OH ppting the $Th(OH)_4$ dilute to ~ 200 cc with water and digest for several minutes.

(9) Centrifuge and pour off supn.

(10) Repeat steps 6 through 9.

(11) Combine the three supernatants from steps 5, 9 and 10. Evaporate combined solutions until ~ 200 cc. volume and transfer to 250 ml cent. bottle.

(12) Add 5 mg La^{+++} carrier and precipitate the $La(OH)_3$ plus $Th(OH)_4$ from any Th^{+4} remaining by the addition of conc. NH_4OH. Discard ppt.

(13) Evaporate the supn to ~ 40 cc and repeat step 12.

(14) Add Na_2CO_3 solution to the supn to ppt $BaCO_3$ (carries Ra) digest for several minutes. Centrifuge.

(15) Dissolve $BaCO_3$ ppt in minimum of conc. HCl (one or two cc's probably enough).

(16) Place in ice bath. Add double or triple volume of ether and bubble in HCl gas until water and organic layers become miscible and the Ba ppts out as the $BaCl_2$. Centrifuge.

(17) Dissolve the ppt in minimum of H_2O.

(18) Repeat steps 16 and 17 twice (total of 3 $BaCl_2$ pptns). Caution: HCl-ether mixtures spatter readily when warmed.

(19) The $BaCl_2$ can be used for α counting or further purification can be made using a resin column.

Remarks:

Usually about 50 gms of Th metal can be bombarded at once in the cyclotron to produce the Ra^{225}. Hence the large centrifuge is necessary for the separation of the original $Th(OH)_4$ pptns and purifications.

The $Th(OH)_4$ ppt is very bulky, occupying more than half of the tube in step 4. However, with the Ba^{++} carrier added and the two reprecipitations of the thorium it is believed much of the Ra is recovered in the supernates.

The amounts of NH_4OH and HNO_3 used should be calculated rather closely so as to allow little excess, otherwise when the supn's are evaporated to ~40 cc (step 13) the solution will be saturated with NH_4NO_3 and interfere with the $BaCO_3$ pptns.

88-1 (cont'd)

In step 13 some of the yield is lost through the solubility of some of the $BaCO_3$. This might be recovered by destroying the NH_4NO_3 and reducing the volume drastically before the carbonate precipitation.

Originally Ba and Ca were added as holdback carriers in the $Th(OH)_4$ ppts. The Ca, however, did not separate as well from the Ba as expected in the later parts of the procedure.

When working up 50 gms of Th, 10 gms at a time, residues might be combined and further recovery of Ba lost in the original procedure might be made. Also the $BaCO_3$ ppt of step 14 (first 10 gms) can be dissolved in conc. HNO_3 and used as carrier for the various steps of succeeding 10 gm portions - thus reducing the total amount of Ba in the final sample.

10 grams is about the maximum amount of thorium practical to work up at one time by this procedure using 250 ml centrifuge bottles.

If carrier free Ra is needed, $BaCO_3$ can be pptd from the water soln of the end of step 18. This $BaCO_3$ can be dissolved in acid pH 1-2 and absorbed on Dowex 50 resin. The Sr, Ba and Ra can then be eluted in that order by citrate at pH 7.5 - 8.0 (See E. R. Tompkins, AECD 1998). This column procedure, however, has not been included in the runs made to date.

89-2

CHEMICAL SEPARATIONS

Element separated: Actinium

Parent material: Tracer Pa^{230}

Milking experiment

Procedure by: Meinke

Time for sep'n: 3-4 hrs.

Equipment required: Standard, centrifuge

Yield: ~ 40%

Degree of Purification: Factor of at least 10^7 from Pa, U and Th.

Advantages: Can separate very small amounts of Ac from large amounts of Pa, U and Th activity. In one experiment separated 500 d/m Ac^{226} from 10^9 total d/m of Pa^{230} and about equivalent amounts of U and 30 minute Th^{226}.

Procedure:

Pa^{230} in 6 N HNO_3 after DIPK extractions (procedure 91-1)

(1) Take 10 cc of Pa soln and add 1/4 mg La^{+++} and 5 mg Ce^{+++} carriers.

(2) Add 10 drops of conc HF to ppt the fluorides. Centrifuge.

(3) Metathesize ppt to La and Ce hydroxides by adding several ml of conc KOH soln. Centrifuge out the hydroxides and wash once with 5 ml alkaline water.

(4) Dissolve ppt in few drops 6 N HCl and dilute to 5 cc.

(5) Add 1/4 mg Zr^{+4} carrier and H_3PO_4 to make 3 N PO_4^{-3}. Discard ppt.

Steps 2 through 5 are repeated alternately or consecutively until the desired degree of purification is obtained. For the purifications noted above, 10 fluoride pptns and 9 phosphate pptns were made. After the 10th fluoride ppt had been metathesized to the hydroxide, the following procedure was used:

(6) Dissolve hydroxide ppt in 10 M HNO_3, make .01 M Fe^{+++} and oxidize Ce^{+++} to Ce^{++++} with solid sodium bismuthate (warm to speed up reaction.) (Ce^{+4} will now carry on the $Zr_3(PO_4)_4$ ppt.)

(7) Repeat step (5).

(8) Repeat (2) and (3).

(9) Dissolve ppt in few drops 6 N HCl, dilute to known volume and plate aliquot for counting.

89-2 (cont'd)

Remarks:

The fluoride cycles decontaminate primarily from Pa, the phosphate from Th. If further purification is required include more cycles in procedure.

Only one milking can be made from a given batch of Pa by this procedure since it is difficult to again get the Pa into an extractable form once fluoride ion has been added.

It has been found that the $LaCl_3$ solution makes a more adherent and thinner plate than the LaF_3 ppt. The amount of La^{+++} carrier used in step (1) should be determined by the amount of bulk that can be tolerated on the final plate.

CHEMICAL SEPARATIONS

Element separated: Thorium

Procedure by: Meinke

Target material: Tracer Pa separated from 60" bbdt of ionium.

Time for sep'n: Several hours.

Type of bbdt: (Milking expt.)

Equipment required: Stirrers and TTA

Yield: As high as 50% possible.

Degree of purification: Decontaminate from 10^7 c/m Pa, 10^6 c/m U and 10^5 c/m Ac.

Advantages: Gives carrier-free Th, a thin plate for pulse analysis and good purification although not speed.

Procedure:

(1) Nitric acid used throughout. Make sample 6 N acid and TTA extract (with .4M TTA in benzene) 5 times with double volume of TTA--- stirring 5 minutes for each extraction. (Removes Pa into TTA ~ 70% or more per pass).

(2) Evaporate to dryness (wash twice with water and take these washings also to dryness) and take up in acid pH 1.0. TTA extract with equal volume (.25M TTA in benzene) stirring 15 minutes. (Th into TTA but not U or Ac.)

(3) Repeat TTA extn of (2) with fresh TTA and combine the extns,

(4) Wash TTA with equal volume of pH 1.0 soln for 15 min. (U contamination into acid.)

(5) Wash TTA with 6 N acid (equal volume) and stir 15 min. (Th into acid).

(6) Repeat parts (2), (3), and (4). (Repeat wash as in (4) if necessary for further U purification.)

(7) Plate out the .25 M TTA on Pt plates and flame.

Remarks: See curves of Hagemann for % extn into TTA vs pH for Th and Ac. At pH of 1 Th should go into the TTA almost completely but U should only go in less than 10% -- perhaps as little as 2%. Ac will not go into TTA until about pH 3 or so and of course Pa goes in up to about 6 or 8N acid.

pH conditions for separating Th from U by TTA extns are quite critical:

Equivalent and molecular weight of TTA is 222 gms.

90-3

CHEMICAL SEPARATIONS

Element separated: Thorium

Procedure by: Meinke

Parent material: Tracer Pa and daughters (both α & K)
Milking experiment

Time for sep'n: ~ 3/4 hr.

Equipment required: standard

Yield: Only ~ 40-50% Th per cycle

Degree of purification: 2-3% Ac carried per cycle - other elements decontaminated by factor of at least 100.

Advantages: Good procedure if Th present in ~ same amount as other activities.

Procedure:

Pa daughters in 6 N HCl after milking from Pa in TTA (9i-1).

(1) To ~ 10 cc daughter soln add 1/2-1 mg Zr^{+4} carrier and enough H_3PO_4 to make ~ 4M in $PO_4^{=}$. Centrifuge ppt (carries Th^{+4}).

(2) Add to the ppt 3 mg La^{+++} carrier and dilute with 1 N HCl. Add HF, digest and centrifuge.

(3) Metathesize the fluoride ppt to hydroxide by adding conc KOH. Centrifuge. Wash once with alkaline water.

(4) Dissolve in HCl and repeat steps 1-3 reducing amount of La carrier.

(5) Plate as the $LaCl_3$ soln, flame and count.

Remarks:

$Zr_3(PO_4)_4$ ppt quite specific for carrying Th^{+4} from other elements in the heavy region. Yield lost in the LaF_3 - $La(OH)_3$ pptns.

Do not use this procedure if more purification needed than given by 2 cycles since the Th yield will be very low.

$LaCl_3$ soln when evaporated sticks to Pt plates much better than the ppts encountered in this procedure.

90-4

Solution of Thorium Metal and Thorium Dioxide

Thorium metal can be dissolved rapidly in conc HCl but a considerable amount of black insoluble residue is formed in the process. If a few drops of $(NH_4)_2SiF_6$ solution (enough to make ~0.0 M) are added to the HCl before solution is started the black residue is dissolved, leaving only a small residue of thorium oxide (< 1%) in the clear solution.

Thorium metal can be dissolved in conc. HNO_3 with the addition of $(NH_4)_2SiF_6$ (or HF) to .01 M. The metal becomes passive to solution from time to time requiring further additions of acid and $SiF_6^=$.

If the excess HNO_3 is evaporated off care should be taken not to allow the solution to go completely to dryness or difficultly soluble ThO_2 will be formed.

If it is desired to dissolve ThO_2, the HNO_3 - $(NH_4)_2SiF_6$ solution should be used and the mixture heated with stirring for several hours. ThO_2 when first formed is much more soluble than after prolonged heating.

Note: A bombardment of 50 mg 13% ionium (Th^{230}) in thorium (Th^{232}) mixture in the dioxide form should be mentioned here. The hydroxide was pptd and heated in a Pt crucible until only the dioxide remained. This dioxide was then packed into a Pt "boat" 1" x 1/2" x .085" and wet with a few drops of sodium silicate soln. The mixture was then dried under a heat lamp, more silicate added and again dried. The boat was then flamed over a Fisher burner.

It was found that a target prepared this way could withstand considerable mechanical shock and also the high target temperature produced by the 60" cyclotron deuteron beam without breaking the silica crust.

It was also found that the target material could be rather easily scraped out of the boat and mostly dissolved in 5 or 6 hours -- after several additions of HNO_3 - $SiF_6^=$ soln.

Newton, Hyde, Meinke

91-1

CHEMICAL SEPARATIONS

Element separated: Protactinium

Procedure by: Meinke

Target material: ~ 10 gms Th metal

Time for sep'n: 1-1/2 - 2 hrs.

Time of bbdt: 60" D+ bbdt and 184" bbdt all particles

Equipment required: Centrifuge, Kjeldahl flasks, dry ice and stirrers.

Yield: Roughly 10% through entire chemistry.

Degree of purification: Separate from all elements by a factor of at least 10^3. For further purification from Cb and Zr do more DIPK washes.

Advantages: Gives carrier-free Pa on weightless plates for pulse analysis and counting. Purification can be made more extensive by repeating individual steps.

Procedures:

(1) Nitric acid used except where indicated otherwise. Dissolve Th metal in conc. HNO_3 ~ .01 M in $(NH_4)_2SiF_6$ soln (25 cc acid and 3 or 4 drops of 1/5 M $SiF_6^=$ soln usually sufficient to dissolve 10 gms Th.).

(2) Dilute to ~ 4 N acid and Th^{+4} con. less than 0.65 M (Greater con. of Th salt interferes with pptn.)

(3) Add to 40 cc $Th(NO_3)_4$ soln in 4 N HNO_3 an excess of $Mn(NO_3)_2$. (1/2 cc of 50% soln sufficient.)

(4) Add 1.5 cc $KMnO_4$ soln (40 mg/cc). (Pa carried quantitatively on 1.5 gm/liter MnO_2 ppt.)

(5) Digest over water bath, centrifuge and pour off supn.

(6) To ppt. add few drops of 4 N acid and dissolve in a few drops of sat. soln of $NH_2OH \cdot HCl$.

(7) Dilute to required volume and repeat pptns. three times, reducing volume each time. Final volume is a few cc's.

(8) Make soln 6 N HNO_3 or HCl. Extract with 2-3 times volume of diisopropyl ketone (DIPK) shaking together for 1/2 min. in Kjeldahl flasks and separating phases by freezing aqueous layer with dry ice - acetone mixture. (Pa into DIPK ~60% yield/pass).

(9) Wash DIPK layer with 3 washs of an equal volume of soln 1 N HNO_3 and 3 N NH_4NO_3 in successive flasks.

(10) Pa then washed into 2 successive portions of .1 N HNO_3.

91-1(cont'd)

(11) DIPK extn repeated once and .1 N solns combined and made 6 N HNO_3.

(12) Equal volume of TTA (.4 M in benzene) stirred for 5 min. with the 6 N acid - (Pa into TTA.)

(13) Organic layer washed once with equal volume 6 N HNO_3.

(14) The Benzene - TTA plated out on platinum.

Remarks: The am't of F^- introduced by the .01 M $(NH_4)_2SiF_6$ is not enough to complex an appreciable amount of the Pa. Traces of Pa coppt with good yield from 1 - 5 N HNO_3 less than .65 M Th^{+4} on 1.5 gm/liter MnO_2 with good separation from macro am't of Th. A concentration factor of at least 10 can be obtained by these pptn cycles.

Any Th and fission product that extract into DIPK are washed out in the acid-salt washes. 0.1 N HNO_3 used to wash Pa out of DIPK keeps Pa from hydrolyzing to the colloid state.

The Pa must never get very near a neutral pH or it will go into the non-extractable colloid.

TTA separates Pa from all elements formed in bbdt except Zr, Cb, and Hf. DIPK extracts only Pa and U at these cons. MnO_2 carries Pa, Zr, Cb and maybe some others, but does eliminate things like I which might solvent extract through the other chemical procedures.

91-2

CHEMICAL SEPARATIONS

Element separated: Protactinium

Procedure by: Meinke

Target material: $Th(NO_3)_4$ or thorium metal

Time for sep'n: 2 minute minimum, average 15 min. with metal

Type of bbdt: 60" & 184" - all particles

Equipment required: stirrer

Yield: 40-80 %

Degree of purification: Factor of at least 100 from all elements present except Zr, Cb, Hf.

Advantages: Fast, weightless plate of Pa, good for alpha pulse analysis. Zr & Cb fission products coming through procedure make Geiger counting of Pa impossible without more chemistry.

Procedure:

(1) Dissolve Th metal in conc. HNO_3 ~ .01 M in $(NH_4)_2SiF_6$ soln. (25 cc. acid and 3 or 4 drops of 1/5 M $SiF_6^=$ sol'n sufficient to dissolve 10 gms. Th.) $Th(NO_3)_4$ can be dissolved directly in 4 N HNO_3.

(2) Dilute to ~ 4 N acid.

(3) Add equal volume of TTA (.4 M in benzene) and stir for 5 minutes. (Pa, Zr, Cb into organic layer).

(4) If want somewhat better purification wash TTA layer with equal volume of 4 N HNO_3. (May lose up to half Pa yield in this wash.)

(5) Plate out benzene-TTA layer on platinum.

Remarks: TTA separates Pa from all elements formed in bbdt except Zr, Cb, & Hf.

This method used for excitation function work where as many as 16 foils are worked up simultaneously. Identical amounts of reagents are added and each sample subjected to the same procedure, giving approximately equal chemical yields for each foil (to within 5 or 10%).

CHEMICAL SEPARATIONS

Element separated: Uranium

Procedure by: Crane

Target materials: ~20 gm of Th metal

Time for sep'n: Several hrs.

Type of bbdt: 184" bbdt

Equipment required: Centrifuge, Kjeldahl flasks, dry ice and stirrers.

Yield: 90%.

Degree of purification: Separate all elements in Th fission by factor greater than 10^6.

Advantages: Gives carrier free Uranium

Procedure:

(1) Nitric acid used except where indicated otherwise. Dissolve Th metal in conc. HNO_3 & ~.01 M in $(NH_4)_2SiF_6$ (50 cc acid and ~6 drops 1/5 M $SiF_6^=$ Solution usually sufficient to dissolve 20 gram Th metal).

(2) Evaporate to near dryness & redissolve in 1 M HNO_3 and saturate with NH_4NO_3.

(3) Ether extract uranium using 3 separate portions of ether and combining; wash twice with .1 M HNO_3 + 10 M NH_4NO_3.

(4) Extract uranium back into water solution. Add La^{+++} carrier ~1 mg/cc solution.

(5) ppt hydroxide with NH_4OH. (carries uranium).

(6) Dissolve in 6 M HNO_3 and add Zr^{+4} scavenger (~1 mg/cc), dilute to 3 N acid.

(7) Add iodic acid to ppt $ZrO(IO_3)_2$ to scavenge solution.

(8) Remove supernatant and ppt La^{+3} as hydroxide.

(9) Dissolve in 1 M HNO_3. Saturate with NH_4NO_3 and ether extract using 3 separate portions of ether and combining.

(10) Wash twice with .1 M HNO_3 + 10 M NH_4NO_3 and re-extract uranium into water.

Remarks: Use one part ether, two parts salt solution in extraction. Wash with equal volume salt solution. Re-extract into half volume water.

In step 7 do not add excess iodic acid or La will also be pptd. Add just enough to ppt the Zr as $ZrO(IO_3)_2$, otherwise much yield will be lost. For ether extraction of uranium see: A. S. Newton, Phys. Rev. 75, 209 (1949).